



Kent Academic Repository

Rizzo, Marzia (2022) *Identification of novel factors regulating *Candida albicans* stress-induced genome instability*. Doctor of Philosophy (PhD) thesis, University of Kent,.

Downloaded from

<https://kar.kent.ac.uk/95760/> The University of Kent's Academic Repository KAR

The version of record is available from

<https://doi.org/10.22024/UniKent/01.02.95760>

This document version

UNSPECIFIED

DOI for this version

Licence for this version

CC BY (Attribution)

Additional information

Versions of research works

Versions of Record

If this version is the version of record, it is the same as the published version available on the publisher's web site. Cite as the published version.

Author Accepted Manuscripts

If this document is identified as the Author Accepted Manuscript it is the version after peer review but before type setting, copy editing or publisher branding. Cite as Surname, Initial. (Year) 'Title of article'. To be published in *Title of Journal*, Volume and issue numbers [peer-reviewed accepted version]. Available at: DOI or URL (Accessed: date).

Enquiries

If you have questions about this document contact ResearchSupport@kent.ac.uk. Please include the URL of the record in KAR. If you believe that your, or a third party's rights have been compromised through this document please see our [Take Down policy](https://www.kent.ac.uk/guides/kar-the-kent-academic-repository#policies) (available from <https://www.kent.ac.uk/guides/kar-the-kent-academic-repository#policies>).

**Identification of novel factors
regulating *Candida albicans*
stress-induced genome
instability**



Thesis submitted to University of Kent for the Degree of Doctor of
Philosophy (Ph.D) in Genetics

Marzia Rizzo

Declaration

No part of this thesis has been submitted in support of an application for any degree or other qualification of the University of Kent, or any other University or Institution of learning.

Marzia Rizzo

February 2022

Disclaimer

Due to the COVID-19 global pandemic, sudden disruption impacted this research. The inability to conduct laboratory research due to university research laboratory closure followed by the restricted access to the research laboratory due to part-time rotation has drastically slowed down the planned research work. Furthermore, the situation created by the global pandemic has also impacted the length of time to order and receive the reagents/chemicals needed from the suppliers leading to the whole process being prolonged and paused. All of this has led to a very limited time to conduct research. Re-planning and decision making was based on the limited time available and therefore the number of experiments conducted was significantly reduced.

*This achievement is not the top of the mountain
but the bottom of the next one.*

Acknowledgments

I would like to thank my parents, who have supported me unconditionally. For their understanding and being patience with me during my “bad days” and be there no matter what.

I would like to thank Dr. Alessia Buscaino not only for the great mentoring which has led me to achieve great results but also for her kindness, and encouragement during these years. For her advice for my future career and her patience and understanding of my difficult times. These three years with her have helped me grow professionally and personally.

I would like to thank also all the AB lab: Sam, Enea, Elise, Cameron, Chole and Matt. Thanks for the everyday shared work and the fun time but also, for the outside lab hours drinks and fun. Sam, for nice time spent together. Enea, for making me laugh so much in the lab, Elise, for helping me during my ‘homeless time’. Chloe, for being such an amazing kind and loving person. Thank you for helping me so much every time I needed, for being there and supporting me. Thanks for the millions of inoculations and pictures taken for me during the writing of this thesis.

I would like to thank also all the KFG group which advises were always helpful and for the pleasant time spent together inside and outside the lab. Jack for being the best desk buddy and being so patient when I was invading his desk. Kevin for the fun times and all the lab advice I could ever get.

Ane and Antoine for the friendships when we started this adventure together.

I would like to thank Mario for our coffee times and for listening and being there when I needed.

Lastly, I would like to thank my two angels, Giada and Simon, which without them I couldn’t get through all of this. Giada, thank you for being my person, I have never felt more connected to a person as I am with you. Thank you for ‘surviving’ with me to all our battles, and for the best time ever spent together. Simon, thank you for being so loving and caring with me. Thank you for your patience especially during my worst stressful time, for

supporting me and listening to all my complaints and helping me with everything was in your power.

Thank you to the University of Kent for funding me during these three years, otherwise this Ph.D would have not be possible.

Table of contents

Declaration	i
Disclaimer	ii
Acknowledgments	iv
Table of contents	vi
ABSTRACT	ix
LIST OF ABBREVIATIONS	x
LIST OF FIGURES	xiii
LIST OF TABLES	xiv
Chapter 1. General Introduction	1
1.1 Fungal pathogens	2
1.1.1 <i>Candida albicans</i>	3
1.2 Cell cycle in yeast	9
1.2.1 Kinetochore	16
1.2.2 Chromosome segregation regulation	19
1.2.3 Chromosome segregation defects	21
1.2.4 SUMOylation and de-SUMOylation mitotic targets	24
1.3 Antifungal drugs	30
1.3.1 Antifungal drug resistance	32
1.3.2 Fluconazole resistance in <i>C. albicans</i>	33
1.4 Genome instability	35
1.4.1 Replication stress	37
1.4.2 Chromosomal Instability	38
1.4.3 Loss of heterozygosity	41
1.4.4 Stress induced genome instability in <i>C. albicans</i>	42
1.5 DNA damage and repair	43
1.5.1 Checkpoint pathway	43
1.5.2 Single strand break	46
1.5.3 Double strand break	49
1.6 Thesis aims	52
Chapter 2. UV stress-induced novel regulators of genome instability	54
2.1 Introduction	55

2.2 Results	57
2.2.1 Genetic library and screening procedure	57
2.2.2 UV Primary screening	58
2.2.3 UV Spotting susceptibility assay	69
2.2.4 Screen of transformants by colony PCR	74
2.1.4 Quantification of survival after UV irradiation	78
2.3 Discussion	81
2.4 Conclusion and future work	84
Chapter 3. MMS stress-induced novel regulators of genome instability	85
3.1 Introduction	86
3.2 Results	88
3.2.1 Genetic library and screening procedure	88
3.1.2 MMS Primary screening	89
3.1.3 MMS Spotting susceptibility assay	101
3.1.4 Growth curves analysis	105
3.3 Discussion	111
3.4 Conclusion and future work	113
Chapter 4. The SUMO protease Ulp2 regulates genome stability and drug resistance in the human fungal pathogen <i>Candida albicans</i>	115
4.1 Article	116
4.2 Supplementary figures	155
4.3 Supplementary Tables	160
Chapter 5. Discussion	161
5.1 Identification of a novel potential regulator of stress-induced genome instability	162
5.2 Ulp2 play a role in cell cycle and genome instability	163
5.3 Ulp2 protein expression and hypersensitivity to genotoxic stress	164
5.4 <i>Ulp2ΔΔ</i> induces genome instability	165
5.5 Stress adaptation and drug resistance	166
Future work	168
Chapter 6. Materials and Methods	169
6.1 Sterilisation	170
6.2 Growth media	170
6.3 SC and SC drop-out: -His/-Arg media	170
6.4 Casitone media	171

6.5 Additives: drugs and antibiotic _____	171
6.6 <i>Candida</i> strains used for the genetic screening _____	172
6.7 Screening methodology _____	173
6.8 Spotting assay serial dilution _____	174
6.9 Colony PCR _____	174
6.10 UV survival quantification _____	175
6.11 Growth curve _____	175
6.12 <i>Candida albicans</i> strain transformant: Lithium acetate transformation _____	176
6.13 HiFidelity PCR and gel electrophoresis _____	177
6.14 CHEF electrophoresis _____	178
6.14.1 Solutions _____	178
6.14.2 Plugs preparation _____	178
6.14.3 Chromosome separation by electrophoresis _____	179
6.15 Fluconazole resistance _____	179
6.16 Caffeine resistance _____	180
6.17 Fluctuation analysis _____	180
6.18 Western Blot _____	181
6.18 Cells fixation for microscopy _____	183
REFERENCES _____	189

ABSTRACT

Candida albicans is a commensal harmless organism which asymptotically colonises the human population. However, this organism can become a life-threatening pathogen causing systemic infections which results fatal especially in immunocompromised patients. During colonisation and infection, *C. albicans* must adapt rapidly to the different environments of the host. *C. albicans* genome is highly plastic, and it can tolerate large-scale genomic changes adapting to the stress environments it encounters. This is because genomic instability increases genetic diversity allowing the selection of the genotypes favourable to adapt to the stress environment. This genetic instability increases virulence and resistance to the common antifungal drugs. However, it remains unknown how stress-induced genetic instability is regulated and what are the driving mechanisms to genome plasticity in the stress environment. By this means, the aim of this project is to identify novel regulators of *C. albicans* stress-induced genome instability.

To this end, I performed different parallel genetic screenings using a homozygous *C. albicans* gene deletion library, using UV radiation and Methyl methanesulfonate (MMS) as DNA damaging agents. This strategy has led to the identification of *ULP2* *C. albicans* gene as novel potential regulator of *C. albicans* genome instability. *ULP2* gene is involved in SUMO deconjugation, and in this project it has proved to be hypersensitive to different genotoxic stresses including UV, MMS, Hydroxy urea (HU), Hydrogen peroxide (H₂O₂) and high temperature. In addition, cell lacking *ulp2ΔΔ* exhibited chromosome mis-segregation defects. The high genome instability of the *ulp2ΔΔ* strain leads to enhanced Fluconazole resistance via selection of novel fitter genotypes. Whole-genome sequencing of *ulp2ΔΔ* fluconazole resistance cells exhibited stress-induced segmental aneuploidies of chromosome R and chromosome I. Furthermore, intrachromosomal repetitive elements are the site of formation of complex novel genotypes with adaptive potential. To sum up, these results show that *C. albicans* *ULP2* gene regulates genome plasticity and drug resistance.

LIST OF ABBREVIATIONS

(6-4)PPs: 6-4 photoproducts

3'-dRP: 3' deoxyribose

5'-dRP: 5' deoxyribose

8-oxoG or OG: 8-oxo-7,8-dihydro-2'-deoxyguanosine

AP: Apurinic/aprimidinic

APC/C: Anaphase-promoting complex/cyclosome

APC^{Cdc20}: Cdc20-dependent anaphase-promoting complex

ATP: Adenosine triphosphate

BER: base excision repair

BIR: Break-induced replication pathway

BP: Base pairs

CCAN: Constitutive centromere-associated network

CDKs: Cyclin-dependent kinases

Chr5L: Chromosome 5L

CIN: Chromosomal instability

CNV: Copy number variation

CCNVs: Chromosome copy number variation

CPDs: Cyclobutene pyrimidine dimers

DNA: Deoxyribonucleic Acid

DSB: Double strand break

dsDNAs: Double stranded DNAs

Fapy: Formamidopyrimidine

G₁: Gap phase 1

G₂: Gap phase 2

GCRs: Gross chromosomal rearrangements

GG-NER: global genome NER

GlcNAc: N-acetylglucosamine

GUT: Gastrointestinal induced transition

H₂O₂: Hydrogen peroxide

HU: Hydroxy urea

HR: Homologous recombination

i(5L): Isochromosome 5L

LOH: Loss of heterozygosity

M: Mitosis

MAP: Mitogen-activated protein

MEN: mitotic exit network

MMS: Methyl methanesulfonate

MRS: Major repeat sequence

MRX: Mre11-Rad50-Xrs2

MTL: Mating-type-like

NER: Nucleotide excision repair

ORI: Replication origins

PIKK: Phosphatidylinositide 3-kinase-related kinase

PKA: Protein kinase A

Pol II: Polymerase II

PTMs: Post-translational modifications

rDNA: Ribosomal DNA

RF: Replication fork

ROS: Reactive oxygen species

RPA: Replication proteins A

S: Synthesis phase

SAC: Spindle assembly checkpoint

SAP: Secreted aspartyl proteinases

SIN: Septation initiation network

SMC: Structural maintenance chromosome

SNPs: Single nucleotide polymorphisms

SPOC: Spindle position checkpoints

SSBR: Single-strand break repair

SSBs: Single strand breaks

ssDNA: Single-stranded DNA

SUMO: Small ubiquitin-like modifier

TC-NER: Transcription-coupled NER

TLO: Telomere associated genes

TLS: Translesion synthesis

UV: Ultraviolet radiation

whole-Chr: Whole-chromosome

WGS: Whole genome sequencing

WT: Wild type

LIST OF FIGURES

Figure 1.1 *C. albicans* different morphologies

Figure 1.2 Schematic organisation of the major classes of genetic repeats in *C. albicans* genome

Figure 1.3 Cell cycle in budding yeast

Figure 1.4 Chromosome segregation during cell cycle

Figure 1.5 Schematic representation of cell division in filamentous forms.

Figure 1.6 Kinetochore organisation

Figure 1.7 Chromosome mis-segregation

Figure 1.8 SUMOylation pathway

Figure 1.9 Chemical structures of representative antifungal drugs

Figure 1.10 DNA damages and DNA repair pathways

Figure 2.1 UV Primary screening

Figure 2.2 UV Spotting susceptibility assay

Figure 2.3 Screening of transformants by colony PCR

Figure 2.5. Quantification of survival to UV radiation of final selected homozygous deletion isolates

Figure 2.6. Percentage of filamentous form in final selected homozygous deletion isolates.

Figure 3.1 MMS Primary screening

Figure 3.2 MMS Spotting susceptibility assay

Figure 3.3 Growth curves of *C. albicans* MMS selected strains

LIST OF TABLES

Table 2.1: Deletion mutants indicated with red circle in figure 2.1

Table 2.2: Deletion mutants indicated with blue circle in figure 2.1

Table 2.3: Deletion mutants indicated with green circle in figure 2.1

Table 2.4. Gradient of sensitivity to UV radiation from spotting susceptibility assay

Table 2.5 Genes sizes and expected sizes bands from PCR reactions

Table 2.6 Successful homozygous knockout isolates verified by colony PCR

Table 2.7 Unsuccessful homozygous knockout isolates verified by colony PCR

Table 2.8. List of homozygous knockout isolates selected from step 3.

Table 3.1: Mutants indicated with red circle for MMS screening in figure 3.1

Table 3.2: Mutants indicated with blue circle for MMS screening in figure 3.1

Table 3.3: Deletion mutants indicated with green circle in figure 3.1

Table 3.4. Gradient of sensitivity to MMS from spotting susceptibility assay in figure 3.2

Table 6.1 YPAD: yeast extract, peptone, adenine, dextrose media

Table 6.2 SC and SC drop-out: -His/-Arg media

Table 6.3 Casitone media

Table 6.4 Additives

Table 6.5 Strains used in this study

Table 6.6 Primers used in this study

Table 6.7 Plasmids used in this study

Table 6.8.A PCR Master mix reagents

Table 6.8.B PCR cycles protocol

Table 6.9.A HiFidelity reagents protocol

Table 6.9.B PCR Hi fidelity protocol

Chapter 1. General Introduction

1.1 Fungal pathogens

The fungal kingdom includes around 6 million species (Taylor et al., 2014). More than 600 species are associated with humans, this association can be as commensals or as pathogens. Globally, the incidence of invasive fungal infections is increasing, while the antifungal resistance by pathogenic fungi is also increasing (Konopka et al., 2019). Three main fungal pathogens can be represented by *Aspergillus* species, *Cryptococcus* species and *Candida* species. The *Aspergillus* species are commonly found in different environments and substrates. Some *Aspergillus* species such as *A. fumigatus* and *A. flavus* can cause serious respiratory disease in humans (Mousavi et al., 2016). In addition, *Aspergillus* species can cause infections in animals and plants and produce toxins which lead to food spoilage (Konopka et al., 2019). *Cryptococcus* species are environmental fungal pathogens commonly found in soil, trees, and avian habitations. Two species, *C. neoformans* and *C. gattii*, can cause serious diseases affecting the lungs or the central nervous system (Konopka et al., 2019; Normile et al., 2020). As mentioned above for *Aspergillus* and *Cryptococcus*, humans do not represent the primary environmental niche. However, when the immune system is compromised, they can cause dangerous diseases. *Candida* species instead are present in the human's microbiome. However, when the host defences are compromised, *Candida* can become a pathogen and cause systemic infections (Sun et al., 2020). Five *Candida* species are commonly associated with pathogenicity, *C. albicans*, *C. glabrata*, *C. tropicalis*, *C. parapsilosis*, and *C. krusei*. Of these, *C. albicans* remains the most commonly isolated in clinics (Turner and Butler, 2014). In the 1950s, medical progress such as immunosuppressive therapy, indwelling medical devices and the development of chemotherapy allowed fungal pathogens to exploit humans. In the same time frame, the first description of candidiasis was reported consequent of treatments with antibiotic which caused disequilibrium in the microbiota with loss of the 'good' bacteria (Konopka et al., 2019).

To parasite a human, fungal pathogens need to be able to accomplish four criteria. First: grow at physiological and febrile temperatures. Second: reach different tissues by penetrating host tissue barriers. Third: be able to get nutrients and digest components of host tissues. Fourth: able to escape the host immune system (Köhler et al., 2015). Nowadays, four classes of antifungal drugs are available to treat life-threatening infection. Fungi as eukaryotes share basic and cell biology with humans which makes this a limiting factor in developing antifungal drugs that selectively target fungi. Another threat which comes from the fungal species is the developing of resistance to antifungal drugs. An emerging fungal pathogen, *Candida auris*, has already developed multidrug resistance to all four class of antifungal drugs (Sun et al., 2020). Therefore, fungal infections have become a global threat which is evolving rapidly urging new target therapy for fast adapting fungal pathogens.

1.1.1 *Candida albicans*

C. albicans is the most prevalent fungal species in humans. It is a commensal organism which asymptotically colonizes the mouth, gastrointestinal tract, genitourinary tracts, and skin (Achkar and Fries, 2010; Alonso-Monge et al., 2021; JM and BC, 2010; Kashem and Kaplan, 2016). It is often harmless in healthy individuals, however a different range of stimuli in the host environment (i.e., drugs, pH nutritional constituents) or host immune system (immunocompromised individuals or response to chemotherapy) lead *C. albicans* to overgrow and become a pathogen (Mayer et al., 2013a). *C. albicans* can cause oral and vaginal infections and in severe cases, it can penetrate into tissue and disseminate through the bloodstream causing life threatening diseases (Hube, 2004). *C. albicans* belongs to the CTG fungi clade, in which the members of this clade are characterised by different genetic code in which CUG codons codify for serine rather than leucine (Santos et al., 2011). The members of the CTG clade are also related by the common feature of adaptation to stress environments (Krassowski et al., 2018). It was shown by (Simões et al.,

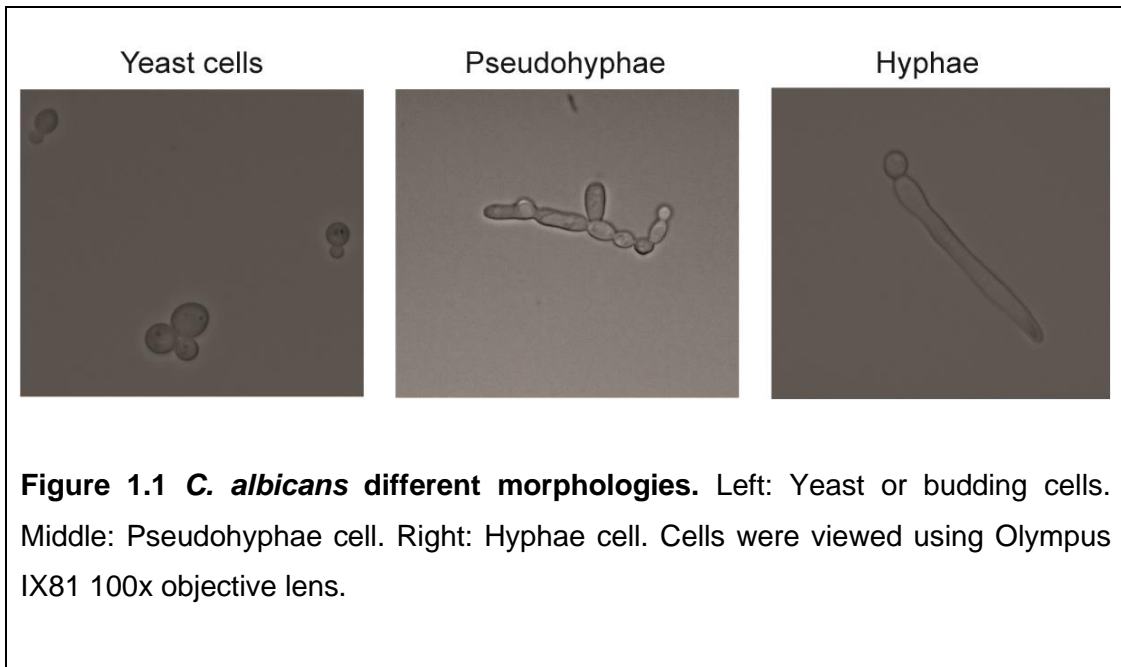
2016) that under normal conditions, CUG sites incorporate serine 97% of the times. However, under stress conditions leucine incorporation is more frequent.

Phenotypic diversity: *C. albicans* can exist in different morphotypes. For example, *C. albicans* can switch between (i) white-opaque, (ii) white-grey-opaque (iii) yeast to GUT and (iv) yeast to hyphae. White and opaque cells are different in appearance, in gene expression and mating behaviour. The master regulator for white-opaque switching is the transcription factor *WOR1* (Zordan et al., 2006). Under normal conditions, this switching occurs at a very low rate. However, decreasing temperature, level of oxygen and increasing of CO₂ can induce *C. albicans* to switch to the opaque state (Huang et al., 2009; Ramírez-Zavala et al., 2008). Mating plays the main role in white-opaque transition. The mating type locus MTL, **a/a** or α/α , where **a** and α represent the mating forms, control the switching **a/a** (Soll, 2004). In addition, a tristable phenotypic switch has been demonstrated by (Tao et al., 2014), in which *C. albicans* can undergo a white-grey-opaque transition. The grey forms differ in colony appearance but also in gene expression (Tao et al., 2014). Furthermore, *C. albicans* during the passage in the gastrointestinal tract can switch its morphology resulting in gastrointestinal induced transition (GUT) cells which differ in morphology (cells results elongated) and in gene expression, with higher levels of genes for phosphate uptake in addition to transcription factors for cell surface, secreted proteins and cell wall remodelling enzymes (Pande et al., 2013). *C. albicans* can also switch its morphology from budding yeast form to filamentous form as described in the next section.

Yeast-hyphae switch: *C. albicans* is normally present in yeast form. However, when it becomes pathogenic, this organism can undergo rapid and reversible phenotypic changes from budding yeast to pseudo-hyphae to hyphae form (figure 1.1) (Li and Nielsen, 2017; Tyc et al., 2014). Pseudohyphae cells represent the intermediate cell type between yeast cells and hyphae. They are formed of chains of elongated yeast cells with constrictions at the septal junctions. Hyphae cells are tube-like, uniform in width and lack septal constrictions. Hyphae possesses a specialised

organelle, known as Spitzenkörper which induces growth of the hyphal tip mediating the vesicle secretion figure 1.5 (Berman, 2006; Berman and Sudbery, 2002; Thompson et al., 2011a) .

Environmental stimuli affect *C. albicans* morphology such as pH < 6 induces *C. albicans* cells to grow in yeast form, in contrast, pH > 7 induces hyphal form. In addition, conditions such as starvation, the presence of the amino sugar N-acetylglucosamine (GlcNAc), the host physiological temperature and CO₂ induce formation of hyphal forms (Mayer et al., 2013b). The transition from yeast to hyphae forms has proven to be essential for host invasion and virulence (Thompson et al., 2011b). The hyphae forms have proved to be more invasive compared to yeast forms. However, yeast forms are considered responsible for dissemination (Mayer et al., 2013b). Hyphal forms can invade the epithelial layers by mechanical force in which hyphae can grow between epithelial cells and/or penetrating them. Hyphae cells can cause the rupture of endothelial cells followed by phagocytosis, in addition *C. albicans* can lyse macrophages and neutrophils (Thompson et al., 2011a).



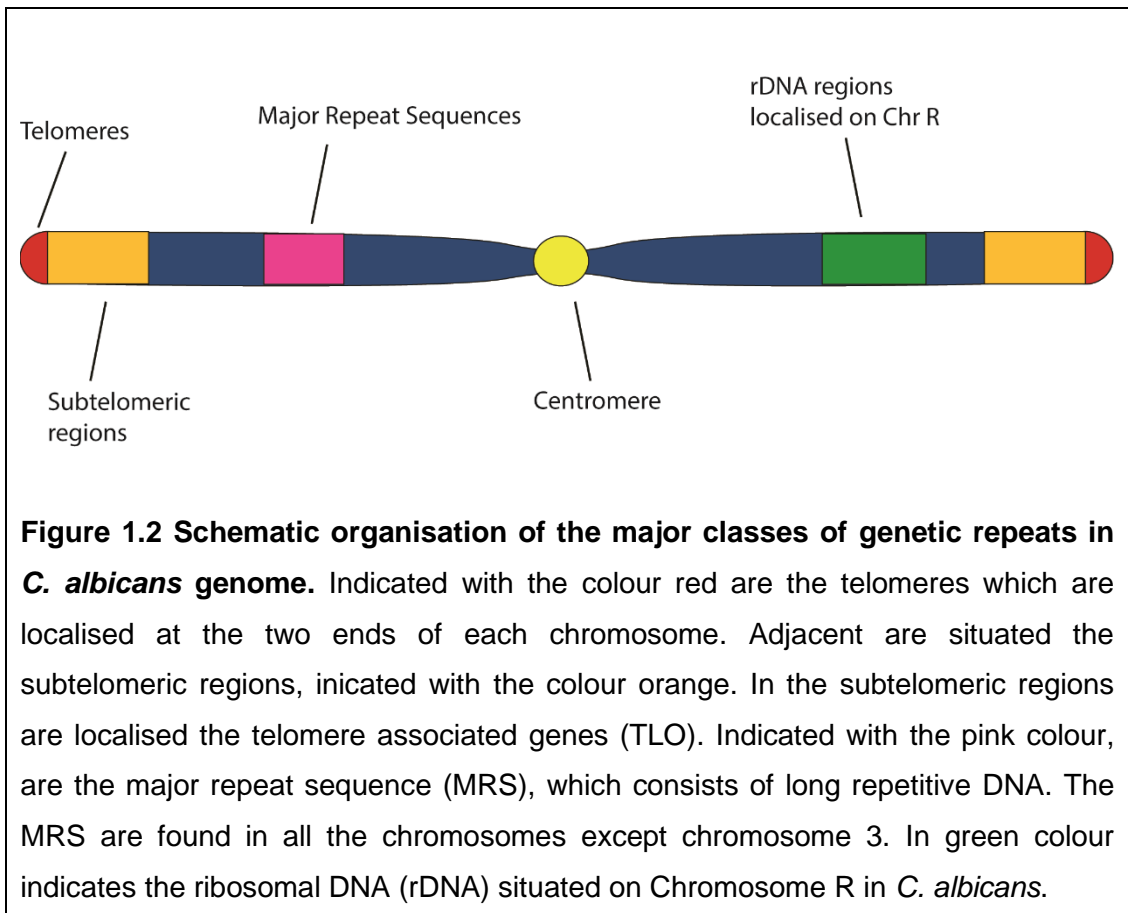
Genome organisation: *C. albicans* possesses a diploid genome formed of eight pairs of chromosomes with sizes between 0.85 to 3.3 Mb consisting of 16 Mb in total, harbouring around 6,100 genes (Jones et al.,

2004a; Van het Hoog et al., 2007a). The eight regional centromeres have unique DNA sequence on each chromosome bound to histone H3-variant proteins Cse4. In addition, *C. albicans* centromeres lack of repeated DNA elements and transposons (Mishra et al., 2007) (see section 1.2.1 for more detailed description on centromere and kinetochore). Replication in *C. albicans* begins from multiple genetic loci known as DNA replication origins (ORI) and they can be of two types: arm ORIs, located in the chromosomal arms; and centromeric ORIs, located close to the centromere. The arm ORIs are featured by the presence of 15-bp AC-rich sequence and nucleosome depleted regions while the centromeric ORIs replicates earlier (Koren et al., 2010; Legrand et al., 2019; Tsai et al., 2014).

Telomeres, specialised nucleoprotein structures have two main roles in maintenance of genome integrity: protect by capping the chromosomes ends and maintain the telomere length promoting chromosome end replication (Singh et al., 2002; Yu, 2012). In most organisms, telomeric DNA consists of short repetitive sequences which are rich in G-residues (Singh et al., 2002). The strand which contains the G-rich residues is longer compared to the complementary strand and forms 3' single-stranded over-hang named G-tail (Yu, 2012). The telomeres are maintained by telomerase, a specialised reverse transcriptase which uses its RNA component as a template to synthesise the G-rich strand of the telomere repeats (Singh et al., 2002; Yu, 2012). In *S. cerevisiae* and *S. pombe*, telomeres consist of short irregular repeats (Singh et al., 2002). On the contrary, *C. albicans* have an unusual long and regular repeat unit which is 23-bp-long (Mceachern and Hicks, 1993). Adjacent to the telomeric repeats are present genomic regions enriched for repetitive genetic elements, called subtelomeres. These subtelomeric regions are rich in transposable elements and known to be the hotspots for recombination events and mutations (Dunn and Anderson, 2019). In *C. albicans*, telomere associated genes (TLO), as the name suggests, are localised in the subtelomeric regions. In *C. albicans* genome there are 15 TLOs in which all except one *TLO* gene are located within 12 kb of a telomere. The other *TLO* named *TLO34* (since it is located between *TLO3* and *TLO4*) is located internally on chromosome 1 (Anderson et al.,

2012; Haran et al., 2014; Van het Hoog et al., 2007b). The TLO genes can be classified in four clades based on gene structure. The α clade consist of 6 members which are highly expressed; the β clade holds only one gene; the γ clade contains 7 members; lastly, the ψ clade which includes a pseudogene (Anderson et al., 2012). They are all oriented with transcription proceeding toward the centromere. The TLO genes encode proteins with homology for the N-terminal Med2 domain, a component of the Mediator complex (Haran et al., 2014). The mediator is a multi-subunit complex which function is transcription regulation, it interacts with RNA polymerase II (Pol II) and the general initiation factors at target gene promoter (Flanagan et al., 2018; Karijolich and Hampsey, 2012). In addition, the mediator complex plays an important role in expression of genes correlated to virulence and resistance to antifungal drugs (Liu and Myers, 2017; Nishikawa et al., 2016; Uwamahoro et al., 2012). The TLO/Med2 constitutes part of the Mediator's tail in association with Med3 and Med15 (Flanagan et al., 2018). It is believed that *TLO* and *MED3* play a role in virulence due to the inability to form germ tubes in cells lacking *MED3* (Zhang et al., 2012).

C. albicans genome possesses the major repeat sequence (MRS) which consists of long repetitive DNA found in all the chromosomes except chromosome 3. MRS is formed by three subunits: a 6 kb end named RB2, a 2kb central part with multiple repeats known as RPS and a 8kb centromere proximal sequence called HOK (Lephart and Magee, 2006). The MRS are assembled into transcriptionally permissive chromatin carrying marks for both heterochromatin and euchromatin (Freire-Benítez et al., 2016). The MRS are associated with genome rearrangements such as chromosome translocations, chromosome length polymorphisms in clinical isolates (Asakura et al., 1991; Diaz-Guerra et al., 1997; Lockhart et al., 1995).



In *C. albicans*, ribosomal DNA (rDNA) units as tandem repeats are grouped on chromosome R. The rDNA unit sizes are usually around 12 kb repeated 50 to 200 times. Each unit of rDNA includes two highly conserved 35 S and 5 S ribosomal genes, these two rRNA genes are separated by two non-transcribed regions, NTS1 and NTS2 (Freire-Benítez et al., 2016; Jones et al., 2004b). It was shown by Rustchenko et al., 1993 that the numbers and sizes of rDNA units differ in clinical isolates. In addition, among different strains the variability of chromosome R was attributable to the length of rDNA clusters. The same study also shows that at 37°C there is a higher accumulation of the number of rDNA units (Rustchenko et al., 1993).

Altogether these DNA repeats can undergo recombination events which are associated with genome rearrangements such as DNA insertions and/or deletions, copy number variation, karyotypic variation and loss of heterozygosity, driving to genome instability (Todd et al., 2019). Genome instability in *C. albicans* is described in section 1.4.4. Schematic

representation of the organisation of the major classes of genetic repeats in *C. albicans* is illustrated in figure 1.2.

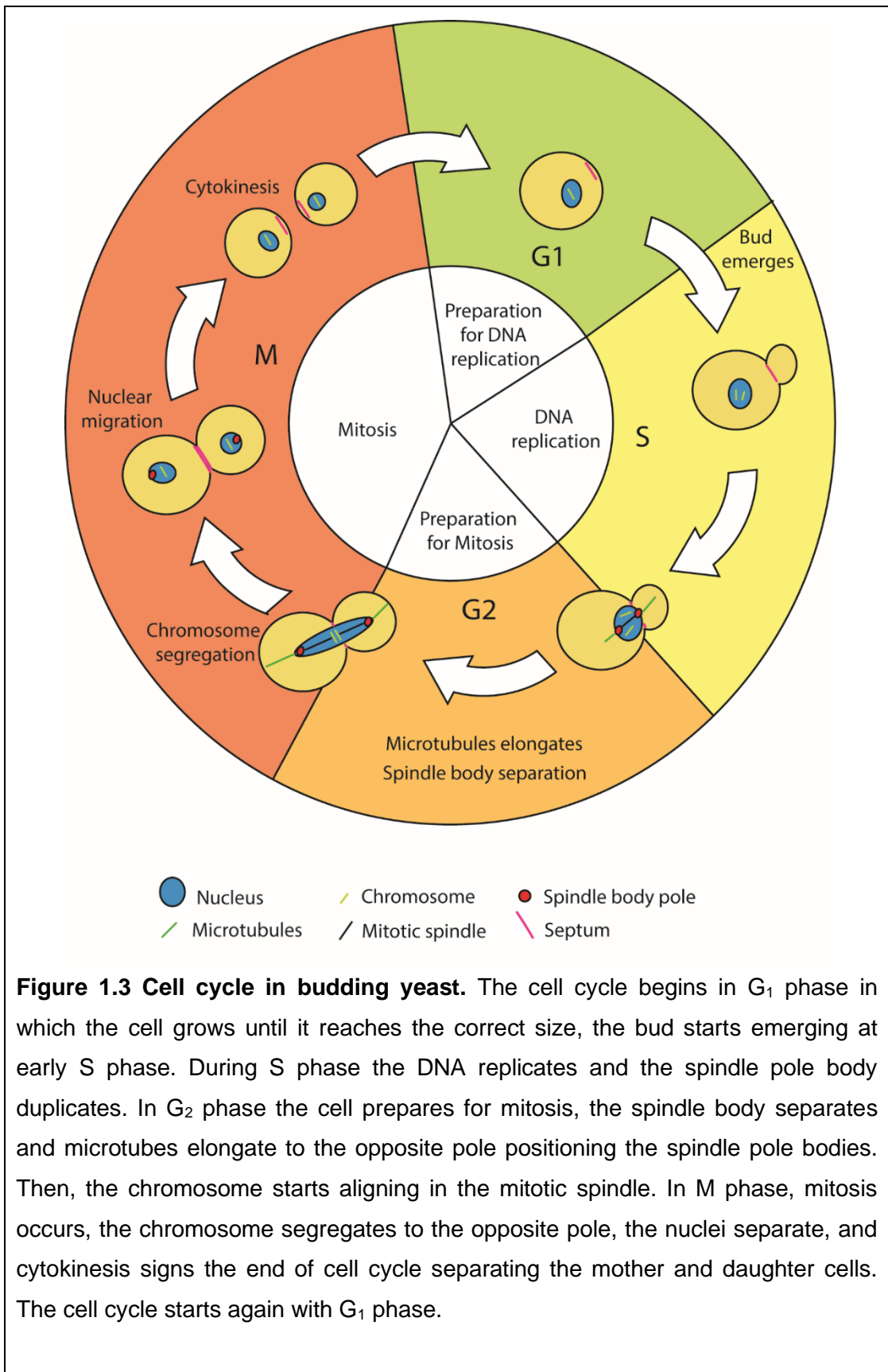
1.2 Cell cycle in yeast

The cell cycle is represented by a succession of events whereby a single cell grows, replicates its DNA, and divides into two daughter cells with identical genetic information. The cell cycle can be divided into four phases: gap phase 1 (G_1), synthesis phase (S), gap phase 2 (G_2), and mitosis (M) (figure 1.3). In the first phase G_1 the cell grows and prepare to progress to the next phase. During S phase the entire genome is duplicated, and two identical copies of each chromosome, called sister chromatids, remain physically associated. The third phase G_2 the chromosome condense to prepare for the last phase. During M phase, the sister chromatids are separated, and segregation of chromosomes occurs (Griffiths et al., 2000). The cell cycle progression is tightly regulated to ensure genome integrity, in particular, DNA damage, stalled DNA replication forks or spindle attachments defects is controlled by cell cycle checkpoints and can cause cell cycle arrest (Rhind and Russell, 1998). The general checkpoints surveillance during the cell cycle begins at G_1 phase with the check of cell size and the absence of DNA damage before entering in the S-phase. At G_2 phase, the checkpoints verify that the DNA synthesis is concluded, and the DNA is not damaged. In the last phase of cell cycle, M phase, the checkpoints verify that the DNA replication is finalised, and the chromosomes aligned. In addition, the mitotic spindle must be bi-oriented such that the sister chromatids migrated in both poles. Once all of these requirements are fulfilled the cell can correctly divide (Barnum and O'Connell, 2014). The cell cycle checkpoints are mainly controlled by cyclin-dependent kinases (CDKs) and cyclins. The CDKs are active only combined with a regulatory cyclin subunit (Barnum and O'Connell, 2014).

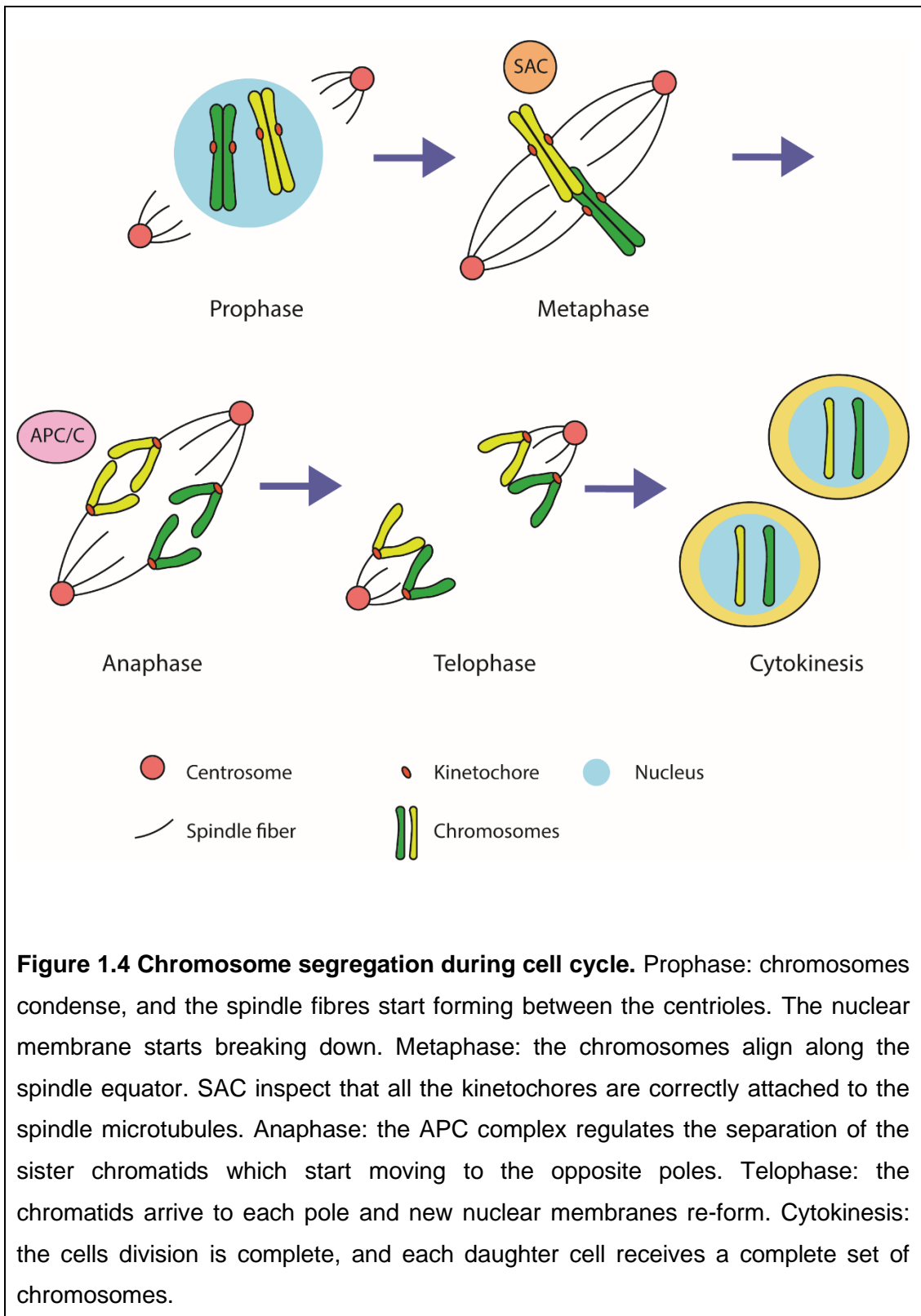
In *C. albicans*, Cdc28 is the central coordinator for the cell cycle division, its activity is regulated by the temporal association with cyclins (Sherlock et al., 1994). In G_1 phase the binding of Cdc28 cyclins Ccn1 and Cln3 induce apical growth and bud elongation (Bachewich and Whiteway,

2005; Côte et al., 2009). With the cell cycle progressing towards the G₂ phase, the G₁ cyclins are degraded, and new binding occurs with the G₂ cyclins Clb2 and Clb4. However, Clb4 is also detected in early S-phase (Ofir and Kornitzer, 2010). Furthermore, Clb2 and Clb4 cyclins inhibit the polarised growth and induce isotropic bud expansion (Bensen et al., 2005). For the mitotic exit, cytokinesis and cell separation, Cdc15 plays a crucial role (Bates, 2018a). Alteration of Ccn1 result in defective hyphal colony formation (J. D. J. Loeb et al., 1999), while cells with Clb2 deletion are inviable, on the contrary deletion of Cdc28, Cln3, Clb4 or Cdc15 induce filamentous forms (Bensen et al., 2005).

In fission yeast, the only CDK involved in the cell cycle regulation is represented by Cdc2, and its activity is regulated by the association with specific cyclins during the cell cycle. Rum1 inhibits Cdc2 maintaining low levels of Cdc2 activity throughout late M-phase and G₁ phase. During the late G₁ phase Cig1 and Puc1 associate with Cdc2 and degrade Rum1 by phosphorylation, increasing the levels of Cdc2. In S-phase, Cdc2 can bind to Cig2. Cdc13 levels increase in G₂ and are maintained high until end of M-phase (Moser and Russell, 2000).



In addition, mitosis can be divided into four substages: prophase, metaphase, anaphase, and telophase (figure 1.4). The first phase is prophase in which chromatin begin to condense into chromosomes. Since the chromosomes were duplicated in the S-phase, each chromosome is present in double copies consisting of two sister chromatids attached through the centromere. The mitotic spindle begins to form. This array of microtubules is responsible for separating the sister chromatid in the opposite pole. Lastly, the nuclear membrane breaks down. During the second phase, metaphase, the sister chromatids align at the centre of the cell and the centromere are attached to the spindle fibers (Pierce, 2012). The mitotic checkpoint also known as spindle assembly checkpoint (SAC) inspect that all the kinetochores are properly attached to the spindle microtubules (Musacchio and Salmon, 2007). Once this requirement is satisfied the cell goes in the next stage called anaphase (Pierce, 2012). In this phase the anaphase-promoting complex/cyclosome (APC/C) regulates the separation of sister chromatids (Yamano, 2019) by degrading the nuclear protein Pds1 (Agarwal and Cohen-Fix, 2002). The degradation of Pds1 allows Esp1 protein to cleave cohesion and enable the sister chromatid separation (Ho et al., 2015). Motor proteins generate forces allowing the migration of the chromosomes towards the spindle poles. The last phase, called telophase, is characterised by the arrival of the chromosome at each spindle pole and nuclear membrane re-forming. In this way, each daughter cell has a complete set of chromosomes within its own nuclei. Cytokinesis then divides the cytoplasm between the two cells (Pierce, 2012).



Since cytokinesis occurs at the mother-bud neck, it is essential that the mitotic spindle and the nuclear division take place at the point of maximum constriction between the mother and daughter cell as shown in

figure 1.3 (Merlini and Piatti, 2011). In the budding form, the septin ring appears before the formation of the bud. Then the bud grows across the septin ring (Warenda and Konopka, 2002). In the event of spindle mispositioned, the spindle position checkpoints (SPOC) arise and delay the mitotic exit providing time for the realignment of the spindle (Merlini and Piatti, 2011). In the pseudohyphal cells, after cytokinesis the cells remain attached forming branching filamentous cells appearing as elongated buds (Berman, 2006). Despite their morphology, pseudohyphae cells share features as synchronous cell division and septation in the position of the mother bud neck, characterising them from true hyphae (Veses and Gow, 2009). Furthermore, pseudohyphal cells grow slower in a polarised manner and remain in G₂ phase longer compared to yeast cells (Berman, 2006). In contrast, hyphae cells show more tube-like filaments and no obvious constrictions at the site of septation. The evagination and germ elongation is continuous from the tip, and it shows high polarised growth (Berman, 2006; Sudbery, 2011). The evagination takes place before the cell cycle starts. At the tip of the germ tube, the septin ring is formed and it stays fixed as the cell continues elongating. The nuclei migrate and divide into the germ tube where mitosis occurs. After mitosis, one nucleus migrates into the mother cell and the other migrates in the apical site of the septin ring. In addition, a septin band is formed at the mother germ tube junction as showed in figure 1.5 (Berman, 2006; Sudbery, 2011).

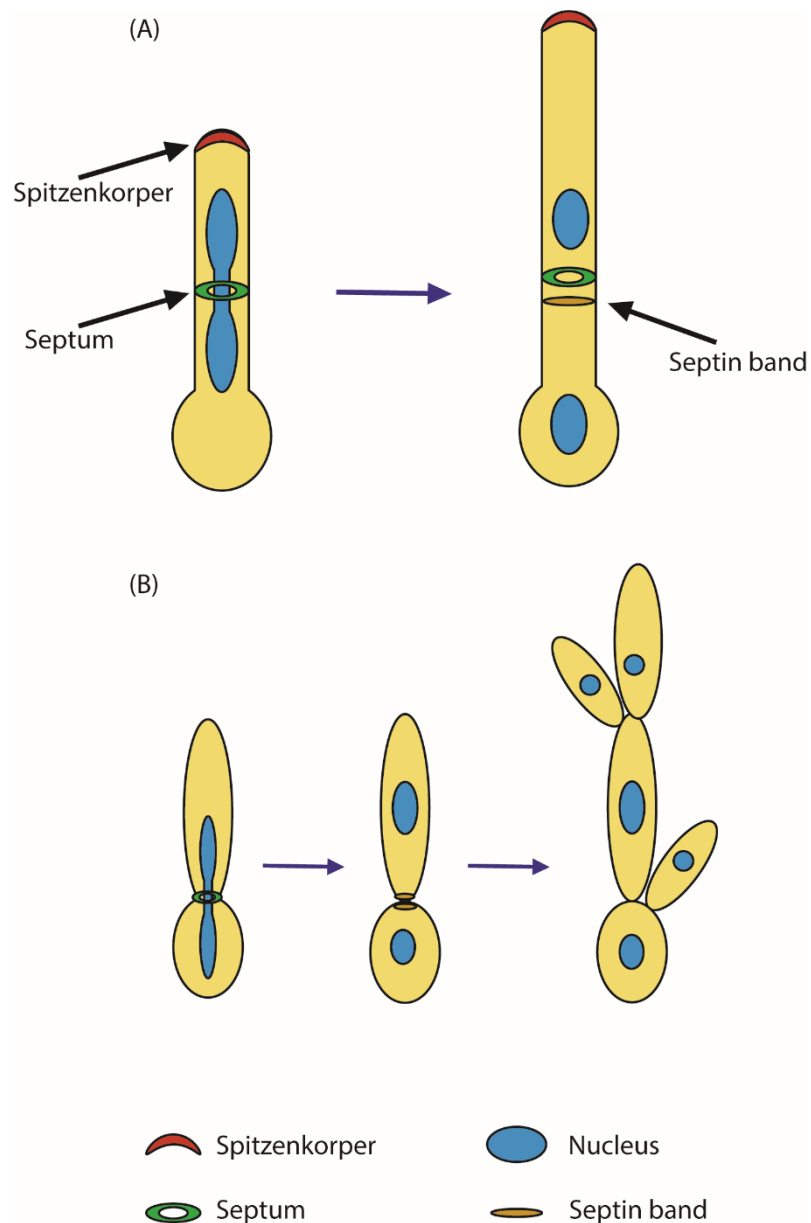


Figure 1.5 Schematic representation of cell division in filamentous forms.

(A) hyphae formation: A single germ tube evaginates from the mother cell, septum ring marks the evagination point and stays fixed as the cell continues elongating. The two nuclei migrate and separate into the germ tube during mitosis. At the end of mitosis one nucleus migrate into the mother cell and the other into the germ tube. The septin band remains at the circumference of germ tube neck.

(B) pseudohyphae cells formation, the cells remain attached creating a branching filamentous cell. Pseudohyphae cells maintain the septing at the mother bud neck.

1.2.1 Kinetochores

Centromeres are chromosomal regions which are crucial for chromosome segregation. Specialised proteins assemble on the centromere to form the kinetochore which binds to microtubules, during mitosis, allowing the segregation of chromosomes. In eukaryotes, organisation of centromeres can be grouped into three main types: (i) *point centromeres* such as the one found in the model system well studied in *S. cerevisiae*. This types of centromeres have a defined DNA sequence that is short in length ~120bp;; (ii) *long regional centromere* such those found in *S. pombe* that possess centromere having a length of ≥ 40 kb, and it includes repetitive sequences and unique DNA elements; (iii) *small regional centromere* typically of *C. albicans* (Cole et al., 2011; Roy et al., 2013; Steiner et al., 1993) further described in this section.

C. albicans possesses regional centromeres with a 3-5 kb length with a unique DNA sequence on each of its 8 chromosomes, characterised by short nucleosome-length satellite repeats present in untranscribed AT-rich region (Sanyal and Carbon, 2002a). In *C. albicans*, neocentromeres can form adjacent to the native centromere, following deletion of native centromeric sequences (Ketel et al., 2009). At centromeric regions, the histone H3 is replaced by H3-variant proteins Cse4 (CENP-A homolog) which act as epigenetic mark of centromeres from yeast to humans (Allshire and Karpen, 2008). Disruptions of CENP-A lead to chromosomes segregation and cell-cycle progression defects (Aristizabal-Corrales et al., 2019; Régnier et al., 2005). Kinetochores are multi-subunit protein complexes that assemble at the surface of the centromere connecting chromosomes to the microtubules of the mitotic spindles. Kinetochores are organised into two main layers figure 1.6 (i) *inner kinetochore* where subunits bind to CENP-A, connecting the chromosomal DNA and form the platform to assemble the kinetochore. This layer is often named as constitutive centromere-associated network (CCAN); (ii) *outer kinetochore* which forms connections with microtubules. These kinetochore layers are spatially distributed from the DNA to the spindle microtubules. In addition to this,

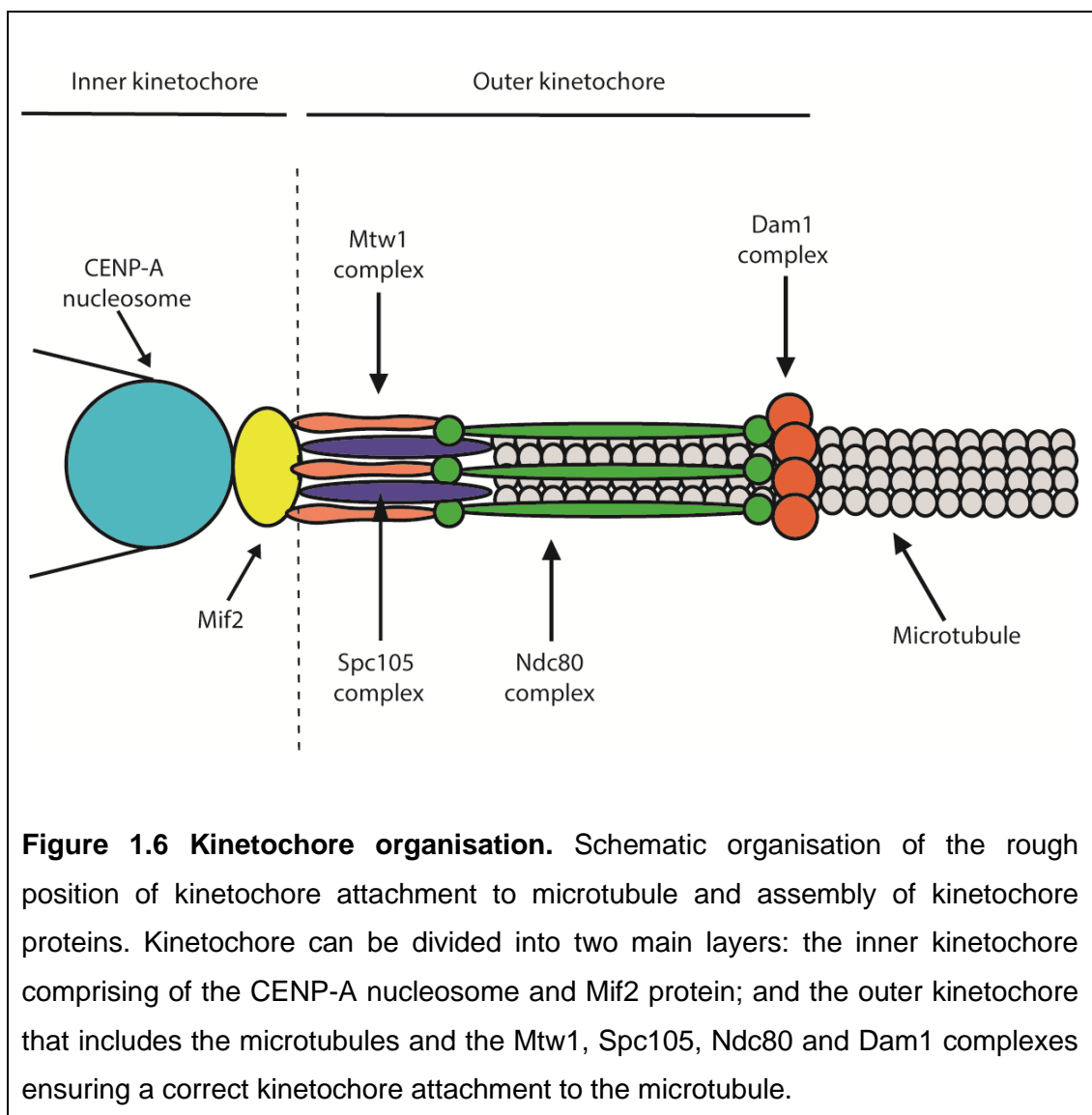
regulatory proteins control the kinetochores activities (Cheeseman, 2014; Musacchio and Desai, 2017).

It is believed that CENP-A is the initiator of kinetochore formation (Allshire and Karpen, 2008), however, it needs the assistance of a histone chaperone for integration at the centromere. This chaperone is known as Scm3 in budding as fission yeast (De Rop et al., 2012). CENP-A can regulate the localization of most of the kinetochore proteins. However, CaMtw1p can regulate CENP-A localization (Thakur and Sanyal, 2012). The recruitment of CENP-A can involve genetic and epigenetic factors. In *S. cerevisiae* it occurs in S-phase and anaphase, at S and G₂ phase for *S. pombe* and anaphase for *C. albicans* (Roy et al., 2013).

In order to segregate the chromosomes during mitosis, the kinetochore is required to physically connect with the microtubule polymers of the mitotic spindle (Cheeseman, 2014). CENP-A has an essential role for chromosome segregation. However, other kinetochore proteins such as Mif2 (CENP-C homolog), Mtw1 (Mis12 homolog), Ndc80 complex (Hec1 homolog) and Dam1 complex together with CENP-A are crucial to mediate the kinetochore-microtubules attachment (Roy et al., 2011; Sanyal et al., 2004; Sanyal and Carbon, 2002b; Thakur and Sanyal, 2012, 2011). More specifically the Ndc80 complex directly binds and forms clusters along the microtubules (DeLuca and Musacchio, 2012). Furthermore, Dam1 complex forms a ring around the microtubules which allow the complex to slide down the microtubules in response to force (Westermann et al., 2005).

Kinetochores are highly regulated to ensure accurate kinetochore – microtubule attachments. Kinetochore regulatory proteins phosphorylate the kinetochore substrates regulating its function (Cheeseman, 2014). These regulators are represented in yeast by Ipl1 (Aurora B homolog in human, ark1 in fission yeast) Cdc5 (Plk1 in humans and plo1 in *S. pombe*), Mps1, Bub1 and Cdc28 (Elowe, 2011; Gascoigne and Cheeseman, 2013; Lampson and Cheeseman, 2011; Liu et al., 2012; Liu and Winey, 2012). An important kinetochore regulation is to prevent improper microtubule attachments. Aurora B can phosphorylate multiple components of the kinetochore-

microtubule destabilising the incorrect attachment. This phosphorylation has the combined effect of removing the improper kinetochore-microtubule attachments and resetting the kinetochore for a fresh opportunity to be bi-oriented, whereas correct attachments are stabilised. However, Aurora B exhibits tension-sensitivity which results in decreasing of phosphorylation on bi-oriented kinetochores. Indeed, Aurora B is located away from the outer kinetochore in the presence of tension which distorts the kinetochore structure (Cheeseman, 2014; Liu and Lampson, 2009).



1.2.2 Chromosome segregation regulation

Chromosome segregation is a complex process to ensure that the mother and daughter cells receive the exact set of duplicated chromosomes during cell division. Accuracy of chromosome segregation is essential; it depends on the correct attachment and alignment of chromosome to the segregation machinery (Marston, 2014).

During prophase, a protein complex named condensin compacts the chromosomes. Cohesin proteins hold together the two sister chromatids produced after replication (Petreaca, 2013). In yeast cohesin is a multiprotein complex (structural maintenance chromosome (SMC) proteins) formed by Smc1 and Smc3 that together with Scc1/Mcd1 subunit (also known as kleisin) form a ring which (Marston, 2014). In addition, Scc3 subunit binds to Scc1 completing cohesin (Haering et al., 2002). Finally, Pds5 associate with cohesin stabilising the ring (Kulemzina et al., 2012). The cohesin ring requires Scc2 and Scc4 to be loaded onto chromosomes (Ciosk et al., 2000). It has been proposed that the centromere is a cohesin-loading site, however the chromosomal features/factors recognised by Scc2 and Scc4 for cohesin are still to be defined (Marston, 2014). Loading of cohesin during G₁ phase may involve ATP hydrolysis by the Smc1 and Smc3 ATPase head domain that allow the ring to open and bind to DNA (Marcos-Alcalde et al., 2017). Once bound to chromatin, Eco1 facilitates the establishment of cohesin by Smc3 acetylation (Marston, 2014).

In anaphase the sister chromatids separate. This process requires breakage of sister chromatid cohesin, and it is induced by Aurora B, Cdc5, condensin I and Wapl (cohesin-associated protein) (Gandhi et al., 2006; Lipp et al., 2007; Sumara et al., 2002). Cdc5 plays a role in phosphorylating Scc3 subunit of cohesin. Aurora B induces the dissociation of cohesin throughout the regulation of condensin I binding to chromatid (Lipp et al., 2007). Wapl instead plays a crucial role in removing cohesin (Haarhuis et al., 2013). Indeed, cells lacking Wapl result in reduction of cohesin dissociation (Gandhi et al., 2006).

During anaphase the loss of sister chromatids cohesin is induced by the enzyme separase Esp1 which cleaves Scc1 subunit (Uhlmann et al., 1999). This process is irreversible, and it cannot be re-established until the next cell cycle replication. Improper/ unregulated/ ectopic separase activation, before bi-orientation of chromosomes on the mitotic spindle can lead to segregation errors and aneuploidy (Uhlmann, 2001). Separase activation is regulated by the securin Pds1 (in fission yeast cut2) that inhibits separase before anaphase (Luo and Tong, 2017). During anaphase, the Cdc20-dependent anaphase-promoting complex (APC^{Cdc20}) degrade securin which is crucial for the activation of separase (Qiao et al., 2016). Lastly, the cohesin cleavage result in the separation of the sister chromatids and it is followed by the pulling forces applied by the spindle poles which segregate the chromosome in the two poles of the cells (Malumbres, 2015).

The last step for a complete cell division is the mitotic exit after successful chromosome segregation followed by cytokinesis. For this, in this section *S. cerevisiae*'s MEN pathway is described. In budding yeast, the exit from mitosis and cytokinesis activation is regulated by mitotic exit network (MEN) which is represented by GTPase kinase cascade (Bettignies and Johnston, 2003). The MEN in *C. albicans* has been investigated, however, deletion of *S. cerevisiae* MEN' s components such as Tem1, Dbf2 and Cdc14 have shown different phenotypes suggesting different features for *C. albicans* (Bates, 2018b; Clemente-Blanco et al., 2006; González-Novo et al., 2009; Milne et al., 2014). The mitotic exit process requires inactivation of Cdk1 and dephosphorylation of its substrate. This GTPase cascade begins with Tem1 which signals via the kinase Cdc15 which follows the activation of Dbf2 and Dbf20. These two kinases together with the coactivator Mob1 release Cdc14 from the nucleolus. Cdc14 inactivates Cdk1 leading to cyclin destruction. Dbf2 phosphorylates the cytokinesis machinery activating cytokinesis process (Hotz and Barral, 2014; Milne et al., 2014).

In *C. albicans*, Tem1 and Dbf2 are essential components for the MEN pathway, regulating filaments formation and spindle organisation in addition to signalling for ring contraction, respectively (González-Novo et al., 2009;

Milne et al., 2014). In contrast, Cdc14 is not essential, and it interacts with the RAM pathways (Clemente-Blanco et al., 2006). On the other hand, Cdc15 showed to be essential for mitotic exit and cytokinesis. Cells lacking *CDC15* exhibiting filaments formation that emerged from large budded cells. In addition, the filaments formed in *cdc15ΔΔ* mutants lose viability and arrest the cells with hyper-extended spindle which suggest the essential role of Cdc15 in signalling for the mitotic exit and cytokinesis (Bates, 2018b).

In fission yeast, MEN is replaced with septation initiation network (SIN) which is represented by a similar cascade to MEN. SIN regulates initiation of cytokinesis at the end of anaphase and cytokinesis occurs by constriction of actomyosin ring and the formation of septum (McCollum and Gould, 2001).

1.2.3 Chromosome segregation defects

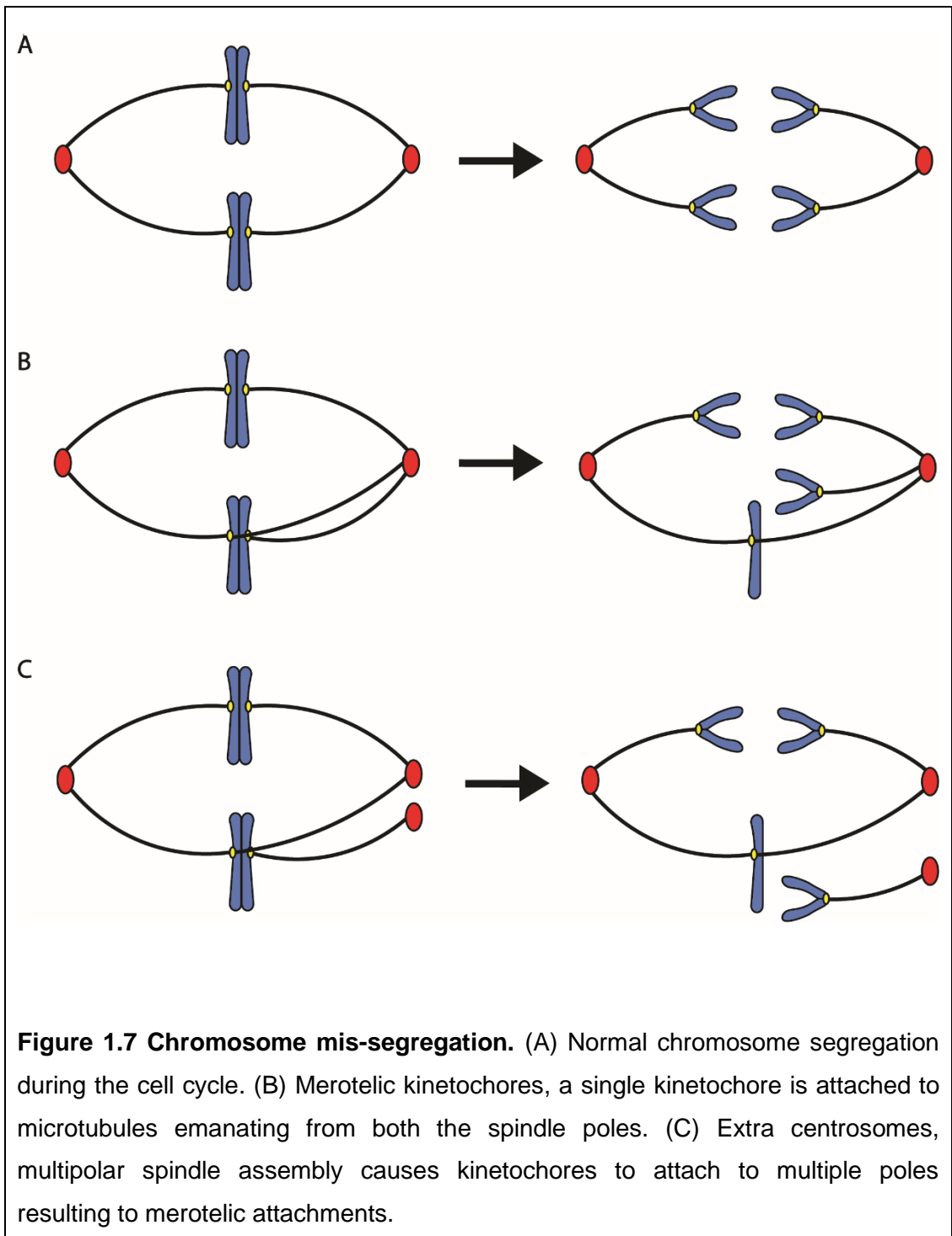
Despite the presence of multiple surveillance mechanisms, errors leading to an imbalanced chromosome segregation can occur. During mitosis different cellular defects can lead to chromosome mis-segregation giving rise to whole chromosome aneuploidy and genomic imbalance. These cellular defects include: (i) aberrant mitotic spindle, mispositioning, and checkpoints (ii) merotelic kinetochores, (iii) supernumerary centrosomes (Ganem and Pellman, 2012).

(i) *aberrant mitotic spindle, mispositioning, and checkpoints.* The formation of a proper mitotic spindle is crucial for chromosome segregation. In particular, defects in the mitotic spindle or chromosome attachment lead to the activation of the spindle checkpoint (Chen et al., 1999). In budding and fission yeast, mutations in *MAD* and *BUB* genes (components of the spindle checkpoints), leads to the increase of the chromosome mis-segregation rate even in the presence of proper mitotic spindle. In addition, Mad and Bub might regulate the transition from metaphase to anaphase during cell cycle (Chen et al., 1999; Hoyt et al., 1991; Li and Murray, 1991; Vanoosthuysen et al., 2004) During the interphase of the cell cycle, it is important that the

mitotic spindle is aligned with the bud neck formed in the constriction between the mother and daughter cell (Merlini and Piatti, 2011). Mutations in *KAR9* and *BIM1* genes, encoding for Karyogamy protein (Kar9) and Bim1, respectively, lead to mispositioning of the spindle randomly in the cell (Miller and Rose, 1998; Schwartz et al., 1997). However, the action dynein and its cofactors Bik1 and Kip2, can correct the misposition of the spindle (Carvalho et al., 2004; Grava et al., 2006). However, double deletion of genes encoding for dynein and Kar9 lead to abnormal nuclear segregation which is lethal for yeast cells (Grava et al., 2006; Miller and Rose, 1998).

(ii) *Merotelic kinetochores*. The proper attachment of the kinetochores to the microtubules emanating from the opposite spindle poles is crucial for a correct chromosome segregation. However, merotelic kinetochores attachment can occur and it leads to a single kinetochore attached to microtubules emanating from both the spindle poles. This phenomenon emerges in the early stage of mitosis, and it is corrected by Aurora B which directly modulates the kinetochore-microtubule attachments (Gregan et al., 2011). On the contrary, if it persists it results in the merotelic chromosome lagging in the anaphase (figure 1.7 B) (Compton, 2011; Gregan et al., 2011). The merotelic chromosome have been associated with chromosomal instability leading to cancer for humans (Cimini, 2008).

(iii) *Supernumerary centrosomes*. Another factor which is associated with chromosome instability and cancer is the presence of extra centrosomes. The supernumerary centrosomes lead to multipolar spindle assembly which cause kinetochores attachments to multiple poles leading to merotelic attachments (figure 1.7 C). This is followed by chromosome mis-segregation and aneuploidy (Compton, 2011; Ganem et al., 2009).



1.2.4 SUMOylation and de-SUMOylation mitotic targets

SUMOylation is one type of post-translational modifications (PTMs). PTMs are covalent modifications of proteins by proteolytic cleavage followed by the addition of modifying group. They mainly consist of methylation, phosphorylation, acetylation, ubiquitination, SUMOylation, glycosylation, and ADP-ribosylation (Ramazi et al., 2020). PTMs play a crucial role in numerous biological processes by affecting the structure and dynamics of proteins. PTMs can be involved in signal transduction, gene expression regulation and gene activation, DNA repair and cell cycle control (Ramazi and Zahiri, 2021). In this section, SUMOylation and its role in chromosome segregation will be described in further detail.

The small ubiquitin-like modifier (SUMO) proteins are highly conserved in eukaryotes. Humans have four genes which encode for the four SUMO proteins: SUMO 1, 2, 3 and 4; while *S. cerevisiae*, *C. albicans* and *S. pombe* have only one gene named *SMT3* in *S. cerevisiae* and *C. albicans* and *PMT3* in *S. pombe*. (Ryu et al., 2020; Sahu et al., 2020). Despite this, in *S. cerevisiae* *SMT3* gene is essential, in *C. albicans* and *S. pombe* disruption in *SMT3* does not result in lethality (Johnson and Hochstrasser, 1997; Michelle D Leach et al., 2011; Tanaka et al., 1999a).

In the SUMOylation pathway, SUMO is linked to its substrate via an isopeptide bond between the C-terminal carboxyl group of SUMO and the ϵ -amino group of the lysine residue on the substrate proteins (Johnson, 2004a). More specifically, SUMOylation occurs on the lysine residues situated in the consensus motif ψ KxE, where ψ represent any large hydrophobic residue, K represent lysine, x any amino acid and E is glutamic acid (Sampson et al., 2001; Yang et al., 2006).

In yeast protein SUMOylation is catalysed by the heterodimeric E1 activating enzyme consisting of Aos1 and Uba2 (Fub2 in *S. pombe*), the E2 conjugating enzyme Ubc9, and the E3 ligases Siz1, Mms21m Cst9, and Wos1 (Pli1 correspond to E3 ligase in *S. pombe*). Of these components, Smt3, Aos1, Uba2, Ubc9 and Mms21 are not considered essential for viability (Sahu et al., 2020). In *C. albicans*, localisation of Smt3p, for the

yeast form, has been reported at the bud neck, instead Smt3p is localised at the septation site in hyphae forms (Martin and Konopka, 2004).

In *C. albicans*, *SMT3* deletion results in slower growth and sensitivity to different stress conditions such as temperature, oxidative stress and cell wall stress and defects in nuclear and cell segregation. In addition, *smt3ΔΔ* cells exhibit heterogeneous population of elongated and pseudohyphae cells (Michelle D. Leach et al., 2011). The SUMO ligases deletion, lead to hyphal formation and increases virulence (Islam et al., 2019). Although these mutants exhibit sensitivity to different stresses, this might suggest a potential role in the response to stress conditions for SUMO (Gupta et al., 2020).

SUMOylation is characterised by enzymes cascade that can be summarised in five main steps as showed in figure 1.8. First step, SUMO-specific proteases act on freshly synthesised SUMO, generating a mature SUMO with C-terminal carboxyl GG motif exposed. Secondly, SUMO-activating enzyme (E1) ATP-dependent, activates the C-terminus of SUMO inducing adenylation of the SUMO C-terminal followed by bond formation between the thiol group of cysteine in the E1 enzyme and the C-terminal glycine of SUMO protein. Thirdly, the E1 enzyme transfer the SUMO moiety to a SUMO-conjugating enzyme (E2) through the thioester linkage. Fourthly, the SUMO ligase (E3) mediates the transfer of SUMO to a lysine side chain(s) of a substrate protein. Lastly, the SUMO-specific protease cleaves the isopeptide bond between SUMO and the target protein, generating an unSUMOylated target protein and a free SUMO (Johnson, 2004a; Ryu et al., 2020; Sahu et al., 2020). In figure 1.8 there is a schematic representation of SUMOylation process.

As mentioned above, SUMOylation is reversed by specific proteases of the Ulp family which cleave SUMO at the C terminus (Johnson, 2004a). There are nine SUMO proteases in humans, two in *S. cerevisiae* and *S. pombe*, Ulp1 and Ulp2 (Ryu et al., 2020) and three in *C. albicans* Ulp1, Ulp2 and Ulp3. The two deSUMOylating enzymes have different functions and localization. Ulp1 is localised in the nuclear pore complex instead Ulp2 is

localised to the nucleus (Jongjitwimol et al., 2014a; Li and Hochstrasser, 2000). In addition, Ulp1 and Ulp2 have different substrate specificities.

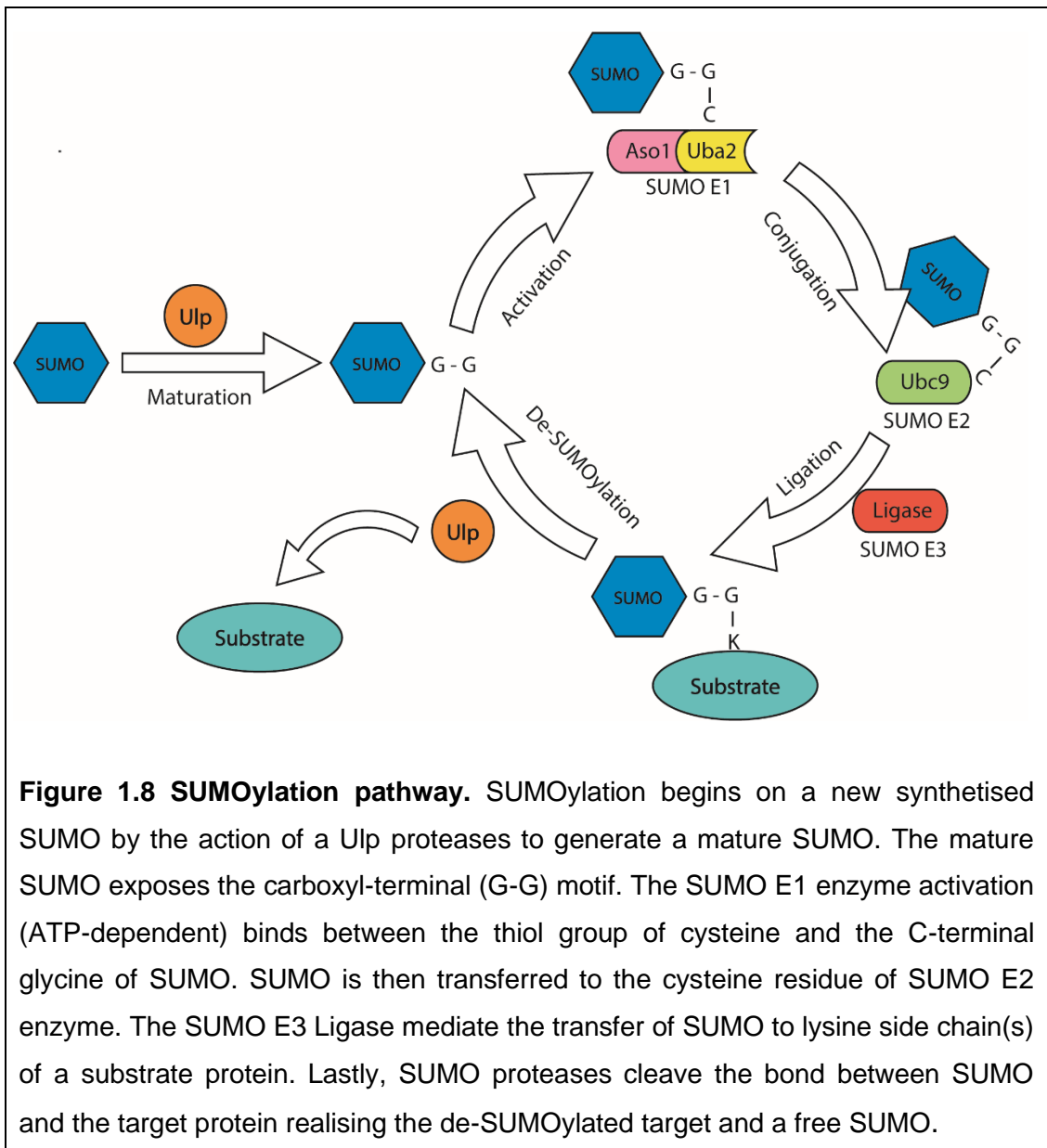


Figure 1.8 SUMOylation pathway. SUMOylation begins on a new synthesised SUMO by the action of a Ulp proteases to generate a mature SUMO. The mature SUMO exposes the carboxyl-terminal (G-G) motif. The SUMO E1 enzyme activation (ATP-dependent) binds between the thiol group of cysteine and the C-terminal glycine of SUMO. SUMO is then transferred to the cysteine residue of SUMO E2 enzyme. The SUMO E3 Ligase mediate the transfer of SUMO to lysine side chain(s) of a substrate protein. Lastly, SUMO proteases cleave the bond between SUMO and the target protein realising the de-SUMOylated target and a free SUMO.

In *C. albicans*, little is known about the Ulp family. From this study, it can be anticipated that *ULP1* deletion does not compromise cell growth and cell morphology. In addition, it does not show sensitivity to stress conditions. On the contrary, cells lacking *ULP2* exhibit slower growth, pseudohyphae cells, chromosome segregation defects and hypersensitivity to different stress agents. *ULP3* deletion is lethal.

In *S. cerevisiae*, *ulp1ΔΔ* cells are non-viable while *ulp2ΔΔ* cells show abnormal phenotypes such as slower growth, sensitivity to stress and high temperature, spindle defects, and aneuploidy (Li and Hochstrasser, 2000). During mitosis, cells lacking *ULP2* exhibit higher frequency of precocious centromere separation and defect in cohesion maintenance (Bachant et al., 2002), hypersensitivity to DNA damage and chromosome segregation defects (Schwienhorst et al., 2000).

In *S. pombe*, *ULP1* mutants exhibit growth defects with elongated and irregular morphologies. In addition to nuclear abnormalities and multiple septation (Taylor et al., 2002). Deletion in *ULP2* leads to growth defects and sensitivity to different stresses (Jongjitwimol et al., 2014b).

The mechanism of action of SUMO consists of altering the substrate binding interactions with the other macromolecules. To date, there are three models of this mechanism of action. The first mechanism hypothesises that the linked SUMO itself might interact with other proteins. The second mechanism of action theorises that both SUMO and the substrate are the determinants of the interactions surface. The third model suggests that SUMO can alter the conformation of the substrate by exposing or masking the binding sites of the modified protein (Johnson, 2004b). The molecular consequences of SUMOylation depends on the specific target proteins and it appears to be very diverse, influencing different aspects of the target protein within the cell, including activity, localisation, and stability (Geiss-Friedlander and Melchior, 2007). Despite this, the mode of action is not fully understood, in yeast, SUMOylated PCNA leads to the recruitment of the DNA helicase Srs2 to the site replication forks (Geiss-Friedlander and Melchior, 2007; Papouli et al., 2005). During replication, the recruitment of Srs2 by PCNA prevents unscheduled recombination events by preventing ubiquitination at the specific lysine residues. This is an independent regulated event and it depends on the different upstream signals coming from the DNA damage and the specific cell cycle phase (Geiss-Friedlander and Melchior, 2007). In many cases, the regulation of SUMOylation takes place at the level of the target itself and it can include other post-translational modifications. For example, phosphorylation can act as a negative regulator for SUMOylation

by masking the SUMO-acceptor site. The localisation of certain SUMO enzymes can be modulated by environmental stimuli. During most of the cell cycle, the E3 ligase Siz1 is localised in the nucleus. However, in G₂/M phase it translocates to the bud neck where it sumoylates septins (Geiss-Friedlander and Melchior, 2007; Johnson and Gupta, 2001).

SUMOylation mitotic targets: SUMO conjugation and deconjugation are crucial processes for mitosis and chromosome segregation (Wan et al., 2012). The first evidence of SUMOylation and deSUMOylation's role in centromere and kinetochore were given by the overexpression of SUMO (Smt3) or SUMO protease (Ulp2) which suppresses the temperature sensitivity of *MIF2* (CENP-C in human) mutation (Wan et al., 2012). Little is known about SUMOylation in *C. albicans*. For this, findings in *S. cerevisiae* are reported in this section.

During mitosis, the APC complex is responsible for the degradation of B type cyclins. SAC regulates and monitors the spindle formation and inhibits APC prior to correct alignment of all the chromosomes (Dasso, 2008). It was shown that the APC complex was inactivated in cells lacking *SMT3* leading to mitotic arrest. The same process happens for *UBC9* deletion cells (Dieckhoff et al., 2004). In addition, *uba2ΔΔ* results in hypersensitivity to microtubule drugs and mitotic arrest (Dasso, 2008; Schwienhorst et al., 2000). In fission yeast, *pmt3Δ* cells exhibit slower growth and *cut* phenotype (Tanaka et al., 1999b). In addition, mutations in *AOS1* and *UBC9* result in chromosome segregation errors (al-Khodairy et al., 1995; Shayeghi et al., 1997).

There are different SUMOylation mitotic targets associated with centromere, kinetochore which in turn are linked with chromosome segregation:

(i) *Kinetochore:* In the budding yeast *S. cerevisiae*, kinetochore proteins which are de-SUMOylated by Ulp2 are Ndc10, Cep3 and Bir1. These proteins mediate the attachment of chromosomes to spindle

microtubules substrates. Mutations in the lysine residues in the consensus motif of these proteins results in chromosome instability, mis-localisation from mitotic spindle, and defective anaphase spindles (Montpetit et al., 2006). The kinetochore protein Ctf3 shows to be a binding site for the de-sumoylase Ulp2. Indeed, Ctf3 alteration which unable ulp2 activity result in accumulation of sumoylated inner kinetochore proteins and chromosome segregation defects (Quan et al., 2021).

(ii) *Cohesin and Condensin*: Cohesin is crucial for chromosome segregation, for this it is controlled by PTMs. In particular, SUMOylation plays an important role for the sister chromatid cohesion. During DNA replication, Smc1, Pds5 and Scc1 have shown SUMOylation peak, confirming that cohesin subunits become targets for SUMOylation (Almedawar et al., 2012).

To form cohesin, Smc1 and Smc3 proteins associate with Scc1 and Scc3. The proteins Smc1, Smc3 and Scc1 were identified as SUMO targets (Dasso, 2008). The Smc subunits need an ATP binding and hydrolysis cycle by the nucleotide binding domain during cohesin loading and establishment. Smc1 mutation abolish ATP binding and interaction with Scc1 subunit which interfere with sumoylation (Almedawar et al., 2012).

Pds5 protein represent another target of Ulp2. During prophase, Smc proteins and kleisin subunits form the cohesin ring (Marston, 2014). The Pds5 protein associates with cohesin stabilising and modulating its binding to the chromosomes (Kulemzina et al., 2012). Pds5 is SUMOylated in a cell cycle manner with SUMOylation increasing during mitosis. Ulp2 overexpression suppress the precocious dissociation of cohesin in Pds5 mutants which leads to a sister chromatid separation similar to wild type cells. The double mutant for Pds5 and Ulp2 instead is lethal or very sick. This might reinforce the concept of Pds5 interaction with cohesin and suggest the important role of SUMOylation on Pds5 in the disruption of this interaction and promote the release of cohesin and sister chromatid separation (Dasso, 2008; Stead et al., 2003).

Some of the Condensin complex subunit Smc4, Ycs4, Brn1 are considered potential SUMOylation targets (Dasso, 2008). Currently, Ycs4 has demonstrated to be sumoylated before mitosis with higher sumoylated forms during anaphase (D'Amours et al., 2004).

Topoisomerase II α (Topo II α) is one of the SUMO targets. This isomerase is required for mitotic chromosome separation, its role is indeed to resolve the catenation of centromeric DNA (Porter and Farr, 2004). It was seen by (Bachant et al., 2002) that in *ulp2 $\Delta\Delta$* strain, the Topo II is mis-regulated with accumulation of its SUMOylated forms. In addition, *ulp2 $\Delta\Delta$* cells result in delayed metaphase and centromeric cohesion defects. This might suggest the specific Topo II deSUMOylation modification by *ulp2* is responsible for the regulation of centromeric cohesion (Bachant et al., 2002).

Great advances have been made in identifying the SUMOylation mitotic targets. However, links and targets in *C. albicans* remain uncovered.

1.3 Antifungal drugs

Antifungal drugs are used to fight fungal infections especially in immunosuppressed and post-transplantation patients (Low and Rotstein, 2011). Antifungal drugs can be fungistatic or fungicidal. As definition, fungistatic drugs inhibit growth of fungi, while fungicidal drugs kill the fungal pathogen (Graybill et al., 1997). Currently, there are four classes of antifungal drugs with different modes of action, polyenes, azole, allaylamines and echinocandins.

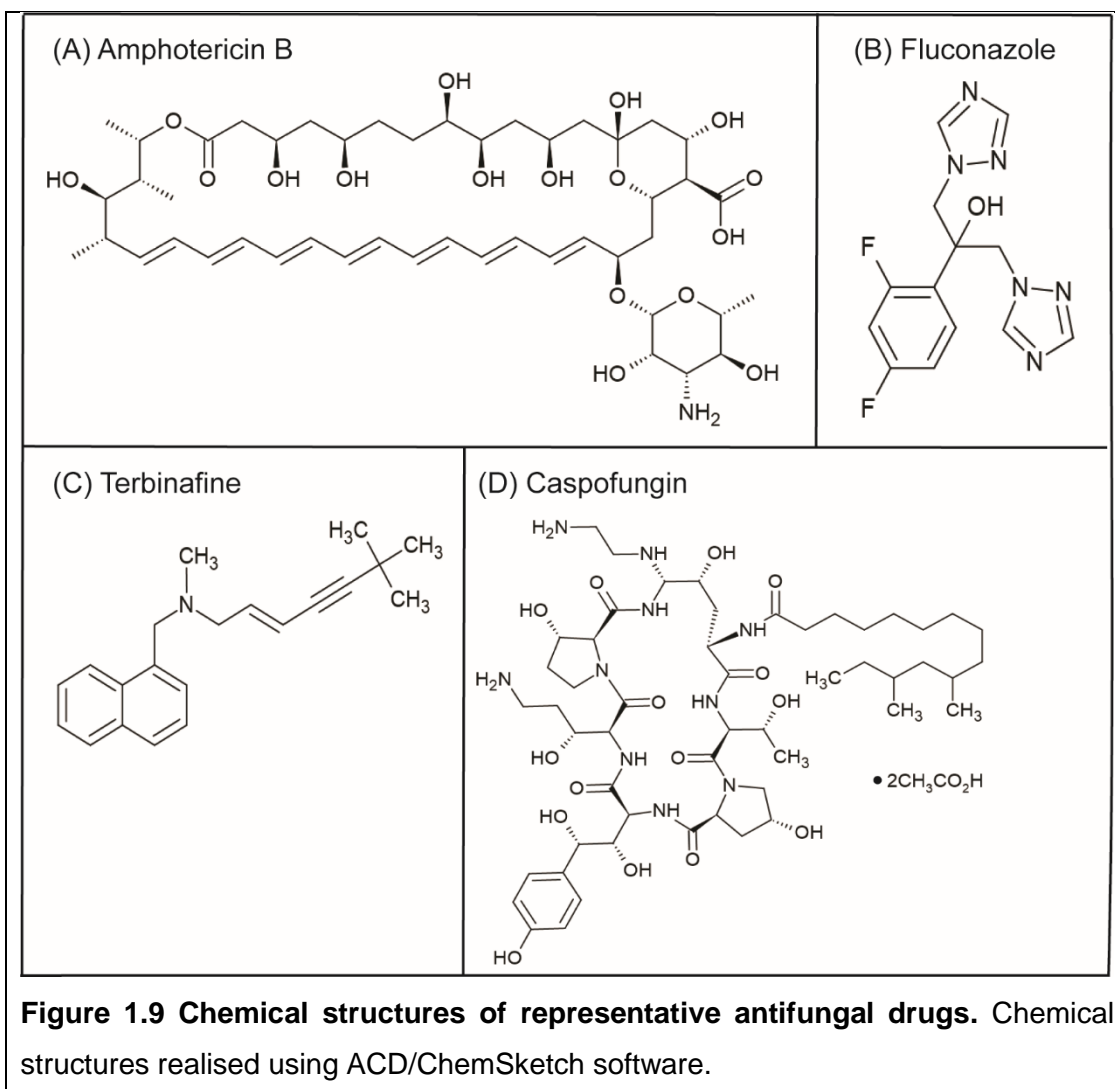
Polyene: This class of antifungal drug acts by binding ergosterol compromising cell integrity by increasing the membrane permeability which leads to cell death (Brajtburg et al., 1990). The only systemic polyene used in clinic is Amphotericin B (figure 1.9 A). However, since its higher affinity for ergosterol compared to its functional analog cholesterol in mammalian cells, Amphotericin B is less toxic for humans. Regardless, it can cause acute and chronic side effects known as nephrotoxicity (Georgopapadakou, 1998).

Azole: This class of antifungal drugs are first in line for *Candida* infections. Azoles are fungistatic and include imidazoles (such as ketoconazole and miconazole) and triazoles (fluconazole, itraconazole and voriconazole). Fluconazole (figure 1.9 B) is the most used azole drug in the clinic (Cowen et al., 2002). Azoles antifungal activity inhibit cytochrome P-450-dependent-14 α -sterol demethylase (encoded by *ERG11*). This enzyme is involved in the conversion of lanosterol to ergosterol. More specifically, to inhibit the ergosterol biosynthesis pathway, the free nitrogen atom of azole ring binds to an iron atom within the heme group of the enzyme. This does not allow the activation of oxygen and the demethylation of lanosterol leading to the inhibition of ergosterol synthesis (Berkow and Lockhart, 2017). The inhibition of 14 α -demethylase leads to the depletion of ergosterol and accumulation of unusual sterols (14 α -methylated sterols) (François et al., 2006; Ghannoum and Rice, 1999). This results in altered plasma membrane with consequent compromised permeability and fluidity which leads to cell growth arrest. Azole's efficacy is owed to its precise nature of interaction with each kind of P-450 lanosterol 14 α -demethylase which amplifies the inhibitory effect in different fungal species. However, the active site conformations of lanosterol can vary between fungal species and mammalian P-450 lanosterol 14 α -demethylase (involved in cholesterol biosynthesis). This links to the inclination of the wide use of azoles antifungal drugs in the clinic (François et al., 2006).

Allaylamines: this class of antifungal drug acts by interfering with ergosterol biosynthesis by inhibiting the enzyme squalene epoxidase. This enzyme interferes with ergosterol biosynthesis pathway leading to depletion of ergosterol and accumulation of toxic sterols (Cowen et al., 2002; Wellehan et al., 2016). The allaylamines are fungicidal, however they have limited use in clinic due to poor pharmacokinetics. Currently, Terbinafine (figure 1.9 C) is the only allaylamines antifungal used in the clinic (Cowen et al., 2002).

Echinocandins: This class of antifungal drug have a peculiar mechanism of action, echinocandins inhibits the β -(1,3)-D-glucan synthase. This enzyme is an essential component of the cell wall integrity, therefore blocking its synthesis compromises the cell wall integrity. The echinocandins

are fungistatic against *Aspergillus* species and fungicidal against most *Candida* species. The echinocandins include three antifungal agents: caspofungin (figure 1.9 D), micafungin, and anidulafungin (Sucher et al., 2009).



1.3.1 Antifungal drug resistance

Antifungal drug resistance has significantly increased in the last decade. Since 1970, the death rate caused by candidiasis has escalated drastically. This can be associated with changes in medical practice and widespread use of immunosuppressive and chemo therapies, in addition to

indiscriminate use of broad-spectrum antibacterial agents and indwelling intravenous devices (Ghannoum and Rice, 1999).

For 30 years, amphotericin B was considered the only drug available for fungal infections (Ghannoum and Rice, 1999). However, amphotericin B can cause nephrotoxicity as a side effect, for this therapy is limited (Georgopapadakou, 1998). The new discovery of azole agents, imidazoles and triazoles were widely used as a result of their ability to treat local fungal infections safely and effectively (Ghannoum and Rice, 1999). In particular, fluconazole has been extensively used to treat patients with systemic fungal infections. Despite the effectiveness of azole agents, limitation for these antifungal drugs occur in treatment against *Aspergillus* species and against *Candida krusei* and *Candida glabrata* (François et al., 2006).

1.3.2 Fluconazole resistance in *C. albicans*

Fluconazole resistance in *C. albicans* has been widely investigated. Several mechanisms have been associated with genes of the ergosterol biosynthesis pathways but also drug transporters, loss of heterozygosity and aneuploidy (Berkow and Lockhart, 2017).

Drug targets alteration: Overexpression of *ERG11* in many *C. albicans* clinical isolates has been reported (Feng et al., 2017; Rosana et al., 2015). In some cases, the level of overexpression is minimal, this compromises the valuation of the direct impact of this overexpression on the resistant phenotype (Monroy-Pérez et al., 2016; Morais Vasconcelos Oliveira et al., 2021). In addition, strains exhibited *UPC2* overexpression, Upc2p is a zinc cluster transcription factor induced upon ergosterol depletion (Berkow and Lockhart, 2017). It positively regulates the expression of *ERG* genes in ergosterol synthesis (MacPherson et al., 2005). Mutation in *UPC2* lead to gain-of-function (GOF) which contributes to increase *ERG11* expression and consequently decreases the susceptibility to fluconazole resulting in fluconazole resistance (Flowers et al., 2012).

Mutation in *ERG11* coding region can lead to amino acid substitutions changing the protein structure. In this way the fluconazole loses its affinity reducing the binding which results in drug susceptibility (Berkow and Lockhart, 2017; Sanglard et al., 1998).

In addition to *ERG11*, the *ERG3* gene plays a critical role for the pathogenesis and resistance to fluconazole treatment during oral mucosal infections (Zhou et al., 2018). *ERG3* encode for sterol $\Delta^{5,6}$ -desaturase which catalyses the formation of methylated sterols in the presence of azole agents (Sanglard et al., 2003). The inactivation of this enzyme allows it to bypass the toxic production of methylated sterols and therefore allows the cell to gain polyenes and azoles resistance (Berkow and Lockhart, 2017; Kelly et al., 1997; Martel et al., 2010; Sanglard et al., 2003).

Drug transporters: In *C. albicans* there are two classes, the ABC proteins, and the MFS pumps. These pumps are located in the plasma membrane. The ABC proteins are primary transporters ATP dependent, the MFS pumps are secondary transporters which use the proton-motive force across the plasma membrane. The ABC transporters comprise a multigene family including *CDR1* and *CDR2* genes (Cannon et al., 2009). Among the MFS family, the *MDR1* gene is shown to be involved in drug resistance. Strains with deletion of the upper mentioned genes showed hyper susceptibility to fluconazole (Ramage et al., 2002). Upregulation of *CDR1* and *CDR2* genes was observed in fluconazole-resistant isolates (Chen et al., 2010). The *CDR1* and *CDR2* upregulation lead in GOF mutations in the transcriptional activator *TAC1* (Coste et al., 2004). In *C. albicans*, 17 different point mutations have been identified in clinical isolates and are likely to be linked to *TAC1* GOF mutations (Coste et al., 2009). Regarding the MFS class, only *MDR1* has been associated with azole resistance in *C. albicans* clinical isolates. *MRR1*, a multidrug resistance regulator, has been identified as the central regulator of *MDR1*. Points mutations in the *MRR1* regulator (leading to GOF) induce constitutive overexpression of *MDR1* efflux pump and consequently multidrug resistance (Morschhäuser et al., 2007).

Aneuploidy and loss of heterozygosity. In *C. albicans* it was reported the formation of an isochromosome 5 and its association with fluconazole resistance. The increased resistance can be associated with the duplication of the segment with additional copies of *ERG11*, and *TAC1* (Selmecki et al., 2008). See section 1.4.4.

Loss of heterozygosity (LOH) is involved in the fluconazole resistance. Point mutations arise in the heterozygous state and then evolve to homozygosity. Mainly the genes implicated are *ERG11*, *TAC1*, and *MRR1* (Berkow and Lockhart, 2017; Alix Coste et al., 2007). See section 1.4.4.

1.4 Genome instability

Eukaryotic cells have developed specific features to preserve the genome which include checkpoints to supervise DNA integrity, in specific coordinate pathways of DNA replication and repair, and monitor the correct cell-cycle progression and chromosome segregation. Indeed, genome stability is crucial to preserve and accurately transmit the genetic material from generation to generation. In contrast, genome instability can result in a wide-ranging of mutations frequency which include inherited or acquired defects in DNA repair, DNA replication, cell cycle propagation or chromosome segregation. These alterations of the genomic materials depending on the mechanism can accumulate in the DNA at different levels, such as mutations, chromosomal gain/losses, chromosomal rearrangements, copy number variation (CNV) or LOH (Aguilera and García-Muse, 2013). More specifically, mutation generated during events of genome instability can include point mutations within a gene in which a change in single nucleotide alters the DNA sequence. This can be the result of mistakes during the DNA replication or defective DNA repair pathways (Aguilera and García-Muse, 2013; Zeman and Cimprich, 2014). In addition, this kind of mutation can be induced exogenously after exposure to ultraviolet radiation (UV) (Budden and Bowden, 2013). Conversely, gross chromosomal rearrangements (GCRs) and chromosome number variation can be caused by the disruption

of mitotic checkpoint or chromosome segregation apparatus. Altogether, these instabilities can be associated with DNA breaks, single stranded DNA gaps generated by stalling/collapsed replication forks. These can also be caused by secondary DNA structures, or defect from the replication machinery, S-phase checkpoints, or double stranded break repair machinery. Depending on the type of damage, DNA can be repaired by specific DNA repair pathways (further described in section 1.5) (Aguilera and Gómez-González, 2008).

Genome instability can be enhanced in specific DNA regions which contain gaps and breaks, these are known as fragile sites. They can be of two types: common which represent the 95% of all known fragile sites, and rare which account for the remaining 5%. They are associated with hotspots for translocations, gene amplifications, integration of exogenous DNA and other DNA rearrangements (Aguilera and Gómez-González, 2008). They are associated with trinucleotide repeats which include GC-rich repeats or long AT-rich nucleotide repeats (Durkin and Glover, 2007). A common aspect to the different types of DNA repeats is to form unusual secondary structures such as hairpins or DNA triplexes (Mitas et al., 1995; Wells, 1996). These secondary structures might be formed on the lagging strand during replication block. This is supported by different studies showing defects in replication factors as DNA polymerases, DNA ligase or PCNA, and defect in S-phase checkpoints as Mec1, Rad53, Rad17 or Rad24 lead to high instability of repetitive DNA (Callahan et al., 2003; Lahiri et al., 2004; Schweitzer and Livingston, 1999). Consequently, fragile sites are exposed when replication is stalled leading to formation of DSBs and rearrangements (Aguilera and Gómez-González, 2008).

Another source of genome instability which leads to the formation of breaks and secondary structures is transcription. This phenomenon is caused mainly by the exposure of ssDNA during transcription. In particular, the single stranded DNA (ssDNA) can form R loops with the nascent mRNA and create RNA-DNA hybrid. In addition, the ssDNA can form stem-loops which interfere with DNA replication (Aguilera and Gómez-González, 2008).

Cells, in addition to DNA repair systems, have evolved genes guarding the genome stability. These are known as suppressor genes or proteins. It was shown that mutations in specific endonuclease, helicase, and nucleosome assembly factors, can increase recombination replication defects leading to DNA breaks (Aguilera and Gómez-González, 2008). Additionally, replication failure can be the most frequent product of DSB. This is seen especially when replication mutants exhibit growth defects enhanced by the presence of mutation in *RAD52*, an homologous recombination (HR) substrate (Chen et al., 1998; Tishkoff et al., 1997). Studies have screened and identified non-essential genes which can prevent the formation of GCRs. However, mutations in these genes can cause GCRs only when combined with mutation in other genes (Myung et al., 2001; CD Putnam et al., 2009; Putnam et al., 2012).

1.4.1 Replication stress

During replication the opened genomic DNA can lead to genome instability, and this is mainly caused by the increased ssDNA at stressed replication forks which makes it vulnerable to DNA breaks. To avoid this, cells have evolved checkpoints response as DNA surveillance, the S-phase checkpoints are essential to preserve genome integrity and they are the response to replication fork (RF) stalling/collapse (Aguilera and Gómez-González, 2008).

There are different DNA breaks generated by replication stress. To start with, the formation of ssDNA nick can suspend the synthesis of the newly formed strand which might lead to DSBs. Another DNA break can be caused by transient pausing or longer delay of the replication forks leaving the leading-strand and the lagging-strand separated (Aguilera and García-Muse, 2013; Pagès and Fuchs, 2003). This can lead to DSB in one of the nascent double stranded DNAs (dsDNAs) or it can lead to fork regression inducing a Holliday junction also referred as “chicken-foot” structure (Aguilera and García-Muse, 2013; Heyer, 2004). Lastly, the RF can block only one of the DNA strands without stopping the fork progression. If the RF blocks the

lagging-strand synthesis, this causes ssDNA gap or DSB (Aguilera and Gómez-González, 2008).

Under normal conditions, depending on the type of DNA damage caused by replication stress, different pathways can intervene to repair the damage. These can be break-induced replication pathway (BIR), translesion synthesis (TLS) or HR (section 1.5.3.1).

However, one of the most frequent DNA lesions caused by DNA replication stress is the DNA base damage. Apurinic/apyrimidinic (AP) sites are originated by spontaneous depurination leading to abasic site which can block DNA replication. This form of lesion is potentially highly mutagenic and lethal if not repaired (Boiteux and Guillet, 2004; Ciccia and Elledge, 2010a). DNA base damage can be caused also by exogenous DNA damage agents such as UV radiation or reactive oxygen species (ROS). These can form bulkier DNA lesions which can distort the DNA structure leading to bends obstructing replication (Rastogi et al., 2010a) (section 1.5.1.1).

1.4.2 Chromosomal Instability

Chromosomal instability (CIN) is the event of genome instability in which chromosomes are unstable. CIN lead to either the whole chromosome or parts of chromosomes to be duplicated or deleted. However, the only GCRs able to survive are those which comprises a centromere and two telomeres. In particular, a chromosome that lacks a centromere will not be dragged to either pole at anaphase and consequently it will not be included in the progeny nucleus (Griffiths et al., 2000). CIN events can be classified in two main subclasses: (i) *chromosome structure rearrangements*, (ii) *chromosome copy number variation*. Both these alterations can affect the genes activity and transmission by changing the position, order, or genes number. This can result in alteration of genetic imbalance which can be detrimental (Hartwell et al., 2020).

(i) *Chromosome structure rearrangements* is a type of chromosome abnormality which involve changes in the structure of the native

chromosome. There are four different types of rearrangements: duplication, deletion, inversion, and translocations. These events are caused by DSBs followed by DNA repair that fuses the broken ends, if the two broken ends are re-joined correctly the original chromosome is repaired. However, if the incorrect ends are re-joined, it results in a new chromosome arrangement of genes.

Chromosome duplication is the event in which a part of the chromosome generates an extra copy of that chromosome region. These duplicated regions can be immediately located next to the original one, this case generating a tandem duplication. On the contrary, if the duplicated regions is in another location in the genome, it generates an insertional duplication or displaced duplication (Griffiths et al., 2000; Pierce, 2012).

A chromosome deletion is the loss of a part of the chromosome segment. It can occur within a gene leading to its inactivation, this deletion is known as intragenic deletion. Alternatively, deletions can take place in different genes (multigenic deletions) in which consequences of these deletions are more severe of the intragenic deletion resulting in the disruption of normal gene balance (Griffiths et al., 2000). If the deletion fragment includes the centromere, then the chromosome can not segregate during mitosis or meiosis and it will be lost. The deletion fragment can include essential genes, in this case this alteration is lethal for the cell (Pierce, 2012).

Chromosome inversion is the event in which a segment of a chromosome is detached, flipped of 180 degrees, and reinserted. Inversions can be pericentric if it includes the centromere as part of inversion or paracentric if the inverted fragment does not include the chromosome centromere. If there are no breaks within a gene, inversion can only change the orientation of the gene with only mild effects. However, the altered gene orientation can lead to functional changes due to regulators of gene expression which can be relocated outside the target resulting in abnormal levels of genes products (Pierce, 2012; Pla-Victori, 2020).

Chromosomal translocation is the event when a segment of a chromosome detaches and reattaches to a different non homologous

chromosome. In humans, this type of mutation can have deleterious effects such as cancer or neuropsychiatric disorders (Tabarés-Seisdedos and Rubenstein, 2009). However, translocation can be reciprocal or nonreciprocal. Reciprocal translocation occurs when the segment of chromosome is exchanged between two nonhomologous chromosome avoiding gain/loss of genetic materials. The nonreciprocal translocation arises when a segment of chromosome is transferred to a nonhomologous chromosome without reciprocal exchange of segments (Pierce, 2012).

(ii) *Chromosome copy number variation (CNVs)* is the events in which the number of copies of any DNA sequence, larger than 1000bp, varies from one individual to another. The CNVs can include chromosomal duplication, deletions, inversions, and translocations (Hartwell et al., 2020). CNVs can be generally described as chromosomes gain or loss, this lead the cell nucleus to possess an abnormal number of chromosomes. This phenomenon is known as aneuploidy. Aneuploidy is the result of chromosomal mis-segregation during mitosis and/or meiosis (Griffiths et al., 2000). Yeast strains with higher rate of aneuploidy often have a defect in the SAC, this is due to SAC function which ensures that chromosomes are correctly orientated in the spindle before anaphase. This checkpoint can be activated by two types of kinetochore defects: lack of kinetochore occupation by the microtubules and lack of tension between sister kinetochores (McCulley and Petes, 2010). Furthermore, there are other factors which can cause chromosome mis-segregation such as UV irradiation, exposure to drugs stress, heat shock or physical stress. For example, studies have shown that aneuploidy can confer increased stress and drug resistance in the pathogenic fungus *C. albicans* (Pavelka et al., 2010; Selmecki et al., 2015, 2009).

Aneuploidy and other alteration in gene copy number can lead to differential gene expression levels of the genes that are gained or lost. In the case of genes within duplicated regions, an increased expression level was shown. However, for deletion genes the opposite phenomenon occurs. Overexpression of genes involved in transcription factors and methylation pathway can result in altered expression or in epigenetic changes in

downstream target genes (Kojima and Cimini, 2019). In addition, in aneuploid yeast strain, proteins aggregate formation due to the limited quality-control system are likely to be compromised leading to misfolded proteins accumulation causing proteotoxic stress (Oromendia et al., 2012). Overall, under certain conditions, gene expression levels may provide fitness benefits which can dominate the costs of maintaining the aneuploidy. In particular, adaptation to stress environment, drug resistance, colonisation of hosts and virulence can promote pathogenic taxa evolutionary diversification (Selmecki et al., 2015, 2009; Yona et al., 2012)

1.4.3 Loss of heterozygosity

Loss of heterozygosity (LOH) is the event that affect the loss of one of the two alleles of a diploid by deletion, gene conversion, or chromosome loss (Aguilera and García-Muse, 2013). LOH can uncover genetic variability by exposing the phenotypes associated with recessive alleles. The length of LOH can extent from short LOH tracts formed via gene conversion or double crossover to long LOH tracts which can be formed via single crossover event or by non-reciprocal events such as BIR which generate a region of homozygosity from the recombination site to the telomere (A. Forche et al., 2011). Defects in centromere/kinetochore/mitotic spindle function can lead to whole-chromosome (whole-Chr) LOH resulting in aneuploidy. Compared to their euploid parental strain, most of aneuploid strains grow lesser. However, under stress conditions aneuploid strains exhibit a stronger fitness. For example, in *C. albicans*, LOH events have been observed in strains growing under antifungal stress. In particular, homozygosis of hyperactive alleles of ERG11 and other genes which can provide advantages for drugs (Forche et al., 2011).

1.4.4 Stress induced genome instability in *C. albicans*

C. albicans exhibit extensive genomic diversity, its genome contains a large number of DNA repeats sequence breakpoints, long repeats as TLO, MRS and rDNA which are associated with genome rearrangements. These are sources of genome instability and can provide adaptive phenotypes in presence of stress environments, across different strain background as clinical strains, environmental and experimental evolved isolated (Todd et al., 2019). As mentioned above, *C. albicans* genome is highly plastic labile and it can undergo from small-scale DNA mutations, i.e., single nucleotide polymorphisms (SNPs) and indels, to large-scale genome rearrangements as aneuploidy, GCRs, and LOH. These genetic alterations prevail in the stressed environments such as host physiological conditions, for example: pH, temperature, microbiota environment, oxidative stress, and drugs (Avramovska and Hickman, 2019a; Berman and Hadany, 2012; Forche et al., 2011). Different types of stress condition lead to different type of altered genetic response which is directly correlated to the type of DNA damage induce by the stress condition (Brown et al., 2014). However, the mechanisms that regulate genome instability in *C. albicans* are still to be determined.

C. albicans strains can manifest the formation of whole chromosome and segmental aneuploidy with the acquisition of resistance to azole drugs. More specifically, it was shown by (Selmecki et al., 2006) a gross rearrangement with segmental aneuploidy which has risen to the formation of an isochromosome 5L [i(5L)] after fluconazole exposure. This isochromosome is composed of two identical arms flanking a centromere, it presents increased gene copy numbers of chromosome 5L (Chr5L) which is 2-fold higher than chromosome 5R. The isochromosome 5 formation confers resistance to fluconazole and this does not have fitness cost in untreated cells (Yang et al., 2021). More specifically, two genes on Chr5L actively contribute to Fluconazole resistance: *ERG11*, and *TAC1* (Selmecki et al., 2008). Fluconazole is the most common azole antifungal drug, and it affect the production of ergosterol which is required for cell wall integrity. Fluconazole function targets the ergosterol biosynthetic enzyme lanosterol

demethylase (known as cytochrome P450) which is encoded by *ERG11*. Fluconazole blocks the ergosterol production leading to formation of secondary toxic sterols which impose membrane stress. *TAC1* encode a transcriptor factor that upregulates the expression of two efflux pumps, *CDR1* and *CDR2* located on chromosome 3. The increased copy number aneuploidy of *ERG11* and *TAC1* in the isochromosome 5 allows fluconazole to be pumped out more efficiently (Shapiro et al., 2011). Aneuploidy formation is a flexible mechanism which confer fitness advantages to the cell under stress condition. However, when the stress condition is removed the cell can lose the extra-chromosome (Selmecki et al., 2006).

Temperature stress such as febrile temperature (39°C) can increase the rate of LOH and aneuploidy. This might be caused by a limitation in heat shock protein chaperones and cochaperones (*SGT1*, *STI1* and *CDC37*) the role of which is involved in the assembly of functional kinetochore, spindle pole bodies, centromeres, and mitotic checkpoints (Forche et al., 2011).

1.5 DNA damage and repair

Cells are under constant threat of DNA damage that can change the basic structure of the DNA. The damage can be caused by environmental sources such as chemicals and radiation or it can arise from cellular processes as oxidative stress and breaks from replication fork stalling. DNA damage, if not repaired, can give rise to mutations which can ultimately lead to cell death. However, cells have evolved specific DNA repairs systems and checkpoints which can detect and repair the DNA damage.

1.5.1 Checkpoint pathway

The first response to DNA damage is governed by the DNA damage checkpoint signal-transduction pathways. This is represented by a signalling cascade which begins with the PIKK proteins (Phosphatidylinositide 3-kinase-related kinase) *Mec1* and *Tel1* kinases (respectively, the ATR and

ATM mammalian ortholog) (Ciccia and Elledge, 2010b). Mec1 and Tel1 respond to different types of DNA damages. Mec1 and tel1 are partially redundant, a double mutant *mec1 $\Delta\Delta$ tel1 $\Delta\Delta$* has synergistically higher sensitivity to DNA damaging agents, increased rate of genome rearrangements, and inability to maintain normal telomeres length compared to single mutants (Ciccia and Elledge, 2010b; Morrow et al., 1995; Ritchie et al., 1999; Ritchie and Petes, 2000). During the cell cycles, Mec1 is important in S and G₂ phases, on the contrary Tel1 is crucial for γ -H2AX formation at site of DSBs during the G₁ phase (CD. Putnam et al., 2009).

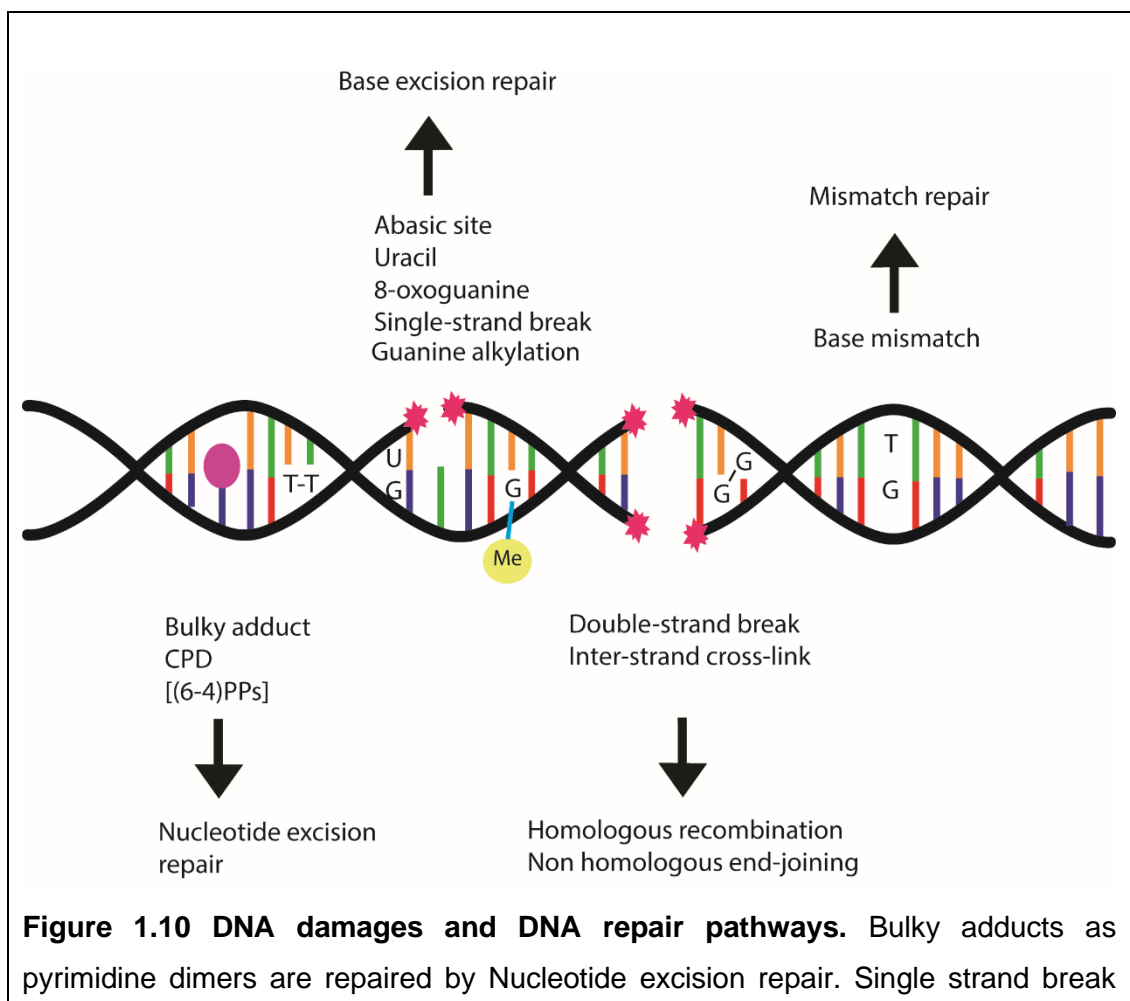
Mec1 is recruited in replication proteins A (RPA)-coated ssDNA, while Tel1 is recruited on blunt-edged DSB ends with short ssDNA tails (Shiotani and Zou, 2009). Mec1 binds to Ddc2, a protein that recognises ssDNA bound by the RPA forming Mec1-Ddc2-RPA complex. After the PCNA-like Ddc1-Mec3-Rad17 complex (homologs of 9-1-1 complex in fission yeast and mammals) is loaded on top of the partial duplex DNA throughout Rad24-Rfc2-5 clamp (CD. Putnam et al., 2009). The colocalization of Ddc1 subunit with Mec1-Ddc2 complex activate the DNA damage response. In addition, another checkpoint component, Dpb11, can initiate the DNA damage response by activating Mec1-Ddc2 complex (Mordes et al., 2008).

Tel1 is recruited to the Mre11-Rad50-Xrs2 complex together with Sae2 endonuclease on the DSB ends which is then processed by Exo1 and Dna2 nucleases together with Sgs1. While the resection takes place, the ssDNA tail is coated with RPA which recruits Ddc1-Mec3-Rad17 complex and Mec1. The initial steps of resections is determinant, in fact the choice of DNA repair pathway depends on the structure of the DNA ends and on the phase of the cell cycle (Symington and Gautier, 2011).

One of the most important roles of the checkpoint response is to stop the cell cycle progression in the presence of DNA damage. The key component for this is Chk1 which inhibits cyclin-dependent kinases (CDKs) preventing the cell cycle to proceed. Chk1 is activated by the PIKK proteins together with Rad53. Chk1 and Rad53 are diffusible proteins and phosphorylation of Rad53 by Mec1 and Tel1 result to Rad53 activation and

subsequent autophosphorylation which multiply the signal (CD. Putnam et al., 2009). In addition to Mec1 and/or Tel1, Rad53 can be activated by Rad9 or Mrc1 by binding to the specific domains of Rad53. More specifically Rad9 is essential for DNA damage, on the contrary Mrc1 is specific for signalling replication stress. Rad53 activates and recruits Dun1 which is important for dNTP synthesis (CD. Putnam et al., 2009). Indeed, the activation of dNTP synthesis facilitates the survival to DNA damage (Chabes et al., 2003).

Depending on the type of DNA damage, different DNA repair pathways take place (figure 1.10). The damage that can be produced in the double helix of DNA can be classified in two main groups: single strand break, where the damage is localise only in one strand of the DNA double helix; and double strand break, where the break arises in both the strands of the DNA duplex.



damage is repaired by Base excision repair. DNA double strand break can be repaired by two pathways: Homologous recombination and non-homologous recombination. Last, base mismatch is repaired by Mismatch repair pathway.

1.5.2 Single strand break

Single strand breaks (SSBs) are characterised by discontinuities in one of the strands of the DNA. It can occur with the loss of a single nucleotide and with a break at site 5'- and or 3' termini of the damaged strand (Caldecott, 2008). Depending on the type of SSBs damages, breaks are repaired by single-strand break repair (SSBR) pathways such as base excision repair (BER) which base alterations are excised; nucleotide excision repair (NER) which replaces pyrimidine dimers and intrastrand crosslinks; mismatch repair (MMR) in which mispaired DNA bases are substituted with correct bases (Ciccia and Elledge, 2010b).

1.5.2.1 Base excision repair (BER)

The base excision repair (BER) pathway is involved in damaged DNA bases or single strand DNA breaks. These lesions can be the result of spontaneous deamination or the outcome from exposure to environmental alkylating agents (D'Andrea, 2015). The lesion is processed by different DNA glycosylases that cleave damaged bases resulting in an apurinic/apyrimidinic (AP) site. This AP site is then a substrate for the AP endonuclease Ape1. The resulting ssDNA is filled by DNA polymerases and finally processed by DNA ligases (D'Andrea, 2015). In yeast, different DNA glycosylases/AP lyases have been categorized such as Ung1, Ogg1, Ntg1, Ntg2, in addition to AP endonuclease Apn1 and Apn2, and monofunctional DNA glycosylase Mag1. There are different types of modified bases which correspond to a different DNA glycosylase (Maclean et al., 2003).

Spontaneous deamination of cytosine results in the introduction of uracil into DNA, this event can occur also during replication which lead to misincorporation of dUMP instead of dTMP (Andersen et al., 2005; Burgers and Klein, 1986). *UNG1* encode for the uracil-DNA glycosylase (UDG) that removes uracil from the DNA (Schormann et al., 2014).

Reactive oxygen species (ROS) can be formed by normal mitochondrial activity; however, it can extensively cause DNA damage. All the four DNA nucleobases are susceptible to oxidative stress, despite that, guanine is the most frequently oxidized nucleotide. More specifically ROS-induced DNA damage introduces an oxo group to the carbon at 8-position of guanine and a hydrogen atom at N7 position to produce 8-oxo-7,8-dihydro-2'-deoxyguanosine (8-oxoG or OG) (Jovanovic and Simic, 2002; Whitaker et al., 2017). The DNA glycosylase encoded by *OGG1* gene, repair the misincorporation of 8-oxoG with adenine during replication (Ba and Boldogh, 2018).

The two DNA glycosylases, Ntg1 and Ntg2, can also recognize and remove oxidative base damage of pyrimidines. In addition, they can repair damages formed by purine which undergo oxidative stress known as formamidopyrimidine (Fapy) (Greenberg, 2012; You et al., 1999). Furthermore, Ntg1 is more effective in removing cytosine photoproducts generated by UV irradiation, while Ntg2 remove only half of the cytosine photoproducts released by Ntg1 (Alseth et al., 1999; Gellon et al., 2001). In *C. albicans* Ntg2 orthologue was not detected and Ntg1 shows strong similarity to both *S. cerevisiae* Ntg1 and Ntg2 (Nth1 and Ntp1 in *S. pombe*). However, it is still unknown if *C. albicans* Ntg1 is functionally related to *S. cerevisiae* Ntg1 or Ntg2 (Legrand et al., 2008).

The DNA glycosylase Mag1 (Mag2 in *S. pombe*) recognises and remove alkylated bases induced by methylating agents such as methyl methanesulfonate (MMS) (Xiao et al., 2001). It was seen that HR is also involved in repairing the damages cause by MMS as this agent is regularly used to induce DSBs. It might be that the DSBs are formed by the replication

fork collapsing when it encounters the MMS-induced SSBs (Lundin et al., 2005a).

After that, the DNA adducts are removed by the specific DNA glycosylase, the empty AP site can be filled in by two BER sub-pathways. The first approach is mediated by AP endonuclease Apn1 and Apn2 which cleaves the phosphodiester bond leading to a 5' deoxyribose (5'-dRP). The DNA polymerase ϵ fills the gap and the endonuclease Rad27 removes the flap containing the 5'-dRP. Lastly, the strand is sealed by Cdc9 DNA ligase (Boiteux and Guillet, 2004). The second approach is mediated by the DNA glycosylases Ntg1 in *C. albicans* (Ntg1 and Ntg2 in *S. cerevisiae*) which cleaves the AP site leading to 3' deoxyribose (3'-dRP). Consequently, the nick can be processed by Apn1/Apn2, or it can be excised by the flap-endonuclease Rad1-Rad10. Finally, the gap is then filled by the DNA polymerase ϵ and sealed by DNA ligase (Boiteux and Guillet, 2004).

1.5.2.2 Nucleotide excision repair

NER is highly conserved, and it is specialised in removal of a wide class of bulky lesions which cause distortion of DNA helix (Prakash and Prakash, 2000) including UV irradiation induced photoproducts (cyclobutene pyrimidine dimers [CPDs] and 6-4 photoproducts [(6-4)PPs]). In addition to photoproducts, NER can recognise environmental mutagens such as cyclopurines and adducts formed by cancer chemotherapeutic drugs (Schärer, 2013).

NER pathway can be divided into two sub-pathways, differing only in the proteins that recognize DNA damage and converging then for repair steps. (i) *global genome NER (GG-NER)* which can operate anywhere in the genome. (ii) *transcription-coupled NER (TC-NER)* which occurs when the damage is situated in the transcribed strand of active genes (Schärer, 2013).

(i) GG-NER: after the recognition of the distortion of the double helix, Rad16, a chromatin remodelling factor, remodels the chromatin around the lesion which allows Rad4 to bind to the damaged site (Yu et al., 2016). After

binding, Rad4 is protected from degradation thank to the direct interaction with Rad23 which also regulate Rad4 stability (Ortolan et al., 2004).

(ii) TC-NER, is triggered by stalled RNA polymerase II (Pol II) which is recognised by Rad26 and followed by recruitment of Rad4-Rad23 complex (Hanawalt and Spivak, 2008; Ortolan et al., 2004).

After these difference in sub-pathways, the following steps are communal to GG-NER and TC-NER. The first step is the formation of a denaturation bubble which is mediated by the transcription factor TFIIH recruited by Rad23. TFIIH contains two DNA helicases Rad3 and Rad25 and two endonucleases Rad1-Rad10 complex and Rad2 (Prakash and Prakash, 2000). The two helicases create the denaturation bubble consisting of approximately 30 nucleotides while the two endonucleases cut the damaged DNA strand. The dissociation of Rad4-Rad23 complex leads to the recruitment of Rad14 and RPA proteins (Guzder et al., 2006). The TFIIH is released, and the gap is filled by Pol ϵ and lastly sealed by DNA ligase (Guzder et al., 1995; Prakash and Prakash, 2000).

1.5.2.3 Mismatch repair (MMR)

The mismatch repair (MMR) pathway is involved in the correction of base-base mispair and insertion/deletion mispair which can be caused by DNA polymerase misincorporation during replication but also by DNA damage due to genotoxic agents. The DNA mismatches are recognised by Msh2-Msh6 heterodimer which recruits Pms1-Mlh1 complex. This complex acts as a DNA endonuclease which nicks the double strand DNA followed by the excision of the incorrect base. Lastly, DNA polymerase resynthesize the excised DNA (Chakraborty and Alani, 2016; Liu et al., 2020).

1.5.3 Double strand break

Double stand break (DSB) represents the most harmful type of damage for cells. DSBs are generated by the simultaneous break of two

complementary strand of DNA helix. DSBs can be caused by fork collapse or by external DNA damaging agents such as ionizing radiation, chemotherapeutic drugs, or chemicals. DSBs can induce mutations and/or cell death. It can also induce chromosomal rearrangements, where in humans this can lead to many kinds of cancers. However, cells have evolved two main pathways for DNA DSB repair systems: homologous recombination (HR) and non-homologous end-joining (NHEJ) (Jackson, 2002). The phase of the cell cycle plays an important role in the choice between HR and NHEJ repair pathway. HR is generally restricted to the S and G₂ phases, this is due to the availability of sister chromatid to use as template. On the contrary NHEJ seems more prevalent during the G₁ phase, however, it can occur throughout the cell cycle (Symington and Gautier, 2011).

1.5.3.1 Homologous recombination

Homologous recombination (HR) repairs DSBs in DNA using the identical or nearly identical genetic information using sister chromatids. It begins removing some of the nucleotides at the broken strand, continues with invasion, displacement and replication (Pierce, 2012).

DSBs are identified by Mre11-Rad50-Xrs2 (MRX) complex and Tel1. The MRX complex's purpose is to start the initial resection of the ends to the initial 5' -3' end (Symington and Gautier, 2011). MRX complex together with the endonuclease Sae2 creates 3' ssDNA tails (Clerici et al., 2005). The ssDNA becomes substrate for Exo1 or Dna2-Sgs1 that extend the resection at the DNA ends while the RPA proteins bind to the ssDNA protecting the strand from degradation (Nimonkar et al., 2011; Paudyal and You, 2016). RPA recruits Ddc1-Mec3-Rad17 complex and Mec1 while the MRX complex-Sae2 dissociate from the damage site (Symington and Gautier, 2011). In addition, RPA recruits Ddc2 and Rad52 which mediate the substitution of RPA proteins with Rad51 recombinase which is stabilised by Rad59 (Chen et al., 2013; Davis and Symington, 2003). The nucleoprotein filament can begin the homology search encompassing the entire genome. Once the homologous sequence is found the strand invasion can begin with the intact donor

template. This phenomenon is known as D-loop formation, and it is the substrate for the new strand DNA synthesis. After the synthesis of a short DNA stretch the new DNA is reannealed and ligated with the broken arm to restore the chromosome (Aylon and Kupiec, 2004).

Overall, repair by HR can be classified in three main sub-pathways: (i) *single strand annealing*, (ii) *gap repair leading to gene conversion*, and (iii) *break-induced repair*.

(i) *Single strand annealing (SSA)* is a type of DSB repair that involves annealing of homologous repeats which flank the DSB leading to deletion rearrangements between the repeats (Bhargava et al., 2016).

(ii) *Gap repair leading to gene conversion (GC)* take place with the formation of double Holliday Junction (dHJ) and it relates to a short patch of DNA synthesis. It is considered the safest pathway for DSBs; however, it can lead to mutation but rarely to genetic rearrangements (Sakofsky et al., 2012).

(iii) *Break-induced repair (BIR)* occurs through the invasion of one broken end into an intact donor chromosome. This pathway take place during replication collapse in S-phase, and it can start a unidirectional replication fork which duplicate the donor template until the end of the chromosome. Furthermore, BIR elongates telomeres in absence of telomerase preserving the chromosome ends (Lydeard et al., 2010). BIR can result in genomic instabilities and various type of chromosome rearrangements if the donor template come from a different chromosome (Sakofsky et al., 2012). There are two main classes of chromosome rearrangements that can be led by BIR: translocation and half-crossover.

Translocation can occur when the BIR initiated invasion take place at non-allelic position of DNA repeat leading to non-reciprocal translocation. This translocation is initiated by DSBs close to repeated sequence which lead to invasion into a homologous sequence located somewhere else in the genome (Sakofsky et al., 2012). An example of translocation is the study conducted by (Lydeard et al., 2007) in which an HO endonuclease creates a DSB next to the *CAN1* gene situated on chromosome V. The DSB shares

homology with a 3' segment of the *CAN1* gene inserted in the chromosome XI. This has led to strand invasion and restore of *CAN1* gene. Furthermore, translocation initiated by BIR can occur at locations of transposons.

Half-crossover (HC) is a type of chromosome rearrangements associated with BIR in which a fusion between donor and recipient chromosome occurs. This fusion lead to the loss of the remaining parts of the participating chromosomes (Sakofsky et al., 2012).

1.5.3.2 Non homologous end-joining

Another mechanism to repair DSBs is the non-homologous end-joining pathway (NHEJ). The term “non-homologous” is due to the mechanism of repair in which the broken ends are directly ligates without a homologous template (Moore and Haber, 1996). For this reason, it is rarely error-free with sequences deletions of various lengths (Jackson, 2002). This pathway is uniquely dependent on two components: Ku complex and DNA ligase IV. More specifically, the DSB is bound and recognised by the Mre11-Rad50-Xrs2 complex followed by the binding of the heterodimer Yku70 and Yku80 (Ku complex). Yku80 and Xrs2 bind Dnl4 and Lif1 respectively, which then recruit the DNA ligase IV (Daley et al., 2005).

1.6 Thesis aims

C. albicans possess a highly labile genome which can tolerate large-scale rearrangements such as aneuploidy, CNV and LOH. These genetic variations are essential for this pathogen to adapt to the stress environment. However, it is still unknown how these mechanisms are regulated. For this, the aim of this study is to identify and investigate a novel regulator of stress-induced genome instability in *C. albicans*.

To identify a novel regulator of stress-induced genome instability a parallel genetic screening using two DNA damaging agents (UV and MMS) are used. For this genetic screening, a *C. albicans* homozygous gene deletion library is used to identify the potential candidates as regulators of

genome instability. Several steps will select one suitable candidate from the parallel genetic screenings. To determine the potential stress-induced regulator, 3 major steps will be followed:

1. Identification and selection of a potential regulator by performing two parallel genetic screenings using UV radiation as source to induce SSB DNA damage and MMS as DNA damaging agents inducing DSB.

2. Investigate whether the deletion of the gene considered as potential regulator leads to genotoxic stress and increased genome instability.

3. Examine whether the loss of the stress-induced potential gene leads to drug resistance throughout the selection of a novel genotypes.

Chapter 2. UV stress-induced novel regulators of genome instability

2.1 Introduction

DNA damage can be caused by different types of DNA lesions such as misincorporation of bases during replication; deamination of bases, depurination and depyrimidination caused by hydrolytic damage; oxidative damage due to UV or ionising radiation inducing free radicals, modified bases caused by alkylating agents (Rastogi et al., 2010b; Sinha and Häder, 2002). UV radiation is an efficacious source for DNA damage, it can alter the normal state of the double helix by inducing different mutagenic and cytotoxic DNA lesions which can interfere with genome integrity (Rastogi et al., 2010b). Specifically, UV irradiation can excite pyrimidine bases which give rise to three main classes of DNA lesions: cyclobutene pyrimidine dimers (CPDs), 6-4 photoproducts (Sinha and Häder, 2002) and 8-oxoGua (Rastogi et al., 2010b). These lesions, lead to distortion of the DNA structure causing bends which obstruct transcription and replication. Consequently, these lesions can cause secondary breaks leading to DSBs (Rastogi et al., 2010b).

C. albicans is the most common commensal fungal species in humans. However, it can become an opportunistic pathogen with high lethality rate in immune suppressed patients (Mayer et al., 2013a). In the host, *C. albicans* faces stressful environments and for this it must adapt rapidly in order to survive under stressful conditions. The stressful environment can promote mutagenesis generating different types of genetic variations which *C. albicans* can act upon (Avramovska and Hickman, 2019b). Genome rearrangements such as chromosome length polymorphism and chromosome copy number variation have been widely reported (Diogo et al., 2009; Ene et al., 2018; Forche et al., 2009; Smith and Hickman, 2020). Furthermore, these genetic changes have been associated with drug resistance (A Coste et al., 2007; Zhu et al., 2010). *C. albicans* is clinically relevant as it can evolve antifungal resistance resulting in an emerging worldwide problem (Pappas et al., 2018). In a study in which *C. albicans* clinical isolates were taken from patients with oral candidiasis, genetic variations including single-nucleotide polymorphisms, copy number variations and LOH were detected (Ford et al., 2015). As mentioned in

section 1.3.2 and section 1.4.4, *C. albicans* can develop resistance to the antifungal drug Fluconazole and gain a segmental aneuploidy of the left arm of chromosome 5. This allows the pathogenic yeast to adapt to the stressful condition conferring fitness advantages (Selmecki et al., 2006). In addition, DNA damages, errors in DNA replication and DNA damage checkpoint pathways compromise genome integrity if not properly repaired. In *C. albicans*, defects in DSBs repair can increase genome instability (Legrand et al., 2007), while mutation in DNA damage checkpoint *MEC1* results in increased LOH frequency (Ahn et al., 2004), as well as *RAD52* deletion can increase rate of LOH and form chromosome instability (Andaluz et al., 2011).

As mentioned above, *C. albicans* isolates can exhibit extensive genomic plasticity caused by different types of events which include LOH events, SNPs and indels, changes in gene and chromosome copy numbers (Ene et al., 2019). However, the plastic genome of *C. albicans* has been proven to contribute to the developing and selection of genotypes which it is favourable to adapt and grow in the stress environment. The genome instabilities that are developed in response to an extreme selective environment can provide a quick means of adaptations throughout genetic changes which confer to *C. albicans* fitness advantages (Siegel and Amon, 2012).

Despite this, the regulators of stress induced genome instability have yet to be established. To identify potential regulator of *C. albicans* genome instability, I have performed a genetic screen using UV radiation as source of DNA damage, the genetic screen has identified 5 potential genes that showed sensitivity to UV radiation and high percentage of filamentous forms.

2.2 Results

2.2.1 Genetic library and screening procedure

The first step of this project was to identify novel regulators of genome instability in *C. albicans*. To do so, a genetic screen was performed using a homozygous *C. albicans* gene deletion library (Noble et al., 2010a). This library includes homozygous deletion strains affecting 674 genes. These genes are involved in a broad spectrum of cellular processes and represents around 11% of the *C. albicans* genome. Each mutant was constructed in the strain SN250 (Table 6.5), derivative of SC5314 *C. albicans*, where one allele was deleted with the His marker and the second allele deleted with the Leu marker (Noble et al., 2010b).

This library is composed of 16 plates in total, containing two independent homozygous knockout isolates for each gene. To identify target genes, UV irradiation was used as source of damaging agent to induce single strand break after spotting the cell lines into YPAD solid media (further detail in section 6.7). The energy of irradiation was $7.5\mu\text{W}/\text{cm}^2$ which led to a sub lethality rate in *C. albicans*.

The process of the UV screening was divided in 4 main stages:

1. *Primary screening*: in which the whole genetic library was subjected to UV irradiation, and a first selection of UV sensitive mutants were selected. Literature research of the location and function of each gene was performed to select deletion mutants whose gene location/function is focused in one or more of the following functional groups: nuclear location, response to stress, cell cycle.
2. *Spotting susceptibility assay*: the selected sensitive mutants from the primary screening were subject to serial dilutions and UV irradiation in order to select the most sensitive candidates.
3. *Confirmation of deletion mutants by colony PCR*: absence of the target genes was verified by colony PCR.

4. *Quantification of survival after UV irradiation*: the final selected knockouts were screened by quantification of survival after UV irradiation. In addition, the quantification of filamentous forms was investigated.

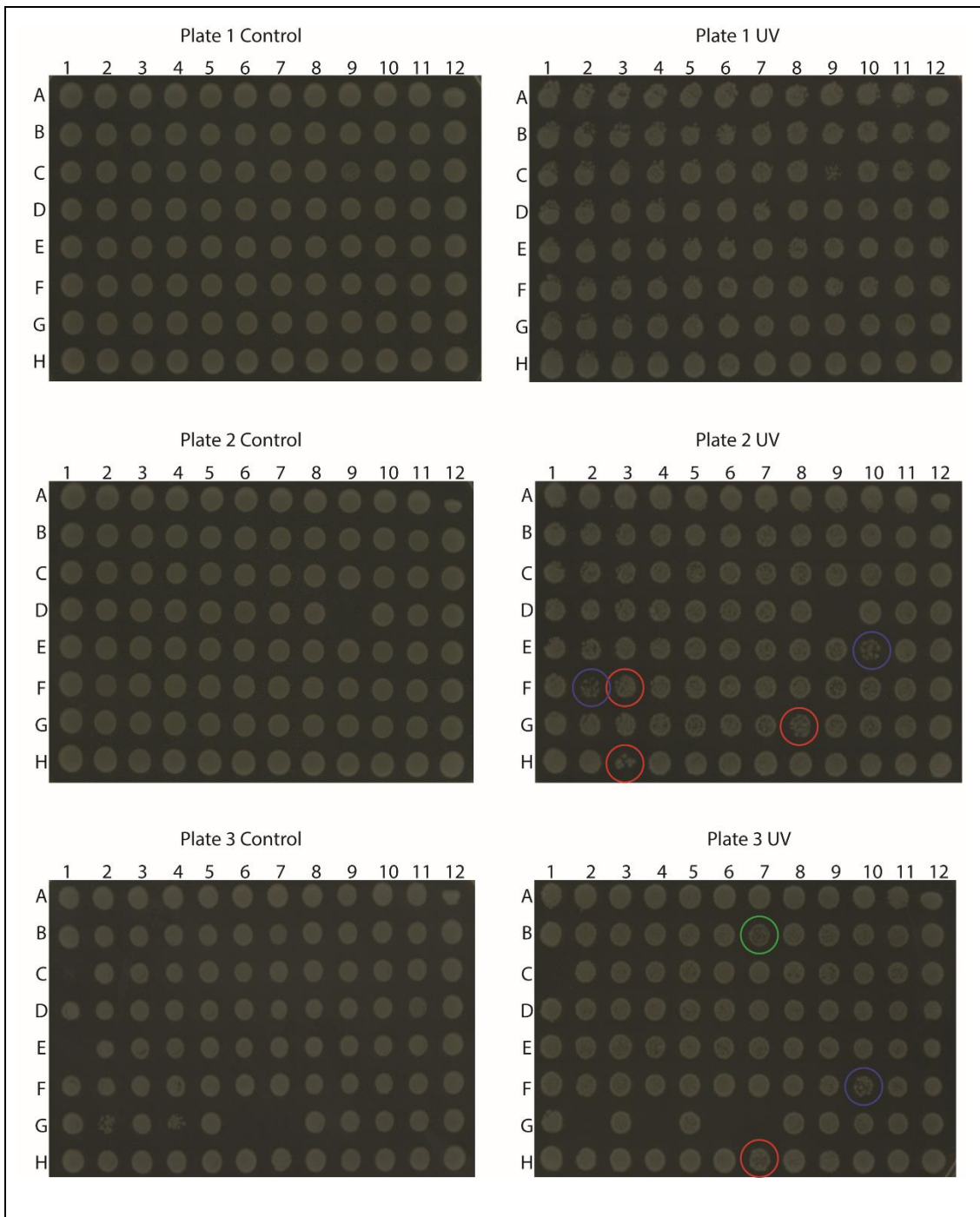
2.2.2 UV Primary screening

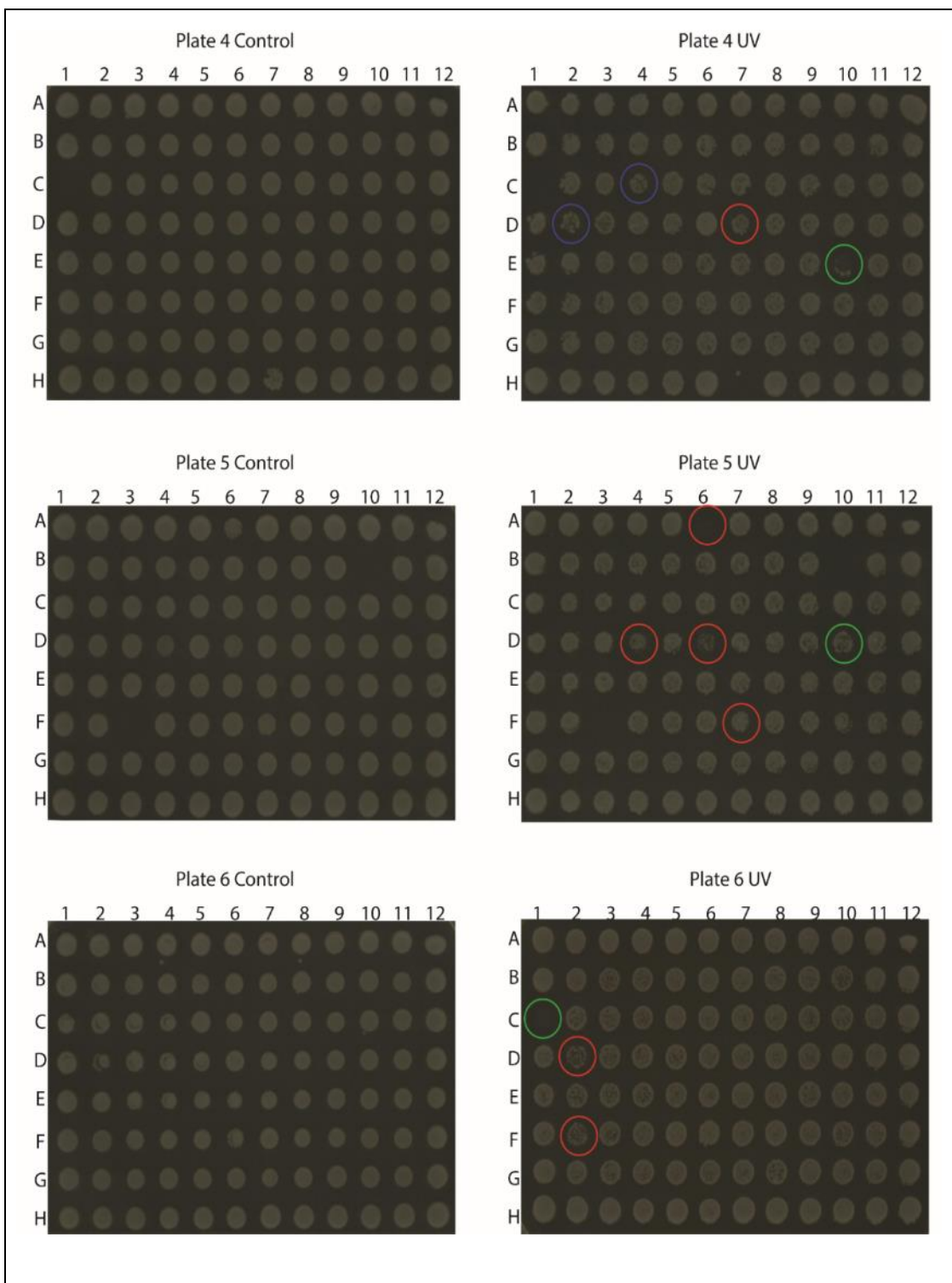
The first step of this genetic screening was the primary identification of which homozygous deletion strains show sensitivity to UV irradiation. Each library plate, containing around 96 different deletion mutants, was spotted in two large YPAD plates (145x20) using a replica plater for 96 well plates. Then, the plates subjected to UV stress were UV irradiated with a power density of $7.5\mu\text{W}/\text{cm}^2$ and grown in the dark for 48h at 30°C (screening methodology details in section 6.7).

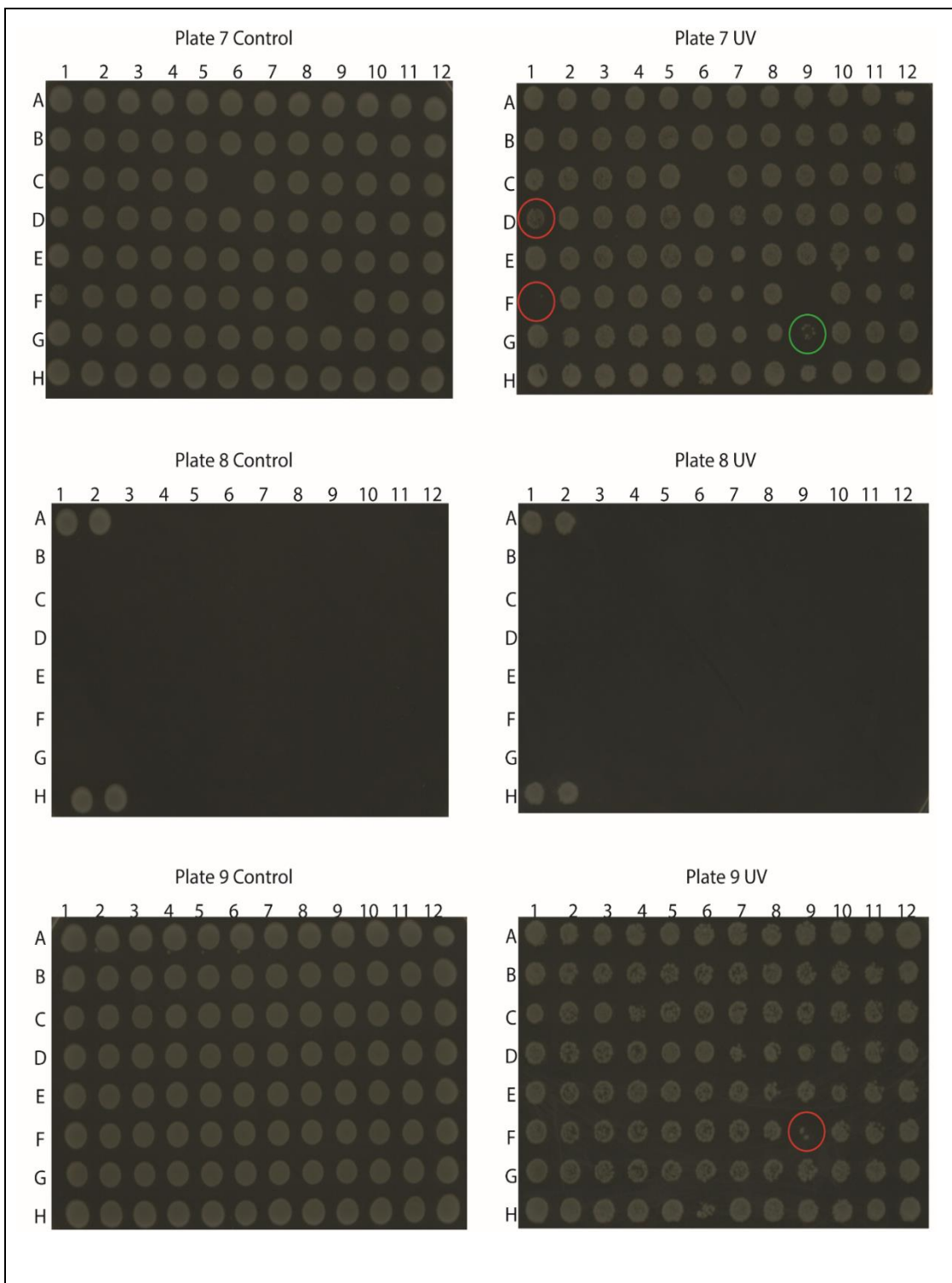
In the initial stage of screening, a total of 43 deletion strains were identified to be sensitive to UV radiation as shown in Figure 2.1 and indicated with red, blue, and green circles. After investigating the functions and locations of each gene selected, the mutants were categorised in different functional groups: nuclear location (NL), response to stress (SR), cell cycle (CC), transporter (TR), lipid metabolism process (LMP), vacuole location (VL) and DNA repair system component (DRS). In the case of unknown functions for *C. albicans* selected genes, literature research on *S. cerevisiae* was used as reference due to its close evolutionary correlation with *Candida* clade (Hendriks et al., 1989).

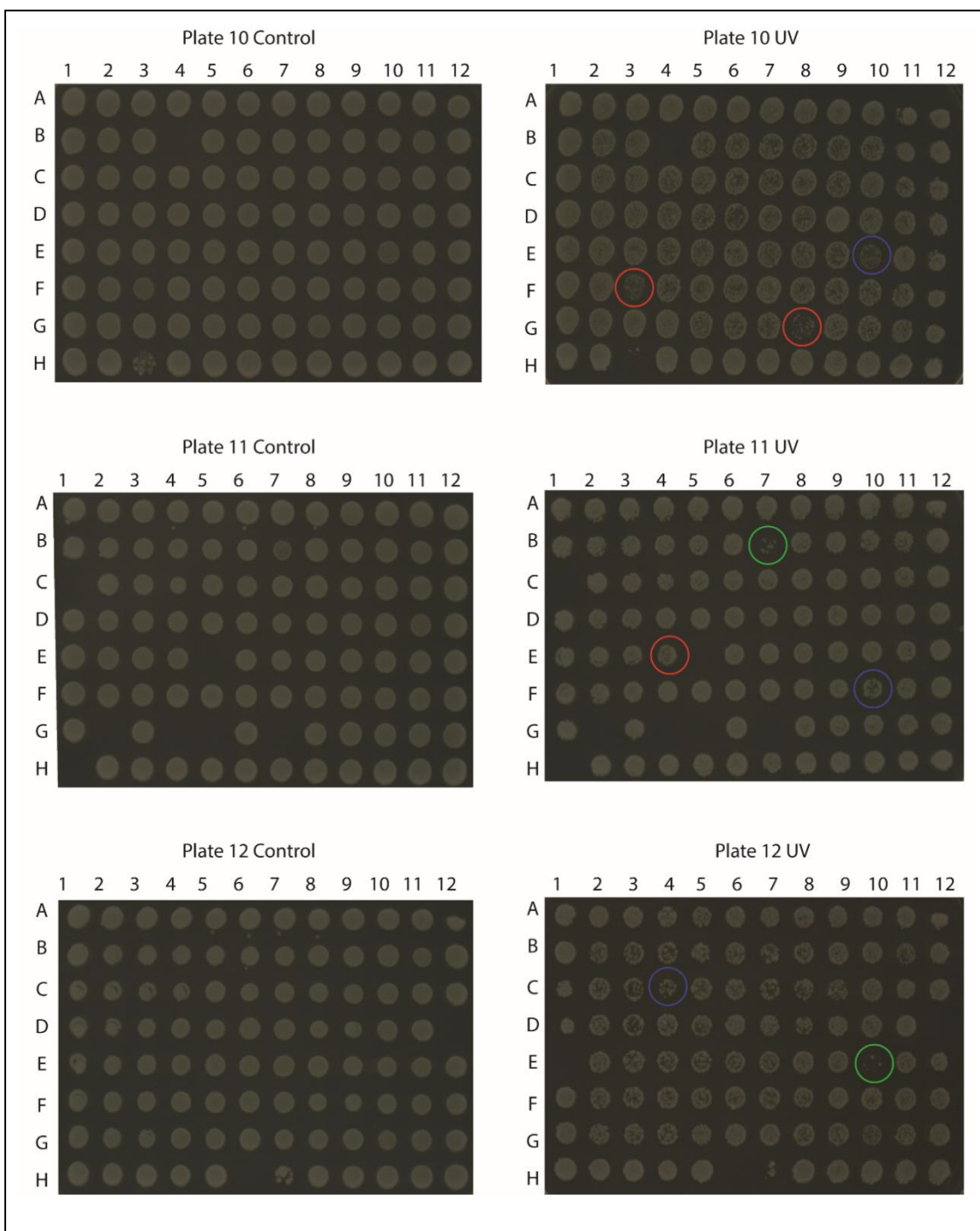
To differentiate the mutants sensitive to UV and selected for the next steps, a colour code was applied. The colour red indicates the UV sensitive mutants whose gene function is in line with the aim of this study and are categorised by the functional group of NL, SR, and CC. Therefore, the red-circled strains were selected for the second step of the screening. These mutants are listed in Table 2.1 The colour blue, instead, was chosen to indicate mutants sensitive to UV irradiation but excluded from this screening due to localisations and/or genes functions categorised as LMP and VL

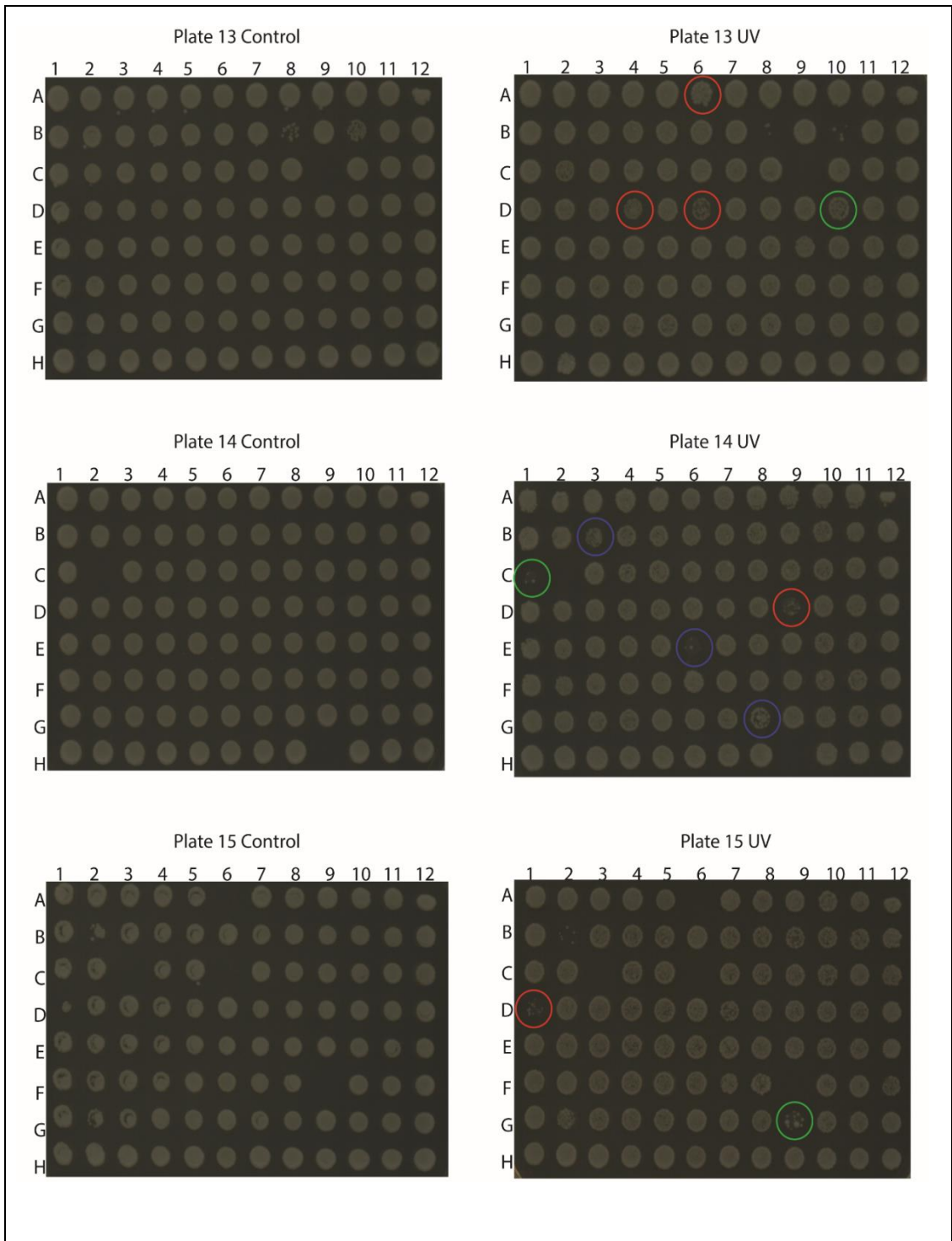
which were considered outside the aim of this study (Table 2.2). Lastly, the colour green was used to indicate mutants for target genes which were already known to have a role in the DNA repair system (Table 2.3). Figure 2.1 shows all the 16 plates of the homozygous deletion library used in this study with the deletion strains showing sensitivity to UV irradiation and their relative colour code.











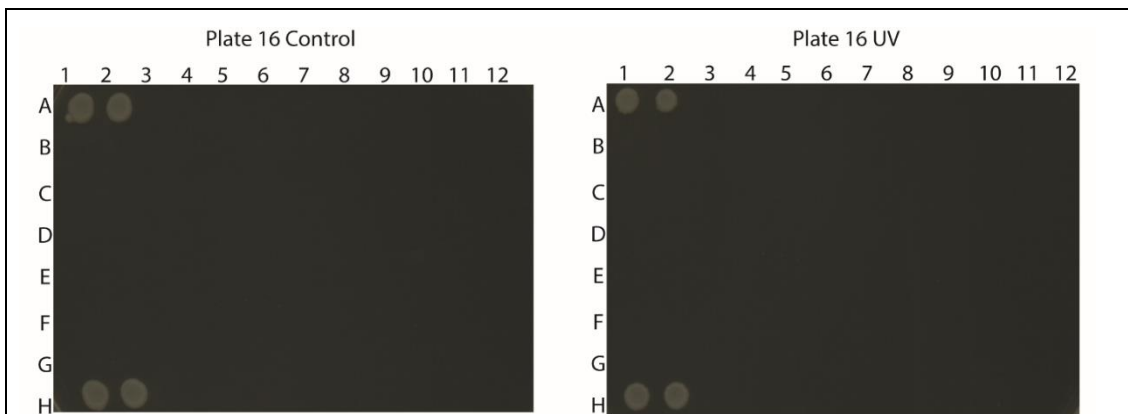


Figure 2.1 UV Primary screening. All 16 plates of the genetic library containing the *C. albicans* homozygous deletion strains were plated on YPAD using a 96 well plate replica plater and then UV irradiated with a power density of $7.5\mu\text{W}/\text{cm}^2$ (right) and grown in the dark for 48h at 30°C . The growth of the mutants was compared with the YPAD control plate (left) and sensitive mutants were selected for the next step. Red circles indicate the deletions strains sensitive to UV with functional role in CC, NL and SR. Blue circles indicate the mutants sensitive to UV but excluded due to functional roles outside the aim of this project. Green circles indicate deletion strains with functional role in DNA repair pathways. Three biological repeats were performed for all the 16 plates of *C. albicans* homozygous deletion strains genetic library.

Table 2.1: Deletion mutants indicated with red circle in figure 2.1. The mutants in this table were identified with the functional group of stress response (SR), cell cycle (CC) and nuclear localisation (NL). These deletion mutants showed sensitivity to UV radiation and therefore they were selected for the next step.

Plate number	Mutant No.	Systematic name	Gene name	Well No.	Relevant role for the genetic screening	Functional group
2 - 10	230	ORF19.333	FCY2	F3	Protein abundance increases upon DNA replication stress in <i>S. cerevisiae</i> (Tkach et al.,	SR

					2012) and multi drug resistance in <i>Candida</i> species (Chapeland-Leclerc et al., 2005)	
2 - 10	253	ORF19.564	KAR3	G8	Microtubule motor protein required for mitotic division (Sherwood and Bennett, 2008)	SR, CC, NL
2	265	ORF19.663	GIN4	H3	Required from transition to pseudohyphae to hyphae and for the formation of septin ring (Wightman et al., 2004)	CC, NL
3	493	ORF19.2378		H7	Protein abundance increases upon DNA replication stress in <i>S. cerevisiae</i> (Tkach et al., 2012)	SR
4	584	ORF19.3207	CCN1	D7	G ₁ cyclin, important for transition G ₁ /S phase (Sinha et al., 2007)(J. Loeb et al., 1999a)	CC, NL
5 - 13	674	ORF19.3944	GRR1	A6	F-box protein component of the SCF ubiquitin-ligase complex required for cell cycle progression (Lu et al., 2019)	CC, NL
5 - 13	729	ORF19.4312	SPT8	D4	TBP-binding transcription coregulator involved in histone acetylation, chromatin organization(Belotserko vskaya et al., 2000), subunit of SAGA complex, localizes to nucleus(Bhaumik and Green, 2002)	NL
5 - 13	734	ORF19.4353	ULP2	D6	SUMO deconjugation enzyme(Hochstrasser, 2001), involved in cell cycle progression(Li and Hochstrasser, 1999), sequestered to the nucleolus under stress conditions(Sydorsky et al., 2010). Trigger multi chromosome aneuploidy in <i>S. cerevisiae</i> (H.-Y. Ryu et al., 2016)	CC, NL
5	779	ORF19.4670	CAS5	F7	Transcription factor	SR, NL

					which couples stress responses, drug resistance and cell cycle regulation (Xie et al., 2017)	
6	904	ORF19.5662	PEP7	D2	Might be involved in virulence (Franke et al., 2006)	SR
6	944	ORF19.6011	SIN3	F2	component of histone deacetylase complexes and important for host colonisation (Tyc et al., 2016)	SR, CC, NL
7 - 15	1064	ORF19.7186	CLB4	D1	cell cycle cyclin (Ofir and Kornitzer, 2010)	CC, NL
7	1091	ORF19.7353	KIP3	F1	Mitotic spindle organisation (McCoy et al., 2015)	SR, CC, NL
9	89	ORF19.4567		F9	No <i>S. cerevisiae</i> orthologous	
11	379	ORF19.1567		E4	vCLAMPs component involved in stress resistance (Mao et al., 2021)	SR
14	918	ORF19.5776	TOM1	D9	heat stress response (Sasaki et al., 2000)	CC

Table 2.2: Deletion mutants indicated with blue circle in figure 2.1. These mutants identified with the functional group of transporters (TR), lipid metabolism process (LMP), vacuole location (VL), showed sensitivity to UV radiation, however they were excluded from this study.

Plate number	Mutant No.	Systematic name	Gene name	Well No.	Role	Functional group
2 - 10	225	ORF19.290	KRE5	E10	UDP-glucose:glycoprotein glucosyltransferase activity (Herrero et al., 2004)	LMP
2	229	ORF19.328	NPR2	F2	putative urea transporter in (Navarathna et al., 2011)	TR
3 - 11	415	ORF19.1814	STT4	F10	Putative phosphatidylinositol-4-kinase (Vernay et al., 2012)	TR, LMP

4 - 12	554	ORF19.2975	YPT7	C4	YPT/RAB component induced during mating process (Zhao et al., 2005)	TR
4	573	ORF19.3122	ARR3	D2	Arsenite transporter in (R Wysocki et al., 1997)	TR
14	863	ORF19.5300		B3	integral membrane ER chaperone (Kimura et al., 2005)	TR
14	932	ORF19.5915	DUR35	E6	Putative urea transporter in (Kumar et al., 2011)	TR
14	980	ORF19.6411		G8	Involved in vacuole trafficking in (Dove et al., 2002)	VL

Table 2.3: Deletion mutants indicated with green circle in figure 2.1. The target genes for these mutants are known to play a role in the DNA repair system and for this they were identified with the functional role of DNA repair system component (DRS). The following deletion mutants showed sensitivity to UV radiation.

Plate number	Mutant No.	Systematic name	Gene name	Well No.	Role	Functional group
3 - 11	307	ORF19.895	HOG1	B7	Component of MAP kinase pathway respond to oxidative stress(Haghnazari and Heyer, 2004)	DRS
4 -12	603	ORF19.3407	RAD18	E10	Postreplication repair(S et al., 1993)	DRS
5 -13	741	ORF19.4412	REV1	D10	Error-free translesion synthesis	DRS
6 - 14	884	ORF19.5485	MEC3	C1	DNA damage checkpoint (Kondo et al., 1999)	DRS
7 - 15	1124	ORF19.8485	RAD32	G9	DNA polymerase (Manohar et al., 2018)	DRS

From the 43 deletion strains showing sensitivity to UV radiation, 22 of them are indicated with the red circles in figure 2.1, some of these deletion mutants include duplicates (see table 2.1 plate number). The 22 homozygous deletion strains have gene localisation and/or known roles which correlate with possible sources of genome instability. For example, one of the selected strains, which gene has main function in cell cycle is *GRR1* (Lu et al., 2019). The *grr1ΔΔ* strain (Figure 2.1 plate 5, well A6) shows strong sensitivity to UV radiation compared to the control. In *C. albicans*, *GRR1* is responsible for stabilisation of two cell cycle cyclins and pseudohyphal growth. Indeed, when *GRR1* is deleted, the cells are unable to separate (Li et al., 2006). An example of stress response selected strain is *cas5ΔΔ* (Fig.2.1 plate 5, well F7), which shows sensitivity to UV radiation, although it is less compared to *grr1ΔΔ*. *CAS5* gene regulate cell dynamics and response to stress in *C. albicans* (Xie et al., 2017). For the nuclear localisation, *ULP2* gene represent a good example. *Ulp2ΔΔ* strain (Figure 2.2 plate 5 and plate 13, well D6) shows sensitive to UV radiation, In addition it was seen that in *S. cerevisiae*, cells deleted for *ULP2* exhibit multichromosome aneuploidy (H.-Y. Ryu et al., 2016). Other deletion strains, sensitive to UV radiation, indicated with the red circle in figure 2.1 represent at this stage good candidates for the aim of this screening and they are listed in Table 2.1. Of all the genes selected for the next step, relevant functions in *C. albicans* were researched in literature. However, ORF19.2378 function in *C. albicans* hasn't been reported. In *S. cerevisiae*, the ortholog is named PKR1 (YMR123W) and it is a V-ATPase assembly factor which is in the endoplasmic reticulum. In spite of this, *pkr1* protein levels increases in response to DNA replication stress but deep investigation on this hasn't been achieved. Therefore, SMART analysis of protein domain was performed. However, this results in an uncharacterized protein in both *C. albicans* and *S. cerevisiae*. Following this, BLAST analysis of *C. albicans* protein sequence highlighted identities of 100% with *S. cerevisiae* in addition to hits with an E-value of $1.9e^{-40}$. This indicates strong similarity between *C. albicans* ORF19.2378 and *S. cerevisiae* PKR1. Therefore, at this stage of the screening, we consider ORF19.2378 for the next steps.

In figure 2.2, 11 UV sensitive strains are indicated with the blue circles. However, their gene's function and/or localisation is not focused on NL, SR and/or CC, for this reason, they excluded for the next steps of the screening. Most knockout isolates are transporters (TR) such as *npr2ΔΔ* and *dur35ΔΔ* in which both are involved in putative urea transporter (Kumar et al., 2011; Navarathna et al., 2011). *Kre5ΔΔ* was also marked as not suitable due to function classified into lipid metabolism process (LMP) (Herrero et al., 2004). Lastly, another example of not suitable candidate is *orf19.6411ΔΔ* for its vacuole location (VL) (Dove et al., 2002). In table 2.2 are listed all the sensitive UV strains excluded from this study at this stage of the screening.

Finally, the target genes of the 10 sensitive homozygous deletion strains indicated by the green circles (listed in table 2.3) are already acknowledged to be components of the DNA repair system pathways such as *hog1ΔΔ* (Figure 2.1 plate 3 and plate 11, well B7), *rad18ΔΔ* (Figure 2.1 plate 4 and plate 12, well E10), *rev1ΔΔ* (Figure 2.1 plate 5 and plate 13, well D10), *mec3ΔΔ* (Figure 2.1 plate 6 and plate 14, well C1), *rad32ΔΔ* (Figure 2.1 plate 7 and plate 15, well G9). All these deletion mutants show sensitivity to UV radiation as expected, and they were used as positive control in this study.

2.2.3 UV Spotting susceptibility assay

The gene deletion homozygous deletion library used for this project contains two independent homozygous knockout isolates for each gene. The second stage of this screening focused on the phenotypic analysis performed to quantify growth defects between the two homozygous knockout isolates for each target gene and the wild-type SN250 strain after UV irradiation. Serial dilution of each mutant was spotted onto YPAD plate and then UV irradiated with $7.5\mu\text{W}/\text{cm}^2$, same energy of UV irradiation used during the first stage of the screening (further details in the methodology in section 6.8). After irradiation, the plates were grown in the dark and protected from natural light for 48h at 30 degrees. Three mutants, *mec3ΔΔ* strain, *rad18ΔΔ* strain and *rad32ΔΔ* strain, known to have a role in DNA

repair pathways (Kondo et al., 1999; Manohar et al., 2018; S et al., 1993) were used as positive control for the spotting susceptibility assay. This genetic library containing two independent homozygous knockout isolates for each target gene. Each gene selected as UV sensitive was tested for both copies of the homozygous deletion strains. The results of this assay indicate different grade of sensitivity to UV radiation as shown in figure 2.2. A gradient scale to define the phenotype grade was made to classify the degrees of UV sensitivity, going from 4 as strongest phenotype comparable to the positive control, to value 1 as phenotype almost identical to control plate and wild type. In table 2.4, the gradient value given to each deletion strain is indicated.

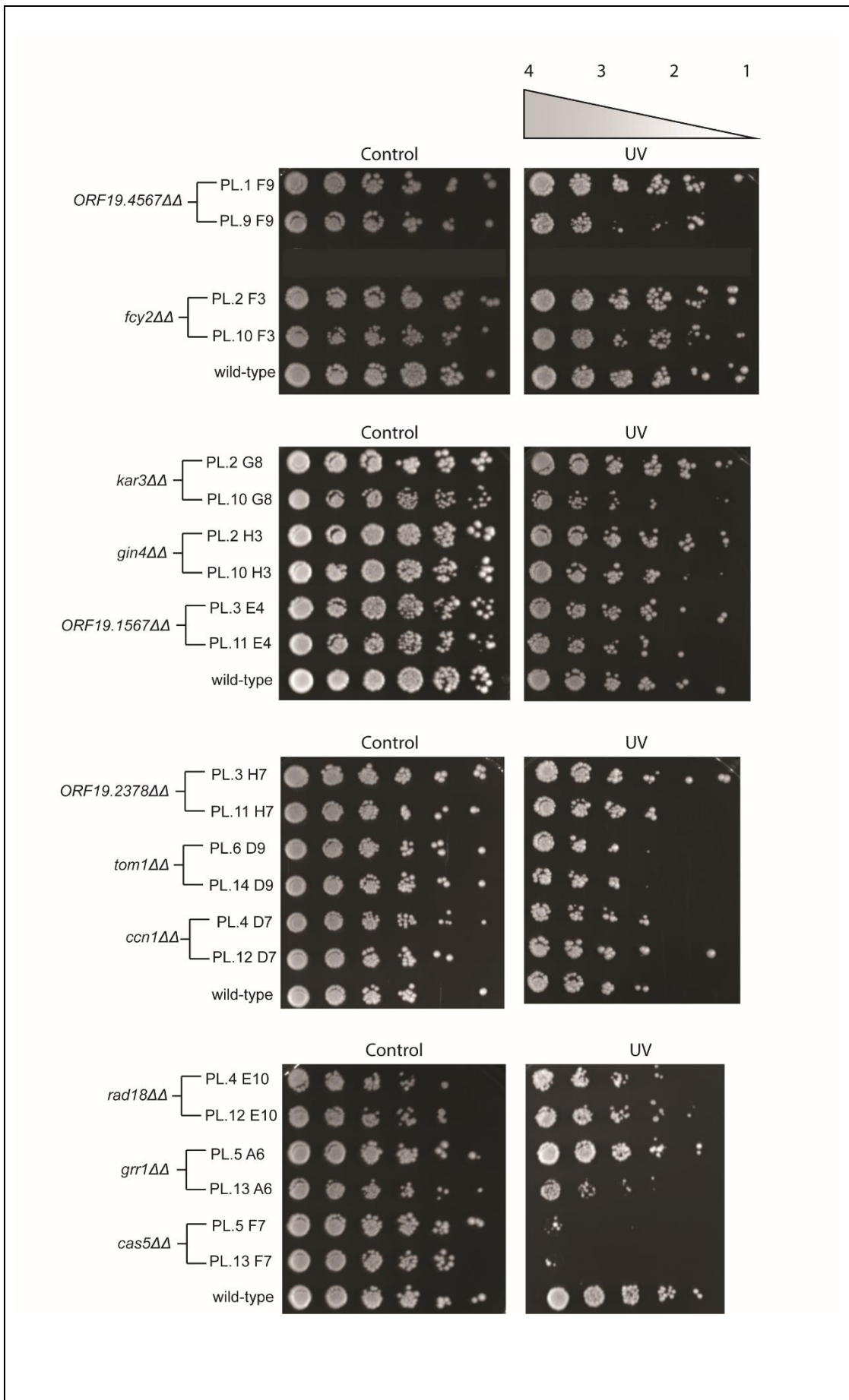
From figure 2.2 it showed that deletion strains: *ccn1ΔΔ*, *rad18ΔΔ*, *cas5ΔΔ*, *spt8ΔΔ*, *mec3ΔΔ*, *pep7ΔΔ*, *tom1ΔΔ*, *clb4ΔΔ*, *rad32ΔΔ* showed sensitivity to UV irradiation in both copy of the deletion strains for the same target gene. In addition, the deletion strains: *orf19.4567ΔΔ*, *kar3ΔΔ*, *orf19.1567ΔΔ*, *orf19.2378ΔΔ*, *grr1ΔΔ*, *ulp2ΔΔ*, *sin3ΔΔ*, *kip3ΔΔ* exhibit different sensitivity between the two copies of the homozygous deletion strains for the same target gene. This can be caused by mistakes during the disruption of one copy of the target gene leading to the wrong homozygous deletion isolates.

In table 2.4 the different gradient values given based on the phenotype of the spotting susceptibility assay after UV radiation are listed. It is interesting to note that the deletion mutants involved in cell cycle such as *kip3ΔΔ* (PL. 7), *kar3ΔΔ* (PL. 10), *ccn1ΔΔ*, *grr1ΔΔ* (PL. 10) and *ulp2ΔΔ* (PL. 13) and nuclear localisation as *spt8ΔΔ* showed very strong sensitivity to UV radiation with gradient of UV sensitivity of 3 and gradient 4 for *kip3ΔΔ* suggesting the crucial roles of the genes of interested. However, *clb4ΔΔ* showed phenotype gradient of value 2. In yeast, *clb3* and *clb4* cyclins are not crucial for mitosis and it is believed that cell lacking *CLB3* and/or *CLB4* do not exhibit any obvious phenotype due to function being substituted by *clb1* and *clb2* (Richardson et al., 1992). Cell lacking *GIN4* and *ORF19.2378* didn't display strong sensitivity to UV irradiation in both copies, this is due to the

fact that in both copies of the deletion mutants respective genes weren't successfully deleted (see section 2.2.2). Regarding the stress response knockout isolates, *fcy2ΔΔ*, *pep7ΔΔ*, *sin3ΔΔ*, *orf19.1567ΔΔ* show weak sensitivity to UV radiation. This might imply that those genes of interested might not have an essential role for UV stress response. On the other hand, *cas5ΔΔ* exhibits very strong sensitivity to UV radiation. Cas5 orchestrates stress response, drug resistance and cell cycle regulation in which (under normal condition) it was determined that 56 out of 604 genes have Cas5-dependent RNA Pol II binding. In cells lacking CAS5, 75% of those genes have reduced RNA Pol II binding (Xie et al., 2017).

The positive control *mec3ΔΔ* and *rad32ΔΔ* showed, as expected, strong sensitivity to UV radiation. Although *rad18ΔΔ* UV sensitivity was ranked with value 3, this might be due to the fact that *RAD18* might not be an essential component required for NER or for UV survival response (Armstrong et al., 1994; Fabre et al., 1989). Two deletion mutants, *cas5ΔΔ* and *kip3ΔΔ* (PL. 7) have shown a similar phenotype to *mec3ΔΔ* and *rad32ΔΔ*.

As a consequence of these results, the absence of the target genes was investigated designing primers within the target genes and verified by PCR.



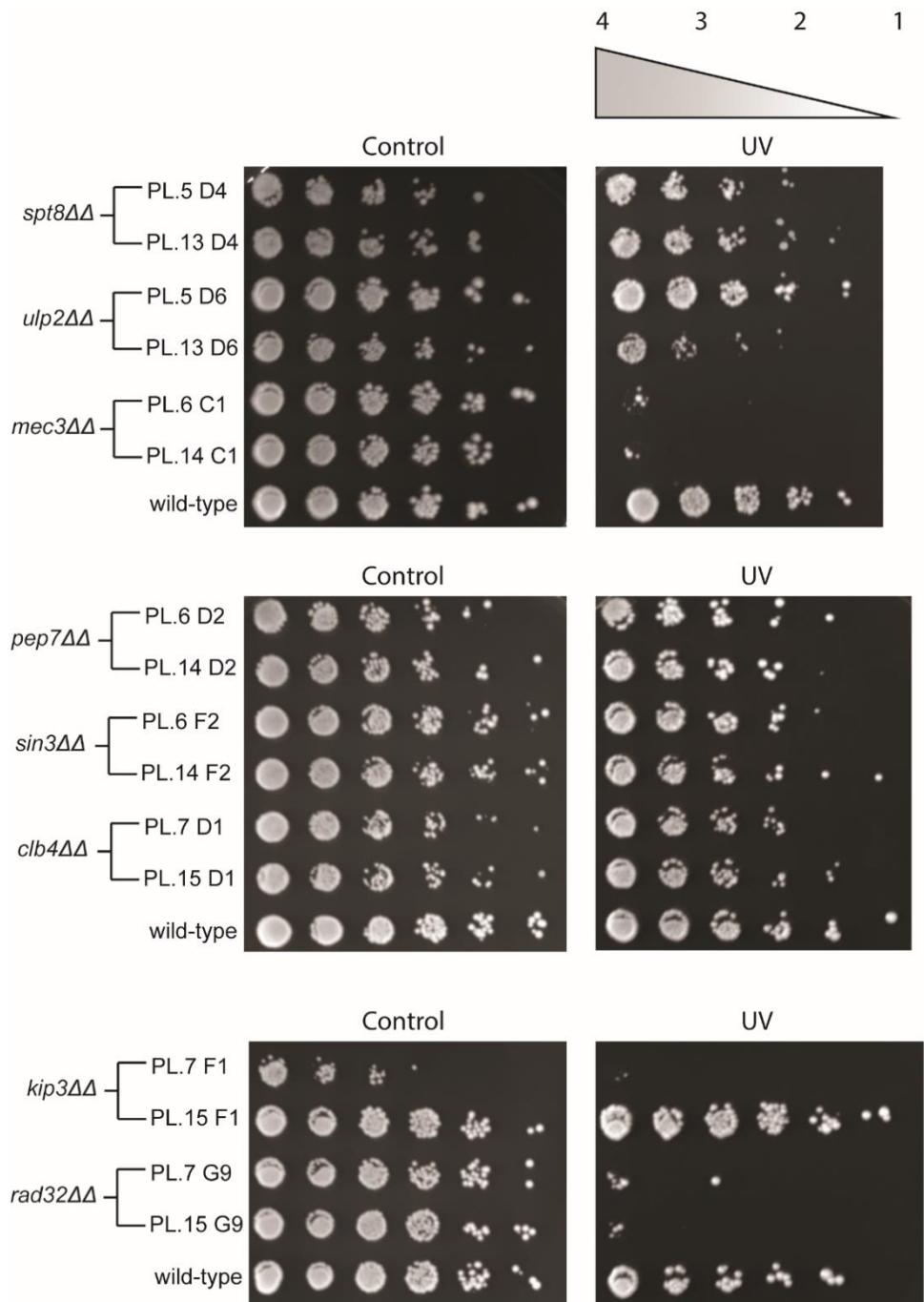


Figure 2.2 UV Spotting susceptibility assay. Serial dilution of the selected deletion strains was spotted on YPAD plates followed by UV irradiation with power of density $7.5\mu\text{W}/\text{cm}^2$ and grown for 48 hours at 30°C . The gradient of sensitivity to UV radiation is summarised in table 2.4. Three biological replicates were performed for this assay. The black square was used to cover a strain unrelated to this study.

Table 2.4. Gradient of sensitivity to UV radiation from spotting susceptibility assay

Plate No.	Mutant	Phenotype grade	Plate No.	Mutant No.	Phenotype grade
1	<i>orf19.4567ΔΔ</i>	1	5	<i>spt8ΔΔ</i>	3
9	<i>orf19.4567ΔΔ</i>	2	13	<i>spt8ΔΔ</i>	3
2	<i>fcy2ΔΔ</i>	1	5	<i>ulp2ΔΔ</i>	1
10	<i>fcy2ΔΔ</i>	1	13	<i>ulp2ΔΔ</i>	3
2	<i>kar3ΔΔ</i>	1	6	<i>mec3ΔΔ</i>	4
10	<i>kar3ΔΔ</i>	3	14	<i>mec3ΔΔ</i>	4
2	<i>gin4ΔΔ</i>	1	6	<i>pep7ΔΔ</i>	2
10	<i>gin4ΔΔ</i>	2	14	<i>pep7ΔΔ</i>	2
3	<i>orf19.1567ΔΔ</i>	1	6	<i>tom1ΔΔ</i>	3
11	<i>orf19.1567ΔΔ</i>	2	14	<i>tom1ΔΔ</i>	3
3	<i>orf19.2378ΔΔ</i>	1	6	<i>sin3ΔΔ</i>	2
11	<i>orf19.2378ΔΔ</i>	2	14	<i>sin3ΔΔ</i>	1
4	<i>ccn1ΔΔ</i>	3	7	<i>clb4ΔΔ</i>	2
12	<i>ccn1ΔΔ</i>	3	15	<i>clb4ΔΔ</i>	2
4	<i>rad18ΔΔ</i>	3	7	<i>kip3ΔΔ</i>	4
12	<i>rad18ΔΔ</i>	2	15	<i>kip3ΔΔ</i>	1
5	<i>grr1ΔΔ</i>	1	7	<i>rad32ΔΔ</i>	4
13	<i>grr1ΔΔ</i>	3	15	<i>rad32ΔΔ</i>	4
5	<i>cas5ΔΔ</i>	4			
13	<i>cas5ΔΔ</i>	4			

2.2.4 Screen of transformants by colony PCR

As mentioned above, the library contains two copies of the homozygous deletion isolates for the same target gene. For this, mutants that showed sensitivity to UV radiation from the first step of the screening were tested for both copies of the homozygous deletion strains in step 2 and step 3 of this screening. As showed in figure 2.2, the following mutants *orf19.4567ΔΔ*, *kar3ΔΔ*, *orf19.1567ΔΔ*, *orf19.2378ΔΔ*, *grr1ΔΔ*, *ulp2ΔΔ*, *sin3ΔΔ*, *kip3ΔΔ* exhibited different phenotypes between the two copies of the strains after UV irradiation, despite presumed deletion for the same target gene. For this, the aim of the third stage of the screening is to genetically

confirm the absence of the target genes of both copies of the homozygous knockout isolates.

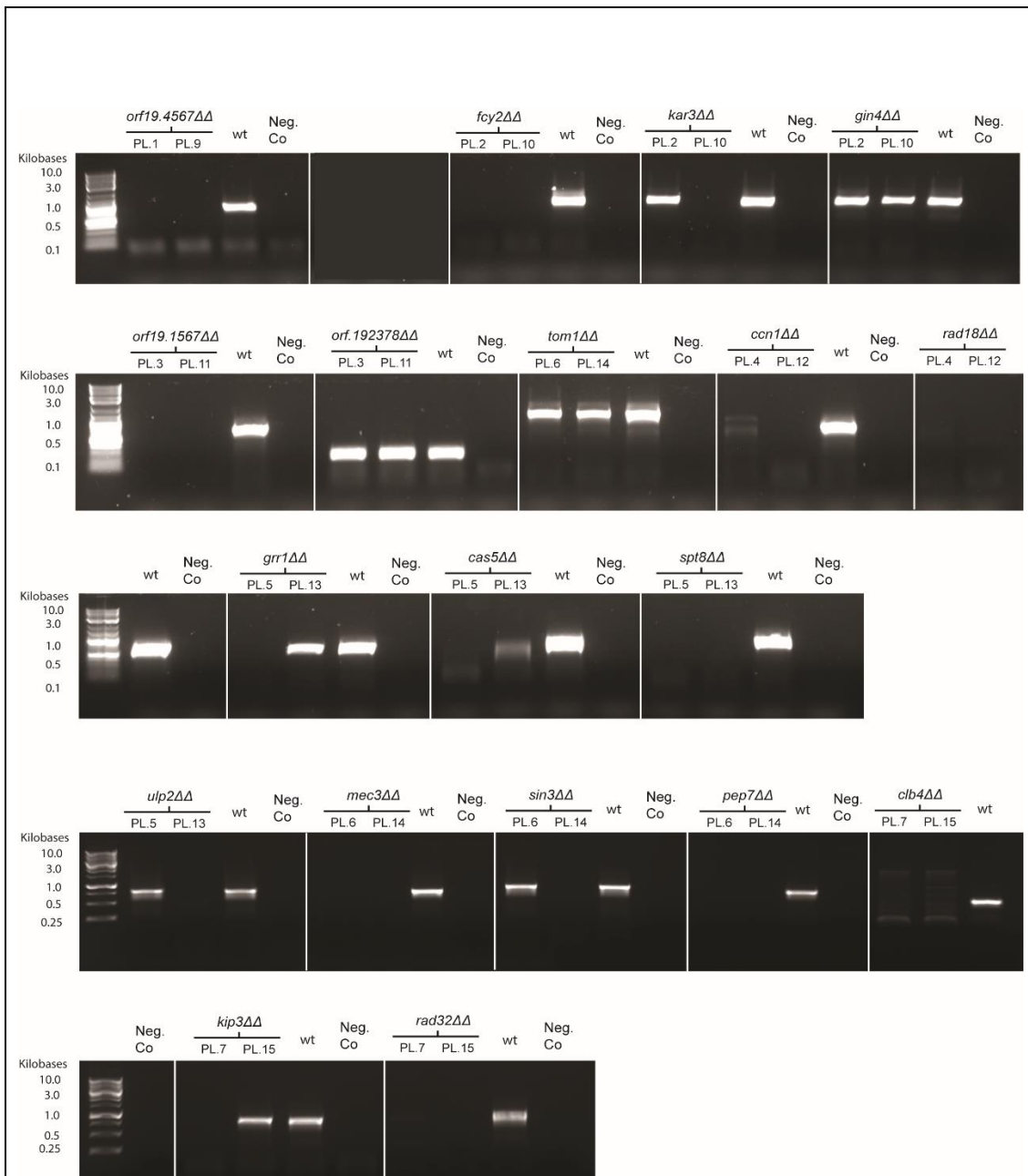


Figure 2.3 Screening of transformants by colony PCR. The absence of the gene from the selected deletion strains of the second step was verified. The wildtype strain was used as positive control and ddH₂O as negative control. The PCR amplicons were then verified in 1% agarose gel throughout gel electrophoresis. In table 2.5 are listed the genes sizes and the expected sizes from the PCR reactions used with the primers listed in table 6.6.

Table 2.5 Genes sizes and expected sizes bands from PCR reactions.

Gene name	Gene size (bp)	Expected gene size from PCR (bp)
<i>ORF19.4567</i>	3105	1026
<i>FCY2</i>	1581	803
<i>KAR3</i>	2064	876
<i>GIN4</i>	4050	920
<i>ORF19.1567</i>	912	829
<i>ORF19.2378</i>	354	259
<i>TOM1</i>	9861	1436
<i>CCN1</i>	2082	802
<i>RAD18</i>	1137	758
<i>GRR1</i>	2343	776
<i>CAS5</i>	2466	747
<i>SPT8</i>	2313	900
<i>ULP2</i>	1476	812
<i>MEC3</i>	960	749
<i>SIN3</i>	3360	898
<i>PEP7</i>	1338	856
<i>CLB4</i>	1461	593
<i>KIP3</i>	2919	902
<i>RAD32</i>	1923	894

To confirm the absence of the target genes, colony PCR using primers designed to anneal inside the target gene allowed to verify the integrity of the homozygous knockout mutants. The primers used are listed in table 6.6 and detailed methodology is described in section 6.9. The wildtype was used as a positive control and ddH₂O for the negative control. The PCR amplicons were then verified in 1% agarose gel throughout gel electrophoresis. Interestingly, for 6 knockout isolates only one of the two mutants were knocked out for that specific gene. In table 2.6 the homozygous knockout strains in which the target gene was fully deleted are listed. On the contrary, in table 2.7 are shown the strains which target genes was not fully or partially deleted and for this reason excluded from further steps of the screening. The knockout isolate *mec3ΔΔ* strain, *rad18ΔΔ* strain

and *rad32ΔΔ* strains used as positive control were also included to this stage of the screening.

Table 2.6 Successful homozygous knockout isolates verified by colony PCR

Plate No.	Mutant No.	Plate No.	Mutant No.
1	<i>orf19.4567ΔΔ</i>	13	<i>spt8ΔΔ</i>
9	<i>orf19.4567ΔΔ</i>	13	<i>ulp2ΔΔ</i>
2	<i>fcy2ΔΔ</i>	6	<i>mec3ΔΔ</i>
10	<i>fcy2ΔΔ</i>	14	<i>mec3ΔΔ</i>
10	<i>kar3ΔΔ</i>	14	<i>sin3ΔΔ</i>
3	<i>orf19.1567ΔΔ</i>	6	<i>pep7ΔΔ</i>
11	<i>orf19.1567ΔΔ</i>	14	<i>pep7ΔΔ</i>
12	<i>ccn11ΔΔ</i>	7	<i>clb4ΔΔ</i>
4	<i>rad18ΔΔ</i>	15	<i>clb4ΔΔ</i>
12	<i>rad18ΔΔ</i>	7	<i>kip3ΔΔ</i>
5	<i>grr1ΔΔ</i>	7	<i>rad32ΔΔ</i>
5	<i>cas5ΔΔ</i>	15	<i>rad32ΔΔ</i>
5	<i>spt8ΔΔ</i>		

Table 2.7 Unsuccessful homozygous knockout isolates verified by colony PCR

Plate No.	Mutant No.	Plate No.	Mutant No.
2	<i>kar3ΔΔ</i>	6	<i>sin3ΔΔ</i>
2	<i>gin4ΔΔ</i>	6	<i>tom1ΔΔ</i>
10	<i>gin4ΔΔ</i>	14	<i>tom1ΔΔ</i>
3	<i>orf19.2378ΔΔ</i>	13	<i>grr1ΔΔ</i>
11	<i>orf19.2378ΔΔ</i>	13	<i>cas5ΔΔ</i>
4	<i>ccn1ΔΔ</i>	15	<i>kip3ΔΔ</i>

Importantly, the results of spotting susceptibility assay (figure 2.2) correspond with the results of the colony PCR results (figure 2.3). For example, the *kip3ΔΔ* mutant (PL. 7) exhibits strong sensitivity to UV radiation which is consistent with the absence of the target gene by PCR (figure 2.3). In contrast, *kip3ΔΔ* (PL. 15) deletion strain does not exhibit sensitivity to UV

radiation. In agreement with this result, the colony PCR demonstrated that the *kip3*ΔΔ (PL. 15) was incorrect as the KIP3 gene was detected. Similarly, PCR analyses demonstrates that *kar3*ΔΔ (PL. 2), *grr1*ΔΔ (PL. 13), *ulp2*ΔΔ (PL. 5) and *sin3*ΔΔ (PL. 6) are incorrect and indeed are not sensitive to UV radiation. Instead, the other copies of the aforementioned deletion strains are correct and sensitive to UV irradiation. As shown in figure 2.3. However, the phenotypes of *orf19.2378*ΔΔ and *gin4*ΔΔ deletion strains do not show sensitivity to UV radiation and the colony PCR of both copies of *orf19.2378*ΔΔ and *gin4*ΔΔ shows the presence of the target genes into the genome which results in the wrong homozygous deletion isolates. The phenotype of *tom1*ΔΔ shows medium weak UV sensitivity (value 3). However, the colony PCR showed the presence of the genes in both the deletion strains for *TOM1*. This might be due to artefact during the transformation process. Therefore, *gin4*ΔΔ, *orf19.2378*ΔΔ and *tom1*ΔΔ were excluded from this study. Following, the colony PCR for *ccn1*ΔΔ, *clb4*ΔΔ, *fcy2*ΔΔ, *cas5*ΔΔ, *pep7*ΔΔ, *orf19.1567*ΔΔ, *spt8*ΔΔ, *orf19.4567*ΔΔ, *mec3*ΔΔ, *rad18*ΔΔ and *rad32*ΔΔ show successful deletion of target genes in both the copied of the knockout isolates.

2.1.4 Quantification of survival after UV irradiation

The results from the previous three steps of this genetic screening allowed the selection of a total of 13 genes out of 674 target genes (Table 2.8). Having established that these 13 final selected homozygous deletion isolates were sensitive to UV radiation from the first two steps of the screening, in addition to the confirmation of target genes deletion from the third step of the screening, the last step was to quantify the survival of these final mutants after UV irradiation. The quantification of survival was conducted by counting the number of colonies forming at 30 °C in the dark, 48 hours after the UV irradiation (7.5μW/cm²) (methods details in section 6.10). As expected, the positive control deletion strains, *mec3*ΔΔ, *rad18*ΔΔ, and *rad32*ΔΔ showed strong UV sensitivity (figure 2.5). Interestingly, five of

the selected deletions strains: *kip3ΔΔ*, *spt8ΔΔ*, *grr1ΔΔ*, *kar3ΔΔ* and *ulp2ΔΔ* showed significantly higher sensitivity to UV radiation compared to the WT strain ($p < 0.05$ figure 2.5). Defects in *C. albicans* stress response and DNA repair leads to filamentation forms (Bachewich et al., 2005; Bai et al., 2002). Therefore, the presence and quantification of filamentous forms has been investigated for all the 13 final selected mutants in no stress conditions. Interestingly, deletion strains: *kip3ΔΔ*, *spt8ΔΔ*, *grr1ΔΔ*, *kar3ΔΔ* and *ulp2ΔΔ* (showing high sensitivity to UV radiation) also exhibited the highest filamentous forms formations (figure 2.6). Interestingly, *spt8ΔΔ*, and *grr1ΔΔ* showed a percentage of filamentous forms higher compared to the positive control *mec3ΔΔ*. For this, the combination of strong UV sensitivity in all the steps of this screening added to the higher filamentous forms, and their functional roles in cell cycle, stress response and nuclear localisation (further described in the next section) lead these five deletion strains (*kip3ΔΔ*, *spt8ΔΔ*, *grr1ΔΔ*, *kar3ΔΔ* and *ulp2ΔΔ*) to be considered as final potential candidates. The following deletion strains *orf19.4567ΔΔ*, *fcy2ΔΔ*, *clb4ΔΔ*, *pep7ΔΔ*, *orf19.1567ΔΔ* and *sin3ΔΔ* did not exhibit strong sensitivity to UV radiation as showed in figure 2.5. These results are in accordance with the results of spotting susceptibility assay in figure 2.2. However, cell lacking *CCN1* and *CAS5* show a more percentage of survival compared to the survival to UV radiation from the spotting assay (figure 2.2). The cause of this might be explained by laboratory mistakes during the procedure of step 2 or step 4 of the screening. Furthermore, in figure 2.6, *CCN1* and *CLB4* deletions mutants exhibit formation of filamentous forms. However, these results are inconsistent with studies showing that *CLB4* and *CCN1* regulates morphogenesis in *C. albicans* (J. Loeb et al., 1999b).

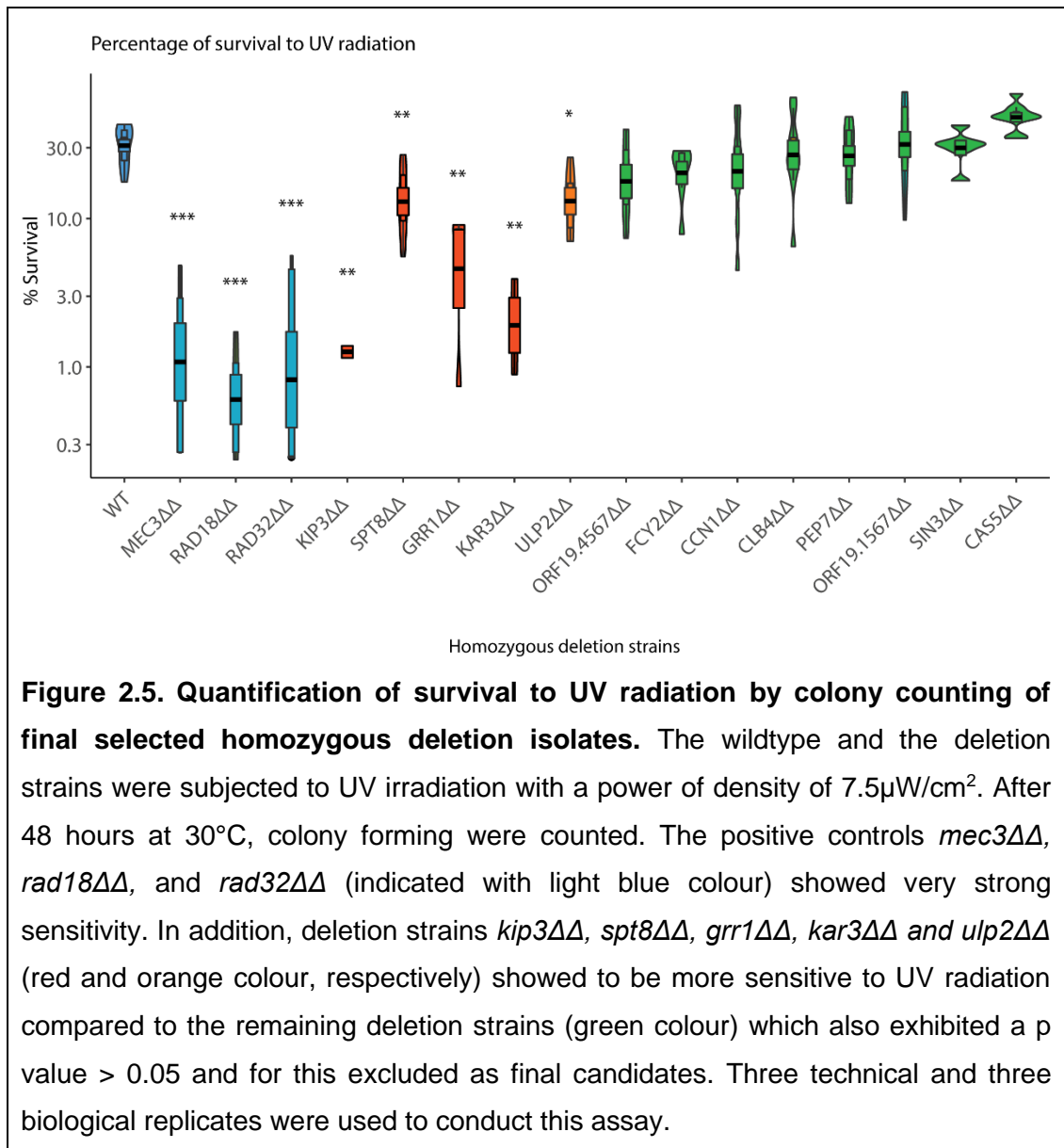
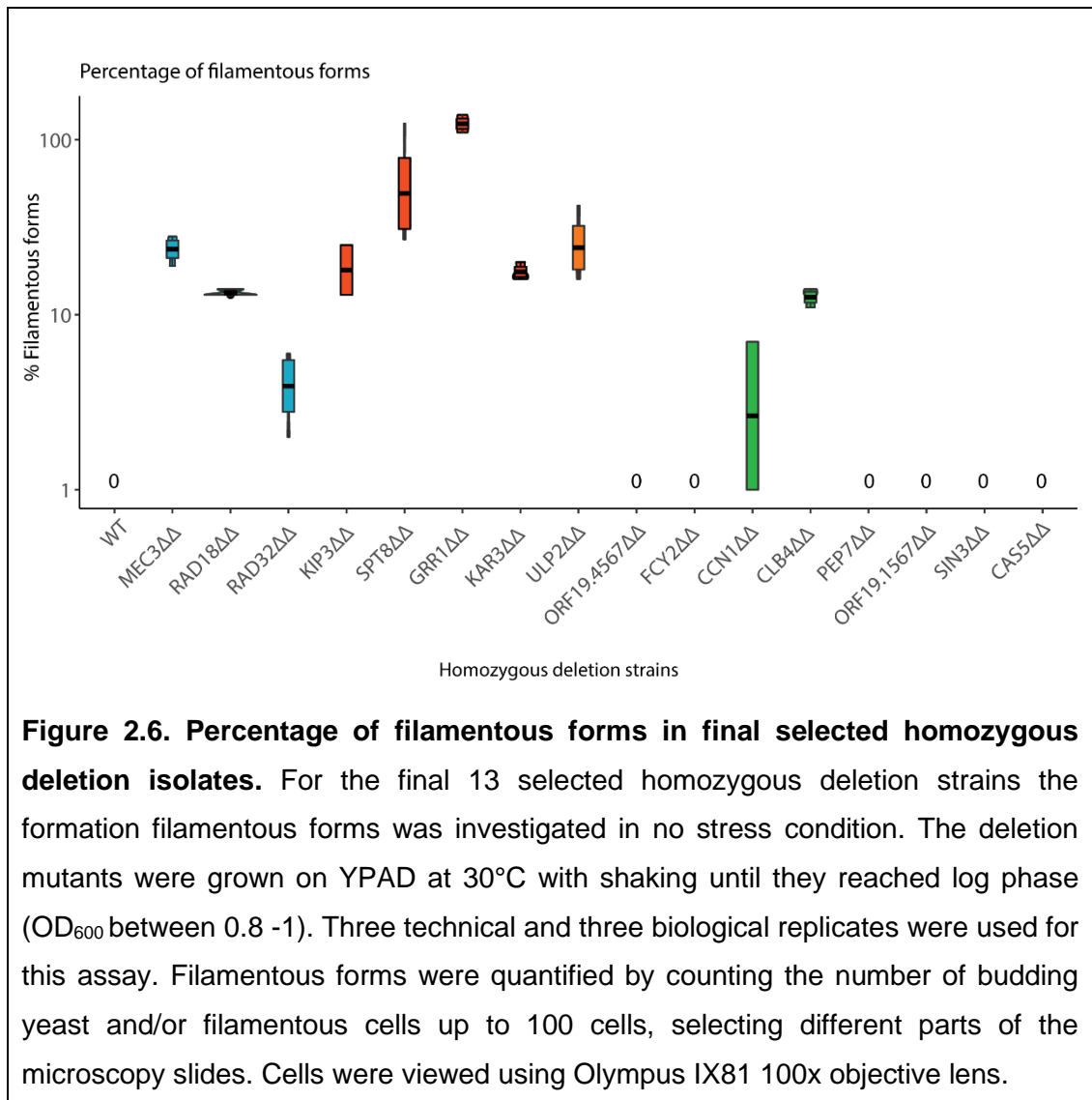


Table 2.8. List of homozygous knockout isolates selected from step 3.

Mutant No.	Mutant No.
<i>orf19.4567ΔΔ</i>	<i>spt8ΔΔ</i>
<i>kic1ΔΔ</i>	<i>ulp2ΔΔ</i>
<i>fcy2ΔΔ</i>	<i>pep7ΔΔ</i>
<i>kar3ΔΔ</i>	<i>sin3ΔΔ</i>
<i>orf19.1567ΔΔ</i>	<i>clb4ΔΔ</i>
<i>ccn1ΔΔ</i>	<i>kip3ΔΔ</i>
<i>grr1ΔΔ</i>	



Overall, the four steps of this genetic screening subjected to UV radiation as DNA damaging agents led to the identification of five potential candidates as regulators for genome instability in *C. albicans*. More detailed investigation is needed. Further description of roles and functions of the five final selected deletion strains for this UV genetic screening are described in the next section.

2.3 Discussion

The CTG clade contains different opportunistic pathogenic yeast of *Candida* genus including *Candida albicans*. This clade displays a particular genetic code in which the CTG codon is translated as serine instead of

leucine (Santos et al., 2011; TA et al., 2018). Genome instability has been correlated with the yeast belonging to the CTG clade (M et al., 2019; Todd et al., 2019). As genome plasticity is a consequence of DNA damage which is not naturally repaired, this study is using UV light as a DNA damage agent to induce single strand break. The aim is to identify potential novel regulators which may play a role in genome instability in *C. albicans*. To do so, a genetic screening of homozygous deletion strains targeting 674 different genes in *C. albicans* was used.

The genetic screen led to the selection of 13 deletion mutants (Table 2.8) Of the 13 selected mutants, 5 of them (*kip3ΔΔ*, *spt8ΔΔ*, *grr1ΔΔ*, *kar3ΔΔ* and *ulp2ΔΔ*) have exhibited higher sensitivity to UV irradiation with statistically significance. All these 5 potential candidates have shown higher UV radiation sensitivity, and also shown higher filamentous forms compared to wild type. Here the investigation of specific roles for the final 5 candidates is presented.

The first target gene is *KIP3*. Not much information of KIP3 is reported in *C. albicans*, for this protein BLAST analysis have reported 100% identity with *S. cerevisiae* KIP3. Kip3 in *S. cerevisiae*, is involved in mitotic spindle (McCoy et al., 2015). This Kinesin-like protein is part of kinesin-8-family proteins which are necessary to regulate microtubule dynamics (Cottingham and Hoyt, 1997). Accurate chromosome segregation is fundamental during mitosis, to do so sister chromatids need to be orientated on microtubules of the mitotic spindle. Kip3 protein has been shown to play a role during anaphase in synchronize the poleward kinetochore movements (Tytell and Sorger, 2006a). In particular, *kip3* has also shown to play a role in nuclear migration. *Kip3ΔΔ* interferes with movement of the nucleus toward the bud and mitotic spindle orientation (DeZwaan et al., 1997). When considered together, the functions of *KIP3* gene are in accordance with the aim of the study but also with the sources of genome instability. Its highest sensitivity to UV compared to the rest of the selected genes lead to consider this gene as one of the potential candidates for this study.

The second candidate of the UV sensitivity screening is *SPT8* gene. It encodes a subunit of SAGA complex (Spt-Ada-Gcn5-acetyltransferase) which allows the acetylation of H3 histone and deubiquitylation of H2B histones. These two activities, acetylation and deubiquitylation are necessary for transcriptional initiation and elongation (Liu et al., 2019). Interestingly, SAGA may also have a role in preserve the genome integrity. It was shown that deletion of *GCN5* results in the damage to UV irradiation, lacking acetylation to lysine 9 and 14 of H3. In particular, both *GCN5* and *ADA2* may regulate nucleotide excision repair (NER) which removes DNA damage induced by UV radiation (Ferreiro et al., 2006). As demonstrated by (Sterner et al., 1999) double mutant for *spt8ΔΔ* and *gcn5ΔΔ* show severe defective phenotypes under different type of stress, which show that disruption of one subgroups can interfere with the whole SAGA complex. From the same study, it was shown also that Spt8 is crucial for SAGA interaction with TATA binding protein (TBP).

The third candidate is *GRR1*, a component of the F-box protein of SCF ubiquitin-ligase complex. It regulates the stability of several proteins involved in cell division. Grr1 targets *cln1* and *cln2* for degradation, these are two G1 cyclins responsible for regulating the G1/S phase transition. These initial cell cycle steps activate several numbers of genes which are involves in DNA replication and spindle body duplication. DNA damage inhibits the cell cycle by inhibiting the activation of G1/S-cyclin dependant kinase (CDK) complex (JP and S, 2007; Landry et al., 2012; SI, 2003). Additionally, (Butler et al., 2006) showed that deletion of *GRR1* gene leads to pseudo and hyphae forms under normal conditions which associated *GRR1* function in controlling the switch of morphology in *C. albicans*. This is also consistent with the investigation of morphology conducted in this study, indeed *GRR1* mutant was present only in pseudo and hyphae forms as showed in figure 4.2.

The fourth candidate of this genetic screening is *KAR3* gene. In *C. albicans*, *kar3* is required for normal mitotic spindle formation and nuclear division (Meluh and Rose, 1990). In *KAR3* mutant the cells exhibit abnormal morphologies with tendency to form pseudo and hyphae forms, delayed

anaphase, mitotic spindle instability and mitotic arrest (Middleton and Carbon, 1994; Page et al., 1990; Tytell and Sorger, 2006b). In addition, (Sherwood and Bennett, 2008) has shown *kar3* proteins to be localised in the spindle pole bodies in mitotically dividing cells. Defects in mitotic spindle lead cells to abnormal chromosome segregation which lastly lead to genome instability (Skoneczna et al., 2015). The results of *KAR3* mutant, showing sensitivity to UV radiation (figure 2.1 and 2.2) and high formation of filamentous form (figure 4.2) motivate the choice to be a potential candidate.

The last candidate from this genetic screening is *ULP2*. This gene will be further investigated in this thesis (Chapter 4).

2.4 Conclusion and future work

This first UV genetic screening has scrutinised the potential candidates of novel regulators for genome instability in *C. albicans*. From the genetic library containing homozygous deletion strains targeting 674 different genes, five of them showed strong sensitivity to UV radiation. These five potential genes *KIP3*, *SPT8*, *GRR1*, *KAR3*, and *ULP2* demonstrated to be sensitive to UV radiation in all the steps of this genetic screening with cell cycle appearing to be the main role for all the five final candidates. However, no concrete conclusion can be produced at this point as deeper investigations are necessary. To establish the potential candidate which will be then subjected to further analysis, the genetic library is required to be exposed to a different stress condition. In the next chapter, MMS is used as another source of DNA damage. The comparison of the final selected deletion mutants between the two genetic screenings will identify the candidate which will be subjected to further investigation on genome instability.

Chapter 3. MMS stress-induced novel regulators of genome instability

3.1 Introduction

Genome stability is essential for the cell to preserve and transmit the accurate genetic material from generation to generation. Cells can be challenged by extrinsic and intrinsic factors which can result in single strand breaks (SSBs) and double strand breaks (DSBs). This accumulation of DNA lesions can lead to cell death, apoptosis or aberrant proliferation (Symington and Gautier, 2011). To safeguard the genome, cells have evolved two main DNA repair systems to deal and repair DSBs: homologous recombination (HR) and non-homologous end joining (NHEJ) (Jackson, 2002). DNA repair system pathways are further described in section 1.5.3. When DSB DNA damage occurs, the phase of the cell cycle plays a crucial role in the choice of the pathway to use to repair the damage. During S and G₂ phases, HR is the preferred pathway to use due to the availability of the sister chromatids to use as template. The NHEJ pathway is used throughout the cell cycle with more prevalence during the G₁ phase (Symington and Gautier, 2011). The cell responds to the DNA damage by arresting the cell cycle and initiating the whole DNA repair complex. However, when the unrepaired damage persists after 6-8 hours, the cell adapts and continues the cell cycle (Kaye et al., 2004; Morrow et al., 1997; Toczyski et al., 1997). Double strand break DNA when unrepaired can lead to gross chromosomal rearrangements, whole or partial loss of chromosomes. The breakage of a chromosome generates two fragments in which one of them lacks the centromere, leading to a compromised chromosome segregation (Kaye et al., 2004). Errors during the segregation process can lead to imbalances of the genome between the two cells, leading to a phenomenon known as aneuploidy. Aneuploidy leads to an abnormal number of chromosomes in the cells with the gain or loss of the whole chromosome (Aguilera and Gómez-González, 2008). In humans, aneuploidy is the cause of genetic disorders such as Down's syndrome, karyotype mosaicism, and cancer (Ben-David and Amon, 2019; Biesscker and Spinner, 2013; Hassold and Hunt, 2001). A double-edged sword is the acquisition of aneuploidy in the pathogenic yeast *C. albicans* which can have a harmful effect on humans. As widely mentioned before in this thesis, *C. albicans* can develop resistance to antifungal drugs through the acquisition of

a segmental aneuploidy during stressful exposure to fluconazole (Selmecki et al., 2006). The acquisition of *C. albicans* aneuploidy or gross chromosomal rearrangement confers fitness advantages and drug resistance to the pathogen, but at the same time drug resistance represents a worldwide problem for patients with weakened immune system (Diogo et al., 2009; Ene et al., 2018; Forche et al., 2009; Pappas et al., 2018; Smith and Hickman, 2020).

In this chapter, the *C. albicans* gene deletion library is exposed to methyl methanesulfonate (MMS), a DNA damaging agent inducing DSBs. MMS is a DNA alkylating agent which modifies guanine and adenine to 7-methylguanine and 2-methylguanine, respectively. These modified bases lead to base mispairing and replication blocks (Beranek, 1990; Lundin et al., 2005b). In the budding yeast it was seen that low doses of MMS induce DSBs, this might be due to the multiple SSBs (Choy and Kron, 2002). In addition, it was hypothesised that DSBs generated during replication are caused by the MMS-induced SSBs leading to replication fork collapsing and resulting in DSB (Lundin et al., 2005b; Pascucci et al., 2005).

This MMS genetic screening has led to the identification of 4 final candidates: *PPH3*, *PTC2*, *CLB4* and *ULP2*.

3.2 Results

3.2.1 Genetic library and screening procedure

The homozygous *C. albicans* gene deletion library (Noble et al., 2010a) previously used for the UV genetic screening was subjected to a different stress in order to identify novel regulators of genome instability in *C. albicans*. For this second screening, MMS was used as source of damaging agent. The aim of this chapter is to compare the deletion mutants between the two DNA damaging agents used in this study and identify the potential candidate sensitive to UV and MMS.

The process of the MMS screening follows the principle of the UV genetic screening with one less step (screens by colony PCR) caused by the disruption of laboratory closure due to COVID-19 pandemic. Overall, this MMS genetic screening was divided in 3 main steps:

1. *Primary screening*: all the 16 plates of the genetic library were plates in YPAD media with the addition of 0.005% MMS. A first selection of MMS sensitive deletion mutants was performed comparing the sensitive mutants to YPAD plates control. Then, literature research of gene locations and functions was carried to gain an understanding of the existing research and chose which genes location/functions in CC, SR, and NL.
2. *Spotting susceptibility assay*: The mutants selected from the first step of this genetic screening were subjected to a spotting susceptibility assay. The serial dilutions were plated in YPAD and YPAD 0.005% MMS.
3. *Growth curves*: the final selected deletion mutants from the previous 2 steps were screened by the analysing the growth curve in the presence of MMS damaging agent.

From these steps, 40 mutants were selected, the phenotype of these mutants was compared with the phenotype from the UV screening (if available) and further literature research was performed in order to choose

the ideal candidate as regulator of genome instability from the 2 genetic screenings.

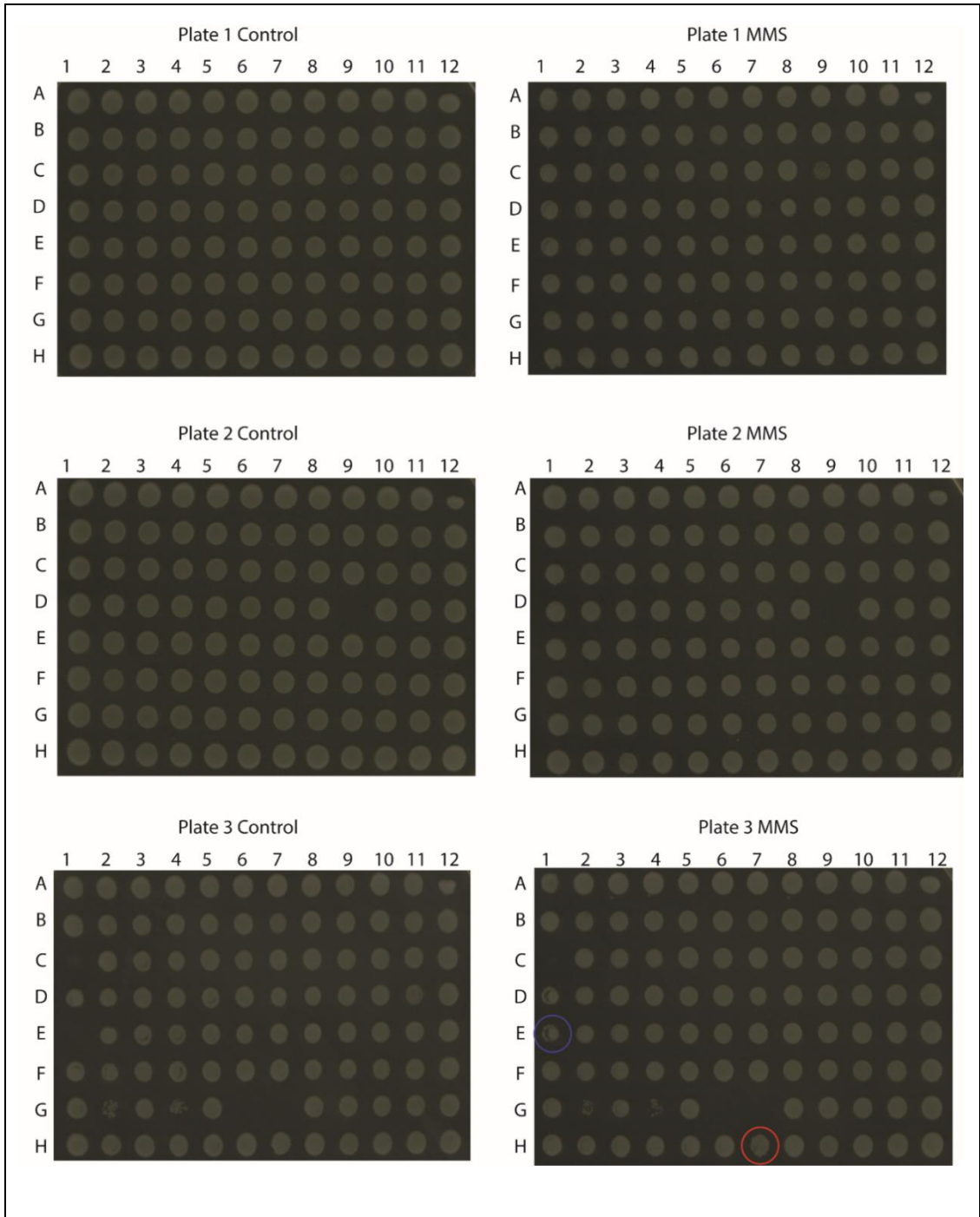
3.1.2 MMS Primary screening

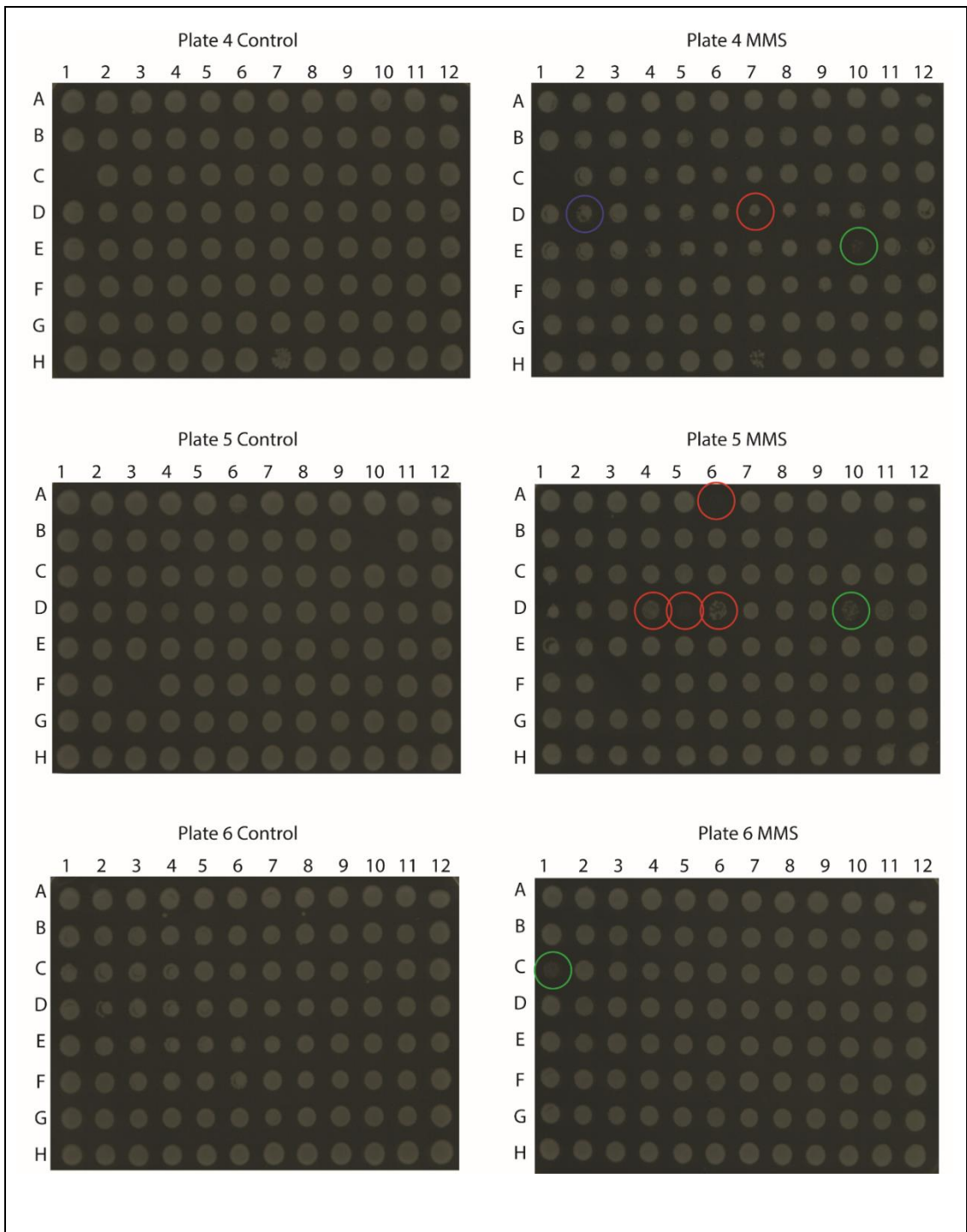
For the first step of this genetic screening the primary investigation of which homozygous deletion strains show sensitivity to MMS was performed. Each library plate, consisting of around 96 different deletion mutants, was spotted in two large petri dishes plates (145x20), one containing YPAD media with 0.005% MMS and the other YPAD media. The strains were spotted using a 96-replica plater and thereafter incubated at for 48h at 30°C (details in section 6.7).

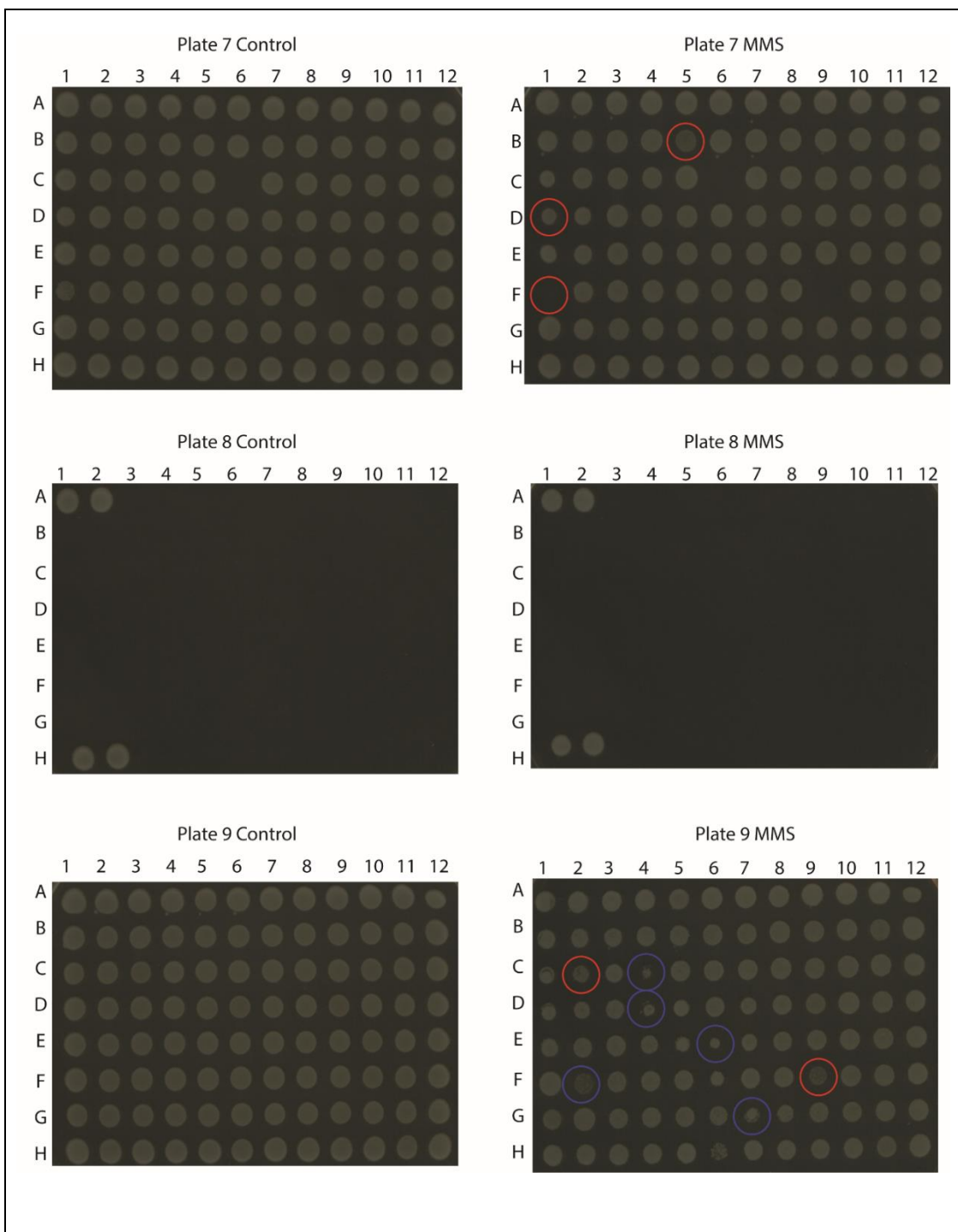
As used in chapter 2 for the UV genetic screening, the same colour code and selection methodology was applied to this chapter as shown in figure 3.1. As mentioned in section 2.2.1, the colour red was used to identify deletion mutants sensitive to MMS drug with functions/location of the deleted gene in line with this study. The colour blue was used to distinguish the deletion strains sensitive to MMS but with functions/location not conforming with the aim of this project. And finally, the colour green was used for DNA repair components deletions strains. The functional groups were kept the same as the one previously mentioned in section 2.2.1, with the addition of: enzymes (ENZ), no defined information (ND), plasma membrane (PLM), and cell wall (CW) indicated with colour blue.

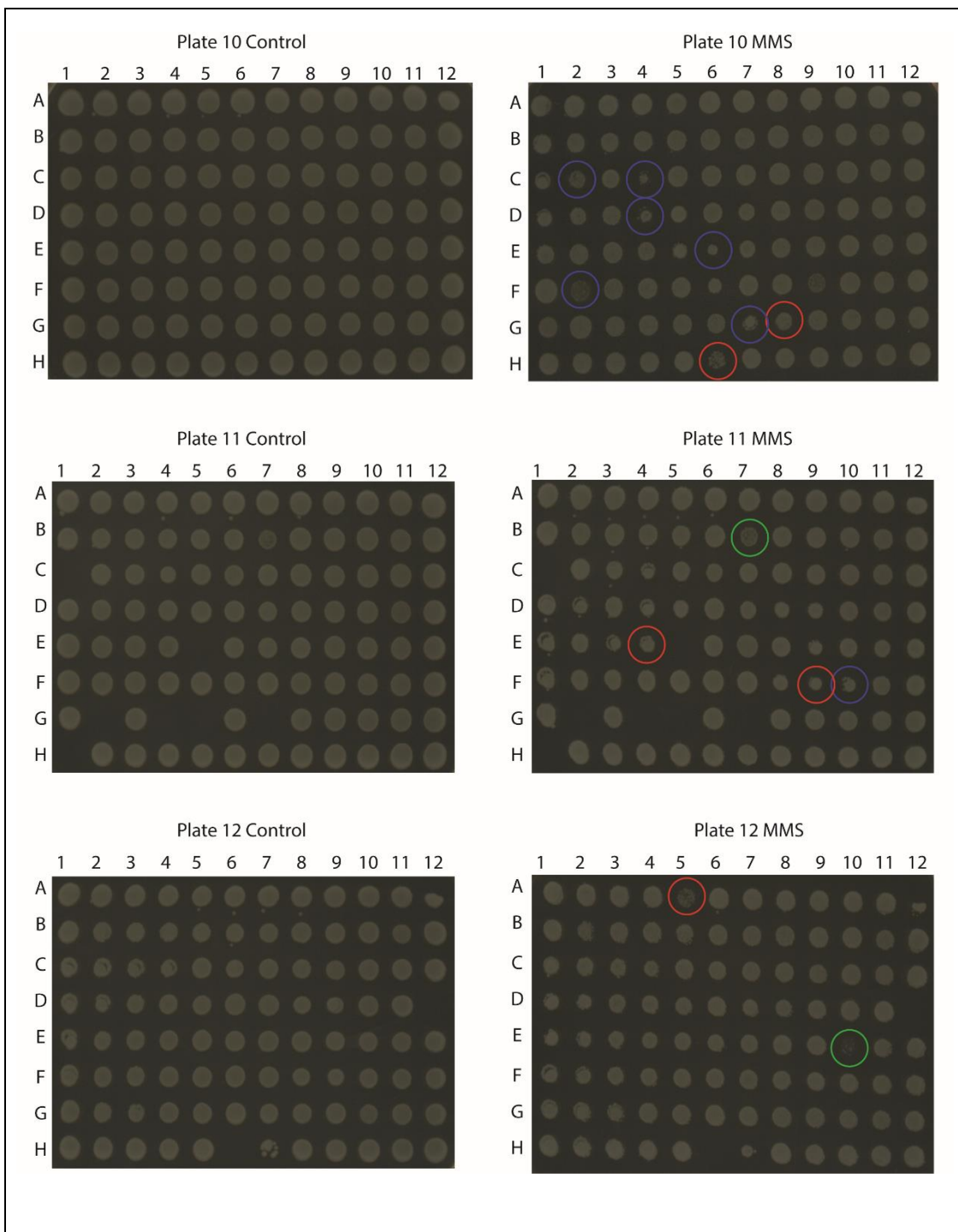
In this first step of the MMS genetic screening a total of 40 deletion mutants (Tables 3.1, 3.2 and 3.3) were identified as being sensitive to the MMS DNA damaging agent (Figure 3.1 red, blue and green circles). From the total of 40 deletion mutants, 19 were indicated with the red circles in figure 3.1 and listed in table 3.1. Of these 14 mutants were also sensitive to UV irradiation. The five mutants sensitive to MMS but not to UV radiation are indicated in table 3.1. All the five deletion mutants sensitive exclusively to the MMS drug were categorised with the functional group of stress response. Of these five, *gpd2ΔΔ* strain (figure 2.1 plate 10 H6) showed sensitivity to MMS

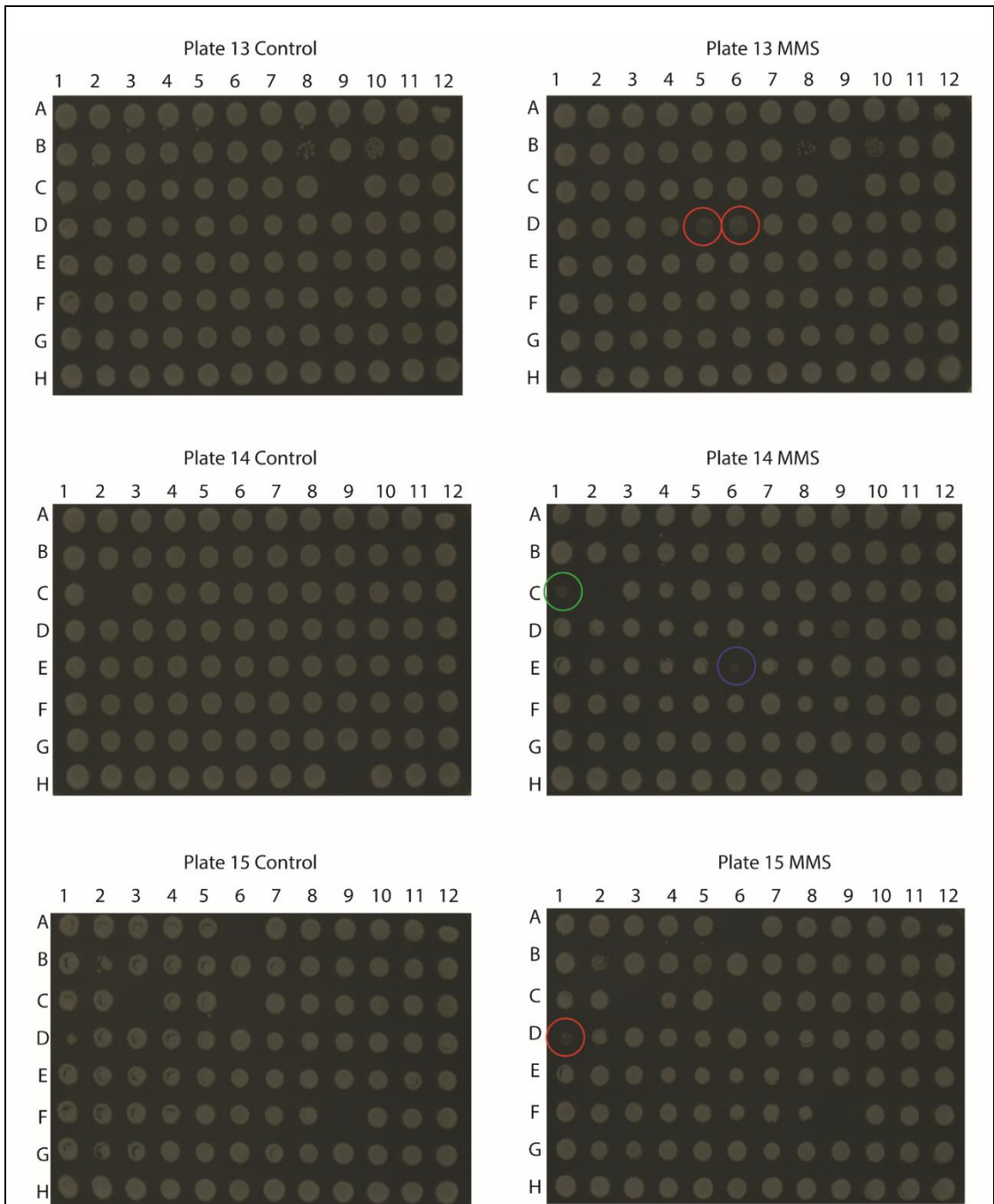
compared to control. The *GPD2* gene plays an important role in osmotic stress adaptation (Enjalbert et al., 2003; Jacobsen et al., 2018a), the *gpd2ΔΔ* sensitivity to MMS might be linked to the fact that hyperosmolarity can cause DNA DSBs (Kültz, 2005). In addition, Gpd2 protein can act as a novel virulence factor which can facilitate *C. albicans* immune evasion (Luo et al., 2013). *Ras1ΔΔ* (figure 2.1 plate 11 E9) is the second deletion mutant which show sensitivity to MMS damaging agent but no sensitivity to UV light. Ras1 is a G-protein which regulates many biological processes such as white-opaque switching and hyphal growth (David, 2013; Piispanen et al., 2013a). Furthermore, the Ras family plays crucial role in regulating adaptations for virulence (Pentland et al., 2018). *Ptc2ΔΔ* deletion mutant (figure 2.1 plate 12 A5) shows sensitivity to MMS. *PTC2* gene regulates DNA damage-related protein phosphatases and it also plays a role in virulence (Feng et al., 2019a). Interestingly, the same study has investigated the virulence in double mutant for *ptc2ΔΔ* and *pph3ΔΔ* showing decreased virulence. *Pph3ΔΔ* deletion strain is another selected mutant sensitive to MMS drug (figure 2.1 plate 5-13 D5). *PPH3* is a gene which play a crucial role in the dephosphorylation of Rad53 after DNA damage (O'Neill et al., 2007). *Pph3ΔΔ* sensitivity to MMS was already documented in Feng et al., 2019a study. The last deletion strain sensitive only to MMS is *ccc1ΔΔ* (figure 2.1 plate 7 B5). *CCC1* is an important component of the Mrs4-Ccc1-Smf3 pathway which is involved in cellular iron level. However, this pathway is crucial also for other biological process such as cell-wall stability, antifungal tolerance, filamentous growth and virulence (Xu et al., 2014). These 19 deletion strains showing sensitivity to MMS were carried for the next steps of the MMS genetic screening.











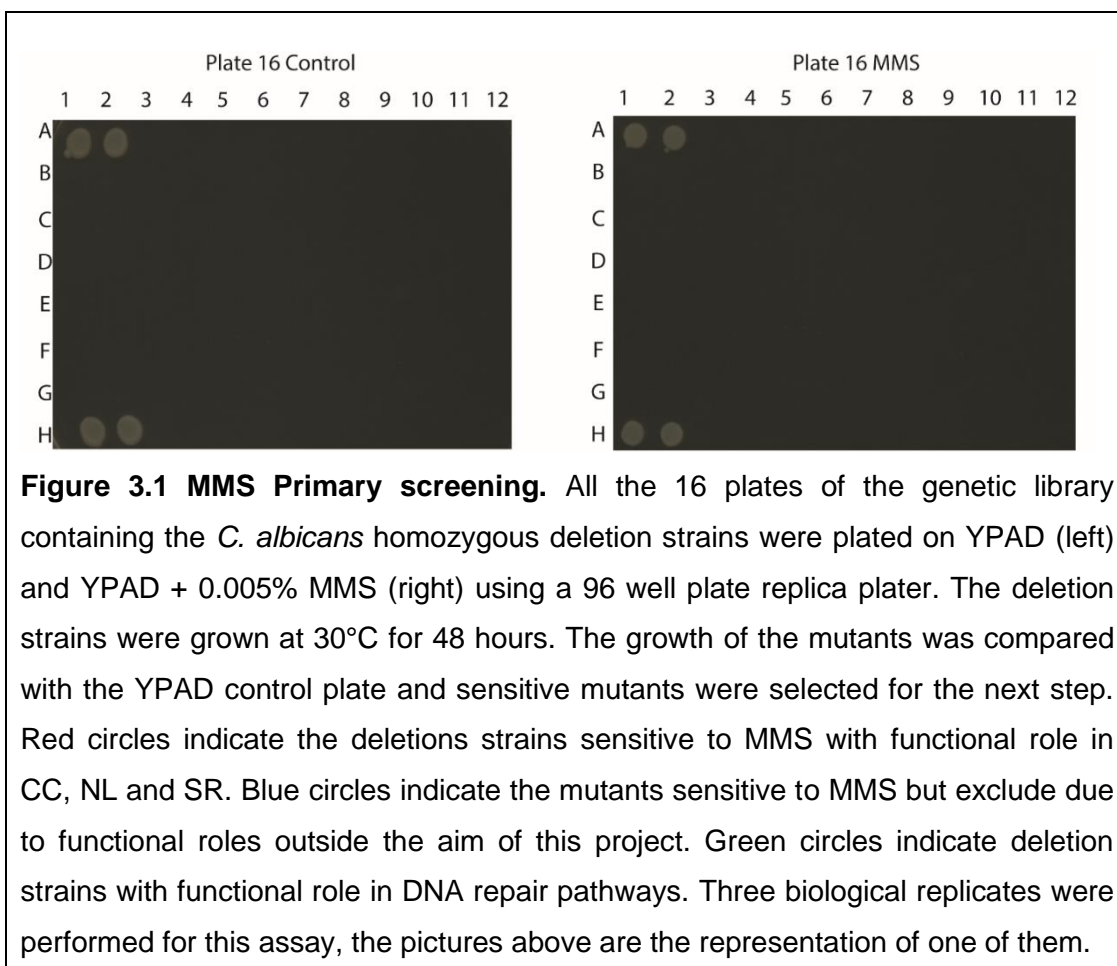


Table 3.1: Mutants indicated with red circle for MMS screening in figure 3.1. The mutants in this table were identified with the functional group of stress response (SR), cell cycle (CC) and nuclear localisation (NL). These deletion mutants showed sensitivity to UV and/or MMS drug, therefore they were selected for the next step.

Plate number	Mutant No.	Systematic name	Gene name	Well No.	Relevant role for the genetic screening	Functional group	DNA damage agent sensitivity
3	493	ORF19.2378		H7	Protein abundance increases upon DNA replication stress in <i>S.</i>	SR	UV, MMS

					<i>cerevisiae</i> (Tkach et al., 2012)		
4	584	ORF19.3207	CCN1	D7	G ₁ cyclin, important for transition G ₁ /S phase (Sinha et al., 2007) (J. Loeb et al., 1999a)	CC, NL	UV, MMS
5	674	ORF19.3944	GRR1	A6	F-box protein component of the SCF ubiquitin-ligase complex required for cell cycle progression (Lu et al., 2019)	CC, NL	UV, MMS
5	729	ORF19.4312	SPT8	D4	TBP-binding transcription coregulator involved in histone acetylation, chromatin organization (Belotserkovskaya et al., 2000), subunit of SAGA complex, localizes to nucleus (Bhaumik and Green, 2002)	NL	UV, MMS
5 - 13	733	ORF19.4350	PPH3	D5	Mediate genotoxin-induced filamentous growth and regulating Rad53 dephosphorylation (Sun et al., 2011)	SR	MMS
5 - 13	734	ORF19.4353	ULP2	D6	SUMO deconjugation enzyme(Hochstrasser, 2001), involved in cell cycle progression(Li and Hochstrasser, 1999), sequestered to the nucleolus under stress conditions(Sydorsky et al., 2010). Trigger multi chromosome aneuploidy in <i>S. cerevisiae</i> (H.-Y. Ryu et al., 2016)	CC, NL	UV, MMS

7	1037	ORF19.6948	CCC1	B5	Component of Mrs4–Ccc1–Smf3 pathway of cellular iron homeostasis involved in oxidative stress response, cell-wall stability, morphogenesis, and virulence (Xu et al., 2014)	SR	MMS
7 - 15	1064	ORF19.7186	CLB4	D1	cell cycle cyclin (Ofir and Kornitzer, 2010)	CC, NL	UV, MMS
7	1091	ORF19.7353	KIP3	F1	Mitotic spindle organisation (McCoy et al., 2015)	SR, CC, NL	UV, MMS
9	89	ORF19.4567	-	F9	No <i>S. cerevisiae</i> orthologous		UV, MMS
10	253	ORF19.564	KAR3	G8	Microtubule motor protein required for mitotic division (Sherwood and Bennett, 2008)	SR, CC, NL	UV, MMS
10	270	ORF19.691	GPD2	H6	osmotic stress adaptation (Jacobsen et al., 2018b)	SR	MMS
11	379	ORF19.1567	-	E4	vCLAMPs component involved in stress resistance (Mao et al., 2021)	SR	UV, MMS
11	406	ORF19.1760	RAS1	E9	G-protein regulating virulence, filamentous forms, and stress resistance (Piispanen et al., 2013b)	SR	MMS
12	508	ORF19.2538	PTC2	A5	interact with the PP4 complex in the DNA damage response pathway (Feng et al., 2019b)	SR	MMS

Regarding the deletion mutants excluded from the study due to functions/locations outside the aim of this study, a total of 15 homozygous deletion isolates were identified as sensitive to MMS. Of these 15 mutants, only 3 mutants, categorised as transporters, were sensitive to UV radiation and MMS drug: *arr3ΔΔ* (figure 3.1 plate 4 D2), *stt4ΔΔ* (figure 3.1 plate 11 F10), and *dur35ΔΔ* (figure 3.1 plate 14 E6) (table 3.2). Of the remaining 12 deletion mutants, half of them are mutants with no defined information and no *S. cerevisiae* ortholog. All the mutants indicated with blue circles and consequently excluded from this study are reported in table 3.2.

Table 3.2: Mutants indicated with blue circle for MMS screening in figure 3.1. These mutants identified with the functional group of transporters (TR), lipid metabolism process (LMP), vacuole location (VL), enzymes (ENZ), no defined information (ND), plasma membrane (PLM), and cell wall (CW) showed sensitivity to UV and/or MMS drug however they were excluded from this study.

Plate No.	Mutant No.	Systematic name	Gene name	Well No.	Functional role	Functional group	DNA damage agent sensitivity
3	374	ORF19.1497	ZCF6	E1	transcription factor ("Candida Genome Database," n.d.), no defined information	ND	MMS
4	573	ORF19.3122	ARR3	D2	Arsenite transporter (Robert Wysocki et al., 1997)	TR	UV, MMS
9	40	ORF19.1797	-	C4	D-arabinose 5-phosphate isomerase GutQ domain (Tzeng et al., 2002) No <i>S. cerevisiae</i> orthologous	ENZ	MMS
9	55	ORF19.2463	PRN2	D4	No defined information No <i>S. cerevisiae</i> orthologous	ND	MMS
9	71	ORF19.3335		E6	Plasma membrane protein ("Candida Genome Database,"	PLM	MMS

					n.d.) No <i>S. cerevisiae</i> orthologous		
9	80	ORF19.3901	-	F2	No defined information No <i>S. cerevisiae</i> orthologous	ND	MMS
9	101	ORF19.4831	MTS1	G7	Sphingolipid C9- methyltransferase (Oura and Kajiwara, 2010)	LMP	MMS
10	164	ORF19.9470	FAV3	C2	No defined information No <i>S. cerevisiae</i> orthologous	ND	MMS
10	174	ORF19.1066 5	-	C4	Protein of unknown function No <i>S. cerevisiae</i> orthologous	ND	MMS
10	204	ORF19.138	FIG1	D4	Plasma membrane involved in Ca ²⁺ uptake in mating- competent opaque cells (Yang et al., 2011)	PLM	MMS
10	219	ORF19.220	PIR1	E6	Cell wall protein (Martínez et al., 2004)	CW	MMS
10	229	ORF19.328	NPR2	F2	Putative urea transporter (D. H. M. L. P. Navarathna et al., 2011)	TR	MMS
10	251	ORF19.557	-	G7	Protein of unknown function No <i>S. cerevisiae</i> orthologous	ND	MMS
11	415	ORF19.1814	STT4	F10	Putative phosphatidylinositol- 4-kinase (Audhya et al., 2000)	TR, LMP	UV, MMS
14	932	ORF19.5915	DUR3	E6	Putative urea	TR	UV, MMS

			5		transporter in (Kumar et al., 2011)		
--	--	--	---	--	-------------------------------------	--	--

With reference to DNA repair components indicated with the green circles in figure 3.1, except *rad32ΔΔ* (figure 3.1 plates 7-15 G9), all the deletions mutants that were sensitive to UV radiation also showed sensitivity to the MMS drug (table 3.3).

Table 3.3: Deletion mutants indicated with green circle in figure 3.1. The target genes for these mutants are known to play a role in the DNA repair system and for this they were identified with the functional role of DNA repair system component (DRS). The following deletion mutants showed sensitivity to UV and MMS drug.

Plate number	Mutant No.	Systematic name	Gene name	Well No.	Functional role	Functional group	DNA damage agent sensitivity
4 -12	603	ORF19.3407	RAD18	E10	Postreplication repair(S et al., 1993)	DRS	UV, MMS
5	741	ORF19.4412	REV1	D10	Error-free translesion synthesis	DRS	UV, MMS
6 - 14	884	ORF19.5485	MEC3	C1	DNA damage checkpoint (Kondo et al., 1999)	DRS	UV, MMS
11	307	ORF19.895	HOG1	B7	Component of MAP kinase pathway respond to oxidative stress(Haghna zari and Heyer, 2004)	DRS	UV, MMS

3.1.3 MMS Spotting susceptibility assay

The second step of this genetic screening investigates the phenotype of the selected deletion strains growing on solid media containing MMS. Serial dilution of each mutant was spotted on YPAD with the addition of 0.005% MMS and incubated at 30°C for 48h (methodology detailed in section 6.8). Previous verification by PCR of the absence of the target genes

(section 2.2.4) allowed the use of only one copy for the mutants which showed UV and MMS sensitivity. Due to circumstances brought about by the beginning of the global pandemic, it was not possible to test both copies of the five new deletion mutants chosen from step one. Only the DNA damage checkpoint *mec3ΔΔ* strain was used as a positive control as shown in figure 3.2. Also, in this screening the same gradient scale used in chapter 2 was used to classify the phenotype grade for the MMS screening. As mentioned in section 2.2.3, the gradient scale starts from value 4 indicating the strongest phenotype comparable to the positive control, and it ends with value 1 which classifies the phenotype as very similar to wild type. Table 3.4 lists the gradient value of the spotting susceptibility assay for each deletion strains in figure 3.2.

Deletion mutants involved in cell cycle such as *grr1ΔΔ*, *ulp2ΔΔ*, and which showed strong phenotype to UV radiation in figure 2.2 showed also strong sensitivity to MMS in for the spotting susceptibility assay (figure 3.2). The gradients for these deletions' mutants were very similar for both the stresses. The same applies for *spt8ΔΔ*, in which it showed strong phenotype to UV and MMS with sensitivity gradient of value 3. However, the remaining cell cycle mutants, *ccn1ΔΔ* and *clb4ΔΔ*, showed a milder phenotype (value 2) on MMS-containing media. For cells lacking *CLB4* this phenotype is very similar to the one obtained after UV irradiation. While cells lacking *CCN1* showed slightly more sensitivity to UV radiation as shown in figure 2.2.

Regarding the two genes classified with functional groups/protein motifs to be cell cycle, nuclear localisation, and stress response *kar3ΔΔ* and *kip3ΔΔ* showed very different phenotypes. *Kar3ΔΔ* deletion strain didn't show any sensitivity to MMS while it displayed strong sensitivity to UV irradiation. This was not an expected result and it is contrary to the MMS sensitivity of *S. cerevisiae kar3ΔΔ* reported by (Svensson et al., 2011). On the contrary, *kip3ΔΔ* deletion mutant displayed strong sensitivity to UV and MMS as comparable as to positive control *mec3ΔΔ*. The deletion mutant *kip3ΔΔ* was already classified as one of the five final selected mutants from the UV genetic screening (section 2.3) and it looks a good candidate for the next step of this genetic screening.

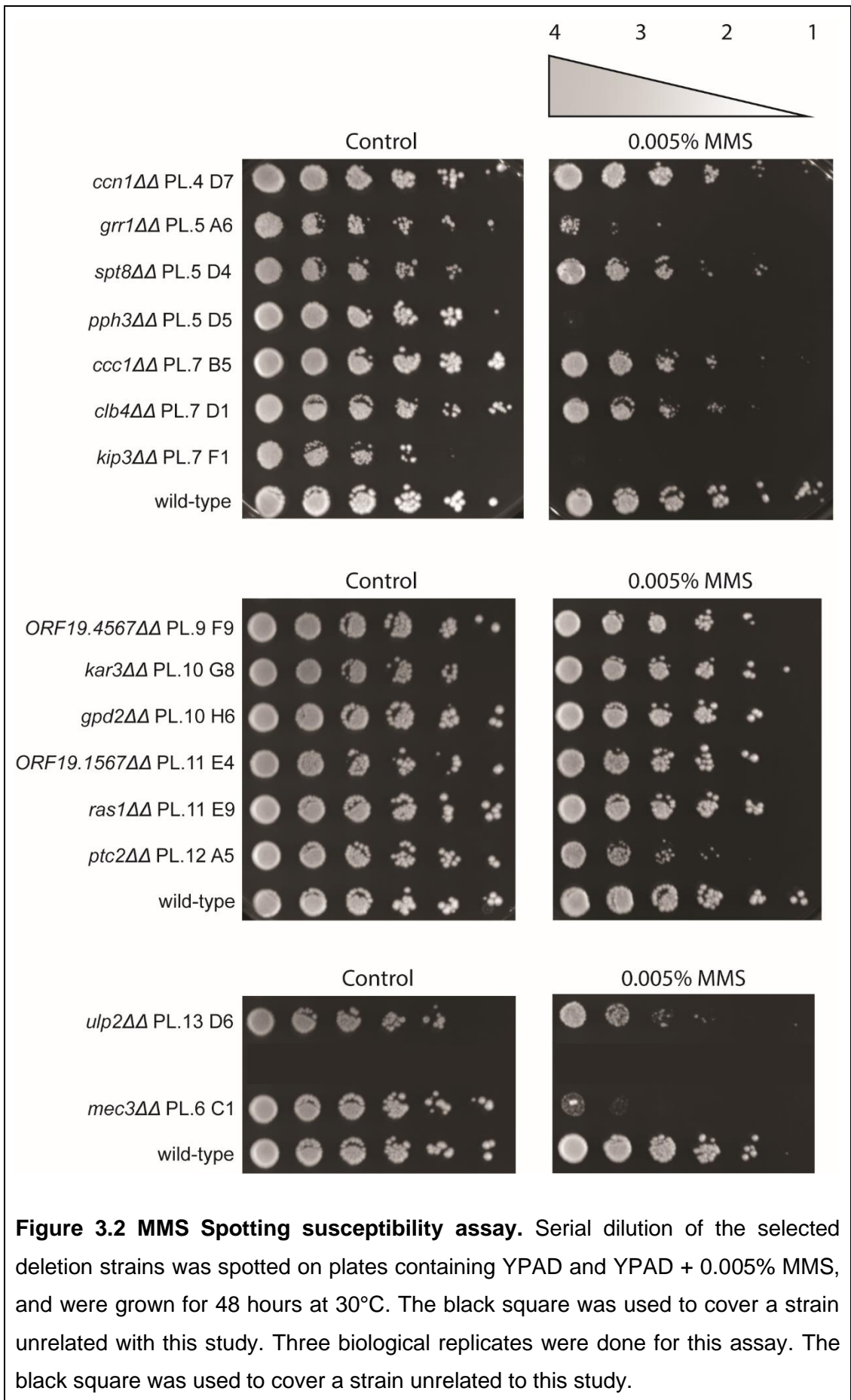


Table 3.4. Gradient of sensitivity to MMS from the spotting susceptibility assay in figure 3.2.

Plate No.	Mutant	Phenotype grade	Plate No.	Mutant No.	Phenotype grade
4	<i>ccn1ΔΔ</i>	2	10	<i>kar3ΔΔ</i>	1
5	<i>grr1ΔΔ</i>	4	10	<i>gpd2ΔΔ</i>	1
5	<i>spt8ΔΔ</i>	3	11	<i>orf19.1567ΔΔ</i>	1
5	<i>pph3ΔΔ</i>	4	11	<i>ras1ΔΔ</i>	1
7	<i>ccc1ΔΔ</i>	2	12	<i>ptc2ΔΔ</i>	3
7	<i>clb4ΔΔ</i>	2	13	<i>pph3ΔΔ</i>	4
7	<i>kip3ΔΔ</i>	4	13	<i>ulp2ΔΔ</i>	3
9	<i>orf19.4567ΔΔ</i>	1	6	<i>mec3ΔΔ</i>	4

Figure 3.2 shows that stress response deletion mutants: *gpd5ΔΔ*, *orf19.1567ΔΔ*, *ras1ΔΔ*, and *orf19.4567ΔΔ* exhibit a very weak phenotype (value 1, table 3.4) in response to MMS. The two deletion strains *orf19.1567ΔΔ* and *orf19.4567ΔΔ* showed weak sensitivity to UV radiation in figure 2.2, which might imply some artefacts in the spotting during the first step of both UV and MMS screening. The deletion mutant *ccc1ΔΔ* exhibited a mild sensitivity to MMS indicated with value 2 in table 3.4. *CCC1* gene encodes for an iron/manganese transporter. In addition, Ccc1 is a component of the Mrs4-Ccc1-Smf3 pathway affecting cellular iron homeostasis (Xu et al., 2014). Therefore, *CCC1* does not seem to have a specific role for the response to DNA damage insults. *Ptc2ΔΔ* deletion strain displayed a sensitivity to MMS classified with value 3. This result is consistent with the study by Feng et al., 2019a where it shows the sensitivity to MMS of *C. albicans ptc2ΔΔ*. In addition, Feng et al., 2019a characterise *PTC2* gene as a potential DNA-damage-related protein phosphatase (Feng et al., 2019a). Furthermore, Leroy et al., 2003 have hypothesised a possible role for *PTC2* in dephosphorylation of Rad53 triggering to inactivation of Rad53-dependent pathway (Leroy et al., 2003). Lastly, *pph3ΔΔ* deletion strain displayed strong sensitivity to MMS as showed in figure 3.2, indicated with the maximum value in table 3.4. This sensitivity is also consistent with

the study by Feng et al., 2019a where in addition it shows *C. albicans* double mutant *ptc2ΔΔ* and *pph3ΔΔ* lead to a decreased virulence in mice.

Following on from these results, the next step was supposed to be the verification of the absence of target genes by PCR colony of *pph3ΔΔ*, *ccc1ΔΔ*, *gpd2ΔΔ*, *ptc2ΔΔ*, and *ras1ΔΔ* homozygous deletion isolates. Unfortunately, I was unable to perform this experiment due to the 2020 Lockdown. For this, the screen of transformants by colony PCR was suspended for the aforementioned deletion strains and the genetic screening continued without verification of the absence of the target genes.

3.1.4 Growth curves analysis

The previous 2 steps of this MMS genetic screening allowed to select a total of 14 /674 genes. From the spotting susceptibility assays, some of the chosen candidates exhibited various phenotypes based on MMS sensitivity. For this, growth curve analysis was performed to examine the growth rate pattern of the deletion mutants, and to compare the mutants' phenotype to the wild type and the positive control *mec3ΔΔ*. As showed in figure 3.3 (A) the wild type showed the typical S shape of the normal growth curve in both YPAD media (blue colour) and in YPAD media with the addition of 0.005% MMS (red colour), (legend at the end of the figure). For the wild type strain (fig 3.3 A) it is possible to distinguish, in both untreated and treated cells, the three major phases of the growth curve: lag, logarithmic, and stationary phase. The presence of MMS in the media causes a longer lag phase. On the contrary, the log phase and stationary phases of a wild type strain growing with and without MMS is very similar. In contrast, the positive control *mec3ΔΔ* strain shows a good growth rate in untreated cells and strong sensitivity to MMS (no S shape) (figure 3.3 B). For this reason, the lag, logarithmic, and stationary phases are not distinguishable for the homozygous deletion strain *mec3ΔΔ* in treated cells. Seeing and considering that the positive controls were used as guide in this genetic screening for the possible candidates of the novel regulators of genome instability, visual analysis and phenotyping comparison with the positive control in MMS media

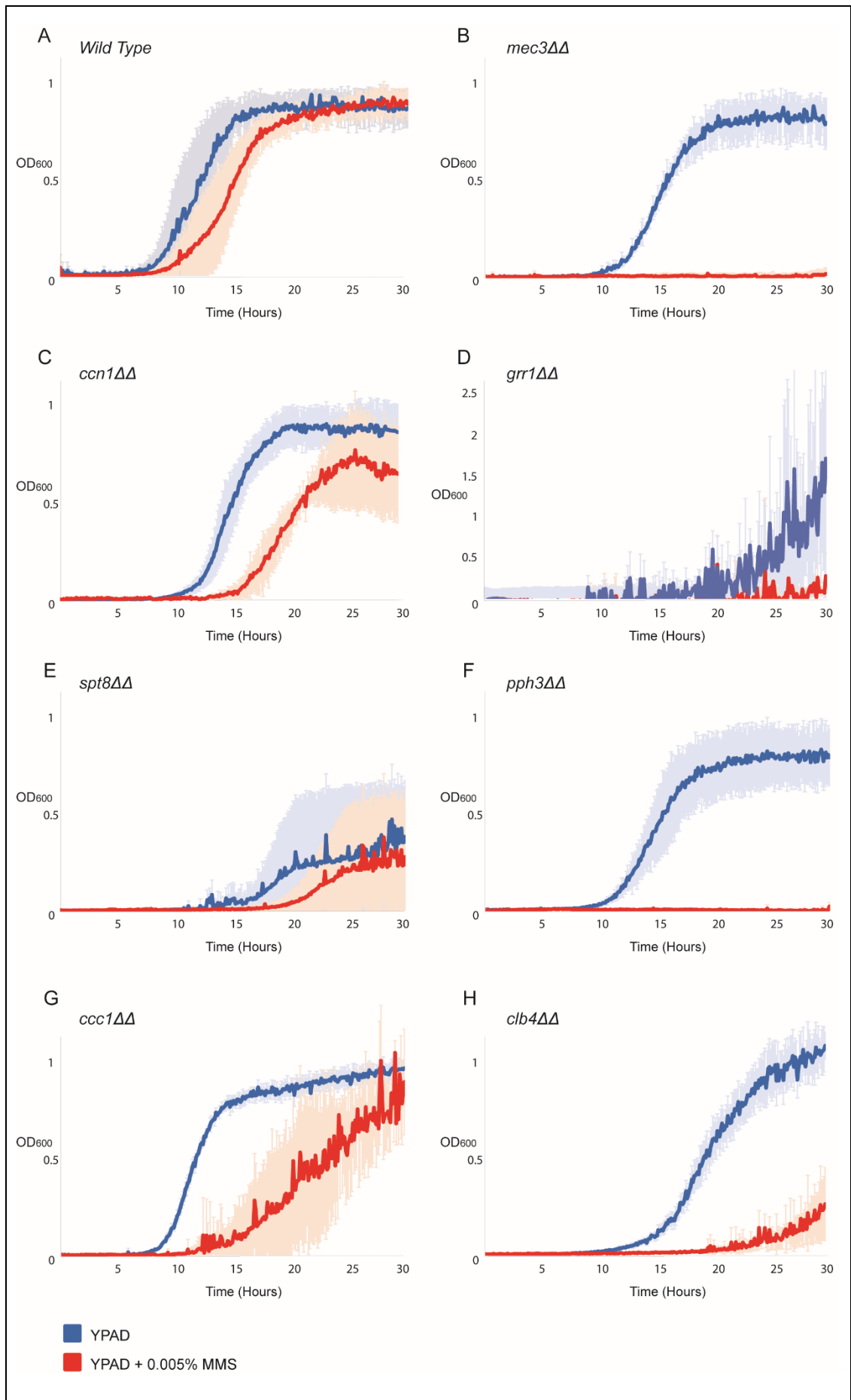
were the parameters used to select for the homozygous deletion strains sensitive to the MMS drug.

Figure 3.3 shows all growth rate curves of the 14 chosen deletion strains. The selected mutants were grown on YPAD and YPAD + 0.005% MMS for 48 hours at 30°C with shaking (methodology detailed in section 6.11). The growth was analysed by the changes of OD₆₀₀ units over the time. As showed in figure 3.3, not all the deletion mutants showed sensitivity to MMS but only 4 exhibited strong sensitivity to MMS (*pph3ΔΔ*, *ptc2ΔΔ*, *clb4ΔΔ*, and *ulp2ΔΔ*). These mutants have the potential to be considered as final candidates for MMS genetic screening.

For the genes classified with the functional group of cell cycle and nuclear localization, cells lacking *CCN1* (figure 3.3 C) show a normal growth in the control media but not much sensitivity to MMS media. This result matches the phenotype shown from this mutant in the spotting susceptibility assay (figure 3.2). However, the lack of MMS sensitivity lead *CCN1* gene to be excluded from the final chosen candidate of this screening.

The deletion mutant *spt8ΔΔ* was considered sensitive to MMS from the spotting susceptibility assay in figure 3.2 (table 3.4 phenotype grade 3). However, cells lacking *SPT8* in the control media YPAD exhibited a strong delay for the start of the log phase with the final OD₆₀₀ around 0.5. A similar result was obtained for *spt8ΔΔ* in media with MMS (figure 3.3 E). Although, *SPT8* gene was one of the five final candidates from the UV genetic screening (chapter 2, section 2.3), considering the weak growth in YPAD control media, this strain cannot be considered as a good final candidate for this genetic screening.

In addition to *SPT8*, another final candidate from the UV genetic screening was *GRR1* (section 2.3). However, the results of *grr1ΔΔ* deletion mutant were inconclusive as figure 3.3 (D) shows, and for this reason it was excluded as final candidate for the MMS screening. The abnormal growth pattern found from the analysis of the growth curve in both YPAD media and MMS media (figure 3.3 D), might be due to the high percentage of filamentous forms of this deletion strain as showed in figure 2.6.



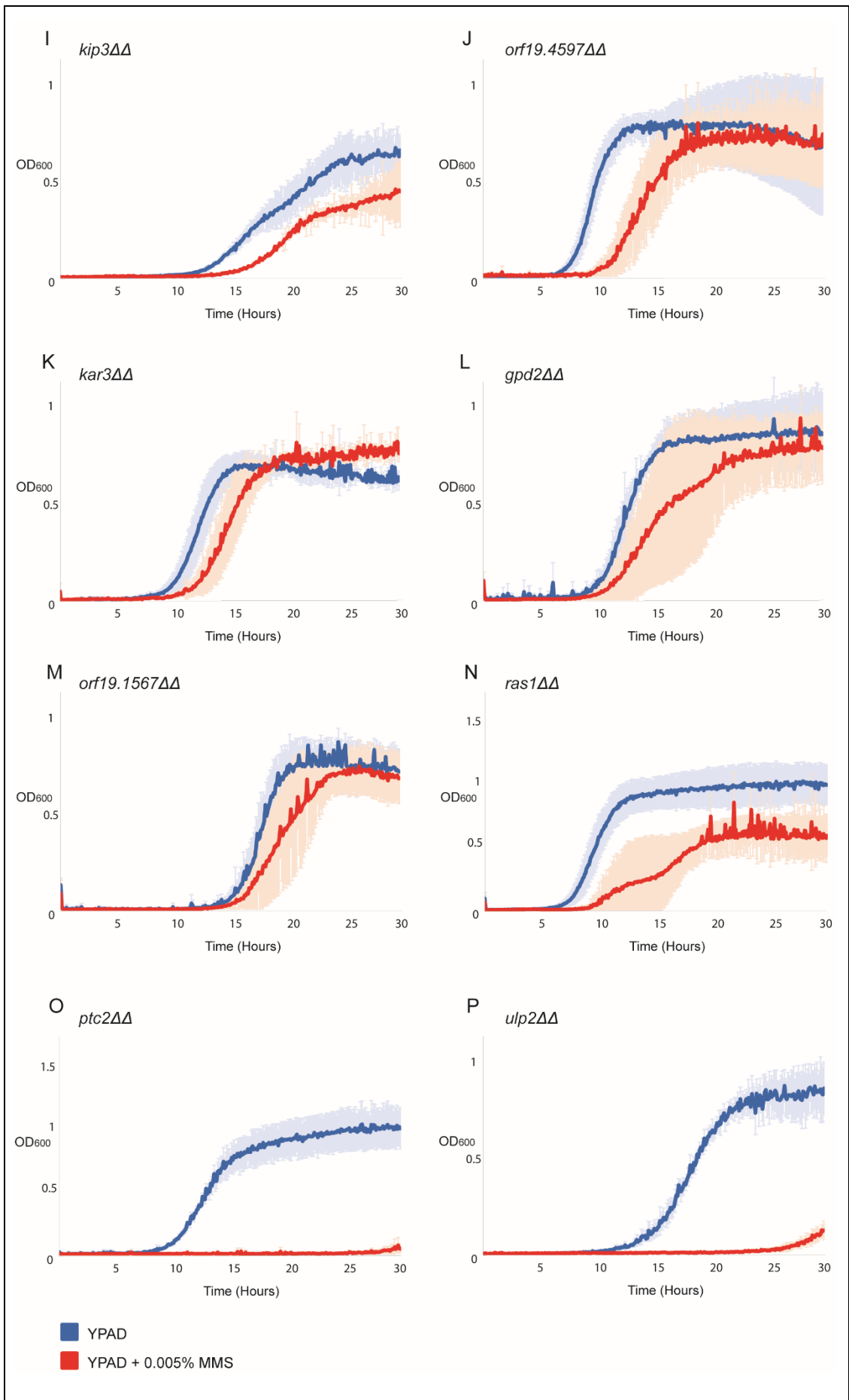


Figure 3.3 Growth curves of *C. albicans* MMS selected strains. The growth curve rate of the selected deletion strains was investigated. Deletion strains were grown at 30 °C with shaking on YPAD media and YPAD + 0.005% MMS. Growth was measured by the changes of OD₆₀₀ units over the time in hours. The growth curve assay was conducted in three technical and three biological replicates.

Interestingly, cells lacking *CLB4* or *ULP2* in figure 3.3 H and P, respectively, showed a very similar phenotype to *mec3ΔΔ* deletion (figure 3.3 B) in media containing 0.005% MMS. These deletion mutants in control media YPAD show normal growth and the typical S shape. More specifically, in YPAD, *clb4ΔΔ* and *ulp2ΔΔ* deletion strains exhibits a prolonged lag phase compared to the wild type (fig 3.3 A). *Clb4ΔΔ* deletion strain showed sensitivity to both UV radiation and MMS drug. The deletion of the target gene does not interfere much with the growth in untreated cells and considering also its crucial role in the cell cycle (Ofir and Kornitzer, 2010) (section 1.2), *CLB4* is considered one of the final potential mutants for this genetic screening. Cells lacking *ULP2* showed strong sensitivity to MMS drug in figure 3.3 (P), in addition it was considered one of the 5 final potential candidates from the UV genetic screening (section 2.3) due to its strong sensitivity to UV radiation. All these results taken in consideration with the role of *ulp2* protein in SUMOylation and chromosome segregation (sections 1.2.2 and 2.5) make *ULP2* gene an ideal final candidate for this genetic screening. This gene will be analysed further in this study.

Regarding the *KIP3* and *KAR3* genes belonging to the functional groups of cell cycle, nuclear localisation, and stress response, the two deletion strains *kip3ΔΔ* and *kar3ΔΔ*, do not exhibit MMS sensitivity (figure 3.3 I and K, respectively). This result, for cell lacking *KAR3*, is in line with the phenotype exhibited in the spotting susceptibility assay (figure 3.2). Despite the fact that *kar3ΔΔ* deletion mutant showed strong sensitivity to UV radiation and for this considered one of the five candidates from the UV genetic screening, the contrary result of non-sensitivity to MMS drug does not allocate *KAR3* as one of the final candidates of the screening. In agreement with this finding, no MMS sensitivity was reported/investigated for

KAR3 gene in *C. albicans*. Similar results are presented for *kip3ΔΔ* deletion mutant. From the figure 3.2 of the spotting susceptibility assay it was expected strong sensitivity to MMS from the analysis of the growth curve for *kip3ΔΔ* deletion strain (figure 3.3 I). However, cells lacking *KIP3* exhibit delayed growth in both untreated and treated cells. Considering the strong sensitivity to UV radiation (figure 2.1 plate 7 well F1, fig. 2.2, 2.5) and MMS drug in the first two stages of this screening (figure 3.1 plate 7 well F1 and fig. 3.2) of cell lacking *KIP3*, and its role in mitotic spindle, anaphase, and nuclear migration (section 2.3), *KIP3* gene could represent an ideal candidate for a potential regulator of genome instability. However, due to laboratory closure it was not possible to verify if the results obtained from the growth curves analysis were a consequence of technical laboratory artefacts. For this reason, with the results obtained *KIP3* is excluded as final candidate of this genetic screening.

Regarding *CCC1* classified in the functional group of stress response, *ccc1ΔΔ* deletion strain shows in figure 3.3 (G) a normal growth rate for untreated cells, but a slower and oblique growth rate in treated cells compared to wild type (fig 3.3 A). The final OD₆₀₀ for treated cells is similar to untreated and this result is comparable to the result in the spotting susceptibility assay (figure 3.2). Due to the lack of strong sensitivity to MMS, *CCC1* is not considered as a final candidate for this screening. The same exclusion is applied for *GPD2*, *ORF19.1567*, and *RAS1* (fig 3.3 L, M, N respectively). All three didn't show strong sensitivity to MMS spotting susceptibility assay (figure 3.2) but also in the growth curves rate (figure 3.3). From the same stress response functional group, *PPH3* and *PTC2*, instead have shown to be two potential final candidates from the genetic screening. Cell lacking *PPH3* (fig 3.3 F) or *PTC2* (fig 3.3 O) showed good growth rate for untreated cells and strong sensitivity for treated cells with phenotype similar to the positive control (fig 3.3 B).

Lastly, *ORF19.4597* didn't show any sensitivity to MMS in either spotting susceptibility assay (fig 3.2) nor in the analysis of the growth rate (figure 3.3 J). For this, it is also excluded from the final candidates.

In conclusion, taken into consideration the results from the previous UV genetic screening, 4 out of 14 selected candidates (*PPH3*, *PTC2*, *CLB4* and *ULP2*) are considered the final candidates of this genetic screening. In the next section, the roles and function of these 4 candidates are investigated and discussed.

3.3 Discussion

The genome of *C. albicans* is highly plastic and it can undergo from different small scale DNA mutations to large-scale genome rearrangements such as aneuploidy, gross chromosomal rearrangements or LOH. All these genetic changes arise when the pathogen is in the presence of stress environments such as higher physiological temperature, changes in pH, drugs or microbiota environment (Avramovska and Hickman, 2019a; Berman and Hadany, 2012; Forche et al., 2011). The diverse species of stress conditions that *C. albicans* can encounter in the host leads to a different type of altered genetic response which is then directly correlated to the type of DNA damage induced by the stress condition (Brown et al., 2014). How *C. albicans* stress-induced genome instability is regulated is still unknown. To elucidate this, I have performed a genetic screening using homozygous deletion isolates targeting 674 different genes. For the genetic screening two different type of DNA damaging agents were used: UV radiation (chapter 2) and MMS drug. The screening was divided in 4 steps for the UV genetic screening and 3 steps for the MMS screening. The first step was the primary screening in which all the 16 plates of the genetic library were plated on YPAD following UV irradiation with a power density of $7.5\mu\text{W}/\text{cm}^2$ (figure 2.1) for the UV screening, and on YPAD+0.005% MMS (figure 3.1) for the MMS screening. The plates with the deletion mutants were kept in the dark and grow for 48h at 30°C. Thereafter, identification of the deletion mutants sensitive to UV radiation or MMS were selected for the second step. The second step was characterised by the spotting susceptibility assay in which the selected mutants were subjected to serial dilution and UV irradiate or plated in YPAD+0.005% MMS. Due to COVID-19 laboratory closure, the third

step was possible to be performed only for the UV genetic screening. The third step investigated the absence of the target genes by colony PCR. The last step was to quantify the survival to UV radiation and the growth rate to MMS, respectively for the UV genetic screening and for the MMS genetic screening. From these steps a final selection of 5 homozygous deletion isolates were identified from the UV genetic screening. While, from the MMS genetic screening a final of 4 deletion isolates were selected. The functions of 5 final candidates from the UV genetic screening are described in section 2.3. Regarding the MMS genetic screening, the 4 final candidates are: *PPH3*, *PTC2*, *CLB4* and *ULP2*.

The first gene to be described is *PPH3*. The deletion mutants for *PPH3* gene showed strong sensitivity from the primary screening (figure 3.1 plate 5 and 13 well D5), followed from the strong phenotype similar to the positive control *mec3ΔΔ* for the spotting susceptibility assay (figure 3.2) and the growth curve rate (figure 3.3). In *C. albicans*, the MMS sensitivity of *PPH3* deletion strain was already reported by Feng et al., 2019a. Studies have reported that Pph3 forms a phosphatase complex with Psy2 and this complex is involved in Rad53 dephosphorylation after DNA damage, especially as response to the DNA-damaging agent MMS (Wang et al., 2012) (O'Neill et al., 2007). However, due to laboratory closure it was not possible to verify the absence of the gene by colony PCR and the presence and/or quantification of filamentous forms. As a result of this, *PPH3* gene could not be considered as a final candidate from this genetic screening.

The second gene is *PTC2*. This gene has showed strong MMS sensitivity in all the steps of this MMS screening (figure 2.1 plate 12 well A5, figure 3.2 and 3.3). It was reported by Feng et al., 2019 that the double mutation of *ptc2ΔΔ* and *pph3ΔΔ* exhibit reduce virulence in *C. albicans* (Feng et al., 2019a). However, as for *PPH3*, with *PTC2* deletion mutants it was not possible to verify the presence of the deleted gene in the genome and the formation of filamentous forms. For these reasons, the results are uncertain and *PTC2* gene was excluded as potential candidate.

The third gene is *CLB4*. Clb4 is a G₂ cyclin which is also detected in the early S-phase (Ofir and Kornitzer, 2010). Clb4 together with Clb2 inhibits the polarised growth and induce the isotropic bud expansion (Bensen et al., 2005). From this study, *CLB4* deletion strains showed sensitivity to both UV radiation and MMS. From the primary screening of both UV and MMS genetic screening (figures 2.1 and 3.1 plate 7 and 15 well D1), *CLB4* showed a mild sensitivity which was classified with value 2 out of 4 in the spotting susceptibility assays for both the stresses (figures 2.2 and 3.2). It exhibited a percentage of survival to UV radiation (figure 2.5) which was higher compared to the positive control but similar to the wild type. On the subject of filamentous forms, *CLB4* displays a higher percentage compared to the wild type but lower compared to the positive control. However, *CLB4* deletion mutant showed strong sensitivity to MMS regarding the growth curve rate as showed in figure 3.3. Despite the results obtained, the mild sensitivity to both UV and MMS are insufficient to considered *CLB4* as a final candidate and therefore potential regulator of genome instability.

The final candidate gene for this genetic screening is *ULP2*. This gene is identified as the potential novel regulator of stress-induced genome instability. The function of *C. albicans ULP2* gene is studied in more detail in this thesis (Chapter 4).

3.4 Conclusion and future work

The second part of the genetic screening identified the final candidate as a potential novel regulator of genome instability in *C. albicans*. From the genetic library containing homozygous deletion strains targeting 674 different genes, *ULP2* was the gene selected after *ulp2ΔΔ* deletions strain showed strong sensitivity to UV and MMS stress. The combination of sensitivity to UV and MMS DNA damaging agents, the specific kinetochore substrates de-SUMOylation, added to the study on *ulp2ΔΔ* leading to chromosome mis-segregation and aneuploidy in *S. cerevisiae* by (Ryu et al., 2020; H. Y. Ryu et al., 2016) provided all the criteria for *ULP2* to be considered as the final

potential candidate. To determine if *ULP2* contribute to the genome plasticity of *C. albicans*, further phenotypic analysis on different genotoxic agents, drug resistance and adaptation is investigated in the next section.

Chapter 4. The SUMO protease Ulp2 regulates genome stability and drug resistance in the human fungal pathogen *Candida albicans*

This chapter contains the preprint article: Marzia Rizzo, Natthapon Soisangwan, Jan Soetaert, Samuel Vega-Estevez, Anna Selmecki and Alessia Buscaino sent to BioRxiv (2021). The SUMO protease Ulp2 regulates genome stability and drug resistance in the human fungal pathogen *Candida albicans*. <https://doi.org/10.1101/2021.12.06.471441>;

Author contributions

MR performed all the experimental work, UV and MMS genetic screenings, new mutants' construction, different genotoxic phenotyping stress assays, serial dilution assays, western blots, fluctuation analysis assays, microscopy cell preparation, drugs resistance over time assays, CHEF and result analysis showed in figures 1 -4 and supplementary figures S1 and S2A.

NS assisted with sequencing analysis showed in figures 3D, 4E, S2B and S3, and bioinformatics

JS assisted with microscopy analysis

SVE assisted with a qPCR assay (not shown)

AS assisted with sequencing analysis and bioinformatics analysis

AB checked and analysed the results, wrote the manuscript.

4.1 Article

1 **TITLE**

2

3 The SUMO protease Ulp2 regulates genome stability and drug resistance in the
4 human fungal pathogen *Candida albicans*

5

6

7 Marzia Rizzo¹, Natthapon Soisangwan², Jan Soetaert³, Samuel Vega-Estevez¹,
8 Anna Selmecki² and Alessia Buscaino^{1#}

9

10 ¹ University of Kent, School of Biosciences, Kent Fungal Group, Canterbury Kent,
11 CT2 7NJ, UK.

12 ² University of Minnesota, Department of Microbiology and Immunology, Minneapolis,
13 Minnesota, United States, 55455

14 ³ Blizard Advanced Light Microscopy (BALM), Queen Mary University of London,
15 London E12AT, UK

16 # Address correspondence to Alessia Buscaino

17 Email: A.Buscaino@kent.ac.uk

18

19

20

21

22

23

24 **Abstract**

25 Stress-induced genome instability in microbial organisms is emerging as a critical
26 regulatory mechanism for driving rapid and reversible adaption to drastic
27 environmental changes. In *Candida albicans*, a human fungal pathogen that causes
28 life-threatening infections, genome plasticity confers increased virulence and
29 antifungal drug resistance. Discovering the mechanisms regulating *C. albicans*
30 genome plasticity is a priority to understand how this and other microbial pathogens
31 establish life-threatening infections and develop resistance to antifungal drugs. We
32 identified the SUMO protease Ulp2 as a critical regulator of *C. albicans* genome
33 integrity through genetic screening. Deletion of *ULP2* leads to hypersensitivity to
34 genotoxic agents and increased genome instability. This increased genome diversity
35 causes reduced fitness under standard laboratory growth conditions but enhances
36 adaptation to stress, making *ulp2 Δ* cells more likely to thrive in the presence of
37 antifungal drugs. Whole-genome sequencing indicates that *ulp2 Δ* cells counteract
38 antifungal drug-induced stress by developing segmental aneuploidies of
39 chromosome R and chromosome I. We demonstrate that intrachromosomal
40 repetitive elements drive the formation of complex novel genotypes with adaptive
41 power.

42

43 Introduction

44 Understanding how organisms survive and thrive in changing environments is a
45 fundamental question in biology. Genetic variation is central to environmental
46 adaptation as it allows selection of certain genotypes better fit to grow in new
47 environments. Different types of genetic change contribute to genetic variability,
48 including (i) mutations such as single-base alteration and small (<100 bp) insertions
49 or deletions (indels), (ii) large (>1 kb) deletions and duplications, (iii) whole-
50 chromosome or segmental-chromosome aneuploidy and (iv) translocations and
51 complex genomic rearrangements [1]. Furthermore, diploid cells can undergo Loss
52 of Heterozygosity (LOH) driven by cross-overs or gene conversions between the two
53 homologous chromosomes [2]. Excessive genome instability is harmful in the
54 absence of selective pressure as it alters the copy-number of many genes, leading to
55 unbalanced protein levels [3]. However, an unstable genome can provide rapid
56 adaptive power in hostile environments [4,5] because it provides genetic diversity
57 upon which selection can act.

58 Genome plasticity – the ability to generate genomic variation – is emerging as a
59 critical adaptive mechanism in human microbial pathogens that need to adapt rapidly
60 to extreme environmental shifts, including changes in temperature, pH and nutrient
61 availability following colonisation of different host environments [6,7]. One such
62 organism is *Candida albicans*, the most common human fungal pathogen and the
63 most prevalent cause of death due to fungal infection. *C. albicans* is part of the
64 normal microflora of most healthy individuals where it colonises the skin, mucosal
65 surface, gastrointestinal and the female genitourinary tract. However, *C. albicans*
66 can become a dangerous pathogen causing a wide range of infections, from
67 superficial mucosal infections to life-threatening disseminated diseases [8]. Azole
68 antifungal agents, such as Fluconazole (FLC), are the most commonly prescribed
69 drugs for treating *Candida* infections [9–11]. FLC targets the enzyme lanosterol 14 α -
70 demethylase, encoded by *ERG11*, blocking biosynthesis of ergosterol, an essential
71 component of the fungal cell membrane [12,13]. As a result, FLC arrests *C. albicans*
72 cell growth without killing the fungus. This fungistatic, rather than fungicidal, mode of
73 action allows for the evolution of drug-resistant strains [14]. One primary mechanism
74 of drug resistance is an increased production of the FLC target, Erg11 enzyme,
75 diluting the activity of the drug [12]. This high target production is often due to

76 increased activity of the transcription factor Upc2 activating *ERG11* transcription [15–
77 18]. Overproduction of efflux pumps, such as the *C. albicans* proteins Cdr1, Cdr2 and
78 Mdr1, can also drive FLC resistance by decreasing intracellular FLC levels [19].
79 In recent years, genome plasticity has emerged as a critical adaptive mechanism
80 causing antifungal drug resistance. *C. albicans* is a diploid organism with a highly
81 heterozygous genome organised into 2×8 chromosomes ($2n = 16$) [20,21].
82 Population studies have identified a remarkable genomic variation among *C.*
83 *albicans* isolates and specific chromosomal variations are selected during host-niche
84 colonisation [22–28]. Indeed, many drug-resistant isolates exhibit karyotypic
85 diversity, including aneuploidy and gross chromosomal rearrangements that can
86 confer resistance due increased copy number of specific genes including *ERG11*,
87 and/or multidrug transporters [7,29,30].

88 *C. albicans* genome instability is not random: it occurs more frequently at specific
89 hotspots that are often repetitive [31–35]. Subtelomeric regions and the *rDNA* locus
90 are among the most unstable genomic sites [34,36]. Indeed, *C. albicans*
91 subtelomeric regions are enriched in transposons-derived repetitive sequences and
92 protein-coding genes [31,37]. Most notable are the telomere-associated *TLO* genes,
93 a family of 14 closely related paralogues encoding proteins similar to the Mediator 2
94 subunit of the mediator transcriptional regulator [38–40]. The majority of *TLO* genes
95 are located at subtelomeric regions except *TLO34*, located at an internal locus on
96 the left arm of Chr1 [38]. The number and position of *TLO* genes vary widely
97 between clinical isolates, indicating significant plasticity with potential consequences
98 for the fitness of the organism [34]. The *rDNA* locus consists of a tandem array of a
99 ~ 12 kb unit repeated 50 to 200 times on chromosome R; *rDNA* length
100 polymorphisms occur frequently [21,34]. In addition to these complex repetitive
101 elements, different types of Long Repeat Sequences (65 bp to 6.5 Kb) dispersed
102 across the *C. albicans* genomes have been shown to drive karyotype variation
103 during adaptation to antifungal drugs and passage through the mouse host [32,33].
104 *C. albicans* genome plasticity is regulated by environmental conditions: the genome
105 is relatively stable under optimal laboratory growth conditions but becomes more
106 unstable under stress conditions [41,42]. For example, FLC treatment drives a global
107 increase in LOH, chromosome rearrangements and aneuploidy [41,42]. This
108 increased genetic variation facilitates selection of fitter genotypes [28,29]. Similarly,

109 higher rates of genomic variation are detected following passage of *C. albicans* *in*
110 *vivo* relative to passage *in vitro* [35,43]. It is unknown if and how stress regulates
111 genome plasticity. The discovery of such regulatory mechanisms will be essential to
112 reveal how resistance to antifungal drugs emerges.

113 This study posits that gene deletions for critical regulators of *C. albicans* genome
114 integrity would cause higher genome variation and rapid adaptation to FLC. To test
115 this hypothesis, we performed a genetic screen to identify modulators of *C. albicans*
116 genome stability. The screen led to the identification of the SUMO protease Ulp2. In
117 the absence of stress, *ULP2* deletion leads to elevated genome instability causing
118 fitness defects and hypersensitivity to genotoxic agents. In contrast, the elevated
119 genome instability of the *ulp2* Δ/Δ strain is advantageous in the presence of high FLC
120 doses. This is because the increased genetic diversity expands the pool of
121 genotypes upon which selection can act, driving adaptation to a new stress
122 environment (FLC), concomitantly rescuing the fitness defects associated with *ULP2*
123 deletion. We also demonstrate that intrachromosomal repetitive elements are sites of
124 genetic diversity that drive the formation of complex novel genotypes with adaptive
125 potential.

126 Results

127 *A systematic genetic screen identifies the Ulp2 as a regulator of C. albicans* 128 *genotoxic stress response*

129 To identify factors regulating *C. albicans* genome integrity, we utilised a deletion
130 library comprising a subset (674/3000) of *C. albicans* genes that are not conserved
131 in other organisms or have a functional motif potentially related to virulence [44]. As
132 defects in genome integrity lead to hypersensitivity to genotoxic agents [45], the
133 deletion library was screened for hypersensitivity to two DNA damaging agents:
134 Ultraviolet (UV) irradiation which induces formation of pyrimidine dimers [46], and
135 Methyl MethaneSulfonate (MMS), which leads to replication blocks and base
136 mispairing [47].

137 Genotoxic stress hypersensitivity was semi-quantitatively scored by comparing the
138 growth of treated versus untreated on a scale of 0 to 4, where 0 indicates no
139 sensitivity, and 4 specifies strong hypersensitivity (Fig 1A). The screen identified 32
140 gene deletions linked to DNA damage hypersensitivity (UV or MMS score ≥ 2).

141 Almost half of these hits (14/32; ~44%) are genes predicted to encode components
142 of the DNA Damage Response pathway (7/32; ~22%) or the cell division machinery
143 (7/32; ~22%) (Table S1). For example, the top 4 hits of the screen were *MEC3*,
144 *RAD18*, *GRR1* and *KIP3* genes. Although *C. albicans MEC3* and *RAD18* are
145 uncharacterised, they encode for proteins, conserved in other organisms, that are
146 universally involved in sensing DNA damage (Mec3) [48] and in DNA post-replication
147 repair (Rad18) [49]. *C. albicans GRR1* and *KIP3* are required for cell cycle
148 progression [50] and mitotic spindle organisation, respectively [51] (Fig 1B and
149 Table S1). ~25% (8/32) of the remaining hits are genes encoding proteins with no
150 apparent orthologous in the two well-studied yeast model systems (*S. cerevisiae* and
151 *S. pombe*). This high percentage is not surprising as one of the criteria used to select
152 target genes for the deletion library was the lack of conservation between *C. albicans*
153 and yeast model systems [44]. The remaining 10 hits are genes encoding for
154 proteins with diverse functions, including stress response (*HOG1*) [52],
155 transcriptional and chromatin regulation (*SPT8*, *SET3*) [53–55], transport (*YPT7*,
156 *DUR35*, *NPR2*, *FCY2*) [56–59], protein folding (*HCH1*) [60], MAP kinase pathway
157 (*STT4*) [61] and cell wall biosynthesis (*KRE5*) [62].

158 One of the highest-ranked genes on our screen is *ULP2* (CR_03820C/ *orf19.4353*:
159 EMS score:3, UV score:3) encoding for a SUMO protease (Fig 1C). SUMOylation is
160 a dynamic and reversible post-translation modification in which a member of the
161 SUMO family of proteins is conjugated to target proteins at lysine residues by E1
162 activating enzymes, E2 conjugating enzymes and E3 ligases [63–65]. SUMO
163 proteases remove the polypeptide SUMO from target proteins, regulating their
164 function, activity or localisation [66,67].

165 *C. albicans ULP2* is an excellent candidate for a modulator of stress-induced
166 genome plasticity for several reasons: (i) post-translation modifications (PTMs), such
167 as SUMOylation, are rapid and reversible. Consequently, PTMs can modulate
168 genome instability in response to rapid and transient environmental changes [68,69],
169 (ii) protein sumoylation is emerging as a critical stress response mechanism across
170 eukaryotes [66,70–73] (iii) *C. albicans* protein sumoylation levels change in response
171 to environmental stresses encountered in the host [74].

172 Colony-Forming Unit (CFU) assays of UV-treated cells confirm the importance of
173 *ULP2* in DNA damage resistance as UV treatment reduced the number of CFU in a
174 *ulp2 Δ/Δ* strain (~14.5% survival) compared to a wild-type (WT) strain (~33.7%

175 survival:) (Fig 1D). Furthermore, the *ulp2* Δ/Δ strain also displayed a reduced growth
176 rate in liquid media containing MMS or Hydroxyurea (HU), a chemotherapeutic agent
177 that challenges genome integrity by stalling replication forks [75] (Fig 1E and 1F).
178 Thus, *ULP2* has a role in the response to a wide range of genotoxic agents.

179 *ULP2 but not ULP1 is required for survival under stress*

180 *C. albicans* contains three putative SUMO-deconjugating enzymes: Ulp1, Ulp2 and
181 Ulp3 (Fig 2A). Sequence comparison between the three *C. albicans* Ulp proteins
182 and the two *S. cerevisiae* Ulps (Ulp1 and Ulp2) reveals that although the *C. albicans*
183 proteins are poorly conserved, the amino acid residues essential for catalytic activity
184 are conserved. This analysis suggests that all *C. albicans* Ulps are active SUMO
185 proteases (Fig 2A and 2B). Accordingly, recombinantly expressed *C. albicans* Ulp1,
186 Ulp2 and Ulp3 have SUMO-processing activity *in vitro* [76]. Similarly to *S. cerevisiae*
187 *ULP1*, *C. albicans* *ULP3* is an essential gene and was not investigated further in this
188 study [77].

189 Previous studies suggested that *C. albicans* Ulp2 is an unstable or a very low
190 abundant protein undetectable by Western blot analysis [76]. We reassessed *ULP2*
191 expression by generating strains expressing, at the endogenous locus, an epitope-
192 tagged Ulp2 protein (Ulp2-HA). Western analyses show that Ulp2-HA expression is
193 readily detected in extracts from independent integrant strains. (Fig 2C). Thus, a
194 stable Ulp2 protein is expressed in cells grown under standard laboratory growth
195 conditions (YPD, 30 °C). To assess whether *C. albicans* *ULP1* and *ULP2* gene share
196 a similar function, we engineered homozygous deletion strains for *ULP1* (*ulp1* Δ/Δ)
197 and *ULP2* (*ulp2* Δ/Δ). Growth analysis demonstrated that deletion of *ULP2* reduces
198 fitness as the newly generated *ulp2* Δ/Δ strain is viable, but cells are slow-growing
199 (Fig 2D and 2E). In contrast, the *ulp1* Δ/Δ strain grows similarly to the WT control in
200 solid and liquid media (Fig 2D and 2E). Phenotypic analysis confirms that *ULP2* is
201 an important regulator of *C. albicans* stress response as, similarly to the deletion
202 library mutant, the newly generated *ulp2* Δ/Δ strain is sensitive to different stress
203 conditions including treatment with DNA damaging agents (UV and MMS), DNA
204 replication inhibitor (HU), oxidative stress (H₂O₂) and high temperature (39°C) (Fig
205 2E) In contrast, deletion of *ULP1* did not cause any sensitivity to the tested stress
206 conditions (Fig 2E).

207 In summary, we could not detect any phenotype associated with deletion of *ULP1*,
208 while loss of *ULP2* leads to poor growth in standard laboratory growth conditions and
209 hypersensitivity to multiple stresses.

210 ***Loss of ULP2 leads to increased genome instability***

211 To assess whether the hypersensitivity to DNA damage agents observed in the
212 *ulp2 Δ/Δ* strain was indeed due to enhanced genome instability, we deleted the *ULP2*
213 gene from a set of tester strains containing a heterozygous *URA3*⁺ marker gene
214 inserted in three different chromosomes (Chr 1, 3 and 7) [41]. We quantified the
215 frequency of *URA3*⁺ marker loss by plating on plates containing the *URA3* counter-
216 selective drug FOA and scoring the number of colonies able to grow on FOA-
217 containing media compared to non-selective (N/S) media. Deletion of *ULP2* leads to
218 a dramatic increase in LOH rate at all three chromosomes (Chr1: ~5000X, Chr3:
219 ~18X, Chr7: ~170X), indicating that *ULP2* is required for maintaining genome
220 stability across the *C. albicans* genome (Fig 3A).

221 In *C. albicans*, hypersensitivity to genotoxic stress often correlates with filamentous
222 growth [45,78–81]. Accordingly, and in agreement with a significant role for *ULP2* in
223 genotoxic stress response, the *ulp2 Δ/Δ* strain displays a higher frequency of
224 abnormal morphologies than a WT strain, including filamentous pseudohyphal-like
225 and hyphal-like cells (Fig 3B). To assess whether the exacerbated *ulp2 Δ/Δ* genome
226 instability is linked to defective chromosome segregation, we deleted the *ULP2* gene
227 in a reporter strain in which *TetO* sequences are integrated adjacent to the
228 centromere (*CEN7*) of one Chromosome 7 homolog and TetR-GFP fusion protein is
229 expressed from an intergenic region [82]. Binding of TetR-GFP to *tetO* sequences
230 allowed visualisation of Chr7 duplication and segregation during the cell cycle. We
231 found that deletion of *ULP2* leads to abnormal Chr7 segregation, including cells with
232 no TetR-GFP signals or multiple TetR-GFP-foci, which was ~5 fold higher in the *ulp2*
233 Δ/Δ strain than the WT control strain (Fig 3C).

234 Previous studies performed in the model system *S. cerevisiae* demonstrated that
235 loss of *ULP2* leads to the accumulation of a specific multichromosome aneuploidy
236 (amplification of both ChrI and ChrXII) that rescues the potential lethal defects of
237 *ulp2* deletion by amplification of specific genes on both chromosomes [83,84]. To
238 determine whether loss of *C. albicans ULP2* results in a specific aneuploidy, we

239 sequenced the genome of 3 randomly selected *ulp2* Δ/Δ colonies by whole genome
240 sequencing (WGS) and compared their genome sequences to the *C. albicans*
241 reference genome. This analysis demonstrates that deletion of *C. albicans* *ULP2*
242 does not select for specific chromosome rearrangements and identifies different
243 genomic variations that are not present in the parental WT strain (Fig 3D and Table
244 S2) [85]. While deletion of *ULP2* leads to very few (<10) *de novo* mutations (Table
245 S2), two of the three colonies underwent extensive LOH on different chromosomes
246 (Fig 3D and Table S2). For example, chromosome missegregation followed by
247 reduplication of the remaining homologue is detected on isolate C1 (C1: ChrR) and
248 the genome of C2 contains a long-track LOH (C2:Chr 3L) that occurred within 4.6 kb
249 of a repeat locus on Chr3L (*PGA18*, [32]) (Fig 3D). Our analysis collectively
250 demonstrates that deletion of *C. albicans* *ULP2* leads to increased genome instability
251 via the formation of extensive chromosomal variation.

252 ***Loss of ULP2 leads to drug resistance via selection of novel genotypes***

253 We hypothesised that the increased genome instability of the *ulp2* Δ/Δ strain would
254 facilitate adaptation to hostile environments via selection of fitter genotypes. To test
255 this hypothesis, we assessed whether WT and *ulp2* Δ/Δ strains differ in their ability to
256 overcome the stress imposed by low or high concentrations of 2 drugs: Fluconazole
257 (FLC) and caffeine (CAF). FLC was chosen because it is the most used antifungal
258 drug in the clinic. CAF was chosen because it is associated with well-known
259 resistance mechanisms [86,87]. Serial dilution analyses demonstrate that the
260 *ulp2* Δ/Δ strain is not sensitive to a low FLC (15 $\mu\text{g}/\text{ml}$) dose while it is sensitive a low
261 CAFF (5mM) doses (Fig 4A and 4B).

262 In contrast, deletion of *ULP2* increases adaptation to high doses FLC and CAF. On
263 plates containing an inhibitory concentration of FLC (128 $\mu\text{g}/\text{ml}$), a WT strain
264 produced only tiny abortive colonies while the *ulp2* Δ/Δ strain produces colonies of
265 heterogenous size (Large and Small, Fig 4C). The starting *ulp2* Δ/Δ strain is highly
266 sensitive to 12 mM CAF (Fig S1A), and therefore a reduced number of *ulp2* Δ/Δ
267 colonies grew at this high drug concentration compared to the WT strain (Fig 4D).
268 Despite this difference, the *ulp2* Δ/Δ strain, but not the WT strain, produces large
269 colonies that can grow on high CAF concentration following passaging in the

270 absence of the drug, indicative of adaptation (Fig 4D, Fig S1B). Thus, deletion of
271 *ULP2* accelerates adaptation to lethal drug concentration.

272 To test whether enhanced drug adaption was linked with selection of novel
273 genotypes, we sequenced the genome of 4 independent *ulp2 $\Delta\Delta$* FLC-adapted
274 isolates (*FLC-1*, *FLC-2*, *FLC-3* and *FLC-4*). *FLC-1*, *FLC-2* and *FLC-3* were randomly
275 selected from the High FLC plates and sequenced immediately. In contrast, *FLC-4*
276 was selected because this isolate was still able to grow on high FLC following
277 passaging in non-selective (N/S) media (Fig S1C). To assess for genotype
278 heterogeneity, three *FLC-4* derived single colonies (*FLC-4a*, *b* and *c*) were
279 sequenced (Fig S2A and B). The WGS analysis demonstrates that all FLC-adapted
280 colonies have a genotype that is distinct from the *ulp2 $\Delta\Delta$* progenitor. We detected
281 very few (<10) *de novo* point mutations, and none of these are common among all
282 the sequenced FLC isolates (Table S3). In contrast, all colonies are marked by an
283 extensive segmental chromosome aneuploidy: a partial deletion (~ 388 Kb) of the
284 right arm of Chromosome R (ChrRR-Deletion). ChrRR-deletion occurs at the
285 ribosomal DNA (25S subunit) and it extends to the right telomere of ChrR
286 (ChrR:1,897,750 bp - 2,286,380 bp), reducing the dosage of 204 genes (Fig 4E,
287 S2A and Table S4). GO analysis revealed that ChrRR-Deletion leads to a reduced
288 dosage of 34/204 genes associated with the "response to stress" pathways and
289 18/204 genes linked to "response to drug" pathways (Table S4). We posit that this
290 reduced gene dosage enables growth in the presence of high FLC. For example,
291 *CKA1*, a gene whose deletion leads to FLC resistance [88], is located within the
292 ChrRR-deletion (Fig 4G).

293 Interestingly, we found that all three *FLC-4* sequences colonies (*FLC-4a*, *b* and *c*),
294 are marked by a second segmental aneuploidy: a partial Chr1 amplification (Chr1-
295 Duplication) (Fig 4E and S2A). This novel Chr1-Duplication amplifies a genomic
296 fragment of ~1.3 Mbp containing 535 protein-coding genes (Table S4). The Chr1-
297 Duplication starts and ends near two distinct DNA repeat sequences with high
298 sequence identity elsewhere in the genome: the 5' breakpoint is within the *TLO34*
299 and its 3' breakpoint is within 3 kb of a *Zeta-1a* Long Terminal Repeat (LTR) (Fig 4G
300 and S3) [32,33,89]. These WGS data led us to hypothesise that a chromosome-
301 chromosome fusion event occurred between the Chr1-Duplication and Chr6 within
302 homologous *TLO* sequences (Fig 4G). Indeed, the *TLO34* gene on Chr1 has high

303 sequence identity with a 380 bp region located at Chr6 (position: 6182-6562 bp). In
304 addition, sequence polymorphisms unique to Chr1-*TLO34* mapped to Chr6 in the
305 *FLC-4* isolate (but not in *FLC-1*, *FLC-2* and *FLC-3*), supporting a novel
306 interchromosomal recombination product between *TLO*-homologous sequences.
307 This model is supported by CHEF gel electrophoresis analyses as, when compared
308 to the *ulp2* Δ/Δ progenitor, the *FLC-4* genome lacks one band corresponding to the
309 shorter Chr6 homologue (blue asterisk), and it contains a new chromosome band of
310 ~2.2 Mb (magenta asterisk) (Fig 4F).

311 We posit that Chr1-Duplication provides a synergistic fitness advantage in response
312 to two independent stressors (the presence of FLC and lack of *ULP2*) by
313 simultaneously changing the dosage of several genes. Indeed, GO analyses
314 demonstrated that 41 genes present in the Chr1-Duplication are associated with a
315 "drug resistance" phenotypes (Table S4). Among these, amplification of *UPC2*
316 encoding for the Upc2 transcription factor is likely to be critical. Indeed, it is well
317 established that *UPC2* overexpression leads to FLC resistance by *ERG11*
318 upregulation [90,91]. Chr1-Duplication likely rescues the fitness defects of the *ulp2*
319 Δ/Δ strain by amplifying two key genes: *CCR4* and *NOT5* (Fig 4G). Ccr4 and Not5
320 are subunits of the evolutionarily conserved Ccr4-Not complex that modulate gene
321 expression at multiple levels, including transcription initiation, elongation, de-
322 adenylation and mRNA degradation [92]. It has been shown that *S. cerevisiae* *CCR4*
323 and *NOT5* overexpression rescue the lethal defects associated with a *ulp2* deletion
324 strain [83].

325 Collectively our data suggest that the combined selective pressure of two
326 independent stresses leads to selection of a chromosome aneuploidy that
327 overcomes both stresses by overexpressing two different sets of genes.

328 Discussion

329 In this study, we demonstrate that the SUMO protease Ulp2 is a critical regulator of
330 *C. albicans* genome plasticity and that the development of drug resistance is
331 accelerated in cells lacking *ULP2*. We unveil a striking flexibility of *C. albicans* cells
332 in their response to complex stresses caused by drug treatment and dysregulation of
333 the SUMO system, leading to the selection of extensive chromosome
334 rearrangements.

335 ***Ulp2 is a critical regulator of C. albicans genome stability***

336 Our study identifies protein SUMOylation as a critical regulatory mechanism of *C.*
337 *albicans* genome stability. SUMOylation is a dynamic and reversible post-translation
338 modification in which a member of the SUMO family of proteins is conjugated to
339 target proteins at lysine residues by E1 activating enzymes, E2 conjugating enzymes
340 and E3 ligases [63–65]. SUMO is removed from its target proteins by SUMO-specific
341 Ulp2 proteases [67]. Several observations are in agreement with our findings and
342 suggest that SUMOylation controls stress-induced genome plasticity. Firstly,
343 SUMOylation is a post-translational modification that is rapid and reversible, an
344 essential requirement for a regulator of stress-induced genome plasticity. Secondly,
345 *C. albicans* protein SUMOylation levels are different in normal and stress growth
346 conditions [74]. Thirdly, deletion of genes encoding other components of the *C.*
347 *albicans* SUMOylation machinery lead to filamentation, a phenotype often associated
348 with defective cell division and compromised genome integrity [74,93,94]. Finally, *C.*
349 *albicans* strains lacking the SUMO (Smt3) protein or the E3 ligase Mms21 display
350 nuclear segregation defects [74,93].

351 *C. albicans* Ulp2 likely controls genome plasticity by modulating SUMO levels of
352 several target proteins. SUMO proteases have a broad substrate specificity
353 catalysing SUMO deconjugation of several substrates [95]. In other organisms, it is
354 well known that SUMOylation modulates pathways ensuring genome integrity,
355 including the DNA damage-sensing and repair pathway and the cell division and
356 chromosome segregation pathway [63–66,96–98]. Despite the broad substrate
357 specificity, our data suggest that one significant function of *C. albicans* *ULP2* is to
358 ensure faithful chromosome segregation as high rates of chromosome
359 missegregation is detected in the *ulp2 ΔΔ* strain. Furthermore, the Illumina Genome
360 sequencing analyses demonstrated that lack of *ULP2* is associated with extensive
361 LOH events. Such extensive genomic changes are reminiscent of catastrophic
362 mitotic events associated with defective chromosome segregation [99,100]. The
363 targets of *C. albicans* Ulp2 are unknown, and it will be important to adopt proteomic
364 approaches to identify the entire repertoire of SUMO targets and determine how
365 *ULP2* contributes to *C. albicans* genome plasticity.

366 ***Complex chromosome rearrangements drive adaptation to multiple stress***
367 ***environments.***

368 Our data demonstrate that the *ulp2* Δ/Δ strain is more likely than the WT parental
369 strain to develop resistance to anti-fungal drugs by selecting specific segmental
370 aneuploidies on ChrR (ChrRR-deletion) and Chr1 (Chr1-duplication). These adaptive
371 genotypes confer a growth advantage in response to two independent stressors: the
372 absence of *ULP2* and drug treatment.

373 In agreement with the notion that repetitive elements play a significant role in
374 genome instability, we identified intrachromosomal repetitive elements as drivers of
375 genome instability. Indeed, all the sequenced *FLC*-adapted isolates carry a partial
376 deletion of ChrR originating within the rDNA locus. We have previously
377 demonstrated that the *C. albicans* rDNA locus is a hotspot for mitotic recombination
378 [36], and clinical isolates are often marked by chromosomal aberrations originating
379 from this locus [34]. This rDNA-driven chromosomal aberration leads to the deletion
380 of one copy of 204 genes. We hypothesise that this reduced gene dosage drives
381 *FLC* adaptation. For example, *CKA1*, one of the genes affected by ChrRR deletion,
382 encodes for one of the two *C. albicans* Casein Kinases (Cka1 and Cka2). Deletion of
383 these genes causes *FLC* resistance by controlling the expression of the efflux pump
384 *CDR1* and *CDR2* [88].

385 WGS analysis demonstrated that the *FLC-4* isolate, whose *FLC* resistance is
386 maintained followed by passaging on non-selective media, carries a second
387 segmental aneuploidy: a partial duplication of Chr1 with breakpoints at repetitive
388 elements. We provide evidence suggesting that Chr1 Duplication results from a
389 fusion event between Chr1 and Chr6 due to a novel interchromosomal
390 recombination product between *TLO* homologous sequences. We hypothesise that
391 Chr1-duplication leads to gene dosage changes that are critical for overcoming two
392 independent stresses: the presence of *FLC* and the absence of *ULP2*. Indeed, one
393 of the master regulators of *FLC* resistance, *UPC2*, is located on the Chr1-duplication
394 and its overexpression is likely to allow growth in the presence of *FLC*. *UPC2*
395 encodes a key transcription factor of *ERG11*, the target of *FLC* [91]. It is well
396 established that *UPC2* deletion leads to increased *FLC* susceptibility and that *UPC2*

397 overexpression causes FLC resistance [91,101]. Accordingly, *UPC2* gain-of-function
398 mutations are prevalent among FLC resistant clinical isolates [101].

399 The Chr1-duplication carries two key genes, *CCR4* and *NOT5*, likely to rescue the
400 fitness defects associated with the *ulp2* Δ/Δ strain. Indeed, it has been shown that
401 *CCR4* and *NOT5* overexpression rescues the fitness defects of a *ULP2* deletion
402 strain in *S. cerevisiae* [83]. Crr4 and Not5 are components of the evolutionarily
403 conserved Crr4-Not multiprotein complex that regulate gene expression at all steps
404 from transcription to translation and mRNA decay [102]. It is unknown why
405 overexpression of the Crr4-Not complex rescues the fitness defect of an *ulp2*
406 deletion strain, but it has been suggested that it might be linked to the transcriptional
407 regulation of snoRNA and rRNA genes [84]. Here, for the first time, we demonstrate
408 that segmental aneuploidy can lead to adaptation to different stressors by
409 overexpressing genes located in the same chromosome and independently rescue
410 the two stressors, leading to an overall fitness advantage.

411 **Material and Methods**

412 *Yeast strains and Growth Conditions*

413 Strains used in this study are listed in **Table S5**. Routine culturing was performed at
414 30 °C in Yeast Extract-Peptone-D-Glucose (YPD) liquid and solid media containing
415 1% yeast extract, 2% peptone, 2% dextrose, 0.1 mg/ml adenine and 0.08 mg/ml
416 uridine, Synthetic Complete (SC-Formedium) or Casitone (5 g/L Yeast extract, 9 g/L
417 BactoTryptone, 20 g/L Glucose, 11.5 g/L Sodium Citrate dehydrate, 15 g/L Agar)
418 media. When indicated, media were supplemented with 1mg/ml 5-Fluorotic acid (5-
419 FOA, Melford), 200 μ g/ml Nourseothricin (clonNAT, Melford), 5mM and 12 mM
420 Caffeine (Sigma #C0750), 15 mg/ml and 128 mg/ml Fluconazole (Sigma #F8929),
421 6m H₂O₂ (Sigma #H1009), 12 mM and 22 mM Hydroxyurea (Sigma #H8627),
422 0.005% MMS (Sigma #129925).

423 *Genetic Screening*

424 The genetic screening was performed using a *C. albicans* homozygous deletion
425 library [44] arrayed in 96 colony format on YPD plates (145x20 mm) using a replica
426 plater (Sigma #R2508). Control N/S plates were grown at 30 °C for 48 hours. UV
427 treatment was performed using UVitec (Cambridge) with power density of
428 7.5 μ W/cm² (0.030 J for 4 seconds). Following UV treatment, plates were incubated
429 in the dark at 30°C for 48 hours. For MMS treatment, the library was spotted on YPD

430 plates (145x20mm) containing 0.05% MMS and incubated at 30°C for 48 hours. UV
431 and/or MMS sensitivity of selected strains was confirmed by serial dilution assays in
432 control (YPD) and stress (UV: power density of 7.5 μ W/cm², MMS: 0.05%) plates.
433 Correct gene deletions were confirmed by PCR using gene-specific primers (Table
434 **S6**).

435 *Yeast strain construction*

436 Integration and deletion of genes were performed using long oligos-mediated PCR
437 for gene deletion and tagging [103]. Oligonucleotides and plasmids used for strain
438 constructions are listed in Supplementary Table **S6** and **S7**, respectively. For Lithium
439 Acetate transformation, overnight liquid yeast cultures were diluted in fresh YPD and
440 grown to OD₆₀₀ of 1.3. Cells were harvested by centrifugation and washed once with
441 dH₂O and once with SORB solution (100mM Lithium acetate, 10mM Tris-HCL pH
442 7.5, 1mM EDTA pH 7.5/8, 1M sorbitol; pH 8). The pellet was resuspended in SORB
443 solution containing single-stranded carrier DNA (Sigma-Aldrich) and stored -80 °C in
444 50 μ l aliquots. Frozen competent cells were defrosted on ice, mixed with 5 μ L of
445 PCR product and 300 μ L PEG solution (100mM Lithium acetate, 10mM Tris-HCL pH
446 7.5, 1mM EDTA pH 8, 40% PEG4000) and incubated for 21-24 hours at 30 °C. Cells
447 were heat-shocked at 44°C for 15 minutes and grown in 5mL YPD liquid for 6 hours
448 before plating on selective media at 30 °C.

449 *UV survival quantification*

450 Following dilution of overnight liquid cultures, 500 cells were plated in YPD control
451 plates while 1500 cells were plated in YPD stress plates and UV irradiates with
452 power density of 7.5 μ W/cm² (0.030 J for 4 seconds). Plates were kept in the dark
453 and incubated at 30°C for 48 hours. Colonies were counted using a colony counter
454 (Stuart Scientific). Experiments were performed in 5 biological replicates, and violin
455 plots graphs were generated using R Studio (<http://www.r-project.org/>).

456 *Growth curve*

457 Overnight liquid cultures were diluted to 60 cells/ μ L in 100 μ L YPD and incubated at
458 30 °C in a 96 well plate (Cellstar®, #655180) with double orbital agitation of 400 rpm
459 using a BMG Labtech SPECTROstar nanoplate reader for 48 hours. When indicated,
460 YPD media was supplemented with MMS (0.05%) and HU (22 mM). Graphs show
461 the average of 3 biological replicates and error bars show the standard deviation.

462 *Serial dilution assay*

463 Overnight liquid cultures were diluted to an OD₆₀₀ of 4, serially diluted 1:5 and
464 spotted into agar plates with and without indicated additives using a replica plater
465 (Replica plater for 96-well plates, Sigma Aldrich, #R2383). Images of the plates were
466 then taken using Syngene GBox Chemi XX6 Gel imaging system. Experiments were
467 performed in 3 biological replicates

468 **Protein extraction and Western blotting**

469 Yeast extracts were prepared as described [104] using 1×10^8 cells from overnight
470 cultures grown to a final OD₆₀₀ of 1.5–2. Protein extraction was performed in the
471 presence of 2% SDS (Sigma) and 4 M acetic acid (Fisher) at 90°C. Proteins were
472 separated in 2% SDS (Sigma), 40% acrylamide/bis (Biorad, 161-0148) gels and
473 transfer into PVDF membrane (Biorad) by semi-dry transfer (Biorad, Trans Blot SD,
474 semi-dry transfer cell). Western-blot antibody detection was used using antibodies
475 from Roche Diagnostics Mannheim Germany (Anti-HA, mouse monoclonal primary
476 antibody (12CA5 Roche, 5 mg/ml) at a dilution of 1:1000, and anti-mouse IgG-
477 peroxidase (A4416 Sigma, 0.63 mg/ml) at a dilution of 1:5000, and Clarity™ ECL
478 substrate (Bio-Rad).

479 ***URA3⁺ marker loss quantification***

480 Strains were first streaked on –Uri media to ensure the selection of cells carrying
481 the *URA3⁺* marker gene. Parallel liquid cultures, grown for 16 hours at 30°C in YPD,
482 were plated on synthetic complete (SC) plates containing 1 □mg/ml 5-FOA (5-
483 fluorotic acid; Sigma) and on non-selective SC plates/. Colonies were counted after
484 2 □days of growth at 30°C, the frequency of the *URA3⁺* marker loss was calculated
485 using the formula $F = m/M$, where m represents the median number of colonies
486 obtained on 5-FOA medium corrected by the dilution factor used and the fraction of
487 culture plated and M the average number of colonies obtained on YPD corrected by
488 the dilution factor used and the fraction of culture plated [80]. Statistical differences
489 between results from samples were calculated using the Kruskal-Wallis test and the
490 Mann-Whitney U test for *post hoc* analysis. Statistical analysis was performed and
491 violin plots were generated using R Studio (<http://www.r-project.org/>).

492 ***Microscopy***

493 30 ml of yeast cultures (OD₆₀₀=1) grown in SC were centrifuged at 2000 rpm for 5
494 minute and washed once with dH₂O. Cells were fixed in 10ml of 3.7%
495 paraformaldehyde (Sigma #F8775) for 15 minutes, washed twice with 10ml of

496 KPO₄/Sorbitol (100 mM KPO₄, 1.2 M Sorbitol) and resuspended in 250 µl PBS
497 containing 10 µg of Dapi. Cells were then sonicated and resuspended in a 1% low
498 melting point agarose (Sigma Aldrich) before mounting under a 22mm coverslip of
499 0,17µm thickness. Samples were imaged on a Zeiss LSM 880 Airyscan with a
500 63x/1.4NA oil objective. Airyscan images were taken with a relative pinhole diameter
501 of 0.2 AU (airy unit) for maximal resolution and reduced noise. GFP was imaged with
502 a 488nm Argon laser and 495-550 nm bandpass excitation filter, RFP with a 546nm
503 solid-state diode laser and a 570nm long pass excitation filter. The Dapi channel was
504 imaged on a PMT with standard pinhole of 1AU and brightfield image were captured
505 on the trans-PMT with the same excitation laser of 405nm., Dapi and brightfield
506 images were taken with the same pixel size and bit depth (16bit) as the airyscan
507 images. Images were of a 42.7x42.7µm field of view and with a 33 nm pixel size
508 resolution. z-stacks were taken containing cells of z interval of 500nm. Airyscan
509 Veena filtering was performed with the inbuilt algorithms of Zeiss Zen Black 2.3. Fiji
510 scripts were written to automatically create a maximum intensity projection with
511 standardised intensity scaling for the fluorescence images and overlay them with the
512 best focus image of the brightfield picture. Experiments were performed in 3
513 biological replicates and >100 cells/replicate were counted.

514 ***Drug Selection***

515 Strains were incubated overnight in casitone liquid media at 30°C with shaking. 10⁴
516 cells were plated in small (10cm) casitone plates or plates containing: (i) 128 µg/mL
517 DMSO (Fluconazole Control), (ii) 128 µg/mL Fluconazole or (iii) 12 mM Caffeine.
518 Plates were incubated at 30°C for 7 days. Colonies able to grow on Fluconazole- or
519 Caffeine-containing plates were streaked in non-selective plates and tested by
520 spotting assay in casitone+ DMSO plates, casitone+Fluconazole or
521 casitone+Caffeine plates. Following incubation at 30°C, plates were imaged using
522 Syngene GBox Chemi XX6 Gel imaging system. Experiments were performed in 3
523 biological replicates.

524 ***Whole-genome sequence analysis***

525 All genome sequencing data have been deposited in the Sequence Read Archive
526 under BioProject PRJNA781758, Genomic DNA was isolated using a phenol-
527 chloroform extraction as previously described [29]. Paired-end (2 x 151 bp)
528 sequencing was carried out by the Microbial Genome Sequencing Center (MiGS) on

529 the Illumina NextSeq 2000 platform. Adaptor sequences and low-quality reads were
530 removed using Trimmomatic (v0.33 LEADING:3 Trailing:3 SLIDINGWINDOW:4:15
531 MINLEN:36 TOPHRED33) [105]. Trimmed reads were mapped to the *C. albicans*
532 reference genome (A21-s02-m09-r08) from the *Candida* Genome Database
533 (http://www.candidagenome.org/download/sequence/C_albicans_SC5314/Assembly_21/archive/C_albicans_SC5314_version_A21-s02-m09-r08_chromosomes.fasta.gz).
534 Reads were aligned to the reference using BWA-MEM (v0.7.17) with default
535 parameters [106]. The BAM files, containing aligned reads, were sorted and PCR
536 duplicates removed using Samtools (v1.10 samtools sort, samtools mdup) [107].
537 Qualimap (v2.2.1) analysed the BAM files for mean coverage of the reference
538 genome; coverages ranged from 73.7x to 89.3x coverage [108]. Variant detection
539 was conducted using the Genome Analysis Toolkit (Mutect, v2.2-25) [109]. Variants
540 were annotated using SnpEff (V4.3) [110] using the SC5314 reference genome fasta
541 and gene feature file above. Parental variants were removed, and all remaining
542 variants were verified visually using the Integrative Genomic Viewer (IGV, v2.8.2)
543 [111].

544 ***Read depth and breakpoint analysis***

545 Whole-genome sequencing data were analysed for copy number and allele ratio
546 changes as previously described [32,33]. Aneuploidies were visualised using the
547 Yeast Mapping Analysis Pipeline (YMAP, v1.0) [112]. BAM files aligned to the
548 SC5314 reference genome as described above were uploaded to YMAP and read
549 depth was determined and plotted as a function of chromosome position. Read
550 depth was corrected for both chromosome-end bias and GC-content. The GBrowse
551 CNV track and GBrowse allele ratio track identified regions of interest for CNV and
552 LOH breakpoints, and more precise breakpoints were determined visually using IGV.
553 LOH breakpoints are reported as the first informative homozygous position in a
554 region that is heterozygous in the parental genome. CNV breakpoints were identified
555 as described previously [32,33].

556 **Contour-clamped homogeneous electric field (CHEF) electrophoresis**

557 Intact yeast chromosomal DNA was prepared as previously described [113].
558 Briefly, cells were grown overnight, and a volume equivalent to an OD₆₀₀ of 7 was
559 washed in 50 mM EDTA and resuspended in 20 µl of 10 mg/ml Zymolyase 100T
560 (Amsbio #120493-1) and 300 µl of 1% Low Melt agarose (Biorad® # 1613112) in
561 100 mM EDTA. Chromosomes were separated on a 1% Megabase agarose gel (Bio-

563 Rad) in 0.5X TBE using a CHEF DRII apparatus. Run conditions as follows: 60-120s
564 switch at 6 V/cm for 12 hours followed by a 120-300s switch at 4.5 V/cm for 12
565 hours, 14 °C. The gel was stained in 0.5x TBE with ethidium bromide (0.5 µg/ml) for
566 30 minutes and destained in water for 30 minutes. Chromosomes were visualised
567 using a Syngene GBox Chemi XX6 gel imaging system.

568

569 **Acknowledgments**

570 We thank Judith Berman for reagents, strains and materials and A. Pidoux for critical
571 reading of the manuscript. This work was supported by BBSRC (BB/T006315/1 to
572 A.B and S.V.E), a University of Kent GTA PhD studentships (to M.R.), a University of
573 Minnesota UMR Fellowship with the Bioinformatics and Computational Biology
574 program (to N.S), the National Institutes of Health (R01AI143689) and Burroughs
575 Wellcome Fund Investigator in the Pathogenesis of Infectious Diseases Award
576 (#1020388) to A.S.

577 **References**

- 578 1. Sui Y, Qi L, Wu JK, Wen XP, Tang XX, Ma ZJ, et al. Genome-wide mapping of
579 spontaneous genetic alterations in diploid yeast cells. *Proc Natl Acad Sci U S*
580 *A*. 2020;117: 28191–28200. doi:10.1073/pnas.2018633117
- 581 2. Bennett RJ, Forche A, Berman J. Rapid Mechanisms for Generating Genome
582 Diversity: Whole Ploidy Shifts, Aneuploidy, and Loss of Heterozygosity. [cited
583 11 Aug 2021]. Available: <http://perspectivesinmedicine.cshlp.org/>
- 584 3. Pavelka N, Rancati G, Zhu J, Bradford WD, Saraf A, Florens L, et al.
585 Aneuploidy confers quantitative proteome changes and phenotypic variation in
586 budding yeast. *Nature*. 2010;468: 321–325. doi:10.1038/nature09529
- 587 4. Siegel JJ, Amon A, Koch DH. New Insights into the Troubles of Aneuploidy.
588 *Annu Rev Cell Dev Biol*. 2012;28: 189–214. doi:10.1146/annurev-cellbio-
589 101011-155807
- 590 5. Rancati G, Pavelka N, Fleharty B, Noll A, Trimble R, Walton K, et al.
591 Aneuploidy underlies rapid adaptive evolution of yeast cells deprived of a
592 conserved cytokinesis motor. *Cell*. 2008;135: 879–93.
593 doi:10.1016/j.cell.2008.09.039

- 594 6. Rancati G, Pavelka N. Karyotypic changes as drivers and catalyzers of cellular
595 evolvability: A perspective from non-pathogenic yeasts. *Semin Cell Dev Biol.*
596 2013;24: 332–338. doi:10.1016/j.semcdb.2013.01.009
- 597 7. Selmecki A, Forche A, Berman J. Genomic plasticity of the human fungal
598 pathogen *Candida albicans*. *Eukaryot Cell.* 2010;9: 991–1008.
599 doi:10.1128/EC.00060-10
- 600 8. Teoh F, Pavelka N. pathogens How Chemotherapy Increases the Risk of
601 Systemic Candidiasis in Cancer Patients: Current Paradigm and Future
602 Directions. doi:10.3390/pathogens5010006
- 603 9. Pfaller MA, Diekema DJ. Epidemiology of invasive mycoses in North America.
604 *Crit Rev Microbiol.* 2010;36: 1–53. doi:10.3109/10408410903241444
- 605 10. Berman J, Krysan DJ. Drug resistance and tolerance in fungi. *Nat Rev*
606 *Microbiol.* 2020;18: 319–331. doi:10.1038/s41579-019-0322-2
- 607 11. Fisher MC, Hawkins NJ, Sanglard D, Gurr SJ. Worldwide emergence of
608 resistance to antifungal drugs challenges human health and food security.
609 *Science (80-).* 2018;360: 739–742. doi:10.1126/science.aap7999
- 610 12. Berkow EL, Lockhart SR. Fluconazole resistance in *Candida* species: a current
611 perspective. *Infect Drug Resist.* 2017;10: 237. doi:10.2147/IDR.S118892
- 612 13. Heimark L, Shipkova P, Greene J, Munayyer H, Yarosh-Tomaine T,
613 DiDomenico B, et al. Mechanism of azole antifungal activity as determined by
614 liquid chromatographic/mass spectrometric monitoring of ergosterol
615 biosynthesis. *J Mass Spectrom.* 2002;37: 265–269. doi:10.1002/jms.280
- 616 14. Charlier C, Hart E, Lefort A, Ribaud P, Dromer F, Denning DW, et al.
617 Fluconazole for the management of invasive candidiasis: Where do we stand
618 after 15 years? *J Antimicrob Chemother.* 2006;57: 384–410.
619 doi:10.1093/JAC/DKI473
- 620 15. Heilmann CJ, Schneider S, Barker KS, Rogers PD, Morschhäuser J. An
621 A643T mutation in the transcription factor *Upc2p* causes constitutive *ERG11*
622 upregulation and increased fluconazole resistance in *Candida albicans*.
623 *Antimicrob Agents Chemother.* 2010;54: 353–359. doi:10.1128/AAC.01102-09

- 624 16. Whaley SG, Caudle KE, Vermitsky JP, Chadwick SG, Toner G, Barker KS, et
625 al. UPC2A is required for high-level azole antifungal resistance in *Candida*
626 *glabrata*. *Antimicrob Agents Chemother.* 2014;58: 4543–4554.
627 doi:10.1128/AAC.02217-13
- 628 17. Dunkel N, Liu TT, Barker KS, Homayouni R, Morschhäuser J, Rogers PD. A
629 gain-of-function mutation in the transcription factor Upc2p causes upregulation
630 of ergosterol biosynthesis genes and increased fluconazole resistance in a
631 clinical *Candida albicans* isolate. *Eukaryot Cell.* 2008;7: 1180–1190.
632 doi:10.1128/EC.00103-08
- 633 18. Hoot SJ, Smith AR, Brown RP, White TC. An A643V amino acid substitution in
634 Upc2p contributes to azole resistance in well-characterized clinical isolates of
635 *Candida albicans*. *Antimicrob Agents Chemother.* 2011;55: 940–942.
636 doi:10.1128/AAC.00995-10
- 637 19. Morschhäuser J. The development of fluconazole resistance in *Candida*
638 *albicans* – an example of microevolution of a fungal pathogen. *J Microbiol.*
639 2016;54: 192–201. doi:10.1007/s12275-016-5628-4
- 640 20. Jones T, Federspiel NA, Chibana H, Dungan J, Kalman S, Magee BB, et al.
641 The diploid genome sequence of *Candida albicans*. *Proc Natl Acad Sci U S A.*
642 2004;101: 7329–34. doi:10.1073/pnas.0401648101
- 643 21. van het Hoog M, Rast TJ, Martchenko M, Grindle S, Dignard D, Hogues H, et
644 al. Assembly of the *Candida albicans* genome into sixteen supercontigs
645 aligned on the eight chromosomes. *Genome Biol.* 2007;8: R52.
646 doi:10.1186/gb-2007-8-4-r52
- 647 22. Hirakawa MP, Martinez D a, Sakthikumar S, Anderson MZ, Berlin A, Gujja S,
648 et al. Genetic and phenotypic intra-species variation in *Candida albicans*.
649 2015; 1–13. doi:10.1101/gr.174623.114.
- 650 23. Tso GHW, Reales-Calderon JA, Tan ASM, Sem X, Le GTT, Tan TG, et al.
651 Experimental evolution of a fungal pathogen into a gut symbiont. *Science (80-*
652 *).* 2018;362: 589–595. doi:10.1126/SCIENCE.AAT0537
- 653 24. Forche A, Cromie G, Gerstein AC, Solis N V., Pisithkul T, Srifa W, et al. Rapid

- 654 Phenotypic and Genotypic Diversification After Exposure to the Oral Host
655 Niche in *Candida albicans*. *Genetics*. 2018;209: genetics.301019.2018.
656 doi:10.1534/genetics.118.301019
- 657 25. Forche A, Magee PT, Selmecki A, Berman J, May G. Evolution in *Candida*
658 *albicans* Populations During a Single Passage Through a Mouse Host.
659 *Genetics*. 2009;182: 799–811. Available:
660 <http://www.genetics.org/content/182/3/799.abstract>
- 661 26. Ene I V., Farrer RA, Hirakawa MP, Agwamba K, Cuomo CA, Bennett RJ.
662 Global analysis of mutations driving microevolution of a heterozygous diploid
663 fungal pathogen. *Proc Natl Acad Sci*. 2018;115: 201806002.
664 doi:10.1073/pnas.1806002115
- 665 27. Ropars J, Maufrais C, Diogo D, Marcet-houben M, Perin A, Sertour N, et al.
666 Gene flow contributes to diversification of the major fungal pathogen
667 *Candida albicans*. 2018. doi:10.1038/s41467-018-04787-4
- 668 28. Forche A, Solis N V., Swidergall M, Thomas R, Guyer A, Beach A, et al.
669 Selection of *Candida albicans* trisomy during oropharyngeal infection results in
670 a commensal-like phenotype. *PLoS Genet*. 2019;15.
671 doi:10.1371/journal.pgen.1008137
- 672 29. Selmecki A, Forche A, Berman J. Aneuploidy and isochromosome formation in
673 drug-resistant *Candida albicans*. *Science*. 2006;313: 367–70.
674 doi:10.1126/science.1128242
- 675 30. Selmecki A, Gerami-Nejad M, Paulson C, Forche A, Berman J. An
676 isochromosome confers drug resistance in vivo by amplification of two genes,
677 *ERG11* and *TAC1*. *Mol Microbiol*. 2008;68: 624–641. doi:10.1111/J.1365-
678 2958.2008.06176.X
- 679 31. Dunn MJ, Anderson MZ. To repeat or not to repeat: Repetitive sequences
680 regulate genome stability in *Candida albicans*. *Genes (Basel)*. 2019;10.
681 doi:10.3390/genes10110866
- 682 32. Todd RT, Wikoff TD, Forche A, Selmecki A. Genome plasticity in *Candida*
683 *albicans* is driven by long repeat sequences. *Elife*. 2019;8.

- 684 doi:10.7554/eLife.45954
- 685 33. Todd RT, Selmecki A. Expandable and reversible copy number amplification
686 drives rapid adaptation to antifungal drugs. *Elife*. 2020;9: 1–33.
687 doi:10.7554/eLife.58349
- 688 34. Hirakawa MP, Martinez DA, Sakthikumar S, Anderson MZ, Berlin A, Gujja S, et
689 al. Genetic and phenotypic intra-species variation in *Candida albicans*.
690 *Genome Res*. 2015;25: 413–25. doi:10.1101/gr.174623.114
- 691 35. Ene I V., Farrer RA, Hirakawa MP, Agwamba K, Cuomo CA, Bennett RJ.
692 Global analysis of mutations driving microevolution of a heterozygous diploid
693 fungal pathogen. *Proc Natl Acad Sci U S A*. 2018;115: E8688–E8697.
694 doi:10.1073/pnas.1806002115
- 695 36. Freire-Benítez V, Gourlay S, Berman J, Buscaino A. Sir2 regulates stability of
696 repetitive domains differentially in the human fungal pathogen *Candida*
697 *albicans*. *Nucleic Acids Res*. 2016;44. doi:10.1093/nar/gkw594
- 698 37. Buscaino. Chromatin-Mediated Regulation of Genome Plasticity in Human
699 Fungal Pathogens. *Genes (Basel)*. 2019;10: 855. doi:10.3390/genes10110855
- 700 38. Anderson MZ, Baller J a, Dulmage K, Wigen L, Berman J. The three clades of
701 the telomere-associated TLO gene family of *Candida albicans* have different
702 splicing, localization and expression features. *Eukaryot Cell*. 2012;11: 612–
703 625. doi:10.1128/EC.00230-12
- 704 39. Haran J, Boyle H, Hokamp K, Yeomans T, Liu Z, Church M, et al. Telomeric
705 ORFs (TLOs) in *Candida* spp. Encode Mediator Subunits That Regulate
706 Distinct Virulence Traits. *PLoS Genet*. 2014;10: e1004658.
707 doi:10.1371/journal.pgen.1004658
- 708 40. Zhang A, Petrov KO, Hyun ER, Liu Z, Gerber SA, Myers LC. The Tlo proteins
709 are stoichiometric components of *Candida albicans* mediator anchored via the
710 Med3 subunit. *Eukaryot Cell*. 2012;11: 874–84. doi:10.1128/EC.00095-12
- 711 41. Forche A, Abbey D, Pisithkul T, Weinzierl MA, Ringstrom T, Bruck D, et al.
712 Stress alters rates and types of loss of heterozygosity in *Candida albicans*.
713 *MBio*. 2011;2. doi:10.1128/mBio.00129-11

- 714 42. Harrison BD, Hashemi J, Bibi M, Pulver R, Bavli D, Nahmias Y, et al. A
715 tetraploid intermediate precedes aneuploid formation in yeasts exposed to
716 fluconazole. *PLoS Biol.* 2014;12: e1001815. doi:10.1371/journal.pbio.1001815
- 717 43. Forche A, Cromie G, Gerstein AC, Solis N V, Pisithkul T. Rapid Phenotypic
718 and Genotypic Diversification After. 2018;209: 725–741.
- 719 44. Noble SM, French S, Kohn LA, Chen V, Johnson AD. Systematic screens of a
720 *Candida albicans* homozygous deletion library decouple morphogenetic
721 switching and pathogenicity. *Nat Genet.* 2010;42: 590–598.
722 doi:10.1038/ng.605
- 723 45. Hakem R. DNA-damage repair; the good, the bad, and the ugly. *EMBO J.*
724 2008;27: 589–605. doi:10.1038/emboj.2008.15
- 725 46. Aboussekhra A, Wood RD. Repair of UV-damaged DNA by mammalian cells
726 and *Saccharomyces cerevisiae*. *Curr Opin Genet Dev.* 1994;4: 212–220.
727 doi:10.1016/S0959-437X(05)80047-4
- 728 47. Beranek DT. Distribution of methyl and ethyl adducts following alkylation with
729 monofunctional alkylating agents. *Mutat Res - Fundam Mol Mech Mutagen.*
730 1990;231: 11–30. doi:10.1016/0027-5107(90)90173-2
- 731 48. T W. DNA damage checkpoints update: getting molecular. *Curr Opin Genet*
732 *Dev.* 1998;8: 185–193. doi:10.1016/S0959-437X(98)80140-8
- 733 49. L di C, BS C. DNA synthesis in UV-irradiated yeast. *Mutat Res.* 1981;82: 69–
734 85. doi:10.1016/0027-5107(81)90139-1
- 735 50. Butler DK, All O, Govena J, Loveless T, Wilson T, Toenjes KA. The *GRR1*
736 gene of *Candida albicans* is involved in the negative control of pseudohyphal
737 morphogenesis. *Fungal Genet Biol.* 2006;43: 573–582.
738 doi:10.1016/j.fgb.2006.03.004
- 739 51. McCoy KM, Tubman ES, Claas A, Tank D, Clancy SA, O’Toole ET, et al.
740 Physical limits on kinesin-5-mediated chromosome congression in the smallest
741 mitotic spindles. *Mol Biol Cell.* 2015;26: 3999–4014. doi:10.1091/mbc.E14-10-
742 1454
- 743 52. Enjalbert B, Smith DA, Cornell MJ, Alam I, Nicholls S, Brown AJP, et al. Role

- 744 of the Hog1 Stress-activated Protein Kinase in the Global Transcriptional
745 Response to Stress in the Fungal Pathogen *Candida albicans*. *Mol Biol Cell*.
746 2006;17: 1018. doi:10.1091/MBE.E05-06-0501
- 747 53. Bhaumik SR, Green MR. Differential requirement of SAGA components for
748 recruitment of TATA-box-binding protein to promoters in vivo. *Mol Cell Biol*.
749 2002;22: 7365–7371. doi:10.1128/MCB.22.21.7365-7371.2002
- 750 54. Sterner DE, Belotserkovskaya R, Berger SL. SALSALSA, a variant of yeast SAGA,
751 contains truncated Spt7, which correlates with activated transcription. *Proc*
752 *Natl Acad Sci U S A*. 2002;99: 11622–11627. doi:10.1073/pnas.182021199
- 753 55. Hnisz D, Majer O, Frohner IE, Komnenovic V, Kuchler K. The Set3/Hos2
754 histone deacetylase complex attenuates cAMP/PKA signaling to regulate
755 morphogenesis and virulence of *Candida albicans*. *PLoS Pathog*. 2010;6:
756 e1000889. doi:10.1371/journal.ppat.1000889
- 757 56. Ferreira T, Brèthes D, Pinson B, Napias C, Chevallier J. Functional analysis of
758 mutated purine-cytosine permease from *Saccharomyces cerevisiae*. A
759 possible role of the hydrophilic segment 371-377 in the active carrier
760 conformation. *J Biol Chem*. 1997;272: 9697–9702.
761 doi:10.1074/jbc.272.15.9697
- 762 57. Rousselet G, Simon M, Ripoche P, Buhler JM. A second nitrogen permease
763 regulator in *Saccharomyces cerevisiae*. *FEBS Lett*. 1995;359: 215–219.
764 doi:10.1016/0014-5793(95)00038-B
- 765 58. ElBerry HM, Majumdar ML, Cunningham TS, Sumrada RA, Cooper TG.
766 Regulation of the urea active transporter gene (*DUR3*) in *Saccharomyces*
767 *cerevisiae*. *J Bacteriol*. 1993;175: 4688–4698. doi:10.1128/jb.175.15.4688-
768 4698.1993
- 769 59. Wichmann H, Hengst L, Gallwitz D. Endocytosis in yeast: Evidence for the
770 involvement of a small GTP-binding protein (*Ypt7p*). *Cell*. 1992;71: 1131–
771 1142. doi:10.1016/S0092-8674(05)80062-5
- 772 60. Talbert PB, Henikoff S. Histone variants—ancient wrap artists of the
773 epigenome. *Nat Rev Mol Cell Biol*. 2010;11: 264–75. doi:10.1038/nm2861

- 774 61. Yoshida S, Ohya Y, Goebel M, Nakano A, Anraku Y. A novel gene, STT4,
775 encodes a phosphatidylinositol 4-kinase in the PKC1 protein kinase pathway of
776 *Saccharomyces cerevisiae*. *J Biol Chem*. 1994;269: 1166–1171.
777 doi:10.1016/s0021-9258(17)42237-x
- 778 62. Herrero AB, Magnelli P, Mansour MK, Levitz SM, Bussey H, Abeijon C. KRE5
779 gene null mutant strains of *Candida albicans* are avirulent and have altered
780 cell wall composition and hypha formation properties. *Eukaryot Cell*. 2004;3:
781 1423–1432. doi:10.1128/EC.3.6.1423-1432.2004
- 782 63. Garvin AJ, Morris JR. SUMO, a small, but powerful, regulator of double-strand
783 break repair. *Philos Trans R Soc B Biol Sci*. 2017;372.
784 doi:10.1098/RSTB.2016.0281
- 785 64. Watts FZ. The role of SUMO in chromosome segregation. *Chromosoma*.
786 2007;116: 15–20. doi:10.1007/s00412-006-0079-z
- 787 65. Cremona CA, Sarangi P, Zhao X. Sumoylation and the DNA Damage
788 Response. *Biomolecules*. 2012;2: 376. doi:10.3390/BIOM2030376
- 789 66. Ryu HY, Ahn SH, Hochstrasser M. SUMO and cellular adaptive mechanisms.
790 *Exp Mol Med*. 2020;52: 931–939. doi:10.1038/s12276-020-0457-2
- 791 67. Felberbaum R, Hochstrasser M. Ulp2 and the DNA damage response:
792 Desumoylation enables safe passage through mitosis. *Cell Cycle*. 2008;7: 52–
793 56. doi:10.4161/cc.7.1.5218
- 794 68. Jaiswal D, Turniansky R, Green EM. Choose your own adventure: The role of
795 histone modifications in yeast cell fate. *J Mol Biol*. 2017;429: 1946.
796 doi:10.1016/J.JMB.2016.10.018
- 797 69. LD V, K G, I DS. Protein Language: Post-Translational Modifications Talking to
798 Each Other. *Trends Plant Sci*. 2018;23: 1068–1080.
799 doi:10.1016/J.TPLANTS.2018.09.004
- 800 70. Morrell R, Sadanandom A. Dealing With Stress: A Review of Plant SUMO
801 Proteases. *Front Plant Sci*. 2019;10: 1–19. doi:10.3389/fpls.2019.01122
- 802 71. K D. Ubiquitin and SUMO Modifications in *Caenorhabditis elegans* Stress
803 Response. *Curr Issues Mol Biol*. 2020;35: 145–158.

- 804 doi:10.21775/CIMB.035.145
- 805 72. JS S, A D. SUMO and the robustness of cancer. *Nat Rev Cancer*. 2017;17:
806 184–197. doi:10.1038/NRC.2016.143
- 807 73. Brown AJP, Budge S, Kaloriti D, Tillmann A, Jacobsen MD, Yin Z, et al. Stress
808 adaptation in a pathogenic fungus. *J Exp Biol*. 2014;217: 144–155.
809 doi:10.1242/jeb.088930
- 810 74. Leach MD, Stead DA, Argo E, Brown AJP. Identification of sumoylation
811 targets, combined with inactivation of SMT3, reveals the impact of sumoylation
812 upon growth, morphology, and stress resistance in the pathogen *Candida*
813 *albicans*. *Mol Biol Cell*. 2011;22: 687–702. doi:10.1091/mbc.E10-07-0632
- 814 75. Bianchis V, Pontis E, Reichard P. THE JOURNAL OF BIOLOGICAL
815 CHEMISTRY Changes of Deoxyribonucleoside Triphosphate Pools Induced by
816 Hydroxyurea and Their Relation to DNA Synthesis*. *J Biol Chem*. 1986;261:
817 16037–16042. doi:10.1016/S0021-9258(18)66672-4
- 818 76. Huaping L, Jie L, Zhifeng W, Yingchang Z, Yuhuan L. Cloning and functional
819 expression of ubiquitin-like protein specific proteases genes from *Candida*
820 *albicans*. *Biol Pharm Bull*. 2007;30: 1851–1855. doi:10.1248/bpb.30.1851
- 821 77. Segal ES, Gritsenko V, Levitan A, Yadav B, Dror N, Steenwyk JL, et al. Gene
822 Essentiality Analyzed by In Vivo Transposon Mutagenesis and Machine
823 Learning in a Stable Haploid Isolate of *Candida albicans*. *MBio*. 2018;9:
824 e02048-18. doi:10.1128/MBIO.02048-18
- 825 78. O'Meara TR, Hay C, Price MS, Giles S, Alspaugh JA. *Cryptococcus*
826 *neoformans* histone acetyltransferase *Gcn5* regulates fungal adaptation to the
827 host. *Eukaryot Cell*. 2010;9: 1193–202. doi:10.1128/EC.00098-10
- 828 79. Berman J. Morphogenesis and cell cycle progression in *Candida albicans*
829 *Curr. Curr Opin Microbiol*. 2006;9: 595–601.
830 doi:10.1016/j.mib.2006.10.007.Morphogenesis
- 831 80. Loll-Krippleber R, d'Enfert C, Feri A, Diogo D, Perin A, Marcet-Houben M, et
832 al. A study of the DNA damage checkpoint in *Candida albicans*: uncoupling
833 of the functions of Rad53 in DNA repair, cell cycle regulation and genotoxic

- 834 stress-induced polarized growth. *Mol Microbiol.* 2014;91: 452–471.
835 doi:10.1111/mmi.12471
- 836 81. Legrand M, Chan CL, Jauert PA, Kirkpatrick DT. The contribution of the S-
837 phase checkpoint genes MEC1 and SGS1 to genome stability maintenance in
838 *Candida albicans*. *Fungal Genet Biol.* 2011;48: 823–30.
839 doi:10.1016/j.fgb.2011.04.005
- 840 82. Burrack LS, Applen Clancey SE, Chacón JM, Gardner MK, Berman J.
841 Monopolin recruits condensin to organize centromere DNA and repetitive DNA
842 sequences. *Mol Biol Cell.* 2013;24: 2807–19. doi:10.1091/mbc.E13-05-0229
- 843 83. Ryu HY, Wilson NR, Mehta S, Hwang SS, Hochstrasser M. Loss of the SUMO
844 protease ULP2 triggers a specific multichromosome aneuploidy. *Genes Dev.*
845 2016;30: 1881–1894. doi:10.1101/gad.282194.116
- 846 84. Ryu HY, López-Giráldez F, Knight J, Hwang SS, Renner C, Kreft SG, et al.
847 Distinct adaptive mechanisms drive recovery from aneuploidy caused by loss
848 of the Ulp2 SUMO protease. *Nat Commun.* 2018;9. doi:10.1038/s41467-018-
849 07836-0
- 850 85. Ma Q, Ola M, Iracane E, Butler G. Susceptibility to Medium-Chain Fatty Acids
851 Is Associated with Trisomy of Chromosome 7 in *Candida albicans*. *mSphere.*
852 2019;4. doi:10.1128/MSPHERE.00402-19
- 853 86. Calvo IA, Gabrielli N, Iglesias-Baena I, García-Santamarina S, Hoe K-L, Kim
854 DU, et al. Genome-Wide Screen of Genes Required for Caffeine Tolerance in
855 Fission Yeast. *PLoS One.* 2009;4: e6619.
856 doi:10.1371/JOURNAL.PONE.0006619
- 857 87. Pfaller M a. Antifungal drug resistance: mechanisms, epidemiology, and
858 consequences for treatment. *Am J Med.* 2012;125: S3-13.
859 doi:10.1016/j.amjmed.2011.11.001
- 860 88. Bruno VM, Mitchell AP. Regulation of azole drug susceptibility by *Candida*
861 *albicans* protein kinase CK2. *Mol Microbiol.* 2005;56: 559–573.
862 doi:10.1111/j.1365-2958.2005.04562.x
- 863 89. Goodwin TJD, Poulter RTM. Multiple LTR-retrotransposon families in the

- 864 asexual yeast *Candida albicans*. *Genome Res.* 2000;10: 174–191.
865 doi:10.1101/gr.10.2.174
- 866 90. MacPherson S, Akache B, Weber S, De Deken X, Raymond M, Turcotte B.
867 *Candida albicans* zinc cluster protein Upc2p confers resistance to antifungal
868 drugs and is an activator of ergosterol biosynthetic genes. *Antimicrob Agents*
869 *Chemother.* 2005;49: 1745–1752. doi:10.1128/AAC.49.5.1745-1752.2005
- 870 91. Silver PM, Oliver BG, White TC. Role of *Candida albicans* transcription factor
871 Upc2p in drug resistance and sterol metabolism. *Eukaryot Cell.* 2004;3: 1391–
872 1397. doi:10.1128/EC.3.6.1391-1397.2004/ASSET/112DA7BA-82B3-42CB-
873 BDEB-198E91B9521D/ASSETS/GRAPHIC/ZEK0060423520006.JPEG
- 874 92. Miller JE, Reese JC. Ccr4-Not complex: the control freak of eukaryotic cells.
875 *Crit Rev Biochem Mol Biol.* 2012;47: 315. doi:10.3109/10409238.2012.667214
- 876 93. Islam A, Tebbji F, Mallick J, Regan H, Dumeaux V, Omran RP, et al. Mms21:
877 A putative SUMO E3 ligase in *Candida albicans* that negatively regulates
878 invasiveness and filamentation, and is required for the genotoxic and cellular
879 stress response. *Genetics.* 2019;211: 579–595.
880 doi:10.1534/genetics.118.301769
- 881 94. Omeara TR, Veri AO, Ketela T, Jiang B, Roemer T, Cowen LE. Global
882 analysis of fungal morphology exposes mechanisms of host cell escape. *Nat*
883 *Commun.* 2015;6: 1–10. doi:10.1038/ncomms7741
- 884 95. Hickey CM, Wilson NR, Hochstrasser M. Function and regulation of SUMO
885 proteases. *Nat Rev Mol Cell Biol.* 2012;13: 755–766. doi:10.1038/nm3478
- 886 96. Suhandynata RT, Quan Y, Yang Y, Yuan W-T, Albuquerque CP, Zhou H.
887 Recruitment of the Ulp2 protease to the inner kinetochore prevents its hyper-
888 sumoylation to ensure accurate chromosome segregation. *PLOS Genet.*
889 2019;15: e1008477. doi:10.1371/JOURNAL.PGEN.1008477
- 890 97. Miyagawa K, Low RS, Santosa V, Tsuji H, Moser BA, Fujisawa S, et al.
891 SUMOylation regulates telomere length by targeting the shelterin subunit
892 Tpz1Tpp1 to modulate shelterin–Stn1 interaction in fission yeast. *Proc Natl*
893 *Acad Sci.* 2014;111: 5950–5955. doi:10.1073/PNAS.1401359111

- 894 98. Montpetit B, Hazbun TR, Fields S, Hieter P. Sumoylation of the budding yeast
895 kinetochore protein Ndc10 is required for Ndc10 spindle localization and
896 regulation of anaphase spindle elongation. *J Cell Biol.* 2006;174: 653–663.
897 doi:10.1083/jcb.200605019
- 898 99. Barra V, Fachinetti D. The dark side of centromeres: types, causes and
899 consequences of structural abnormalities implicating centromeric DNA. *Nat*
900 *Commun.* 2018;9. doi:10.1038/s41467-018-06545-y
- 901 100. Stephens PJ, Greenman CD, Fu B, Yang F, Bignell GR, Mudie LJ, et al.
902 Massive genomic rearrangement acquired in a single catastrophic event during
903 cancer development. *Cell.* 2011;144: 27–40. doi:10.1016/j.cell.2010.11.055
- 904 101. Flowers SA, Barker KS, Berkow EL, Toner G, Chadwick SG, Gygax SE, et al.
905 Gain-of-function mutations in UPC2 are a frequent cause of ERG11
906 upregulation in azole-resistant clinical isolates of *Candida albicans*. *Eukaryot*
907 *Cell.* 2012;11: 1289–1299. doi:10.1128/EC.00215-12
- 908 102. Collart MA. The Ccr4-Not complex is a key regulator of eukaryotic gene
909 expression. *Wiley Interdiscip Rev RNA.* 2016;7: 438–454.
910 doi:10.1002/WRNA.1332
- 911 103. Wilson RB, Davis D, Mitchell AP. Rapid hypothesis testing with *Candida*
912 *albicans* through gene disruption with short homology regions. *J Bacteriol.*
913 1999;181: 1868–74. Available: <http://www.ncbi.nlm.nih.gov/pubmed/10074081>
- 914 104. von der Haar T. Optimized protein extraction for quantitative proteomics of
915 yeasts. *PLoS One.* 2007;2: e1078. doi:10.1371/journal.pone.0001078
- 916 105. Bolger AM, Lohse M, Usadel B. Trimmomatic: a flexible trimmer for Illumina
917 sequence data. *Bioinformatics.* 2014;30: 2114–2120.
918 doi:10.1093/BIOINFORMATICS/BTU170
- 919 106. Li H. Aligning sequence reads, clone sequences and assembly contigs with
920 BWA-MEM. 2013 [cited 17 Nov 2021]. Available:
921 <https://arxiv.org/abs/1303.3997v2>
- 922 107. Li H, Durbin R. Fast and accurate short read alignment with Burrows-Wheeler
923 transform. *Bioinformatics.* 2009;25: 1754–1760.

- 924 doi:10.1093/bioinformatics/btp324
- 925 108. Okonechnikov K, Conesa A, García-Alcalde F. Qualimap 2: advanced multi-
926 sample quality control for high-throughput sequencing data. *Bioinformatics*.
927 2016;32: 292–294. doi:10.1093/BIOINFORMATICS/BTV566
- 928 109. Cibulskis K, Lawrence MS, Carter SL, Sivachenko A, Jaffe D, Sougnez C, et
929 al. Sensitive detection of somatic point mutations in impure and heterogeneous
930 cancer samples. *Nat Biotechnol* 2013 313. 2013;31: 213–219.
931 doi:10.1038/nbt.2514
- 932 110. Cingolani P, Platts A, Wang LL, Coon M, Nguyen T, Wang L, et al. A program
933 for annotating and predicting the effects of single nucleotide polymorphisms,
934 SnPEff: SNPs in the genome of *Drosophila melanogaster* strain w1118; iso-2;
935 iso-3. *Fly (Austin)*. 2012;6: 80–92. doi:10.4161/fly.19695
- 936 111. Thorvaldsdóttir H, Robinson JT, Mesirov JP. Integrative Genomics Viewer
937 (IGV): high-performance genomics data visualization and exploration. *Brief*
938 *Bioinform*. 2013;14: 178–192. doi:10.1093/BIB/BBS017
- 939 112. Abbey D a, Funt J, Lunie-Weinberger MN, Thompson D a, Regev A, Myers CL,
940 et al. YMAP: a pipeline for visualization of copy number variation and loss of
941 heterozygosity in eukaryotic pathogens. *Genome Med*. 2014;6: 1–15.
942 doi:10.1186/s13073-014-0100-8
- 943 113. Schwartz DC, Cantor CR. Separation of yeast chromosome-sized DNAs by
944 pulsed field gradient gel electrophoresis. *Cell*. 1984;37: 67–75.
945 doi:10.1016/0092-8674(84)90301-5
- 946
- 947

948 **Figure Legends**

949 **Fig 1. ULP2 is a regulator of *C. albicans* genotoxic stress response**

950 **(A)** Schematic representation of the screening strategy. 674 *C. albicans* deletion
951 strains were screened using a 96-plate format for hypersensitivity to UV and MMS.
952 Hypersensitivity was scored by comparing the growth of treated vs untreated on a
953 scale of 0 (white) to 4 (magenta). Black *: genes encoding for DNA damage and
954 sensing repair pathway components, Blue *: genes encoding for cell division and
955 chromosome segregation machinery, Green arrow: *ulp2* Δ/Δ **(B)** Data for a plate
956 containing *mec3* Δ/Δ strain (cyan circle). Growth on Non-selective (N/S) media or
957 following UV and MMS treatment is shown. **(C)** Data for a plate containing *ulp2* Δ/Δ
958 strain (magenta circle). Growth on Non-selective (N/S) media or following UV and
959 MMS treatment is shown **(D)** Colony-forming Unit assay of UV treated WT and *ulp2*
960 Δ/Δ strains. % survival is shown. **(E)** Growth curve on WT and *ulp2* Δ/Δ strains
961 grown in non-selective (N/S) liquid media and MMS-containing liquid media. Error
962 bars: standard deviation (SD) of three biological replicates **(F)** Growth curve on WT
963 and *ulp2* Δ/Δ strains grown in non-selective (N/S) liquid media and HU-containing
964 liquid media.

965 **Fig 2. ULP2 is necessary for survival under stress**

966 **(A)** Schematic representation of Ulp1, Ulp2 and Ulp3 protein organisation. The
967 systematic name and the amino acid (aa) number is indicated for each protein. Blue
968 box: putative catalytic UD domain typical of Ulp SUMO proteases **(B)** Protein
969 alignments of the three *C. albicans* Ulp proteins (Ulp1, Ulp2 and Ulp3) and the two *S.*
970 *cerevisiae* proteins (Ulp1 and Ulp2). Magenta arrows: amino acids essential for
971 SUMO protease activity **(C)** HA Western Blot analysis of 4 independent ULP2-HA
972 integrants and the progenitor untagged control (No Tag). Magenta arrow: Ulp2-HA
973 (Magenta arrow). *: non-specific cross-reacting bands serving as a loading control
974 **(C)** Growth curves of WT, *ulp1* Δ/Δ and *ulp2* Δ/Δ strains grown in non-selective (N/S)
975 liquid media. Error bars: standard deviation (SD) of three biological replicates **(D)**
976 Serial dilution assay of WT, *ulp1* Δ/Δ and *ulp2* Δ/Δ strains grown in unstressed (N/S)
977 or stress (UV, MMS, HU, H2O2 and 39 °C) growth conditions.

978 **Fig 3. Loss of ULP2 leads to increased genome instability**

979 (A) Quantification of loss of a heterozygous *URA3*⁺ marker gene inserted in Chr1,
980 Chr3 and Chr7 in WT and *ulp2* Δ/Δ strain. A fold difference of *URA3*⁺ marker loss
981 between *ulp2* Δ/Δ and WT strains is indicated. **: Chr1 (4.11E-07) and Chr7 (6.74E-
982 05) p-value, *: Chr3 (2.87E-02) p-value (B) *Top*: Representative images displaying
983 the morphologies of WT and *ulp2* Δ/Δ strains. *Bottom*: Quantification (%) of yeast
984 and filamentous (hyphae + pseudohyphae) cells in WT and *ulp2* Δ/Δ strains. Error
985 bar: Standard deviation of 3 biological replicates. (C) *Top*: schematics of the CEN7
986 TetO and TetR-GFP system. *Bottom*: nuclear morphology and segregation pattern of
987 centromere 7 (*CEN7*) in WT and *ulp2* Δ/Δ strain. Quantification (%) of abnormal
988 GFP-CEN7 patterns is indicated. Error bar: Standard deviation of 3 biological
989 replicates. (D) Whole genome sequencing analysis of the progenitor (SN152) and
990 three single colonies C1, C2, and C3. Data were plotted as the log₂ ratio and
991 converted to chromosome copy number (y-axis, 1-4 copies) as a function of
992 chromosome position (x-axis, Chr1-ChrR) using the Yeast Mapping Analysis Pipeline
993 (YMAP) [112]. Heterozygous (AB) regions are indicated with grey shading, and
994 homozygous regions (loss of heterozygosity) are indicated by shading of the
995 remaining haplotype, either AA (cyan) or BB (magenta). Two homozygous positions
996 are present in the progenitor (the left side of Chr2 and a small region near the
997 centromere of Chr3), while C1 and C2 underwent loss of heterozygosity of ChrR and
998 Chr3.

999 **Fig 4. Loss of ULP2 leads to drug resistance via selection of novel genotypes**

1000 (A) Serial dilution assay of WT and *ulp2* Δ/Δ strains grown in non-selective (N/S) or
1001 media containing low (15 μ g/ml) concentration of fluconazole (FLC). (B) Serial
1002 dilution assay of WT and *ulp2* Δ/Δ strains grown in non-selective (N/S) or media
1003 containing low (5 mM) Caffeine (CAF). (C) *Left*: Plating assay of *ulp2* Δ/Δ and WT
1004 strain in media containing high (128 μ g/ml) concentration of fluconazole (FLC) or
1005 non-selective (NS) media *Right*: Plating assay quantification. The number of large
1006 (L) and small (S) colonies recovered from fluconazole (FLC) containing media and
1007 non-selective (N/S) media is shown for WT and *ulp2* Δ/Δ strains. (D) *Left*: Plating
1008 assay of *ulp2* Δ/Δ and WT strain in media containing high (12 mM) concentration of
1009 caffeine (CAF) and non-selective (NS) media *Right*: Plating assay quantification. The
1010 number of large (L) and small (S) colonies recovered from caffeine (CAF)-containing

1011 media and non-selective (N/S) media is shown for WT and *ulp2* Δ/Δ strains. (E)
1012 Whole genome sequencing data plotted as in Figure 3D for four single colonies
1013 isolated from 128 μ g/ml fluconazole plates (*FLC1-FLC4*). The chromosome copy
1014 number is plotted along the y-axis (1-4 copies). All four single colonies have a
1015 recurrent segmental deletion of part of ChrRR. Colony *FLC-4* has an amplification of
1016 the middle part of Chr1. Copy number breakpoints and allele ratio changes in *FLC-4*
1017 are indicated in Figure S3. (F) CHEF karyotype gel stained with ethidium bromide of
1018 *ulp2* Δ/Δ progenitor and *FLC-4* isolate. A band (blue *) corresponding to Chr6 is
1019 present in the *ulp2* Δ/Δ progenitor and absent in the *FLC-4* isolate. Conversely, a
1020 new band (magenta *) is present in the *FLC-4* isolate but absent in the *ulp2*
1021 Δ/Δ progenitor. (G) Schematics of segmental aneuploidies detected in *FLC-1*, *FLC-2*,
1022 *FLC-3* and *FLC-4* isolates.

1023

Fig 1

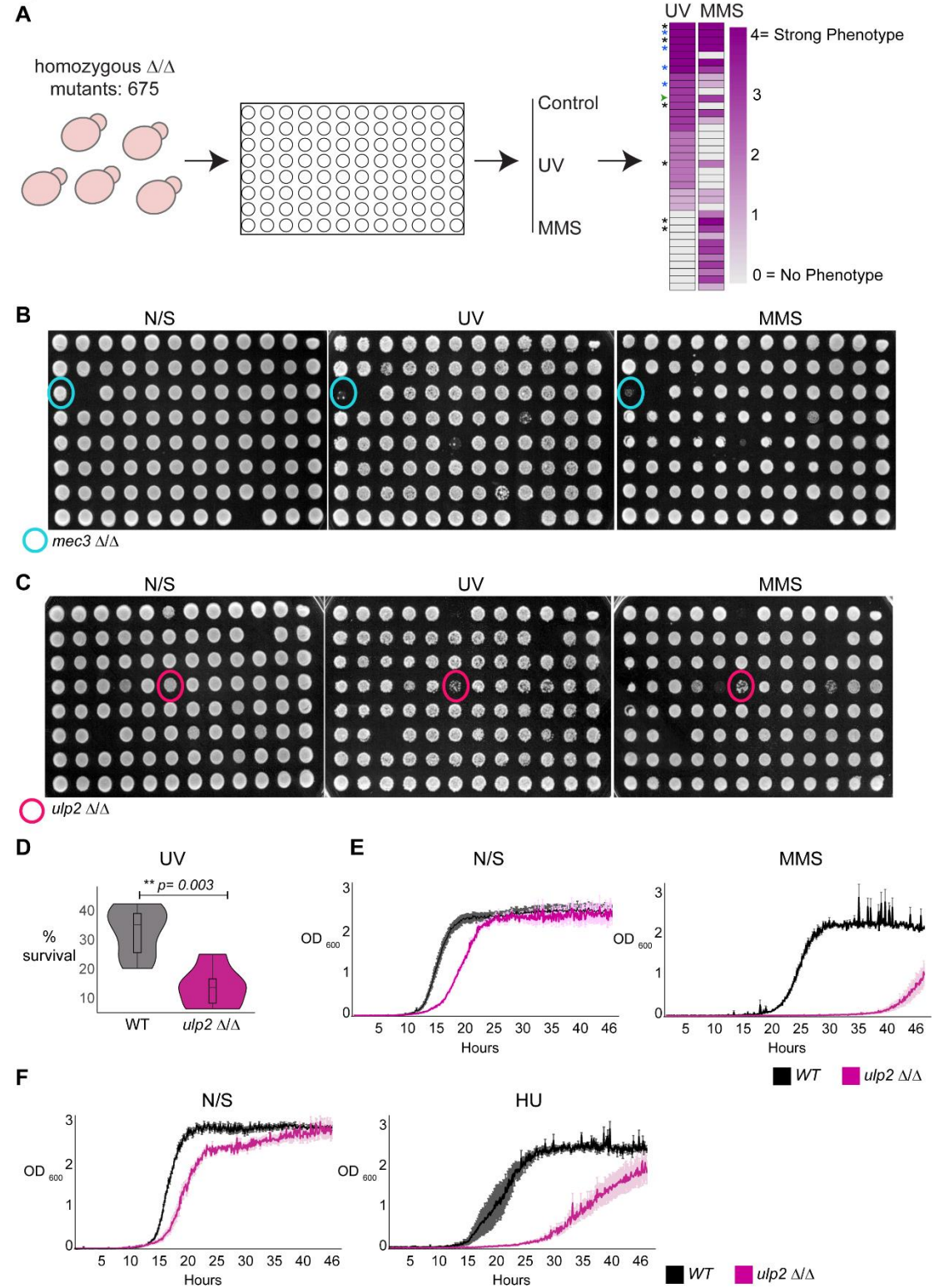


Fig 2

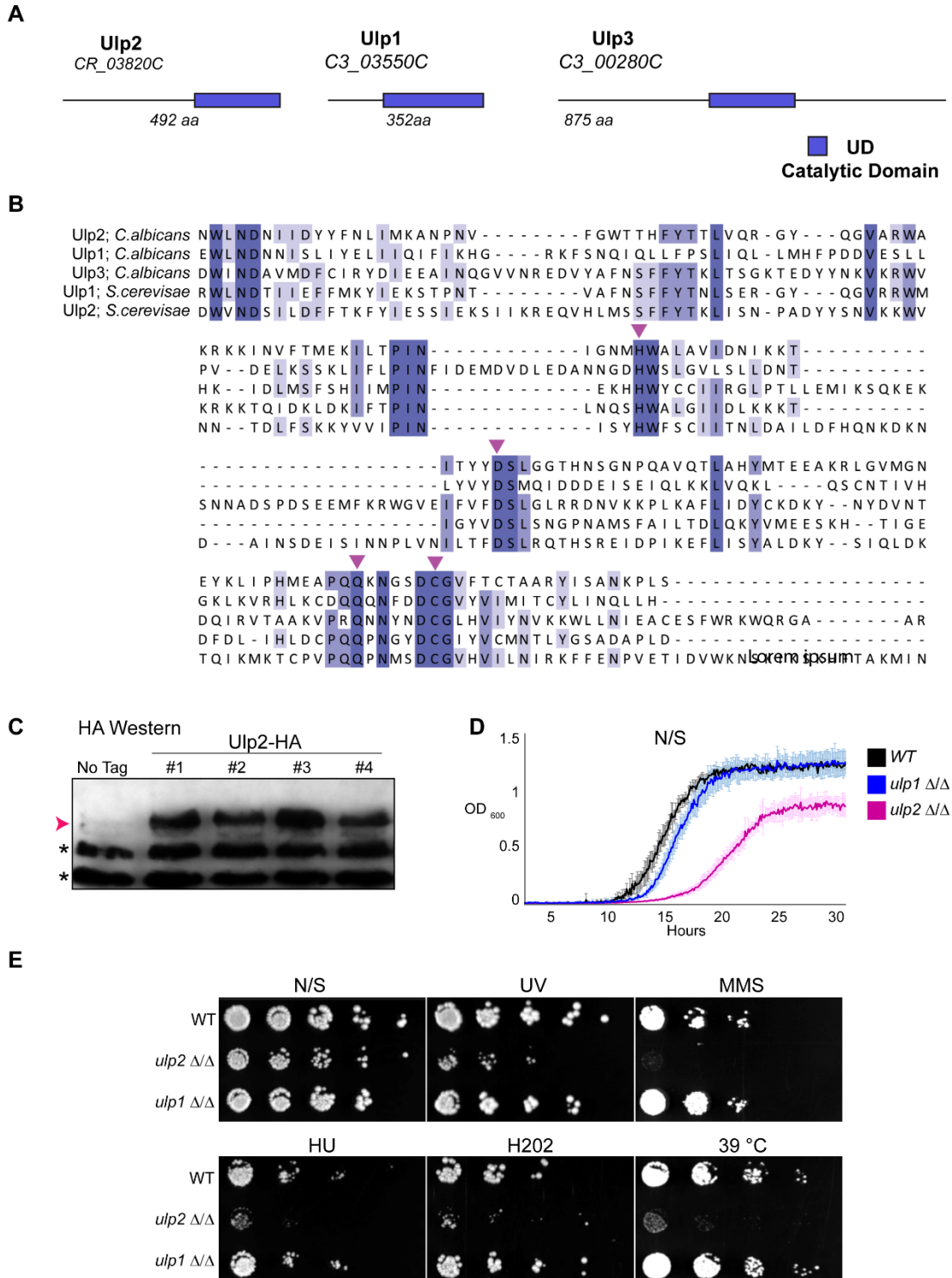


Fig 3

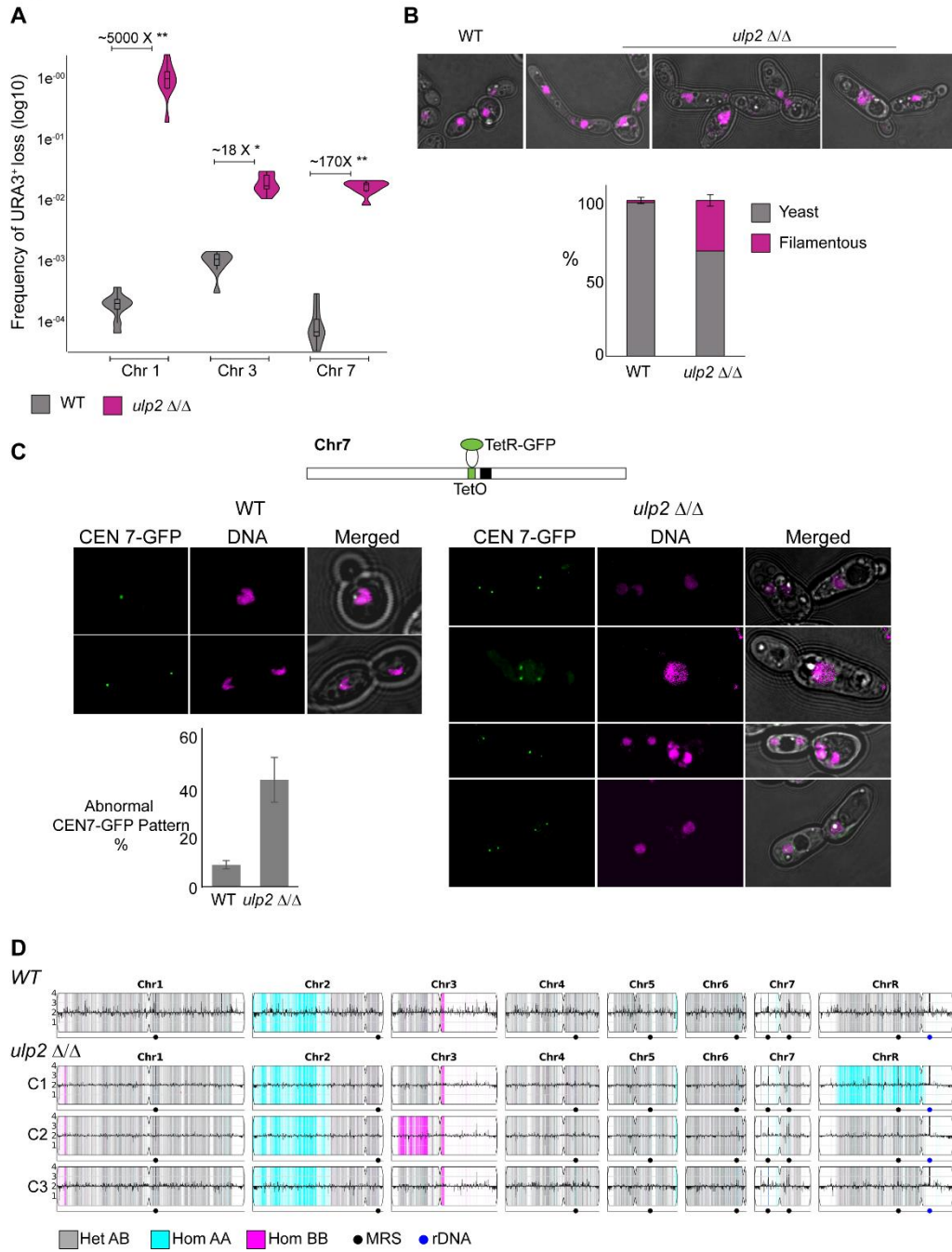
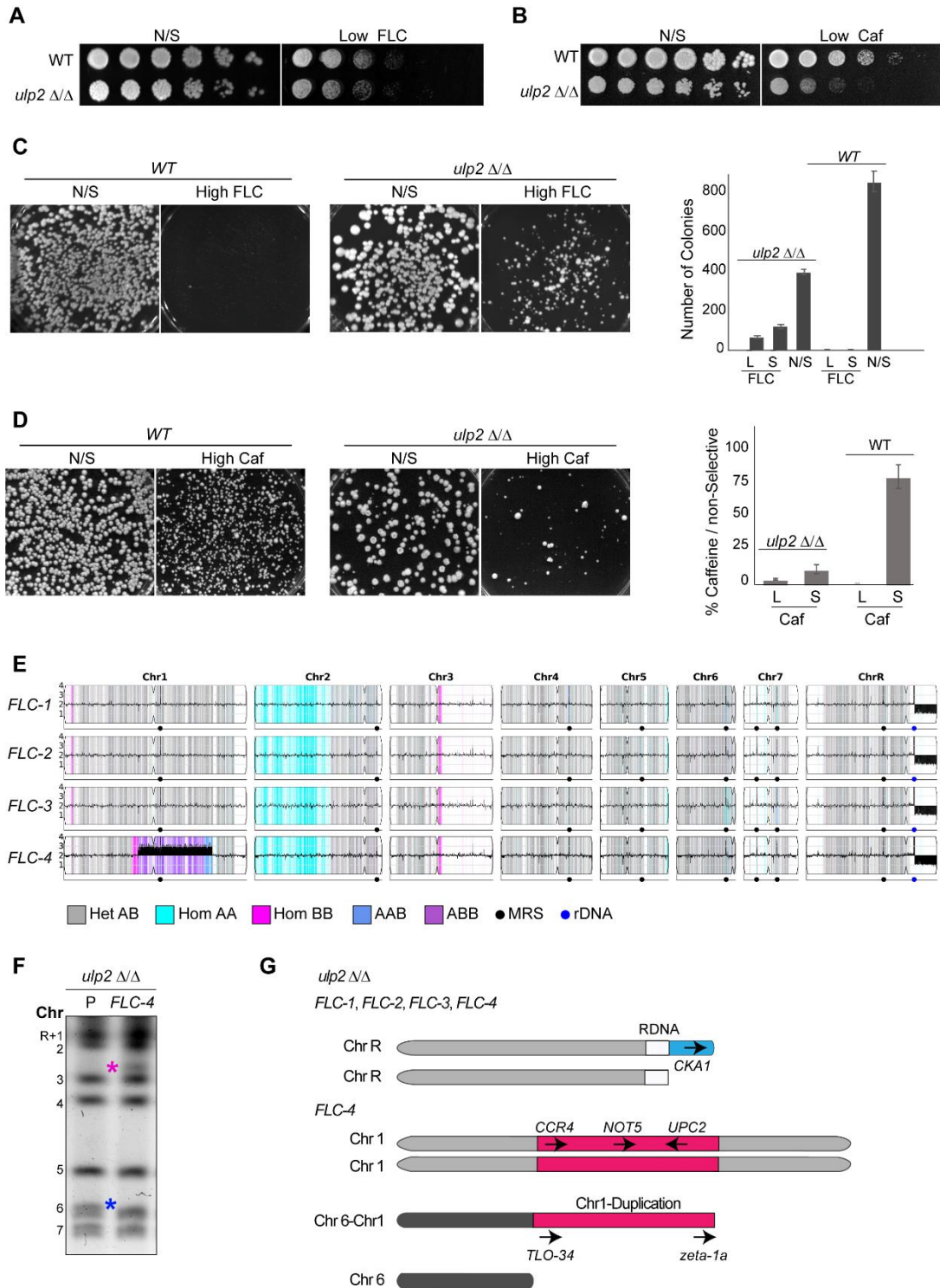


Fig 4

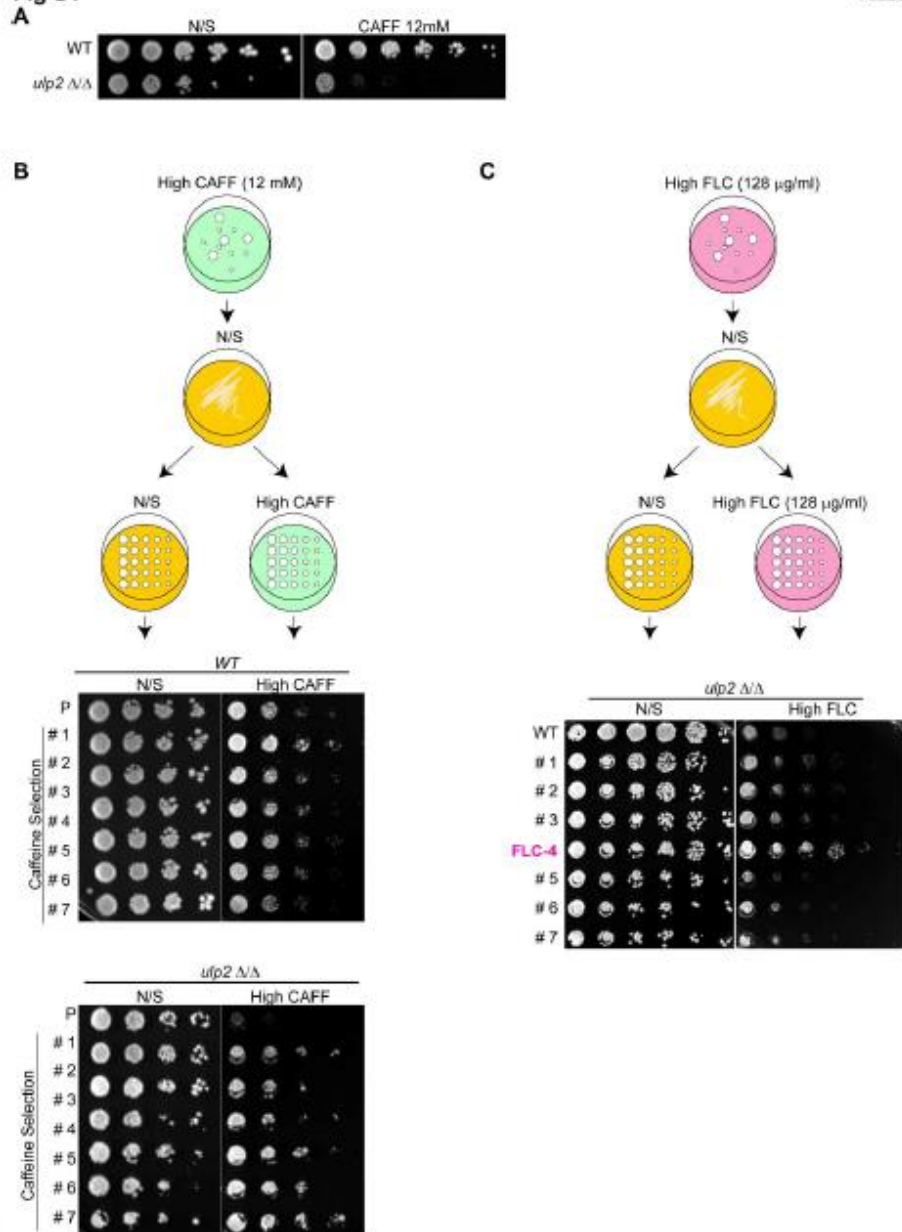
Rizzo et al



4.2 Supplementary figures

Fig S1

Rizzo et al



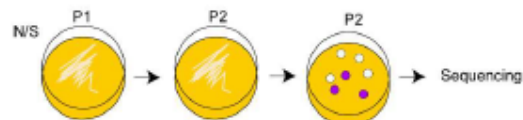
9
 10 Fig S1 (A) Serial dilution assay of WT and *up2* $\Delta\Delta$ strains grown in non-selective
 11 (N/S) media and media containing 12 mM Caffeine (CAF) (B) *Top*: Schematic of
 12 CAFF resistance testing. Single colonies from high CAF plates (12 mM) were
 13 streaked on non-selective (N/S) media before conducting a serial dilution assay in

14 non/selective and High Caffein (12 mM) plates *Bottom*: Serial dilution assay of WT
 15 and *ulp2* Δ/Δ colonies in non-selective media and High caffeine (12 mM CAF)
 16 media. Colonies were selected on high Caffeine (12 mM) and passaged in non-
 17 selective (N/S) media before performing the experiment. (C) *Top*: Schematic of FLC
 18 resistance testing. Single colonies from high FLC plates (128 μ g/ml) were streaked
 19 on non-selective (N/S) media before conducting a serial dilution assay in
 20 non/selective and High FLC plates (128 μ g/ml) *Bottom*: Serial dilution assay of WT
 21 and *ulp2* Δ/Δ colonies in non-selective (N/S) media and High FLC (12 mM CAF)
 22 media. Colonies were selected on High FLC plates (128 μ g/ml) and passaged in
 23 non-selective (N/S) media before performing the experiment. The sequenced *FLC-4*
 24 isolate is highlighted (magenta)

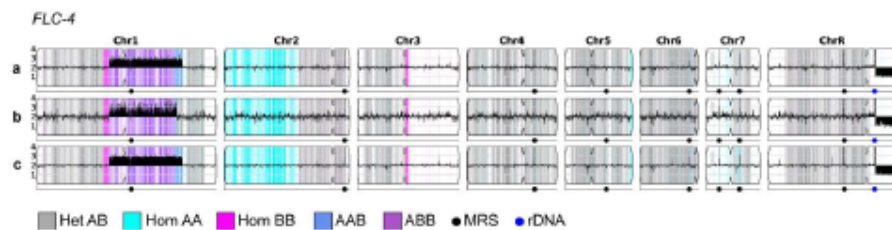
Fig S2

Rizzo et al

A *FLC-4*



B



25

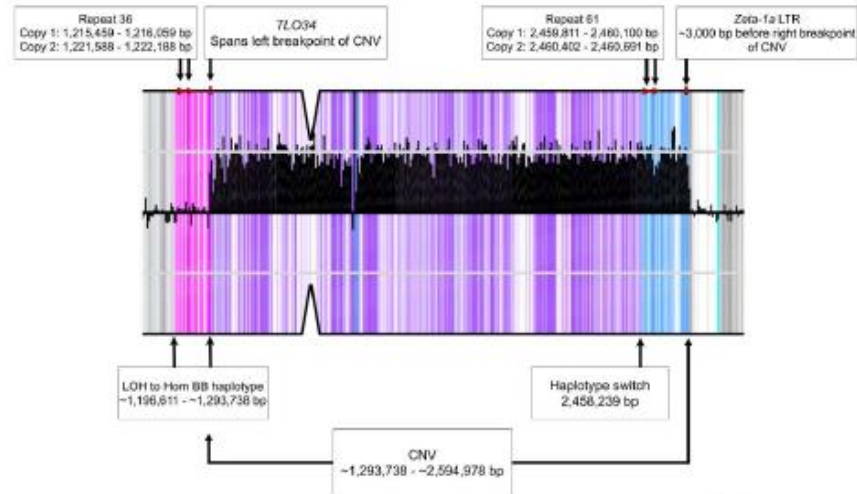
26 **Fig S2 (A)** Schematic of *FLC-4* passaging before sequencing. 3 colonies (magenta)
 27 were sequenced. **(B)** *FLC-4* was selected on 128 μ g/ml FLC, passaged twice on
 28 YPAD, and then plated again for single colonies on 128 μ g/ml FLC. Three single
 29 colonies (magenta) were selected and sent for whole genome sequencing. **(B)**
 30 Whole genome sequence data were plotted as the log₂ ratio and converted to
 31 chromosome copy number (y-axis, 1-4 copies) as a function of chromosome position
 32 (x-axis, Chr1-ChrR) using YMAP. Heterozygous (AB) regions are indicated with gray
 33 shading and homozygous regions are indicated by haplotype AA (cyan) or BB
 34 (magenta). Allele ratio changes that occur within a CNV are indicated as dark blue
 35 (AAB) or purple (ABB). Colony B and C had allele ratio colouring that was corrected
 36 using IGV and allele frequency information. Two homozygous regions were already

37 present in the progenitor (the left side of Chr2 and a small region near the
 38 centromere of Chr3).

Fig S3

Rizzo et al

A *FLC-4*



39 Hom AB Hom AA Hom BB AAB ABB

40 **Fig S3. Copy number and allele ratio changes occur near repeat sequences in**
 41 **FLC-4.** Whole genome sequence data plotted as in Figure S2 for the segmental
 42 amplification of Chr1 in one representative strain (FLC-4-c). Repetitive sequences
 43 are identified at the CNV and allele ratio changes. The position of copy number and
 44 allele ratio changes are approximate and repeat numbers refer to Supplementary file
 45 2 from Todd et al., 2019. From left to right across Chr1: the alleles change from
 46 heterozygous (AB, gray) to homozygous (BB, magenta) at position 1,196,611 bp,
 47 near Repeat 36. The copy number increases from 2 to 3 copies, and the allele ratio
 48 changes to ABB (purple), at the repeat containing *TLO34*. On the other side of the
 49 CNV, there is a haplotype switch from purple (ABB) to dark blue (AAB) near repeat
 50 61. Finally, the copy number decreases from 3 to 2 copies at the repeat containing
 51 Zeta-1a, at which point the allele ratio changes back to AB (gray).

52

4.3 Supplementary Tables

Due to the size of the supplementary tables, it was not possible to include them in this thesis. These tables are available online at this link on BioRxiv:

<https://www.biorxiv.org/content/10.1101/2021.12.06.471441v1.supplementary-material>

Chapter 5. Discussion

5.1 Identification of a novel potential regulator of stress-induce genome instability

To identify a novel regulator of *C. albicans* stress-induce genome instability, I performed a genetic screening using a *C. albicans* gene deletion library comprising homozygous deletion isolates targeting 674 genes, representing the 11% of *C. albicans* genome (Noble et al., 2010a). The two different sources of DNA damaging agents used, UV causing SSBs and MMS leading to DSBs have identified several genes sensitive to one or both of the DNA damaging agents. The sensitivity to one or both sources of stress was scored with a semi-quantitative approach comparing the growth of the deletion isolates in stress condition and non-stress condition. From this, the selected deletion mutants showing sensitivity to the DNA damaging agent were classified into functional groups. The gene with roles in stress response, cell cycle and nuclear localisation were selected for the next steps of the screening. On the contrary, the genes with functional roles in TR, LMP, VC, ENZ, ND, PLM and CW were excluded due to roles outside the aim of this study. Furthermore, genes with roles in DNA repair system (*MEC3*, *RAD18*, *RAD32*, *HOG1*, and *REV1*) were identified.

The results of the UV and MMS genetic screenings showed that after all the screening steps the following genes were identified as final candidates of novel regulators of genome instability: *KIP3*, *SPT8*, *GRR1*, *KAR3*, *ULP2*, *PPH3*, *PTC2*, AND *CLB4*. (i) *KIP3* involved in mitotic spindle (McCoy et al., 2015); (ii) *SPT8* a subunit of SAGA complex (Bhaumik and Green, 2002); (iii) *GRR1* involved in cell division (Landry et al., 2012); (iv) *KAR3* is required for normal mitotic spindle formation and nuclear division (Meluh and Rose, 1990); (v) *ULP2* is a SUMO post translational modifier (Hochstrasser, 2001); (vi) *PPH3* is involved in Rad53 dephosphorylation after DNA damage (O'Neill et al., 2007). (vii) *PTC2* plays a role in virulence and DNA damage-relates protein phosphatases (Feng et al., 2019a). (viii) *CLB4* a G₂ cyclin present also in early S-phase (Ofir and Kornitzer, 2010). From these 8 genes, cells lacking the *ULP2* gene showed strong sensitivity to both the DNA damaging agents and *ULP2* was further investigated in this study.

5.2 Ulp2 play a role in cell cycle and genome instability

Ulp2 is a post-translational modifier protein belonging to small ubiquitin-like modifier (SUMO) protein (Hochstrasser, 2001). SUMO conjugation and deconjugation are essential processes for mitosis and chromosome segregation (Wan et al., 2012). The PTMs showed a crucial role in controlling replication and genome instability (Li and Xu, 2019). Not much information has been reported about Ulp2 in *C. albicans*. However, in *S. cerevisiae*, the de-SUMOylation action of Ulp2 targets kinetochore subunits throughout its SUMO-interacting motif. More specifically, it was seen that mutations in the lysine residues in the consensus motif of Ndc10, Cep3 and Bir1 kinetochore proteins lead to chromosome instability, mislocalisation from mitotic spindle, and defective anaphase spindles (Montpetit et al., 2006). Furthermore, the de-SUMOylation action of Ulp2 also plays a role in the maintenance of centromere cohesin ensuring correct chromosomes segregation (Baldwin et al., 2009). Additionally, *ULP2* gene deletion lead to DNA replication stress sensitivity and hyper-SUMOylate CCAN which takes place in the kinetochore and ensures correct chromosome segregation (Suhandynata et al., 2019).

From this study, *ULP2* deletion strain has showed strong sensitivity to both UV and MMS stresses in all the steps of the genetic screening. From the spotting susceptibility assays it showed strong sensitivity classified with value 3 out of 4 for both UV radiation and MMS. In addition, it showed lower percentage of survival to UV irradiation compared to wild type and higher percentage of filamentous forms. Furthermore, cell lacking *ULP2* exhibits a growth rate phenotype in response to the MMS drug which is very similar to the positive control *mec3ΔΔ* strain.

5.3 Ulp2 protein expression and hypersensitivity to genotoxic stress

After the selection of *ULP2* gene as a potential candidate of stress-induced genome instability from the gene deletion library, investigation of the three putative SUMO deconjugating enzyme showed that the amino acid residues which are essential for the catalytic activity are conserved between *C. albicans* and *S. cerevisiae*. The study by (Huaping et al., 2007) hypothesised that *ulp2* has no detectable expression protein in both the morphological states of *C. albicans*. To investigate this further, the integration at the endogenous locus, of an epitope-tagged *ulp2* protein (Ulp2-HA) proved the expression of Ulp2 by western blot. In contrast to Huaping et al., 2007, my results showed that *ulp2* expression is detectable from independent strains and that the protein expression is stable in non-selective media.

From the results of the genetic screening, *ulp2ΔΔ* showed strong sensitivity to UV and MMS stresses. To confirm these results and investigate if *ULP1* and *ULP2* have different roles, I performed a separate homozygous deletion for *ULP1*, and *ULP2* in SN152 laboratory wild type. In *C. albicans*, *ULP3* gene is essential and for this it was not investigated further in this study. Analysis of the growth rate of *ulp1ΔΔ* and *ulp2ΔΔ* showed that *ulp1ΔΔ* exhibits a growth rate comparable to wild type under normal condition. In contrast, *ulp2ΔΔ* showed delayed growth rate. In accordance with these results, the sensitivity to genotoxic agents has confirmed that cells lacking *ULP2* are sensitive to different types of stress (UV, MMS, HU in both liquid and solid media, H₂O₂, and high febrile temperature (39 °C)). On the contrary, *ulp1ΔΔ* did not show any sensitivity or sensitive phenotype to the different stresses' conditions, concluding that in *C. albicans*, *ULP2* plays an essential role for the survival to stress conditions.

5.4 *Ulp2* $\Delta\Delta$ induces genome instability

The deletion of *ULP2* gene from three strains containing a heterozygous *URA3*⁺ marker in three different chromosomes (chromosome 1, 3, and 7), showed increased LOH rate in all the three chromosomes. These results confirm that *ULP2* gene plays an essential role for genome stability.

From the quantification of filamentous forms in the last step of UV genetic screening, cells lacking *ULP2* exhibited higher formation of filamentous forms. This result was again confirmed with the laboratory engineered strain SN152 *ulp2* $\Delta\Delta$. This led to the conclusion that, the loss of *ULP2* led to an increase of abnormal morphologies and pseudo-filamentous forms.

SUMO conjugation and deconjugation are essential processes for mitosis and chromosome segregation (Wan et al., 2012). For this, to investigate if the deletion of *ULP2* led to chromosome mis-segregation, I removed *ULP2* gene from a strain in which TetO sequence is integrated next to the centromere on one homolog of chromosome 7. In addition, an intragenic region expresses the TetR-GFP fusion protein. As a result, from the binding of TetR-GFP protein to the TetO sequence, the exact localisation of the engineered chromosome 7 during cell cycle was allowed to follow. The outcome of this showed that cell lacking *ULP2* exhibited defects in chromosome segregation with a 5-fold increase compared to wild type.

In *S. cerevisiae*, *ULP2* deletion results in multi-chromosome aneuploidy added to growth defects and DNA damage. This aneuploidy occurs in two specific chromosomes, chromosome I and XII and it can be eliminated with the re-integration of *ULP2* into the genome (Ryu et al., 2020; H. Y. Ryu et al., 2016). However, the results from the CHEF electrophoresis do not exhibit any multi-chromosome aneuploidy. In addition, the sequencing by whole genome sequencing (WGS) of 3 random *ulp2* $\Delta\Delta$ colonies confirms that in *C. albicans* the deletion of *ULP2* does not conceive in specific

chromosome rearrangement, however, it led to specific genomic variations with extensive LOH on different chromosome.

5.5 Stress adaptation and drug resistance

The highly plastic genome of *C. albicans* can provide adaptive genotypes in the presence of stress environment. This has been widely seen in clinical isolates where the stressful environments, for example the presence of drugs, promote mutagenesis generating different types of genetic variation leading to the pathogen adapting in order to survive (Avramovska and Hickman, 2019b; Ford et al., 2015). The different types of stress conditions lead to different type of genetic alteration which is directly correlated to the type of DNA damage induced by the stress condition (Brown et al., 2014). My results showed that *ULP2* gene can provide the selection of specific genotype leading to a specific drug resistance. Using two separate types of stress, fluconazole, and caffeine, *ulp2ΔΔ* didn't show sensitivity to low dose of fluconazole, on the contrary it exhibited sensitivity to low dose of caffeine. Investigating further on adaptations of *ULP2* gene to stress environments, my results showed that cells lacking *ULP2* adapt and survive to high concentration of fluconazole generating small and large colonies while the wild type generated only tiny abortive colonies. Similar results are obtained from caffeine stress. However, cells lacking *ULP2* show decreased number of colonies forming compared to the fluconazole. Furthermore, the passage from stress condition – non stress condition indicate that *ULP2* gene play a role in adaptation to stress environment. To further investigate this, WGS of 3 random colonies selected from high dose of fluconazole (sequenced without performing the passage selective media-nonselective media) and the selected colony (FLC-4) showed resistance to fluconazole after passaging in non-selective media. In addition, these 4 colonies displayed a different genotype compared to the parental *ulp2ΔΔ*. These results showed that all the fluconazole-adapted colonies are defined by a partial deletion of the right arm of chromosome R which take place at the ribosomal DNA. This deletion led to a reduction of dosage for specific genes involved in the response to drug. One of these deleted genes is *CKA1*

the disruption of which lead to fluconazole resistance as shown by (Bruno and Mitchell, 2005).

Further to this, the WGS of FLC-4 showed another segmental aneuploidy represented by a partial duplication of chromosome 1 with breakpoints at repetitive elements. Interestingly, the results showed that this chromosome 1 duplication arose from a fusion event between chromosome 1 and chromosome 6 which emerged within *TLO* homologous sequences. In addition, this segmental aneuploidy is visible by CHEF, in which in FLC-4 the chromosome 6 homolog band is missing, and the extra chromosome is visible above chromosome 3. In addition to this, the evolution of chromosome 1 duplication generates the idea that the combination of two events, the presence of fluconazole and the lack of *ULP2*, led to fitness advantages for *C. albicans*. More specifically, the WGS showed that several genes present in chromosome 1 duplication are involved in drug resistance such as the *UPC2* gene, the overexpression of which leads to fluconazole resistance. The presence of *CCR4* and *NOT5* instead lead to the idea that these two genes rescue the effect cause by the lack of *ULP2* gene. These results are in line with findings in *S. cerevisiae* where *CCR4* and *NOT5* overexpression rescue the fitness defect cause by the *ULP2* depletion.

Future work

This study has identified *ULP2* gene as a novel regulator of *C. albicans* stress-induced genome instability. *ULP2* gene was shown to play an important role in genome instability and chromosome segregation. In addition, *ULP2* deletion causes the selection of specific genotypes which lead to drug resistance and adaptation to stress environment. However, reintroduction of *ULP2* gene in *ulp2ΔΔ* strain was not conducted. Furthermore, the gene expression of genes present in the segmental aneuploidies in FLC-4 was not investigated. Lastly, *ulp2ΔΔ* and FLC-4 phenotypes were not tested in other stress conditions, which might show whether FLC-4 acts as multi-drug resistance. The findings obtained in addition to the aforementioned further investigations might elucidate the possible role of *ULP2* gene in genome instability and drug resistance which might represent in the long term a good candidate for target therapies in pathogenic *C. albicans*.

Chapter 6. Materials and Methods

6.1 Sterilisation

All the media, H₂O, buffer, and solution were sterilised for 18 min at 121 °C and 1.05 Bar (15 psi) pressure using a bench top Prestige Medical autoclave (Coventry, UK). All the solutions and media sensitive to temperature were filtered sterilised (Thermo Scientific™ Nalgene™ Rapid-Flow™ sterile disposable bottle top filters with SFCA Membrane, #10139560, 0.2 µm pore size).

6.2 Growth media

Depending on the type of experiments, different media were used. Mainly, the strains were cultures in rich medium YPAD containing extra adenine hemisulfate and uridine added as growth supplements. For solid media, agar was added. After preparation, the media were autoclaved, or filter sterilised in the case of casitone media. All the media used for this thesis are listed below.

Table 6.1 YPAD: yeast extract, peptone, adenine, dextrose media	
Compound	g/L
Yeast extract (Oxoid, #LP0021)	10
Bactopeptone (BD Biosciences, #211677)	20
Glucose (Fisher, #G/0500/61)	20
Adenine hemisulfate (Merk, #A3159)	0.05
Uridine (Merk, #U3750)	0.08
Agar (Melford Biolaboratories, #9002-18-0)	20

6.3 SC and SC drop-out: -His/-Arg media

The synthetic amino acid complete media (SC) and the synthetic complete media lacking the specific aminoacid his or arg (SC drop-out his/arg) were used for microscopy and as selective media for transformants respectively. SC and SC drop-out media were prepared as shown in table 6.2

Table 6.2 SC and SC drop-out: -His/-Arg media	
Compound	g/L
SC complete mixture drop-out (Formedium DSCCK1000)	2.002
SC drop-out: histidine (Formedium DSCS041S)	1.915
SC drop-out: arginine (Formedium DSCS314S)	1.915
Yeast nitrogen base without aminoacids (Difco #291940)	6.70
Glucose (Fisher, #G/0500/61)	20
Uridine (Merk, #U3750)	0.08
Agar (Melford Biolaboratories, #9002-18-0)	20

6.4 Casitone media

Casitone (pancreatic digest of casein) media was used to assess sensitivity to fluconazole. Once prepared, this media was filter sterilised. For solid media, half of the volume was added to autoclaved agar.

Table 6.3 Casitone media	
Compound	g/L
Yeast extract (Oxoid, #LP0021)	5
BactoTryptone (BD Biosciences, #211705)	9
Glucose (Fisher, #G/0500/61)	20
Sodium Citrate dehydrate	11.5
Agar (Melford Biolaboratories, #9002-18-0)	15

6.5 Additives: drugs and antibiotic

Different additives were added to media both liquid and solid.

Table 6.4 Additives	
Solution	Final concentration
Benomyl (Sigma # 45339)	15ug/mL
Caspofungin (Sigma # 32343)	0.06ug/mL 0.5ug/mL
Camptothecin (Sigma #C9911)	250µM
Caffeine (Sigma #C0750)	12mM
Fluconazole (Sigma #F8929)	5 µg/mL 10 µg/mL 15 µg/mL 128µg/mL 256µg/mL
5- Fluoroorotic acid (Melford #F5001)	1mg/mL
H ₂ O ₂ (sigma #H1009)	6mM
Hydroxyurea (sigma H8627)	12mM 22mM
MMS (Sigma #129925)	0.005%
Nocodazole (Sigma #M1404)	25 µg/mL
Antibiotic	Final concentration
Ampicillin (Melford #A0104)	100 µg/ml
Kanamycin (Sigma # K-4000)	50 µg/ml
Nourseothricin (Melford #N51200)	200 µg/ml

6.6 *Candida* strains used for the genetic screening

The strains used for this screening were obtained from a homozygous *C. albicans* gene deletion library which includes homozygous deletion strain affecting 674 genes (Noble et al., 2010a). The full list of the strains included in the collection is listed in table 6.5. In general, *C. albicans* strains were streaked from a glycerol stock to an agar plate and were cultured overnight on YPAD media or SC media unless it is stated otherwise. The plates were incubated overnight at 30°C and were grown overnight on a platform shaker at ~180 rpm at 30 °C.

6.7 Screening methodology

For the genetic screening, a *C. albicans* homozygous deletion isolated library from (Noble et al., 2010a) was used. The screening was divided into 4 steps:

1. The first step was the primary screening: the library was plated on YPAD plates (145x20mm), for UV radiation stress, the plates were irradiated using UVitec (Cambridge) with power density of $7.5\mu\text{W}/\text{cm}^2$ (0.030 J for 4 seconds), covered with aluminium foil and incubated at 30°C for 48 hours. Regarding the MMS drug stress, the genetic library was spotted on YPAD plates (145x20mm) for the control and YPAD with 0.005% MMS, incubated at 30 degree for 48 hours. In both the stresses, strains which showed sensitivity to UV and/or MMS were selected for the next step, images of plates were taken with Perfection v33 Epson's scanner.

2. The second step was the spotting susceptibility assay: the selected homozygous deletion strains from the primary screening were cultured overnight and then diluted to $\text{OD}_{600} = 4$, thereafter, serially diluted by 1/5 in the subsequent five wells and finally spotted in the specific media plates (section 6.8). YPAD plates were used as control, for UV stress, YPAD plates were followed by UV irradiation of $7.5\mu\text{W}/\text{cm}^2$, lastly for MMS stress the spotting assay was spotted on YPAD plates for control and on YPAD media with the addition of 0.005% MMS. Plates were kept at 30 °C for 48 hours, for UV stress the plates were covered with aluminium foil. Sensitive mutants were then selected for the third steps.

3. The third step was screening by colony PCR: the homozygous deletion strains selected from the second step of the screening were subjected to verification of deletion of the target gene. Primers inside the target gene were designed using SNAPGene Viewer v5.1.2 software (from GSL biotech; available at snapgene.com), a list of the primers used is found in table 6.6 The reagents and protocol are found in section 6.9.

4. The fourth and last step of the genetic screen was: quantification of survival. The quantification of survival of the final selected deletion strains was performed by colony counting after UV irradiation for the UV genetic

screening (section 6.10), instead for the MMS genetic screening, growth curves analysis was performed to final mutants (section 6.11).

6.8 Spotting assay serial dilution

Strains were incubated overnight in YPAD at 30 °C or 39 °C (when specified) with shaking. Cultures were diluted to an OD₆₀₀ =4 and then serially diluted by 1/5 in five subsequent wells and then spotted to the specific agar media using a replica plater (Replica plater for 96 well plates (8x6) Sigma Aldrich, #R2383). Plates were then kept at 30°C or 37 °C (when specified) and covered with aluminium foil for spotting assay subjected of UV radiation. Images of the plates were then taken using Syngene GBox Chemi XX6 Gel imaging system.

6.9 Colony PCR

Single colonies or streaked strains were touched with yellow tip and mixed with 40µL of 0.02 M NaOH inside Eppendorf tubes®. The tubes were boiled at 100 °C for 10 minutes then kept on ice for additional 10 minutes. Lastly, the tubes were centrifuged at 5000 rpm for 2 minutes after 1 µL of the supernatant was added to the PCR Master mix, the list of PCR reagents is shown in table 6.8.A. In table 6.8.B is shown the PCR cycles used.

Table 6.8.A PCR Master mix reagents	
Reagents	Volume for 1 reaction
10x PCRBIO Classic Buffer +30mM Mg (PCR Biosystems®PB609-10)	1.5µL
Forward primer (10µM)	0.6µL
Reverse primer (10 µM)	0.6µL
dTNPs (10 mM stock of mixture of dATP, dCTP, dGTP, dTTP, (VWR))	0.5uL
PCRBIO Classic Taq (1unit/ µL) (PCR Biosystems® PB004619-112-2)	0.13 µL
dH ₂ O	Up to 14µL final volume

Table 6.8.B PCR cycles protocol			
	Temperature (°C)	Time	Cycles
Initial denaturation	94°C	7 minutes	30
Denaturation	94°C	45 seconds	
Anneal	56°C	1 minute	
Extension	72°C	1 minute	
Final extension	72°C	7 minutes	

After the PCR reaction is over the PCR products were checked by gel electrophoresis using 1% agarose gel (Melford Biolaboratories, #MB1200) in 0.5x TBE and ethidium bromide (0.5µg/mL) and imaged with UV by SynGene Gel Doc Imaging System (BioRad).

6.10 UV survival quantification

To quantify the survival to UV irradiation, cells were incubated overnight in YPAD at 30°C with agitation of 200 rpm. The cultures were then diluted to plate 500 cells for control and 1500 cells for UV in YPAD plates. UV plates were irradiated (UVitec, Cambridge) with power density of 7.5µW/cm² (0.030 J for 4 seconds) kept in the dark and incubated at 30°C degree for 48 hours. Colonies were counted using colony counter (Stuart Scientific).

6.11 Growth curve

To evaluate the survival and growth rate, strains were incubated overnight in YPAD at 30°C with agitation. Cells were diluted to 60 cells/µL in 100µL per well in a 96 well plate (Cellstar®, #655180). The plate then was grown at 30 °C with double orbital agitation of 400 rpm in a BMG Labtech SPECTROstar nano plate reader for 48 hours. The OD₆₀₀ and lag time were

used as growth parameters. Growth rate was calculated considering the difference between the Napierian logarithm of growth at two time points during the exponential phase using the following formula:

$$\frac{\ln(V2) - \ln(V1)}{t2 - t1}$$

V1 indicates the growth value at the beginning of the exponential phase and t1 its relative time point, on the contrary V2 indicates the growth value at the end of the exponential phase and its time point (t2).

The Maximum OD was measured in OD units and calculated using the function MAX() in Microsoft® Excel. All the results and graphs were reproduced in Microsoft® Excel.

6.12 *Candida albicans* strain transformant: Lithium acetate transformation

Transformants were constructed using Lithium acetate transformation according to Knop et al. 1999. To make competent cells, overnight cultures in YPAD were diluted in 50mL of fresh YPAD and grown to the desired OD_{600nm} of 1.3. Afterward, cells were harvested by centrifugation at 2000rpm for 5 minutes. Pellets were washed once with dH₂O and once with SORB solution, centrifuged at 3000 rpm for 3 minutes (SORB solution had a final concentration of: 100mM Lithium acetate, 10mM Tris-HCL pH 7.5, 1mM EDTA pH 7.5/8, 1M sorbitol; pH 8 adjusted with diluted acetic acid and autoclaved). The pellet was then resuspended with 360 µL of SORB solution and 40 µL of single stranded carrier DNA (Sigma-Aldrich), previously boiled at 100°C for 10 minutes and then cooled down on ice for 5 minutes. The 400 µL of cells were then aliquoted in 50 µL and kept in -80 °C refrigerator for a maximum of 3 weeks. The day after the frozen competent cells were defrosted on ice, 5 µL of PCR product were added to the cells together with 300 µL PEG solution (final concentration: 100mM Lithium acetate, 10mM Tris-HCL pH 7.5, 1mM EDTA pH 8, 40% PEG4000) and incubated for 21-24

hours at 30 °C. Then, the cells were heat shocked at 44°C for 15 minutes and pelleted twice at 4600 rpm for 30 seconds. Cells were resuspended in 100 µL dH₂O and incubated in 5mL YPAD for 6 hours at 30 °C with shaking for recovery. Finally, the cells were then plated in selective media and incubated at 30 °C for a few days.

6.13 HiFidelity PCR and gel electrophoresis

For the construction of transformant the deletion of genes and gene tagging was performed using long oligos-mediated PCR. To substitute the target gene, the long oligos were constructed using around 70 nucleotides of homology with the Upstream and Downstream region of the gene of interest added to 20 nucleotides of homology to the plasmid of the maker gene. Regarding the gene tagging, the construct was designed with a plasmid containing HA epitope or GFP and a marked gene. High Fidelity PCR reactions were used with long oligos with the reaction showed in table 6.9.A and cycles used are based on table 6.9.B.

Table 6.9.A HiFidelity reagents protocol	
Reagents	Volume for 1 reaction
5x PCR BIO HiFi Buffer (PCR Biosystems® PB608-04)	5µL
Forward primer (10µM)	1 µL
Reverse primer (10 µM)	1µL
Template DNA (500ng)	0.25uL
PCR BIO HiFi Polymerase (1unit/ µL) (PCR Biosystems® PB007610-01-16)	0.25 µL
dH ₂ O	Up to 25 µL final volume

Table 6.9.B PCR Hi fidelity protocol			
	Temperature (°C)	Time	Cycles
Initial denaturation	95°C	1 minute	1
Denaturation	95°C	30 seconds	30
Anneal	58°C	30 seconds	
Extension	72°C	2.5 minute	
Final extension	72°C	7 minutes	1

Then the PCR products were checked by gel electrophoresis using 1% agarose gel (Melford Biolaboratories, #MB1200) in 0.5x TBE and ethidium bromide (0.5µg/mL) and imaged with UV by SynGene Gel Doc Imaging System (BioRad).

6.14 CHEF electrophoresis

6.14.1 Solutions

EDTA 100mM and 50mM were prepared from 0.5M stock. Zymolyase® 100T from *Arthrobacter luteus* (Amsbio, # 120493-1), was used from a stock of 10 mg/ml in 50% glycerol, 1mg of enzyme per 5ml of NDS was used. LET solution was prepared by adding 200mL of 0.5M EDTA, 10ml of 1M Tris (pH=8) and adjusted to 1 litre with water. NDS solution was prepared by adding 200ml of 0.5M EDTA, 50ml of 1M tris pH=8, 50ml of 10% SDS, then adjusted to 1 litre with water.

6.14.2 Plugs preparation

C. albicans strains were cultured overnight in 5ml YPAD media at 30 °C with shaking. The volume of cells corresponding to OD₆₀₀ of 6 was taken and centrifuged at 3000 rpm for 3 minutes at room temperature. The cells were washed with 1ml 50mM EDTA and centrifuged at 3000 rpm for 3 minutes. After, EDTA was remove and cells were resuspended with 20µL of 10mg/ml Zymolyase and 300 µL of 1% low melt agarose (Biorad®, #1613112) in

100mM EDTA. The mixture was transferred in the plug mould and allowed to solidify for 45 minutes and then transferred in tubes containing 2.5 ml LET and 25 μ L of β -mercaptoethanol (Merk, #M6250). The plugs were incubated at 37°C overnight. The next day, LET was removed, and plugs were washed for 30 minutes with 50mM EDTA twice. The NDS-proteinase K solution was added to the tubes containing the plugs and incubated at 50°C in Roller-Blot Hybridizer HB-30 (Techne®) for at least two days. Lastly, the NDS solution was removed, and plugs washed with 50mM EDTA for 30 minute and resuspended in fresh 50mM EDTA, the plugs then could either be stored at 4 °C or used immediately for electrophoresis.

6.14.3 Chromosome separation by electrophoresis

Gel was prepared with 1% agarose (Biorad®, #1613110) and run in CHEF DR II system (Biorad®) in 2 litres of 0.5x TBE at 14 °C. The setting used for the run are 60-120s switching time for 12 hours at 6V/cm followed by 120-300s switching for 26 hours at 4.5 V/cm. The gel was then stained in 0.5x TBE with ethidium bromide (0.5 μ g/ml) for 30 minutes and for another 30 minutes in water. The chromosome separation was visualised under UV light using Syngene GBox Chemi XX6 Gel imaging system.

6.15 Fluconazole resistance

Strains were incubated overnight in casitone media at 30°C incubator with shaking. Cells concentration was calculated using the formula $[OD_{600} \times 3 \cdot 10^7]$ and 10^4 cells were plated in small petri dishes (10cm) containing casitone media with addition of Fluconazole (128 μ g/mL or 256 μ g/mL) and casitone media with DMSO (128 μ g/mL or 256 μ g/mL) added as control. The plates were kept at 30 degree for 7 days covered with aluminium foil. To test resistance or tolerability to Fluconazole of newly formed colonies, spotting assay was performed. Colonies were streaked in non-selective casitone media and the day after cultured in casitone media overnight. Cultures were

then diluted to $OD_{600} = 4$, and thereafter, serially diluted by 1/5 in the following five wells and spotted in casitone plus fluconazole 128 μ g/mL or 256 μ g/mL and casitone media with DMSO 128 μ g/mL or 256 μ g/mL as control using Replica plater for 96 well plates (8x6) Sigma Aldrich, #R2383. The plates were kept at 30 degrees and then imaged using Syngene GBox Chemi XX6 Gel imaging system.

6.16 Caffeine resistance

Strains were incubated overnight in YPAD media at 30°C incubator with shaking. Cells concentration was calculated using the formula [$OD_{600} \times 3 \cdot 10^7$] and 10^4 cells were plated in small petri dishes (10cm) containing YPAD media with addition of 12mM Caffeine Anhydrous (Sigma #C0750). The plates were kept at 30°C for 7 days covered with aluminium foil. To test resistance or tolerability to Caffeine of newly formed colonies, spotting assay was performed. Colonies were streaked in non-selective YPAD media and the day after cultured in YPAD media overnight. Cultures were then diluted to $OD_{600} = 4$ and thereafter, serially diluted by 1/5 in the following five wells and spotted in YPAD plus caffeine and YPAD as control using Replica plater for 96 well plates (8x6) Sigma Aldrich, #R2383. The plates were kept at 30°C and then imaged using Syngene GBox Chemi XX6 Gel imaging system.

6.17 Fluctuation analysis

The first step for fluctuation analysis is to check if the strains carry the *URA3*⁺ marker gene. To do so the strains were streaked in -Uri media. After that, two single colonies were growing overnight in 5 ml YPAD for 16 hours at 30 °C with shaking. Then cells were pelleted at 4000 rpm for 5 minutes, washed with distilled water, centrifuged again, and resuspended in 1mL of distilled water. OD_{600} was calculated and cells were plated on SC plate and SC plates with the addition of 1mg/ml FOA (5-Fluorotic acid, Sigma) at cells density depending on the strain, going from 10^4 to 10^8 cells/plate. The plates

were kept at 30 °C for 48h hours. The colonies formed were counted using colony counter (Stuart Scientific) and data were analysed using Microsoft® Excel and then statistical difference was calculated using Kruskal-Wallis test (Hecke, 2013) and the violin plots were generated using R studio (<http://www.r-project.org/>).

6.18 Western Blot

The first step for Western blot is yeast extracts which was performed as described by (T, 2007). The yeast whole cell extract was prepared by growing the culture overnight and then diluting it to $OD_{600}=0.1$ and letting it grow in 50ml YPAD media at 30 °C with shaking until it reached OD_{600} between 0.6 and 1. Cell were harvested at 4000 rpm for 5 minutes, washed with distilled water and resuspended in 500 μ l of water and centrifuged at 40000 rpm for 5 minutes. The supernatant was discarded, and the pellet was mixed with 200 μ l of lysis buffer [(0.1 M NaOH (Fisher), 0.05 M EDTA (Sigma), 2% SDS (Sigma), 2% β -mercaptoethanol (Sigma)] then it was heated at 90°C for 10 minutes. Afterward, 5 μ l of 4M acetic acid (Fisher) was added and samples vortexed for 30 seconds and incubated at 90°C for 10 minutes. Then, 30 μ l of loading buffer [0.25 M Tris-HCL (Melford) pH = 6.8, 50% glycerol (Fisher) and 0.05 % bromophenol blue (Sigma)] were added and clear lysate was obtained by centrifugation at 13000 rpm for 10 minutes. Before to load, the samples were heated at 90°C for 5 minutes, then centrifuged again at 13000 rpm for 5 minutes and lastly kept on ice. Of those samples, 25 μ l was loaded in 15% SDS polyacrylamide gel for electrophoresis (SDS-PAGE). To construct the gel, premade gel cassettes (Invitrogen) were used. The gel was divided into 2 parts: the running gel and the stacking gel. The running gel was composed of 1.1 ml of dH₂O, 5 ml of 2.5ml of Acrylamide mix 30% (Sigma #SLCF0473), 1.3 ml of 1.5 M Tris (Fisher) pH 8.8, 50 μ l of 10% SDS, 50 μ l of 10 % APS (Fisher) and 2 μ l of TEMED (Sigma). After 1ml of isopropanol (Fisher) was pipetted on top of the running gel to flatten the surface. After the gel solidified, the isopropanol was poured off and 2ml of stacking gel was made with 1.4ml of dH₂O, 330 μ l of

Acrylamide mix 30% (BioRad), 250µl of 1.0 M Tris (Fisher) pH = 6.8, 20µl of 10% SDS, 20µl of ammonium persulfate and 3µl of TEMED (Sigma). The stacking gel was poured on top of the running gel, a comb was inserted, and the gel was left solidifying for 45 minutes. After the gel was positioned in the chamber filled with 300ml of freshly prepared 1x running buffer (10x SDS-PAGE running buffer: 30.3g Tris base, 144.0g glycine, 10g SDS, water up to 1L). 25µl of prepared samples were loaded into the wells and 5µl of protein ladder was loaded as reference. The gel was run at 100 V for ~15 minutes until the dye migrated into the running gel then the voltage was increased to 200 V for ~1 hour until the dye reached the bottom of the gel. After the run was completed, a wet transfer method was applied to transfer the bands of the gel into a PVDF membrane. Firstly, the PVDF membrane was prepared by wetting it in methanol for 30 seconds, soaked briefly in distilled water and then placed in transfer buffer (1x transfer buffer: 10x SDS running 150ml, methanol 300ml, dH₂O 1050 litre) for 10 minutes. Two pieces of western blot filter papers (Invitrogen) were soaked in transfer buffer for 10 minutes together with sponges for transfer. A piece of filter paper was positioned on top of the sponge of transfer on the anode of a Trans-Blot wet transfer cell (BioRad) followed by the PVDF membrane, gel, a second piece of filter paper and a second sponge. The cathode was placed on top and the whole assembly transferred to the tank full of transfer buffer. The run was performed at 100V at 4°C for 1 hour.

After the transfer, the PVDF membrane was transferred to blocking buffer [(5% dried milk powder in PBST (PBST + 0.2% Tween-20 (Sigma #P1379))]and incubated 1 hour at room temperature with shaking. Later, the membrane was rinsed with 1x PBST twice for 10 minutes. Then the membrane was incubated with blocking buffer with the addition of 1:1000 primary antibody Anti-HA, mouse monoclonal primary antibody (12CA5 Roche, 5 mg/ml) at 4°C overnight. The following day, the membrane was rinsed with PBST three times for 10 minutes each, then incubated in a solution containing 5% milk in PBST with 1:25000 secondary anti-mouse antibody [IgG-Peroxidase (A9044 Sigma, 0.63 mg/ml)]. After that, the membrane was washed three times for 10 minutes each with PBST. For the

detection in the Dark room, the membrane was incubated with Clarity™ Western ECL Substrates 1:1 mixture (#170-5060) for 5 minutes before developing. After that, the membrane was exposed to film (Hyperfilm ECL, Amersham #28906837). Time of exposure was adapted depending on the intensity of the bands. Lastly, the film was developed using Compact X4 Automatic Processor (Xograph Healthcare).

6.18 Cells fixation for microscopy

Cultures were grown overnight in SC media, after being grown in 30ml SC media until $OD_{600}=1$. Cells were centrifuged at 2000 rpm for 5 minutes and washed once with dH_2O , after cells were resuspended in 10ml of 3.7% paraformaldehyde (Sigma #F8775) and vortexed for 30 seconds. After 15 minutes of incubation in 3.7% paraformaldehyde, cells were centrifuged at 2000 rpm for 5 minutes and washed once with 10ml of KPO_4 /sorbitol, centrifuged again and resuspended in 200ul of KPO_4 /sorbitol.

Table 6.5 Strains used in this study			
Strain number	Description	Genotype	Source
AB55	SC5314	wildtype	Berman Lab Tel Aviv University
AB54	SN152	MTL a/alpha ura3Δ-iro1Δ::imm434/URA3- IRO1 his1Δ/his1Δ arg4Δ/arg4Δ leu2Δ/leu2Δ	Berman Lab Tel Aviv University
AB140	TetR-GFP, TetO- CEN7	arg-,his-,ura- ORF19.1963::TetR-GFP- Nat::ORF19.1963/ORF19.1963 TetO-HIS::CEN7	
AB653	PHO85/pho85::URA3 (10131)	ura3Δ::λimm434/ura3Δimm434 his1::hisG/his1::hisG PHO85/pho85::URA3	Berman Lab Tel Aviv University
AB655	CLB4/clb4::URA3 (10142)	ura3Δ::λimm434/ura3Δimm434 his1::hisG/his1::hisG CLB4/clb4::URA3	Berman Lab Tel Aviv University
AB663	CRZ1/CRZ1::GFP- URA3 (10806)	ura3Δ::λimm434/ura3Δimm434 his1::hisG/his1::hisG CRZ1/CRZ1::GFP-URA3	Berman Lab Tel Aviv University
AB754	ulp3Δ	MTL a/alpha ura3Δ-iro1Δ::imm434/URA3- IRO1 his1Δ/his1Δ arg4Δ/arg4Δ leu2Δ/leu2Δ ULP3/ulp3::NAT	This work
AB755	<i>Ulp1</i> ΔΔ	MTL a/alpha ura3Δ-iro1Δ::imm434/URA3- IRO1 his1Δ/his1Δ arg4Δ/arg4Δ leu2Δ/leu2Δ ulp1::NAT/ulp1::ARG	This work
AB758	<i>Ulp2</i> ΔΔ	MTL a/alpha ura3Δ-iro1Δ::imm434/URA3- IRO1 his1Δ/his1Δ arg4Δ/arg4Δ leu2Δ/leu2Δ ulp2::NAT/ULP2::ARG	This work

AB746	SN250	his1Δ/his1Δ, leu2Δ::C.dubliniensis HIS1 /leu2Δ::C.maltosa LEU2, arg4Δ /arg4Δ, URA3/ura3Δ::imm ⁴³⁴ , IRO1/iro1Δ::imm ⁴³⁴	(Noble et al., 2010a)
AB765	TetR-GFP, TetO- CEN7, ulp2Δ/ulp2Δ	arg-,his-,ura- ORF19.1963::TetR-GFP- Nat::ORF19.1963/ORF19.1963 TetO-HIS::CEN7 ulp2::ARG/ulp2::NAT	This work
AB803	CLB4/clb4::URA3 ulp2::NAT/ulp2::HIS	ura3Δ::λimm434/ura3Δimm434 his1::hisG/his1::hisG CLB4/clb4::URA3 ulp2::NAT/ULP2::HIS	This work
AB804	CRZ1/CRZ1::GFP- URA3 ulp2::NAT/ulp2::HIS	ura3Δ::λimm434/ura3Δimm434 his1::hisG/his1::hisG CRZ1/CRZ1::GFP-URA3 ulp2::NAT/ulp2::HIS	This work
AB823	PHO85/pho85::URA3 (10131) ulp2::HIS/ulp2::NAT	ura3Δ::λimm434/ura3Δimm434 his1::hisG/his1::hisG PHO85/pho85::URA3 ulp2::HIS/ulp2::NAT	This work

Table 6.6 Primers used in this study			
Sequence	Description	Name	AB Number
CAAATCCATCAATGGATCAG	Check presence arg cassette	Arg4_Rev1	251
CTGGTTGGAACAGAAGATTG	Check presence NAT cassette	Nat_Fw	857
ACTACCTGTTTCTGAACTAT CATCAGTATCATCTAGCAAG	Check MEC3 deletion	mec3_fw mec3_rv	885 886
TATTACTAAATGACGACGACG CCTTCTCTTGGATAAGAATCT	Check <i>CLB4</i> deletion	clb4 fw clb4 rv	887 888
GCAATGGTAATGGTAATGGAT TGGATCACACAAGGCATTAAT	Check KIP3 deletion	kip3 fw kip3 rv	889 890
TGGAATCGAAGCAAGAGGTA ACCAAACGACGGTTGATGTT	Check RAD18 deletion	rad18_fw rad 18 rv	891 892
CATACTGATGCTATATCAGTG TTGTGATAACATTCCACCATG	Check SPT8 deletion	spt8 fw spt8 rv	903 904
ACTCATCACTGCGATATCAG AGCTTCCATATGAGGAATCAA	Check ULP2 deletion	Ulp2_Fw Ulp2_Rv	905 906
CTGCAAGCTCCACAACAAGT GCCTAAATTCATGGCAGCAG	Check CAS5 deletion	cas5 fw cas5 rv	911 912
ATGGTTCCGTCCTCATATGC ATGCATCTGTTATCTGCATACA	Check GRR1 deletion	grr1_fw grr1_rv	913 914
GTCAGTACTCTAACATGAGG GCACGTTTTCCATTCTTCATC	Check <i>SIN3</i> deletion	sin3 fw sin3 rv	915 916
GTGACACGACACTAAGTGTC TACTGCTCATATCCAATACGAA	Check <i>PEP7</i> deletion	pep7 fw pep7 rv	917 918
TTGGAAGTACGTAAGGACAT TAATTTGGCAATATGCTCCT	Check <i>RAD32</i> deletion	rad32 fw rad32 rv	921 922
CGTCGACCATACCATCCAAT TCGATGAATTAGAGGAGAGAG	Check <i>CCN1</i> deletion	ccn1 fw ccn1 rv	925 926
TGGACCAAGCGAATGAGCAA TTCAATGGGGATTCCAGATAG	Check <i>ORF19.1567</i> deletion	ORF19.1567 fw ORF19.1567 rv	927 928
CCACACATGCCTCGTTCATA TATCTTCTGAGGTTGCAGTGG	Check <i>ORF19.2378</i> deletion	ORF19.2378 fw ORF19.2378 rv	929 930
CTGGTGCAACAGCAAATAGA ACCTTCATCGACCAACTCTT	Check GIN4 deletion	gin4 fw gin4 rv	933 934

ACTCTTGGATACCTAATTTCA AATGACACCTTGATACCATG	Check <i>FCY2</i> deletion	fcy2 fw fcy2 rv	941 942
AGGCTTAGACAAGTAGTGAA ACGACACATTTCTTATACGA	Check <i>KAR3</i> deletion	kar3 fw kar3 rv	943 944
TTGATTGCCTCATTGGTGCAA CAGCATCTTGTCTTGCCTTG	Check <i>ORF19.4567</i> deletion	<i>ORF19.4567</i> fw <i>ORF19.4567</i> rv	945 946
GAAAAAAAAACAATACCAGCCAT GATGAAGATTGCTTACACTATTTTC TTCTTTATAACTGGACGTTACTAA gtttcccagtcacgacgtt CATTTTTAGGTATCAAGTTTTGAA AAAAGAAAACAACAGTGGATGTG ATATATATATAATCTTGTACATACA ATTAGtgaattgtgagcggataa	Deletion <i>ulp2</i> with Arg cassette	<i>Ulp2_Arg_Fw</i> <i>Ulp2_arg_Rv</i>	1032 1033
ATTGGAAGAGGAATTGGAGA	Check <i>ulp2</i> deletion	<i>Ulp2_check_Rv</i>	1034
GGGAAAAAAAAACAATACCAGC CATGATGAAGATTGCTTACACTAT TTCTTCTTTATAACTGGACGTTAC TAAgtaaacgacggccagtgaa GGTATCAAGTTTTGAAAAAAGAAA ACAACAGTGGATGTGATATATATA TAATCTTGTACATACAATTAAtgcatca attgacgttgataccac	Deletion <i>ulp2</i> with NAT cassette	<i>Ulp2_nat_Fw</i> <i>Ulp2_nat_Rv</i>	1038 1039
GTATAGTCAAAATGATATGAAAAT AATTCGTAGAAGAATGGTCTATGA AATTTTAGATAATCGTTTACTAGA Tcggatccccgggtaattaa TAGGTATCAAGTTTTGAAAAAAGA AAACAACAGTGGATGTGATATATA TATAATCTTGTACATACAATTAAtgtaa aacgacggccagtgaaattc	Integration HA tag <i>ulp2</i> gene	<i>Ulp2_HA_Nat_Fw</i> <i>Ulp2_HA_Nat_Rv</i>	1042 1043
CGTCCTTCAAGTATTGTAAGTGC CACGGACCAGACGAATGTTGAAC TTTTGAAAATAAGATTAGAAAATgt aaaacgacggccagtgaaat TTACTATTGGATAAATACTACAGA TAATTCTGATTGCTAGAATGTAGA TATATATATAAATAAATTTAGTtgcacat caattgacgttgatac	Deletion <i>ulp1</i> with NAT cassette	<i>Ulp1_nat_fw</i> <i>Ulp1_nat_Rv</i>	1054 1055

CAAGATTGCAGATGCTTGAG	Check ulp1 deletion	Ulp1_check_Rv	1056
GTCCTTTCAAGTATTGTAAGTACC ACGGACCAGACGAATGTTGAACT TTTGAAAATAAGATTAGAAAATgttt cccagtcacgacgtgt TACTATTGGATAAATACTACAGA TAATTCTGATTGCTAGAATGTAGA TATATATATAAATAAATTTAGTgtgg aattgtgagcggataac	Deletion ulp1 allele with arg cassette	Ulp1_arg_Fw Ulp1_arg_rv	1057 1058
AGGATGTGTTTCTTGACAAGCATT TACAGGTAAATTTATCCATAGTCT CGTACTAAACTGTTTTATCAGTAgt aaaacgacggccagtgaa TGATGTTGTTGTTTGTGTATATTT TGATTTTTTCTTTACGTAATCGTTT TCGTTCCCTGCATATATAtgcatcaatt gacgttgatacc	Deletion ulp3 allele with NAT cassette	Ulp3_Nat_Fw Ulp3_Nat_Rv	1059 1060
GCAGATATCTGTGAGACTGA	Check ulp3 deletion	Ulp3_check_Rv	1061

Table 6.7 Plasmids used in this study

Plasmid	Description	AB Number
pHA_NAT	NAT substitution cassette HA tagging	AB17
pR3Arg46spe1	ARG substitution cassette	AB18
pGEM-His1	HIS substitution cassette	AB20

REFERENCES

- Achkar, J.M., Fries, B.C., 2010. *Candida* Infections of the Genitourinary Tract. *Clin. Microbiol. Rev.* 23, 253.
- Agarwal, R., Cohen-Fix, O., 2002. Phosphorylation of the mitotic regulator Pds1/securin by Cdc28 is required for efficient nuclear localization of Esp1/separase. *Genes Dev.* 16, 1371.
- Aguilera, A., García-Muse, T., 2013. Causes of genome instability. *Annu. Rev. Genet.* 47, 1–32.
- Aguilera, A., Gómez-González, B., 2008. Genome instability: A mechanistic view of its causes and consequences. *Nat. Rev. Genet.* 9, 204–217.
- Ahn, J., Urist, M., Prives, C., 2004. The Chk2 protein kinase. *DNA Repair (Amst)*. 3, 1039–1047.
- al-Khodairy, F., Enoch, T., Hagan, I.M., Carr, A.M., 1995. The *Schizosaccharomyces pombe* *hus5* gene encodes a ubiquitin conjugating enzyme required for normal mitosis. *J. Cell Sci.* 108 (Pt 2, 475–486.
- Allshire, R.C., Karpen, G.H., 2008. Epigenetic regulation of centromeric chromatin: old dogs, new tricks? *Nat. Rev. Genet.* 9, 923.
- Almedawar, S., Colomina, N., Bermúdez-López, M., Pociño-Merino, I., Torres-Rosell, J., 2012. A SUMO-dependent step during establishment of sister chromatid cohesion. *Curr. Biol.* 22, 1576–1581.
- Alonso-Monge, R., Gresnigt, M.S., Román, E., Hube, B., Pla, J., 2021. *Candida albicans* colonization of the gastrointestinal tract: A double-edged sword. *PLOS Pathog.* 17, e1009710.
- Alseth, I., Eide, L., Pirovano, M., Rognes, T., Seeberg, E., Bjørås, M., 1999. The *Saccharomyces cerevisiae* Homologues of Endonuclease III from *Escherichia coli*, Ntg1 and Ntg2, Are Both Required for Efficient Repair of Spontaneous and Induced Oxidative DNA Damage in Yeast. *Mol. Cell. Biol.* 19, 3779.
- Andaluz, E., A, B., J, G.-R., A, S., K, B., R, C., J, B., G, L., 2011. Rad52 function prevents chromosome loss and truncation in *Candida albicans*. *Mol. Microbiol.* 79, 1462–1482.
- Andersen, S., T, H., R, S., I, K., HE, K., B, E., H, N., 2005. Incorporation of dUMP into DNA is a major source of spontaneous DNA damage, while excision of uracil is not required for cytotoxicity of fluoropyrimidines in mouse embryonic fibroblasts. *Carcinogenesis* 26, 547–555.
- Anderson, M.Z., Baller, J.A., Dulmage, K., Wigen, L., Berman, J., 2012. The Three Clades of the Telomere-Associated TLO Gene Family of *Candida albicans* Have Different Splicing, Localization, and Expression Features. *Eukaryot. Cell* 11, 1268.

- Aristizabal-Corrales, D., Yang, J., Li, F., 2019. Cell Cycle-Regulated Transcription of CENP-A by the MBF Complex Ensures Optimal Level of CENP-A for Centromere Formation. *Genetics* 211, 861.
- Armstrong, J.D., Chadee, D.N., Kunz, B.A., 1994. Roles for the yeast RAD18 and RAD52 DNA repair genes in UV mutagenesis. *Mutat. Res. Repair* 315, 281–293.
- Asakura, K., Iwaguchi, S., Homma, M., Sukai, T., Higashide, K., Tanaka, K., 1991. Electrophoretic karyotypes of clinically isolated yeasts of *Candida albicans* and *C. glabrata*. *J. Gen. Microbiol.* 137, 2531–2538.
- Audhya, A., Foti, M., Emr, S.D., 2000. Distinct Roles for the Yeast Phosphatidylinositol 4-Kinases, Stt4p and Pik1p, in Secretion, Cell Growth, and Organelle Membrane Dynamics. *Mol. Biol. Cell* 11, 2673.
- Avramovska, O., Hickman, M.A., 2019a. The Magnitude of *Candida albicans* Stress-Induced Genome Instability Results from an Interaction Between Ploidy and Antifungal Drugs. *G3 Genes|Genomes|Genetics* 9, 4019.
- Avramovska, O., Hickman, M.A., 2019b. The Magnitude of *Candida albicans* Stress-Induced Genome Instability Results from an Interaction Between Ploidy and Antifungal Drugs. *G3 Genes, Genomes, Genet.* 9, 4019–4027.
- Aylon, Y., Kupiec, M., 2004. New insights into the mechanism of homologous recombination in yeast. *Mutat. Res.* 566, 231–248.
- Ba, X., Boldogh, Istvan, 2018. 8-Oxoguanine DNA glycosylase 1: Beyond repair of the oxidatively modified base lesions. *Redox Biol.* 14, 669–678.
- Bachant, J., Alcasabas, A., Blat, Y., Kleckner, N., Elledge, S.J., 2002. The SUMO-1 Isopeptidase Smt4 Is Linked to Centromeric Cohesion through SUMO-1 Modification of DNA Topoisomerase II. *Mol. Cell* 9, 1169–1182.
- Bachewich, C., Mantel, A., Whiteway, M., 2005. Cell cycle arrest during S or M phase generates polarized growth via distinct signals in *Candida albicans*. *Mol. Microbiol.* 57, 942–959.
- Bachewich, C., Whiteway, M., 2005. Cyclin Cln3p Links G1 Progression to Hyphal and Pseudohyphal Development in *Candida albicans*. *Eukaryot. Cell* 4, 95–102.
- Bai, C., Ramanan, N., Wang, Y.M., Wang, Y., 2002. Spindle assembly checkpoint component CaMad2p is indispensable for *Candida albicans* survival and virulence in mice. *Mol. Microbiol.* 45, 31–44.
- Baldwin, M.L., Julius, J.A., Tang, X., Wang, Y., Bachant, J., 2009. The yeast SUMO isopeptidase Smt4/Ulp2 and the polo kinase Cdc5 act in an opposing fashion to regulate sumoylation in mitosis and cohesion at centromeres. *Cell Cycle* 8, 3406–3419.
- Barnum, K.J., O’Connell, M.J., 2014. Cell cycle regulation by checkpoints. *Methods Mol. Biol.* 1170, 29–40.

- Bates, S., 2018a. *Candida albicans* Cdc15 is essential for mitotic exit and cytokinesis. *Sci. Reports* 2018 8 1 8, 1–11.
- Bates, S., 2018b. *Candida albicans* Cdc15 is essential for mitotic exit and cytokinesis. *Sci. Reports* 2018 8 1 8, 1–11.
- Belotserkovskaya, R., Sterner, D.E., Deng, M., Sayre, M.H., Lieberman, P.M., Berger, S.L., 2000. Inhibition of TATA-Binding Protein Function by SAGA Subunits Spt3 and Spt8 at Gcn4-Activated Promoters. *Mol. Cell. Biol.* 20, 634.
- Ben-David, U., Amon, A., 2019. Context is everything: aneuploidy in cancer. *Nat. Rev. Genet.* 2019 21 1 21, 44–62.
- Bensen, E.S., Clemente-Blanco, A., Finley, K.R., Correa-Bordes, J., Berman, J., 2005. The Mitotic Cyclins Clb2p and Clb4p Affect Morphogenesis in *Candida albicans*. *Mol. Biol. Cell* 16, 3387.
- Beranek, D.T., 1990. Distribution of methyl and ethyl adducts following alkylation with monofunctional alkylating agents. *Mutat. Res. Mol. Mech. Mutagen.* 231, 11–30.
- Berkow, E.L., Lockhart, S.R., 2017. Fluconazole resistance in *Candida* species: a current perspective. *Infect. Drug Resist.* 10, 237.
- Berman, J., 2006. Morphogenesis and cell cycle progression in *Candida albicans*. *Curr. Opin. Microbiol.* 9, 595–601.
- Berman, J., Hadany, L., 2012. Does stress induce (para)sex? Implications for *Candida albicans* evolution. *Trends Genet.* 28, 197–203.
- Berman, J., Sudbery, P.E., 2002. *Candida albicans*: A molecular revolution built on lessons from budding yeast. *Nat. Rev. Genet.* 2002 3 12 3, 918–931.
- Bettignies, G. de, Johnston, L.H., 2003. The mitotic exit network. *Curr. Biol.* 13, R301.
- Bhargava, R., Onyango, D.O., Stark, J.M., 2016. Regulation of Single-Strand Annealing and its Role in Genome Maintenance. *Trends Genet.* 32, 566–575.
- Bhaumik, S.R., Green, M.R., 2002. Differential Requirement of SAGA Components for Recruitment of TATA-Box-Binding Protein to Promoters In Vivo. *Mol. Cell. Biol.* 22, 7365.
- Biesecker, L.G., Spinner, N.B., 2013. A genomic view of mosaicism and human disease. *Nat. Rev. Genet.* 14, 307–320.
- Boiteux, S., Guillet, M., 2004. Abasic sites in DNA: repair and biological consequences in *Saccharomyces cerevisiae*. *DNA Repair (Amst.)* 3, 1–12.
- Brajtburg, J., Powderly, W.G., Kobayashi, G.S., Medoff, G., 1990.

MINIREVIEW Amphotericin B: Current Understanding of Mechanisms of Action. *Antimicrob. Agents Chemother.* 34, 183–188.

- Brown, A.J.P., Budge, S., Kaloriti, D., Tillmann, A., Jacobsen, M.D., Yin, Z., Ene, I. V., Bohovych, I., Sandai, D., Kastora, S., Potrykus, J., Ballou, E.R., Childers, D.S., Shahana, S., Leach, M.D., 2014. Stress adaptation in a pathogenic fungus. *J. Exp. Biol.* 217, 144.
- Bruno, V.M., Mitchell, A.P., 2005. Regulation of azole drug susceptibility by *Candida albicans* protein kinase CK2. *Mol. Microbiol.* 56, 559–573.
- Budden, T., Bowden, N.A., 2013. The role of altered nucleotide excision repair and UVB-induced DNA damage in melanomagenesis. *Int. J. Mol. Sci.* 14, 1132–1151.
- Burgers, P.M., Klein, M.B., 1986. Selection by genetic transformation of a *Saccharomyces cerevisiae* mutant defective for the nuclear uracil-DNA-glycosylase. *J. Bacteriol.* 166, 905.
- Butler, D.K., All, O., Goffena, J., Loveless, T., Wilson, T., Toenjes, K.A., 2006. The GRR1 gene of *Candida albicans* is involved in the negative control of pseudohyphal morphogenesis. *Fungal Genet. Biol.* 43, 573–582.
- Caldecott, K.W., 2008. Single-strand break repair and genetic disease. *Nat. Rev. Genet.* 2008 9, 619–631.
- Callahan, J., KJ, A., VA, Z., CH, F., 2003. Mutations in yeast replication proteins that increase CAG/CTG expansions also increase repeat fragility. *Mol. Cell. Biol.* 23, 7849–7860.
- Candida Genome Database [WWW Document], n.d. URL <http://www.candidagenome.org/> (accessed 11.28.21).
- Cannon, R.D., Lamping, E., Holmes, A.R., Niimi, K., Baret, P. V., Keniya, M. V., Tanabe, K., Niimi, M., Goffeau, A., Monk, B.C., 2009. Efflux-mediated antifungal drug resistance. *Clin. Microbiol. Rev.* 22, 291–321.
- Carvalho, P., Gupta, M.L., Hoyt, M.A., Pellman, D., 2004. Cell cycle control of kinesin-mediated transport of Bik1 (CLIP-170) regulates microtubule stability and dynein activation. *Dev. Cell* 6, 815–829.
- Chabes, A., Georgieva, B., Domkin, V., Zhao, X., Rothstein, R., Thelander, L., 2003. Survival of DNA Damage in Yeast Directly Depends on Increased dNTP Levels Allowed by Relaxed Feedback Inhibition of Ribonucleotide Reductase. *Cell* 112, 391–401.
- Chakraborty, U., Alani, E., 2016. Understanding how mismatch repair proteins participate in the repair/anti-recombination decision. *FEMS Yeast Res.* 16, 71.
- Chapeland-Leclerc, F., Bouchoux, J., Goumar, A., Chastin, C., Villard, J., Noël, T., 2005. Inactivation of the FCY2 Gene Encoding Purine-Cytosine Permease Promotes Cross-Resistance to Flucytosine and Fluconazole

- in *Candida lusitanae*. *Antimicrob. Agents Chemother.* 49, 3101.
- Cheeseman, I.M., 2014. The Kinetochore. *Cold Spring Harb. Perspect. Biol.* 6.
- Chen, C., Umezū, K., Kolodner, R.D., 1998. Chromosomal Rearrangements Occur in *S. cerevisiae* rfa1 Mutator Mutants Due to Mutagenic Lesions Processed by Double-Strand-Break Repair. *Mol. Cell* 2, 9–22.
- Chen, H., Lisby, M., Symington, L.S., 2013. RPA coordinates DNA end resection and prevents formation of DNA hairpins. *Mol. Cell* 50, 589–600.
- Chen, L.M., Xu, Y.H., Zhou, C.L., Zhao, J., Li, C.Y., Wang, R., 2010. Overexpression of CDR1 and CDR2 genes plays an important role in fluconazole resistance in *Candida albicans* with G487T and T916C mutations. *J. Int. Med. Res.* 38, 536–545.
- Chen, R.H., Brady, D.M., Smith, D., Murray, A.W., Hardwick, K.G., 1999. The Spindle Checkpoint of Budding Yeast Depends on a Tight Complex between the Mad1 and Mad2 Proteins. *Mol. Biol. Cell* 10, 2607.
- Choy, J.S., Kron, S.J., 2002. NuA4 Subunit Yng2 Function in Intra-S-Phase DNA Damage Response. *Mol. Cell. Biol.* 22, 8215.
- Ciccia, A., Elledge, S.J., 2010a. The DNA Damage Response: Making it safe to play with knives. *Mol. Cell* 40, 179.
- Ciccia, A., Elledge, S.J., 2010b. The DNA Damage Response: Making It Safe to Play with Knives. *Mol. Cell* 40, 179–204.
- Cimini, D., 2008. Merotelic kinetochore orientation, aneuploidy, and cancer. *Biochim. Biophys. Acta - Rev. Cancer* 1786, 32–40.
- Ciosk, R., M, S., A, S., T, T., A, T., A, S., K, N., 2000. Cohesin's binding to chromosomes depends on a separate complex consisting of Scc2 and Scc4 proteins. *Mol. Cell* 5, 243–254.
- Clemente-Blanco, A., González-Novo, A., Machín, F., Caballero-Lima, D., Aragón, L., Sánchez, M., de Aldana, C.R.V., Jiménez, J., Correa-Bordes, J., 2006. The Cdc14p phosphatase affects late cell-cycle events and morphogenesis in *Candida albicans*. *J. Cell Sci.* 119, 1130–1143.
- Clerici, M., Mantiero, D., Lucchini, G., Longhese, M.P., 2005. The *Saccharomyces cerevisiae* Sae2 Protein Promotes Resection and Bridging of Double Strand Break Ends *. *J. Biol. Chem.* 280, 38631–38638.
- Cole, H.A., Howard, B.H., Clark, D.J., 2011. The centromeric nucleosome of budding yeast is perfectly positioned and covers the entire centromere. *Proc. Natl. Acad. Sci.* 108, 12687–12692.
- Compton, D.A., 2011. Mechanisms of aneuploidy. *Curr. Opin. Cell Biol.* 23, 109–113.

- Coste, Alix, Selmecki, A., Forche, A., Diogo, D., Bougnoux, M.E., D'Enfert, C., Berman, J., Sanglard, D., 2007. Genotypic Evolution of Azole Resistance Mechanisms in Sequential *Candida albicans* Isolates. *Eukaryot. Cell* 6, 1889.
- Coste, A, Selmecki A, A, F., D, D., ME, B., C, D., J, B., D, S., 2007. Genotypic evolution of azole resistance mechanisms in sequential *Candida albicans* isolates. *Eukaryot. Cell* 6, 1889–1904.
- Coste, A.T., Crittin, J., Bauser, C., Rohde, B., Sanglard, D., 2009. Functional analysis of cis- and trans-acting elements of the *Candida albicans* CDR2 promoter with a novel promoter reporter system. *Eukaryot. Cell* 8, 1250–1267.
- Coste, A.T., Karababa, M., Ischer, F., Bille, J., Sanglard, D., 2004. TAC1, transcriptional activator of CDR genes, is a new transcription factor involved in the regulation of *Candida albicans* ABC transporters CDR1 and CDR2. *Eukaryot. Cell* 3, 1639–1652.
- Côte, P., Hogues, H., Whiteway, M., 2009. Transcriptional Analysis of the *Candida albicans* Cell Cycle. <https://doi.org/10.1091/mbc.e09-03-0210>, 3363–3373.
- Cottingham, F.R., Hoyt, M.A., 1997. Mitotic Spindle Positioning in *Saccharomyces cerevisiae* Is Accomplished by Antagonistically Acting Microtubule Motor Proteins. *J. Cell Biol.* 138, 1041–1053.
- Cowen, L.E., Anderson, J.B., Kohn, L.M., 2002. Evolution of drug resistance in *Candida albicans*. *Annu. Rev. Microbiol.* 56, 139–165.
- D'Amours, D., Stegmeier, F., Amon, A., 2004. Cdc14 and condensin control the dissolution of cohesin-independent chromosome linkages at repeated DNA. *Cell* 117, 455–469.
- D'Andrea, A.D., 2015. DNA Repair Pathways and Human Cancer. *Mol. Basis Cancer Fourth Ed.*
- Daley, J.M., Palmbo, P.L., Wu, D., Wilson, T.E., 2005. Nonhomologous end joining in yeast. *Annu. Rev. Genet.* 39, 431–451.
- Dasso, M., 2008. Emerging roles of the SUMO pathway in mitosis. *Cell Div.* 3, 5.
- David, R., 2013. Ras1 as a switch for *Candida albicans*. *Nat. Rev. Microbiol.* 2013 117 11, 431–431.
- Davis, A., Symington, L., 2003. The Rad52-Rad59 complex interacts with Rad51 and replication protein A. *DNA Repair (Amst).* 2, 1127–1134.
- De Rop, V., Padeganeh, A., Maddox, P.S., 2012. CENP-A: the key player behind centromere identity, propagation, and kinetochore assembly. *Chromosom.* 2012 1216 121, 527–538.
- DeLuca, J., Musacchio, A., 2012. Structural organization of the kinetochore-

- microtubule interface. *Curr. Opin. Cell Biol.* 24, 48.
- DeZwaan, T.M., Ellingson, E., Pellman, D., Roof, D.M., 1997. Kinesin-related KIP3 of *Saccharomyces cerevisiae* is required for a distinct step in nuclear migration. *J. Cell Biol.* 138, 1023–1040.
- Diaz-Guerra, T.M., Martinez-Suarez, J. V., Laguna, F., Rodriguez-Tudela, J.L., 1997. Comparison of four molecular typing methods for evaluating genetic diversity among *Candida albicans* isolates from human immunodeficiency virus-positive patients with oral candidiasis. *J. Clin. Microbiol.* 35, 856–861.
- Dieckhoff, P., Boite, M., Sancak, Y., Braus, G.H., Irniger, S., 2004. Smt3/SUMO and Ubc9 are required for efficient APC/C-mediated proteolysis in budding yeast. *Mol. Microbiol.* 51, 1375–1387.
- Diogo, D., Bouchier, C., d'Enfert, C., Bounoux, M.E., 2009. Loss of heterozygosity in commensal isolates of the asexual diploid yeast *Candida albicans*. *Fungal Genet. Biol.* 46, 159–168.
- Dove, S., RK, M., A, M., DC, H., JD, B., RH, M., 2002. Vac14 controls PtdIns(3,5)P(2) synthesis and Fab1-dependent protein trafficking to the multivesicular body. *Curr. Biol.* 12, 885–893.
- Dunn, M.J., Anderson, M.Z., 2019. To Repeat or Not to Repeat: Repetitive Sequences Regulate Genome Stability in *Candida albicans*. *Genes* 2019, Vol. 10, Page 866 10, 866.
- Durkin, S., Glover, T., 2007. Chromosome fragile sites. *Annu. Rev. Genet.* 41, 169–192.
- Elowe, S., 2011. Bub1 and BubR1: at the interface between chromosome attachment and the spindle checkpoint. *Mol. Cell. Biol.* 31, 3085–3093.
- Ene, I. V., Bennett, R.J., Anderson, M.Z., 2019. Mechanisms of genome evolution in *Candida albicans*. *Curr. Opin. Microbiol.* 52, 47.
- Ene, I. V., Farrer, R.A., Hirakawa, M.P., Agwamba, K., Cuomo, C.A., Bennett, R.J., 2018. Global analysis of mutations driving microevolution of a heterozygous diploid fungal pathogen. *Proc. Natl. Acad. Sci. U. S. A.* 115, E8688.
- Enjalbert, B., Nantel, A., Whiteway, M., 2003. Stress-induced Gene Expression in *Candida albicans*: Absence of a General Stress Response. *Mol. Biol. Cell* 14, 1460.
- Fabre, F., Magana-Schwencke, N., Chanet, R., 1989. Isolation of the RAD18 gene of *Saccharomyces cerevisiae* and construction of rad18 deletion mutants. *Mol. Gen. Genet. MGG* 1989 2153 215, 425–430.
- Feng, Jia, Shan, A., Hu, J., Cao, Z., Lv, R., Feng, Jinrong, 2019a. Genetic interaction between Ptc2 and protein phosphatase 4 (PP4) in the regulation of DNA damage response and virulence in *Candida albicans*. *FEMS Yeast Res.* 19.

- Feng, Jia, Shan, A., Hu, J., Cao, Z., Lv, R., Feng, Jinrong, 2019b. Genetic interaction between Ptc2 and protein phosphatase 4 (PP4) in the regulation of DNA damage response and virulence in *Candida albicans*. *FEMS Yeast Res.* 19, 75.
- Feng, W., Yang, J., Xi, Z., Qiao, Z., Lv, Y., Wang, Yiru, Ma, Y., Wang, Yanqing, Cen, W., 2017. Mutations and/or Overexpressions of ERG4 and ERG11 Genes in Clinical Azoles-Resistant Isolates of *Candida albicans*. *Microb. Drug Resist.* 23, 563–570.
- Ferreiro, J.A., Powell, N.G., Karabetsou, N., Mellor, J., Waters, R., 2006. Roles for Gcn5p and Ada2p in transcription and nucleotide excision repair at the *Saccharomyces cerevisiae* MET16 gene. *Nucleic Acids Res.* 34, 976.
- Flanagan, P.R., Fletcher, J., Boyle, H., Sulea, R., Moran, G.P., Sullivan, D.J., 2018. Expansion of the TLO gene family enhances the virulence of *Candida* species. *PLoS One* 13, e0200852.
- Flowers, S.A., Barker, K.S., Berkow, E.L., Toner, G., Chadwick, S.G., Gygas, S.E., Morschhäuser, J., David Rogers, P., 2012. Gain-of-function mutations in UPC2 are a frequent cause of ERG11 upregulation in azole-resistant clinical isolates of *Candida albicans*. *Eukaryot. Cell* 11, 1289–1299.
- Forche, A., Abbey, D., Pisithkul, T., Weinzierl, M.A., Ringstrom, T., Bruck, D., Petersen, K., Berman, J., 2011. Stress alters rates and types of loss of heterozygosity in *Candida albicans*. *MBio* 2.
- Forche, A., Magee, P.T., Selmecki, A., Berman, J., May, G., 2009. Evolution in *Candida albicans* Populations During a Single Passage Through a Mouse Host. *Genetics* 182, 799.
- Forche, D, A., T, P., MA, W., T, R., D, B., K, P., J, B., 2011. Stress alters rates and types of loss of heterozygosity in *Candida albicans*. *MBio* 2.
- Ford, C.B., Funt, J.M., Abbey, D., Issi, L., Guiducci, C., Martinez, D.A., Delorey, T., Li, B. yu, White, T.C., Cuomo, C., Rao, R.P., Berman, J., Thompson, D.A., Regev, A., 2015. The evolution of drug resistance in clinical isolates of *Candida albicans*. *Elife* 4, 1–27.
- François, I.E.J.A., Cammue, B.P.A., Borgers, M., Ausma, J., Dispersyn, G.D., Thevissen, K., 2006. Azoles: Mode of antifungal action and resistance development. Effect of miconazole on endogenous reactive oxygen species production in *Candida albicans*. *Antiinfect. Agents Med. Chem.* 5, 3–13.
- Franke, K., Nguyen, M., Härtl, A., Dahse, H.-M., Vogl, G., Würzner, R., Zipfel, P.F., Künkel, W., Eck, R., 2006. The vesicle transport protein Vac1p is required for virulence of *Candida albicans*. *Microbiology* 152, 3111–3121.
- Freire-Benéitez, V., Price, R.J., Tarrant, D., Berman, J., Buscaino, A., 2016.

- Candida albicans* repetitive elements display epigenetic diversity and plasticity. *Sci. Reports* 2016 6:1 6, 1–12.
- Gandhi, R., PJ, G., T, H., 2006. Human Wapl is a cohesin-binding protein that promotes sister-chromatid resolution in mitotic prophase. *Curr. Biol.* 16, 2406–2417.
- Ganem, N.J., Godinho, S.A., Pellman, D., 2009. A Mechanism Linking Extra Centrosomes to Chromosomal Instability. *Nature* 460, 278.
- Ganem, N.J., Pellman, D., 2012. Linking abnormal mitosis to the acquisition of DNA damage. *J. Cell Biol.* 199, 871–881.
- Gascoigne, K.E., Cheeseman, I.M., 2013. CDK-dependent phosphorylation and nuclear exclusion coordinately control kinetochore assembly state. *J. Cell Biol.* 201, 23.
- Geiss-Friedlander, R., Melchior, F., 2007. Concepts in sumoylation: a decade on. *Nat. Rev. Mol. Cell Biol.* 2007 8:12 8, 947–956.
- Gellon, L., Barbey, R., Van der Kemp, P.A., Thomas, D., Boiteux, S., 2001. Synergism between base excision repair, mediated by the DNA glycosylases Ntg1 and Ntg2, and nucleotide excision repair in the removal of oxidatively damaged DNA bases in *Saccharomyces cerevisiae*. *Mol. Genet. Genomics* 265, 1087–1096.
- Georgopapadakou, N.H., 1998. Antifungals: mechanism of action and resistance, established and novel drugs. *Curr. Opin. Microbiol.* 1, 547–557.
- Ghannoum, M.A., Rice, L.B., 1999. Antifungal Agents: Mode of Action, Mechanisms of Resistance, and Correlation of These Mechanisms with Bacterial Resistance. *Clin. Microbiol. Rev.* 12, 501.
- González-Novo, A., Labrador, L., Pablo-Hernando, M.E., Correa-Bordes, J., Sánchez, M., Jiménez, J., Aldana, C.R.V. De, 2009. Dbf2 is essential for cytokinesis and correct mitotic spindle formation in *Candida albicans*. *Mol. Microbiol.* 72, 1364–1378.
- Grava, S., Schaerer, F., Faty, M., Philippsen, P., Barral, Y., 2006. Asymmetric recruitment of dynein to spindle poles and microtubules promotes proper spindle orientation in yeast. *Dev. Cell* 10, 425–439.
- Graybill, J.R., Burgess, D.S., Hardin, T.C., 1997. Key issues concerning fungistatic versus fungicidal drugs. *Eur. J. Clin. Microbiol. Infect. Dis.* 16, 42–50.
- Greenberg, M., 2012. The formamidopyrimidines: purine lesions formed in competition with 8-oxopurines from oxidative stress. *Acc. Chem. Res.* 45, 588–597.
- Gregan, J., Polakova, S., Zhang, L., Tolić-Nørrelykke, I.M., Cimini, D., 2011. Merotelic kinetochore attachment: causes and effects. *Trends Cell Biol.* 21, 374.

- Griffiths, A., Miller, J., Suzuki, D., Al., E., 2000. Introduction to Genetic Analysis.
- Gupta, D., Garapati, H.S., Kakumanu, A.V.S., Shukla, R., Mishra, K., 2020. SUMOylation in fungi: A potential target for intervention. *Comput. Struct. Biotechnol. J.* 18, 3484–3493.
- Guzder, S., Y, H., P, S., L, P., S, P., 1995. Reconstitution of yeast nucleotide excision repair with purified Rad proteins, replication protein A, and transcription factor TFIIH. *J. Biol. Chem.* 270, 12973–12976.
- Guzder, S.N., Sommers, C.H., Prakash, L., Prakash, S., 2006. Complex Formation with Damage Recognition Protein Rad14 Is Essential for *Saccharomyces cerevisiae* Rad1-Rad10 Nuclease To Perform Its Function in Nucleotide Excision Repair In Vivo. *Mol. Cell. Biol.* 26, 1135.
- Haarhuis, J.H.I., Elbatsh, A.M.O., Van Den Broek, B., Camps, D., Erkan, H., Jalink, K., Medema, R.H., Rowland, B.D., 2013. WAPL-Mediated Removal of Cohesin Protects against Segregation Errors and Aneuploidy. *Curr. Biol.* 23, 2071–2077.
- Haering, C., J, L., A, H., K, N., 2002. Molecular architecture of SMC proteins and the yeast cohesin complex. *Mol. Cell* 9, 773–788.
- Hahnazari, E., Heyer, W.D., 2004. The Hog1 MAP kinase pathway and the Mec1 DNA damage checkpoint pathway independently control the cellular responses to hydrogen peroxide. *DNA Repair (Amst).* 3, 769–776.
- Hanawalt, P., Spivak, G., 2008. Transcription-coupled DNA repair: two decades of progress and surprises. *Nat. Rev. Mol. Cell Biol.* 9, 958–970.
- Haran, J., Boyle, H., Hokamp, K., Yeomans, T., Liu, Z., Church, M., Fleming, A.B., Anderson, M.Z., Berman, J., Myers, L.C., Sullivan, D.J., Moran, G.P., 2014. Telomeric ORFs (TLOs) in *Candida* spp. Encode Mediator Subunits That Regulate Distinct Virulence Traits. *PLOS Genet.* 10, e1004658.
- Hartwell, L., Goldberg, M.L., Fischer, J.A., Hood, L.E., 2020. Genetics: From Genes to Genomes.
- Hassold, T., Hunt, P., 2001. To err (meiotically) is human: the genesis of human aneuploidy. *Nat. Rev. Genet.* 2001 24 2, 280–291.
- Hecke, T. Van, 2013. Power study of anova versus Kruskal-Wallis test. <http://dx.doi.org/10.1080/09720510.2012.10701623> 15, 241–247.
- Hendriks, L., Goris, A., Neefs, J.M., Van De Peer, Y., Hennebert, G., De Wachter, R., 1989. The Nucleotide Sequence of the Small Ribosomal Subunit RNA of the Yeast *Candida albicans* and the Evolutionary Position of the Fungi among the Eukaryotes. *Syst. Appl. Microbiol.* 12, 223–229.
- Herrero, A., P, M., MK, M., SM, L., H, B., C, A., 2004. KRE5 gene null mutant

- strains of *Candida albicans* are avirulent and have altered cell wall composition and hypha formation properties. *Eukaryot. Cell* 3, 1423–1432.
- Heyer, W.-D., 2004. Recombination: Holliday Junction Resolution and Crossover Formation. *Curr. Biol.* 14, R56–R58.
- Ho, K.L., Ma, L., Cheung, S., Manhas, S., Fang, N., Wang, K., Young, B., Loewen, C., Mayor, T., Measday, V., 2015. A Role for the Budding Yeast Separase, Esp1, in Ty1 Element Retrotransposition. *PLoS Genet.* 11.
- Hochstrasser, M., 2001. SP-RING for SUMO: new functions bloom for a ubiquitin-like protein. *Cell* 107, 5–8.
- Hotz, M., Barral, Y., 2014. The Mitotic Exit Network: new turns on old pathways. *Trends Cell Biol.* 24, 145–152.
- Hoyt, M.A., Totis, L., Roberts, B.T., 1991. *S. cerevisiae* genes required for cell cycle arrest in response to loss of microtubule function. *Cell* 66, 507–517.
- Huang, G., Srikantha, T., Sahni, N., Yi, S., Soll, D.R., 2009. CO(2) regulates white-to-opaque switching in *Candida albicans*. *Curr. Biol.* 19, 330–334.
- Huaping, L., Jie, L., Zhifeng, W., Yingchang, Z., Yuhuan, L., 2007. Cloning and Functional Expression of Ubiquitin-Like Protein Specific Proteases Genes from *Candida albicans*. *Biol. Pharm. Bull.* 30, 1851–1855.
- Hube, B., 2004. From commensal to pathogen: stage- and tissue-specific gene expression of *Candida albicans*. *Curr. Opin. Microbiol.* 7, 336–341.
- Islam, A., Tebbji, F., Mallick, J., Regan, H., Dumeaux, V., Omran, R.P., Whiteway, M., 2019. Mms21: A Putative SUMO E3 Ligase in *Candida albicans* That Negatively Regulates Invasiveness and Filamentation, and Is Required for the Genotoxic and Cellular Stress Response. *Genetics* 211, 579–595.
- Jackson, S.P., 2002. Sensing and repairing DNA double-strand breaks. *Carcinogenesis* 23, 687–696.
- Jacobsen, M.D., Beynon, R.J., Gethings, L.A., Claydon, A.J., Langridge, J.I., Vissers, J.P.C., Brown, A.J.P., Hammond, D.E., 2018a. Specificity of the osmotic stress response in *Candida albicans* highlighted by quantitative proteomics. *Sci. Reports* 2018 8, 1–11.
- Jacobsen, M.D., Beynon, R.J., Gethings, L.A., Claydon, A.J., Langridge, J.I., Vissers, J.P.C., Brown, A.J.P., Hammond, D.E., 2018b. Specificity of the osmotic stress response in *Candida albicans* highlighted by quantitative proteomics. *Sci. Reports* 2018 8, 1–11.
- JM, A., BC, F., 2010. *Candida* infections of the genitourinary tract. *Clin. Microbiol. Rev.* 23, 253–273.

- Johnson, E.S., 2004a. Protein modification by SUMO. *Annu. Rev. Biochem.* 73, 355–382.
- Johnson, E.S., 2004b. Protein modification by SUMO. *Annu. Rev. Biochem.* 73, 355–382.
- Johnson, E.S., Gupta, A.A., 2001. An E3-like factor that promotes SUMO conjugation to the yeast septins. *Cell* 106, 735–744.
- Johnson, P.R., Hochstrasser, M., 1997. SUMO-1: Ubiquitin gains weight. *Trends Cell Biol.* 7, 408–413.
- Jones, T., Federspiel, N.A., Chibana, H., Dungan, J., Kalman, S., Magee, B.B., Newport, G., Thorstenson, Y.R., Agabian, N., Magee, P.T., Davis, R.W., Scherer, S., 2004a. The diploid genome sequence of *Candida albicans*. *Proc. Natl. Acad. Sci. U. S. A.* 101, 7329.
- Jones, T., Federspiel, N.A., Chibana, H., Dungan, J., Kalman, S., Magee, B.B., Newport, G., Thorstenson, Y.R., Agabian, N., Magee, P.T., Davis, R.W., Scherer, S., 2004b. The diploid genome sequence of *Candida albicans*. *Proc. Natl. Acad. Sci. U. S. A.* 101, 7329.
- Jongjitwimol, J., Feng, M., Zhou, L., Wilkinson, O., Small, L., Baldock, R., Taylor, D.L., Smith, D., Bowler, L.D., Morley, S.J., Watts, F.Z., 2014a. The *S. pombe* Translation Initiation Factor eIF4G Is Sumoylated and Associates with the SUMO Protease Ulp2. *PLoS One* 9, e94182.
- Jongjitwimol, J., Feng, M., Zhou, L., Wilkinson, O., Small, L., Baldock, R., Taylor, D.L., Smith, D., Bowler, L.D., Morley, S.J., Watts, F.Z., 2014b. The *S. pombe* Translation Initiation Factor eIF4G Is Sumoylated and Associates with the SUMO Protease Ulp2. *PLoS One* 9.
- Jovanovic, S. V., Simic, M.G., 2002. One-electron redox potentials of purines and pyrimidines. *J. Phys. Chem.* 90, 974–978.
- JP, F., S, L., 2007. Delayed accumulation of the yeast G1 cyclins Cln1 and Cln2 and the F-box protein Grr1 in response to glucose. *Yeast* 24, 419–429.
- Karijolic, J.J., Hampsey, M., 2012. The Mediator complex. *CURBIO* 22, R1030–R1031.
- Kashem, S.W., Kaplan, D.H., 2016. Skin Immunity to *Candida albicans*. *Trends Immunol.* 37, 440.
- Kaye, J.A., Melo, J.A., Cheung, S.K., Vaze, M.B., Haber, J.E., Toczyski, D.P., 2004. DNA Breaks Promote Genomic Instability by Impeding Proper Chromosome Segregation. *Curr. Biol.* 14, 2096–2106.
- Kelly, S.L., Lamb, D.C., Kelly, D.E., Manning, N.J., Loeffler, J., Hebart, H., Schumacher, U., Einsele, H., 1997. Resistance to fluconazole and cross-resistance to amphotericin B in *Candida albicans* from AIDS patients caused by defective sterol $\Delta 5,6$ -desaturation. *FEBS Lett.* 400, 80–82.

- Ketel, C., Wang, H.S.W., McClellan, M., Bouchonville, K., Selmecki, A., Lahav, T., Gerami-Nejad, M., Berman, J., 2009. Neocentromeres Form Efficiently at Multiple Possible Loci in *Candida albicans*. *PLOS Genet.* 5, e1000400.
- Kimura, T., Y, H., Y, S., Y, K., T, I., T, H., M, K., 2005. Interactions among yeast protein-disulfide isomerase proteins and endoplasmic reticulum chaperone proteins influence their activities. *J. Biol. Chem.* 280, 31438–31441.
- Köhler, J.R., Casadevall, A., Perfect, J., 2015. The Spectrum of Fungi That Infects Humans. *Cold Spring Harb. Perspect. Med.* 5.
- Kojima, S., Cimini, D., 2019. Aneuploidy and gene expression: is there dosage compensation? *Epigenomics* 11, 1827.
- Kondo, T., Matsumoto, K., Sugimoto, K., 1999. Role of a Complex Containing Rad17, Mec3, and Ddc1 in the Yeast DNA Damage Checkpoint Pathway. *Mol. Cell. Biol.* 19, 1136.
- Konopka, J.B., Casadevall, A., Taylor, J.W., Heitman, J., Cowen, L., 2019. One Health: Fungal Pathogens of Humans, Animals, and Plants.
- Koren, A., Tsai, H.-J., Tirosh, I., Burrack, L.S., Barkai, N., Berman, J., 2010. Epigenetically-Inherited Centromere and Neocentromere DNA Replicates Earliest in S-Phase. *PLOS Genet.* 6, e1001068.
- Krassowski, T., Coughlan, A.Y., Shen, X.-X., Zhou, X., Kominek, J., Oplente, D.A., Riley, R., Grigoriev, I. V., Maheshwari, N., Shields, D.C., Kurtzman, C.P., Hittinger, C.T., Rokas, A., Wolfe, K.H., 2018. Evolutionary instability of CUG-Leu in the genetic code of budding yeasts. *Nat. Commun.* 2018 91 9, 1–8.
- Kulemzina, I., MR, S., V, V., J, R., J, M., AV, F., C, L., VT, S., G, R., D, I., 2012. Cohesin rings devoid of Scc3 and Pds5 maintain their stable association with the DNA. *PLoS Genet.* 8.
- Kültz, D., 2005. DNA damage signals facilitate osmotic stress adaptation. *Am. J. Physiol. - Ren. Physiol.* 289.
- Kumar, R., S, C., D, S., JS, B., RA, L., HR, C., M, E., 2011. Histatin 5 uptake by *Candida albicans* utilizes polyamine transporters Dur3 and Dur31 proteins. *J. Biol. Chem.* 286, 43748–43758.
- Lahiri, M., TL, G., ER, M., CH, F., 2004. Expanded CAG repeats activate the DNA damage checkpoint pathway. *Mol. Cell* 15, 287–293.
- Lampson, M., Cheeseman, I., 2011. Sensing centromere tension: Aurora B and the regulation of kinetochore function. *Trends Cell Biol.* 21, 133–140.
- Landry, B.D., Doyle, J.P., Toczyski, D.P., Benanti, J.A., 2012. F-Box Protein Specificity for G1 Cyclins Is Dictated by Subcellular Localization. *PLoS Genet.* 8.

- Leach, Michelle D, Stead, D.A., Argo, E., Brown, A.J.P., 2011. Identification of sumoylation targets, combined with inactivation of SMT3, reveals the impact of sumoylation upon growth, morphology, and stress resistance in the pathogen *Candida albicans* 22.
- Leach, Michelle D., Stead, D.A., Argo, E., Brown, A.J.P., 2011. Identification of sumoylation targets, combined with inactivation of SMT3, reveals the impact of sumoylation upon growth, morphology, and stress resistance in the pathogen *Candida albicans*. *Mol. Biol. Cell* 22, 687–702.
- Legrand, M., Chan, C.L., Jauert, P.A., Kirkpatrick, D.T., 2008. Analysis of base excision and nucleotide excision repair in *Candida albicans*. *Microbiology* 154, 2446–2456.
- Legrand, M., CL, C., PA, J., DT, K., 2007. Role of DNA mismatch repair and double-strand break repair in genome stability and antifungal drug resistance in *Candida albicans*. *Eukaryot. Cell* 6, 2194–2205.
- Legrand, M., Jaitly, P., Feri, A., d'Enfert, C., Sanyal, K., 2019. *Candida albicans*: An Emerging Yeast Model to Study Eukaryotic Genome Plasticity. *Trends Genet.* 35, 292–307.
- Lephart, P.R., Magee, P.T., 2006. Effect of the Major Repeat Sequence on Mitotic Recombination in *Candida albicans*. *Genetics* 174, 1737–1744.
- Leroy, C., Lee, S.E., Vaze, M.B., Ochsenbien, F., Guerois, R., Haber, J.E., Marsolier-Kergoat, M.C., 2003. PP2C Phosphatases Ptc2 and Ptc3 Are Required for DNA Checkpoint Inactivation after a Double-Strand Break. *Mol. Cell* 11, 827–835.
- Li, R., Murray, A.W., 1991. Feedback control of mitosis in budding yeast. *Cell* 66, 519–531.
- Li, S.-J., Hochstrasser, M., 2000. The Yeast ULP2 (SMT4) Gene Encodes a Novel Protease Specific for the Ubiquitin-Like Smt3 Protein . *Mol. Cell Biol.* 20, 2367–2377.
- Li, S., Hochstrasser, M., 1999. A new protease required for cell-cycle progression in yeast. *Nature* 398, 246–251.
- Li, W.J., Wang, Y.M., Zheng, X. De, Shi, Q.M., Zhang, T.T., Bai, C., Li, D., Sang, J.L., Wang, Y., 2006. The F-box protein Grr1 regulates the stability of Ccn1, Cln3 and Hof1 and cell morphogenesis in *Candida albicans*. *Mol. Microbiol.* 62, 212–226.
- Li, Z., Nielsen, K., 2017. Morphology Changes in Human Fungal Pathogens upon Interaction with the Host. *J. Fungi* 3.
- Li, Z., Xu, X., 2019. Post-Translational Modifications of the Mini-Chromosome Maintenance Proteins in DNA Replication. *Genes (Basel)*. 10.
- Lipp, J., T, H., I, P., JM, P., 2007. Aurora B controls the association of condensin I but not condensin II with mitotic chromosomes. *J. Cell Sci.*

120, 1245–1255.

- Liu, D., Davydenko, O., Lampson, M., 2012. Polo-like kinase-1 regulates kinetochore-microtubule dynamics and spindle checkpoint silencing. *J. Cell Biol.* 198, 491–499.
- Liu, D., Lampson, M., 2009. Regulation of kinetochore-microtubule attachments by Aurora B kinase. *Biochem. Soc. Trans.* 37, 976–980.
- Liu, G., Zheng, X., Guan, H., Cao, Y., Qu, H., Kang, J., Ren, X., Lei, J., Dong, M.-Q., Li, X., Li, H., 2019. Architecture of *Saccharomyces cerevisiae* SAGA complex. *Cell Discov.* 2019 51 5, 1–4.
- Liu, Q., Zhu, X., Lindström, M., Shi, Y., Zheng, J., Hao, X., Gustafsson, C.M., Liu, B., 2020. Yeast mismatch repair components are required for stable inheritance of gene silencing. *PLOS Genet.* 16, e1008798.
- Liu, X., Winey, M., 2012. The MPS1 family of protein kinases. *Annu. Rev. Biochem.* 81, 561–585.
- Liu, Z., Myers, L.C., 2017. Mediator tail module is required for Tac1-activated CDR1 expression and azole resistance in *Candida albicans*. *Antimicrob. Agents Chemother.* 61.
- Lockhart, S.R., Fritch, J.J., Meier, A.S., Schroppel, K., Srikantha, T., Galask, R., Soll, D.R., 1995. Colonizing populations of *Candida albicans* are clonal in origin but undergo microevolution through C1 fragment reorganization as demonstrated by DNA fingerprinting and C1 sequencing. *J. Clin. Microbiol.* 33, 1501–1509.
- Loeb, J., M, S.-B., I, H., H, L., 1999a. A G1 cyclin is necessary for maintenance of filamentous growth in *Candida albicans*. *Mol. Cell. Biol.* 19, 4019–4027.
- Loeb, J., Sepulveda-Becerra, M., I, H., H, L., 1999b. A G1 cyclin is necessary for maintenance of filamentous growth in *Candida albicans*. *Mol. Cell. Biol.* 19, 4019–4027.
- Loeb, J.D.J., Sepulveda-Becerra, M., Hazan, I., Liu, H., 1999. A G1 Cyclin Is Necessary for Maintenance of Filamentous Growth in *Candida albicans*. *Mol. Cell. Biol.* 19, 4019–4027.
- Low, C.Y., Rotstein, C., 2011. Emerging fungal infections in immunocompromised patients. *F1000 Med. Rep.* 3.
- Lu, Y., Su, C., S, R., Y, Y., H, L., 2019. CO₂ Signaling through the Ptc2-Ssn3 Axis Governs Sustained Hyphal Development of *Candida albicans* by Reducing Ume6 Phosphorylation and Degradation. *MBio* 10.
- Lundin, C., North, M., Erixon, K., Walters, K., Jenssen, D., Goldman, A.S.H., Helleday, T., 2005a. Methyl methanesulfonate (MMS) produces heat-labile DNA damage but no detectable in vivo DNA double-strand breaks. *Nucleic Acids Res.* 33, 3799.

- Lundin, C., North, M., Erixon, K., Walters, K., Jenssen, D., Goldman, A.S.H., Helleday, T., 2005b. Methyl methanesulfonate (MMS) produces heat-labile DNA damage but no detectable in vivo DNA double-strand breaks. *Nucleic Acids Res.* 33, 3799.
- Luo, S., Hoffmann, R., Skerka, C., Zipfel, P.F., 2013. Glycerol-3-Phosphate Dehydrogenase 2 Is a Novel Factor H-, Factor H-like Protein 1-, and Plasminogen-Binding Surface Protein of *Candida albicans*. *J. Infect. Dis.* 207, 594–603.
- Luo, S., Tong, L., 2017. Molecular mechanism for the regulation of yeast separase by securin. *Nature* 542, 255–259.
- Lydeard, J.R., Jain, S., Yamaguchi, M., Haber, J.E., 2007. Break-induced replication and telomerase-independent telomere maintenance require Pol32. *Nat.* 2007 4487155 448, 820–823.
- Lydeard, J.R., Lipkin-Moore, Z., Sheu, Y.-J., Stillman, B., Burgers, P.M., Haber, J.E., 2010. Break-induced replication requires all essential DNA replication factors except those specific for pre-RC assembly. *Genes Dev.* 24, 1133.
- M, L., P, J., A, F., C, d'Enfert, K, S., 2019. *Candida albicans*: An Emerging Yeast Model to Study Eukaryotic Genome Plasticity. *Trends Genet.* 35, 292–307.
- Macleán, M.J., Aamodt, R., Harris, N., Alseth, I., Seeberg, E., Bjørås, M., Piper, P.W., 2003. Base excision repair activities required for yeast to attain a full chronological life span. *Aging Cell* 2, 93–104.
- MacPherson, S., Akache, B., Weber, S., De Deken, X., Raymond, M., Turcotte, B., 2005. *Candida albicans* Zinc Cluster Protein Upc2p Confers Resistance to Antifungal Drugs and Is an Activator of Ergosterol Biosynthetic Genes. *Antimicrob. Agents Chemother.* 49, 1745.
- Malumbres, M., 2015. Keeping Order in Anaphase. *Dev. Cell* 35, 403–404.
- Manohar, K., Peroumal, D., Acharya, N., 2018. TLS dependent and independent functions of DNA polymerase eta (Pol η /Rad30) from Pathogenic Yeast *Candida albicans*. *Mol. Microbiol.* 110, 707–727.
- Mao, X., Yang, L., D, Y., T, M., C, M., J, W., Q, Y., M, L., 2021. The Vacuole and Mitochondria Patch (vCLAMP) Protein Vam6 is Crucial for Autophagy in *Candida albicans*. *Mycopathologia* 186, 477–486.
- Marcos-Alcalde, Í., Mendieta-Moreno, J.I., Puisac, B., Gil-Rodríguez, M.C., Hernández-Marcos, M., Soler-Polo, D., Ramos, F.J., Ortega, J., Pié, J., Mendieta, J., Gómez-Puertas, P., 2017. Two-step ATP-driven opening of cohesin head. *Sci. Reports* 2017 71 7, 1–14.
- Marston, A.L., 2014. Chromosome Segregation in Budding Yeast: Sister Chromatid Cohesion and Related Mechanisms. *Genetics* 196, 31.
- Martel, C.M., Parker, J.E., Bader, O., Weig, M., Gross, U., Warrilow, A.G.S.,

- Rolley, N., Kelly, D.E., Kelly, S.L., 2010. Identification and Characterization of Four Azole-Resistant *erg3* Mutants of *Candida albicans*. *Antimicrob. Agents Chemother.* 54, 4527.
- Martin, S.W., Konopka, J.B., 2004. SUMO Modification of Septin-interacting Proteins in *Candida albicans**. *J. Biol. Chem.* 279, 40861–40867.
- Martínez, A.I., Castillo, L., Garcerá, A., Elorza, M. V., Valentín, E., Sentandreu, R., 2004. Role of Pir1 in the construction of the *Candida albicans* cell wall. *Microbiology* 150, 3151–3161.
- Mayer, F.L., Wilson, D., Hube, B., 2013a. *Candida albicans* pathogenicity mechanisms. *Virulence* 4, 119.
- Mayer, F.L., Wilson, D., Hube, B., 2013b. *Candida albicans* pathogenicity mechanisms. *Virulence* 4, 119.
- McCollum, D., Gould, K.L., 2001. Timing is everything: regulation of mitotic exit and cytokinesis by the MEN and SIN. *Trends Cell Biol.* 11, 89–95.
- McCoy, K.M., Tubman, E.S., Claas, A., Tank, D., Clancy, S.A., O'Toole, E.T., Berman, J., Odde, D.J., 2015. Physical limits on kinesin-5-mediated chromosome congression in the smallest mitotic spindles. *Mol. Biol. Cell* 26, 3999.
- McCulley, J.L., Petes, T.D., 2010. Chromosome rearrangements and aneuploidy in yeast strains lacking both Tel1p and Mec1p reflect deficiencies in two different mechanisms. *Proc. Natl. Acad. Sci.* 107, 11465–11470.
- Mceachernt, M.J., Hicks, J.B., 1993. Unusually large telomeric repeats in the yeast *Candida albicans*. *Mol. Cell. Biol.* 13, 551.
- Meluh, P.B., Rose, M.D., 1990. KAR3, a kinesin-related gene required for yeast nuclear fusion. *Cell* 60, 1029–1041.
- Merlini, L., Piatti, S., 2011. The mother-bud neck as a signaling platform for the coordination between spindle position and cytokinesis in budding yeast. *Biol. Chem.* 392, 805–812.
- Middleton, K., Carbon, J., 1994. KAR3-encoded kinesin is a minus-end-directed motor that functions with centromere binding proteins (CBF3) on an in vitro yeast kinetochore (chromosome segregation, microtubules/mitosis). *Proc. Natd. Acad. Sci. USA* 91, 7212–7216.
- Miller, R.K., Rose, M.D., 1998. Kar9p is a novel cortical protein required for cytoplasmic microtubule orientation in yeast. *J. Cell Biol.* 140, 377–390.
- Milne, S.W., Cheetham, J., Lloyd, D., Shaw, S., Moore, K., Paszkiewicz, K.H., Aves, S.J., Bates, S., 2014. Role of *Candida albicans* Tem1 in mitotic exit and cytokinesis. *Fungal Genet. Biol.* 69, 84–95.
- Mishra, P.K., Baum, M., Carbon, J., 2007. Centromere size and position in

- Candida albicans* are evolutionarily conserved independent of DNA sequence heterogeneity. *Mol. Genet. Genomics* 278, 455–465.
- Mitas, M., A, Y., J, D., IS, H., 1995. The trinucleotide repeat sequence d(CGG)₁₅ forms a heat-stable hairpin containing Gsyn. Ganti base pairs. *Biochemistry* 34, 12803–12811.
- Monroy-Pérez, E., Paniagua-Contreras, G.L., Rodríguez-Purata, P., Vaca-Paniagua, F., Vázquez-Villaseñor, M., Díaz-Velásquez, C., Uribe-García, A., Vaca, S., 2016. High virulence and antifungal resistance in clinical strains of *Candida albicans*. *Can. J. Infect. Dis. Med. Microbiol.* 2016.
- Montpetit, B., Hazbun, T.R., Fields, S., Hieter, P., 2006. Sumoylation of the budding yeast kinetochore protein Ndc10 is required for Ndc10 spindle localization and regulation of anaphase spindle elongation. *J. Cell Biol.* 174, 653–663.
- Moore, J.K., Haber, J.E., 1996. Cell Cycle and Genetic Requirements of Two Pathways of Nonhomologous End-Joining Repair of Double-Strand Breaks in *Saccharomyces cerevisiae*. *Mol. Cell. Biol.* 16, 2164–2173.
- Morais Vasconcelos Oliveira, J., Conceição Oliver, J., Latércia Tranches Dias, A., Barbosa Padovan, A.C., Siqueira Caixeta, E., Caixeta Franco Ariosa, M., 2021. Detection of ERG11 Overexpression in *Candida albicans* isolates from environmental sources and clinical isolates treated with inhibitory and subinhibitory concentrations of fluconazole. *Mycoses* 64, 220–227.
- Mordes, D.A., Nam, E.A., Cortez, D., 2008. Dpb11 activates the Mec1–Ddc2 complex. *Proc. Natl. Acad. Sci. U. S. A.* 105, 18730.
- Morrow, D., DA, T., Y, S., FS, C., P, H., 1995. TEL1, an *S. cerevisiae* homolog of the human gene mutated in ataxia telangiectasia, is functionally related to the yeast checkpoint gene MEC1. *Cell* 82, 831–840.
- Morrow, D.M., Connelly, C., Hieter, P., 1997. “break Copy” Duplication: A Model for Chromosome Fragment Formation in *Saccharomyces Cerevisiae*. *Genetics* 147, 371.
- Morschhäuser, J., Barker, K.S., Liu, T.T., Blaß-Warmuth, J., Homayouni, R., Rogers, P.D., 2007. The transcription factor Mrr1p controls expression of the MDR1 efflux pump and mediates multidrug resistance in *Candida albicans*. *PLoS Pathog.* 3, 1603–1616.
- Moser, B.A., Russell, P., 2000. Cell cycle regulation in *Schizosaccharomyces pombe*. *Curr. Opin. Microbiol.* 3, 631–636.
- Mousavi, B., Hedayati, M.T., Hedayati, N., Ilkit, M., Syedmousavi, S., 2016. *Aspergillus* species in indoor environments and their possible occupational and public health hazards. *Curr. Med. Mycol.* 2, 36.

- Musacchio, A., Desai, A., 2017. A molecular view of kinetochore assembly and function. *Biology (Basel)*. 6.
- Musacchio, A., Salmon, E.D., 2007. The spindle-assembly checkpoint in space and time. *Nat. Rev. Mol. Cell Biol.* 2007 8 5, 379–393.
- Myung, K., Chen, C., Kolodner, R.D., 2001. Multiple pathways cooperate in the suppression of genome instability in *Saccharomyces cerevisiae*. *Nat.* 2001 411 6841 411, 1073–1076.
- Navarathna, D.H.M.L.P., Das, A., Morschhäuser, J., Nickerson, K.W., Roberts, D.D., 2011. Dur3 is the major urea transporter in *Candida albicans* and is co-regulated with the urea amidolyase Dur1,2. *Microbiology* 157, 270.
- Navarathna, P., D.H.M.L., Das, A., Morschhäuser, J., Nickerson, K.W., Roberts, D.D., 2011. Dur3 is the major urea transporter in *Candida albicans* and is co-regulated with the urea amidolyase Dur1,2. *Microbiology* 157, 270.
- Nimonkar, A. V., Genschel, J., Kinoshita, E., Polaczek, P., Campbell, J.L., Wyman, C., Modrich, P., Kowalczykowski, S.C., 2011. BLM–DNA2–RPA–MRN and EXO1–BLM–RPA–MRN constitute two DNA end resection machineries for human DNA break repair. *Genes Dev.* 25, 350–362.
- Nishikawa, J.L., Boeszoermenyi, A., Vale-Silva, L.A., Torelli, R., Posteraro, B., Sohn, Y.J., Ji, F., Gelev, V., Sanglard, D., Sanguinetti, M., Sadreyev, R.I., Mukherjee, G., Bhyravabhotla, J., Buhrlage, S.J., Gray, N.S., Wagner, G., Naar, A.M., Arthanari, H., 2016. Inhibiting Fungal Multidrug Resistance by Disrupting an Activator-Mediator Interaction. *Nature* 530, 485.
- Noble, S.M., French, S., Kohn, L.A., Chen, V., Johnson, A.D., 2010a. Systematic screens of a *Candida albicans* homozygous deletion library decouple morphogenetic switching and pathogenicity. *Nat. Genet.* 2010 42 7, 590–598.
- Noble, S.M., French, S., Kohn, L.A., Chen, V., Johnson, A.D., 2010b. Systematic screens of a *Candida albicans* homozygous deletion library decouple morphogenetic switching and pathogenicity. *Nat. Genet.* 42, 590–598.
- Normile, T.G., Bryan, A.M., Del Poeta, M., 2020. Animal Models of *Cryptococcus neoformans* in Identifying Immune Parameters Associated With Primary Infection and Reactivation of Latent Infection. *Front. Immunol.* 11, 2197.
- O'Neill, B.M., Szyjka, S.J., Lis, E.T., Bailey, A.O., Yates, J.R., Aparicio, O.M., Romesberg, F.E., 2007. Pph3-Psy2 is a phosphatase complex required for Rad53 dephosphorylation and replication fork restart during recovery from DNA damage. *Proc. Natl. Acad. Sci. U. S. A.* 104, 9290–9295.

- Ofir, A., Kornitzer, D., 2010. *Candida albicans* Cyclin Clb4 Carries S-Phase Cyclin Activity. *Eukaryot. Cell* 9, 1311–1319.
- Oromendia, A.B., Dodgson, S.E., Amon, A., 2012. Aneuploidy causes proteotoxic stress in yeast. *Genes Dev.* 26, 2696.
- Ortolan, T.G., Chen, L., Tongaonkar, P., Madura, K., 2004. Rad23 stabilizes Rad4 from degradation by the Ub/proteasome pathway. *Nucleic Acids Res.* 32, 6490.
- Oura, T., Kajiwara, S., 2010. *Candida albicans* sphingolipid C9-methyltransferase is involved in hyphal elongation. *Microbiology* 156, 1234–1243.
- Page, B.D., Satterwhite, L.L., Rose, M.D., Snyder, M., 1990. Meluh and Rose.
- Pagès, V., Fuchs, R.P., 2003. Uncoupling of leading- and lagging-strand DNA replication during lesion bypass in vivo. *Science* 300, 1300–1303.
- Pande, K., Chen, C., Noble, S.M., 2013. Passage through the mammalian gut triggers a phenotypic switch that promotes *Candida albicans* commensalism. *Nat. Genet.* 45, 1088–1091.
- Papouli, E., Chen, S., Davies, A.A., Huttner, D., Krejci, L., Sung, P., Ulrich, H.D., 2005. Crosstalk between SUMO and ubiquitin on PCNA is mediated by recruitment of the helicase Srs2p. *Mol. Cell* 19, 123–133.
- Pappas, P.G., Lionakis, M.S., Arendrup, M.C., Ostrosky-Zeichner, L., Kullberg, B.J., 2018. Invasive candidiasis. *Nat. Rev. Dis. Prim.* 2018 41 4, 1–20.
- Pascucci, B., Russo, M.T., Crescenzi, M., Bignami, M., Dogliotti, E., 2005. The accumulation of MMS-induced single strand breaks in G1 phase is recombinogenic in DNA polymerase β defective mammalian cells. *Nucleic Acids Res.* 33, 280.
- Paudyal, S.C., You, Z., 2016. Sharpening the ends for repair: mechanisms and regulation of DNA resection. *Acta Biochim. Biophys. Sin. (Shanghai)*. 48, 647.
- Pavelka, N., Rancati, G., Zhu, J., Bradford, W.D., Saraf, A., Florens, L., Sanderson, B.W., Hattem, G.L., Li, R., 2010. Aneuploidy confers quantitative proteome changes and phenotypic variation in budding yeast. *Nature* 468, 321.
- Pentland, D.R., Piper-Brown, E., Mühlischlegel, F.A., Gourlay, C.W., 2018. Ras signalling in pathogenic yeasts. *Microb. Cell* 5, 63.
- Petreaca, R.C., 2013. Yeast Chromosomes. *Brenner's Encycl. Genet.* Second Ed. 382–384.
- Pierce, B.A., 2012. *Genetics: A Conceptual Approach*, *Genetics: A Conceptual Approach*. W. H. Freeman.

- Piispanen, A.E., Grahl, N., Hollomon, J.M., Hogan, D.A., 2013a. Regulated proteolysis of *Candida albicans* Ras1 is involved in morphogenesis and quorum sensing regulation. *Mol. Microbiol.* 89, 166–178.
- Piispanen, A.E., Grahl, N., Hollomon, J.M., Hogan, D.A., 2013b. Regulated proteolysis of *Candida albicans* Ras1 is involved in morphogenesis and quorum sensing regulation. *Mol. Microbiol.* 89, 166–178.
- Pla-Victori, J., 2020. The role of genetic counseling in the infertile patient. *Hum. Reprod. Genet.* 295–316.
- Porter, A., Farr, C., 2004. Topoisomerase II: untangling its contribution at the centromere. *Chromosome Res.* 12, 569–583.
- Prakash, S., Prakash, L., 2000. Nucleotide excision repair in yeast. *Mutat. Res. Mol. Mech. Mutagen.* 451, 13–24.
- Putnam, CD., Jaehnig, E.J., Kolodner, R.D., 2009. Perspectives on the DNA damage and replication checkpoint responses in *Saccharomyces cerevisiae*. *DNA Repair (Amst).* 8, 974.
- Putnam, CD, TK, H., RD, K., 2009. Specific pathways prevent duplication-mediated genome rearrangements. *Nature* 460, 984–989.
- Putnam, C.D., Allen-Soltero, S.R., Martinez, S.L., Chan, J.E., Hayes, T.K., Kolodner, R.D., 2012. Bioinformatic identification of genes suppressing genome instability. *Proc. Natl. Acad. Sci.* 109, E3251–E3259.
- Qiao, R., Weissmann, F., Yamaguchi, M., Brown, N.G., VanderLinden, R., Imre, R., Jarvis, M.A., Brunner, M.R., Davidson, I.F., Litos, G., Haselbach, D., Mechtler, K., Stark, H., Schulman, B.A., Peters, J.-M., 2016. Mechanism of APC/CCDC20 activation by mitotic phosphorylation. *Proc. Natl. Acad. Sci.* 113.
- Quan, Y., Hinshaw, S.M., Wang, P.C., Harrison, S.C., Zhou, H., 2021. Ctf3/cenp-i provides a docking site for the desumoylase ulp2 at the kinetochore. *J. Cell Biol.* 220.
- Ramage, G., Bachmann, S., Patterson, T.F., Wickes, B.L., López-Ribot, J.L., 2002. Investigation of multidrug efflux pumps in relation to fluconazole resistance in *Candida albicans* biofilms. *J. Antimicrob. Chemother.* 49, 973–980.
- Ramazi, S., Allahverdi, A., Zahiri, J., 2020. Evaluation of post-translational modifications in histone proteins: A review on histone modification defects in developmental and neurological disorders. *J. Biosci.* 2020 451 45, 1–29.
- Ramazi, S., Zahiri, J., 2021. Post-translational modifications in proteins: resources, tools and prediction methods. *Database* 2021.
- Ramírez-Zavala, B., Reuß, O., Park, Y.N., Ohlsen, K., Morschhäuser, J., 2008. Environmental Induction of White–Opaque Switching in *Candida albicans*. *PLOS Pathog.* 4, e1000089.

- Rastogi, R.P., Richa, Kumar, A., Tyagi, M.B., Sinha, R.P., 2010a. Molecular Mechanisms of Ultraviolet Radiation-Induced DNA Damage and Repair. *J. Nucleic Acids* 2010, 32.
- Rastogi, R.P., Richa, Kumar, A., Tyagi, M.B., Sinha, R.P., 2010b. Molecular Mechanisms of Ultraviolet Radiation-Induced DNA Damage and Repair. *J. Nucleic Acids* 2010, 32.
- Régnier, V., Vagnarelli, P., Fukagawa, T., Zerjal, T., Burns, E., Trouche, D., Earnshaw, W., Brown, W., 2005. CENP-A Is Required for Accurate Chromosome Segregation and Sustained Kinetochores Association of BubR1. *Mol. Cell. Biol.* 25, 3967.
- Rhind, N., Russell, P., 1998. Mitotic DNA damage and replication checkpoints in yeast. *Curr. Opin. Cell Biol.* 10, 749.
- Richardson, H., Lew, D.J., Henze, M., Sugimoto, K., Reed, S.I., 1992. Cyclin-B homologs in *Saccharomyces cerevisiae* function in S phase and in G2. *Genes Dev.* 6, 2021–2034.
- Ritchie, K., JC, M., TD, P., 1999. Interactions of TLC1 (which encodes the RNA subunit of telomerase), TEL1, and MEC1 in regulating telomere length in the yeast *Saccharomyces cerevisiae*. *Mol. Cell. Biol.* 19, 6065–6075.
- Ritchie, K., Petes, T., 2000. The Mre11p/Rad50p/Xrs2p complex and the Tel1p function in a single pathway for telomere maintenance in yeast. *Genetics* 155, 475–479.
- Rosana, Y., Yasmon, A., Lestari, D.C., 2015. Overexpression and mutation as a genetic mechanism of fluconazole resistance in *Candida albicans* isolated from human immunodeficiency virus patients in Indonesia. *J. Med. Microbiol.* 64, 1046–1052.
- Roy, B., Burrack, L.S., Lone, M.A., Berman, J., Sanyal, K., 2011. CaMtw1, a member of the evolutionarily conserved Mis12 kinetochores protein family, is required for efficient inner kinetochores assembly in the pathogenic yeast *Candida albicans*. *Mol. Microbiol.* 80, 14.
- Roy, B., Varshney, N., Yadav, V., Sanyal, K., 2013. The process of kinetochores assembly in yeasts. *FEMS Microbiol. Lett.* 338, 107–117.
- Rustchenko, E.P., Curran, T.M., Sherman, F., 1993. Variations in the number of ribosomal DNA units in morphological mutants and normal strains of *Candida albicans* and in normal strains of *Saccharomyces cerevisiae*. *J. Bacteriol.* 175, 7189–7199.
- Ryu, H.-Y., Ahn, S.H., Hochstrasser, M., 2020. SUMO and cellular adaptive mechanisms. *Exp. Mol. Med.* 2020 526 52, 931–939.
- Ryu, H.-Y., Wilson, N.R., Mehta, S., Hwang, S.S., Hochstrasser, M., 2016. Loss of the SUMO protease Ulp2 triggers a specific multichromosome aneuploidy. *Genes Dev.* 30, 1881.

- Ryu, H.Y., Wilson, N.R., Mehta, S., Hwang, S.S., Hochstrasser, M., 2016. Loss of the SUMO protease ULP2 triggers a specific multichromosome aneuploidy. *Genes Dev.* 30, 1881–1894.
- S, P., P, S., L, P., 1993. DNA repair genes and proteins of *Saccharomyces cerevisiae*. *Annu. Rev. Genet.* 27, 33–70.
- Sahu, M.S., Patra, S., Kumar, K., Kaur, R., 2020. SUMOylation in human pathogenic Fungi: Role in physiology and virulence. *J. Fungi* 6, 1–19.
- Sakofsky, C.J., Ayyar, S., Malkova, A., 2012. Break-induced replication and genome stability. *Biomolecules* 2, 483–504.
- Sampson, D.A., Wang, M., Matunis, M.J., 2001. The Small Ubiquitin-like Modifier-1 (SUMO-1) Consensus Sequence Mediates Ubc9 Binding and Is Essential for SUMO-1 Modification *. *J. Biol. Chem.* 276, 21664–21669.
- Sanglard, D., Ischer, F., Koymans, L., Bille, J., 1998. Amino acid substitutions in the cytochrome P-450 lanosterol 14 α -demethylase (CYP51A1) from azole-resistant *Candida albicans* clinical isolates contribute to resistance to azole antifungal agents. *Antimicrob. Agents Chemother.* 42, 241–253.
- Sanglard, D., Ischer, F., Parkinson, T., Falconer, D., Bille, J., 2003. *Candida albicans* Mutations in the Ergosterol Biosynthetic Pathway and Resistance to Several Antifungal Agents. *Antimicrob. Agents Chemother.* 47, 2404.
- Santos, M.A.S., Gomes, A.C., Santos, M.C., Carreto, L.C., Moura, G.R., 2011. The genetic code of the fungal CTG clade. *C. R. Biol.* 334, 607–611.
- Sanyal, K., Carbon, J., 2002a. The CENP-A homolog CaCse4p in the pathogenic yeast *Candida albicans* is a centromere protein essential for chromosome transmission. *Proc. Natl. Acad. Sci.* 99, 12969–12974.
- Sanyal, K., Carbon, J., 2002b. The CENP-A homolog CaCse4p in the pathogenic yeast *Candida albicans* is a centromere protein essential for chromosome transmission. *Proc. Natl. Acad. Sci. U. S. A.* 99, 12969.
- Sanyal, K., M, B., J, C., 2004. Centromeric DNA sequences in the pathogenic yeast *Candida albicans* are all different and unique. *Proc. Natl. Acad. Sci. U. S. A.* 101, 11374–11379.
- Sasaki, T., Toh-e, A., Kikuchi, Y., 2000. Extragenic suppressors that rescue defects in the heat stress response of the budding yeast mutant tom1. *Mol. Gen. Genet.* 262, 940–948.
- Schärer, O.D., 2013. Nucleotide Excision Repair in Eukaryotes. *Cold Spring Harb. Perspect. Biol.* 5.
- Schormann, N., Ricciardi, R., Chattopadhyay, D., 2014. Uracil-DNA glycosylases—Structural and functional perspectives on an essential

- family of DNA repair enzymes. *Protein Sci.* 23, 1667.
- Schwartz, K., Richards, K., Botstein, D., 1997. BIM1 encodes a microtubule-binding protein in yeast. *Mol. Biol. Cell* 8, 2677–2691.
- Schweitzer, J.K., Livingston, D.M., 1999. The effect of DNA replication mutations on CAG tract stability in yeast. *Genetics* 152, 953.
- Schwienhorst, I., Johnson, E.S., Dohmen, R.J., 2000. SUMO conjugation and deconjugation. *Mol. Gen. Genet. MGG* 2000 2635 263, 771–786.
- Selmecki, A., Forche, A., Berman, J., 2006. Formation in Drug-Resistant. *Science* (80-). 367–370.
- Selmecki, A., Gerami-Nejad, M., Paulson, C., Forche, A., Berman, J., 2008. An isochromosome confers drug resistance in vivo by amplification of two genes, ERG11 and TAC1. *Mol. Microbiol.* 68, 624–641.
- Selmecki, A., K, D., LE, C., JB, A., J, B., 2009. Acquisition of aneuploidy provides increased fitness during the evolution of antifungal drug resistance. *PLoS Genet.* 5.
- Selmecki, A., Maruvka, Y.E., Richmond, P.A., Guillet, M., Shores, N., Sorenson, A., De, S., Kishony, R., Michor, F., Dowell, R., Pellman, D., 2015. Polyploidy can drive rapid adaptation in yeast. *Nature* 519, 349.
- Shapiro, R.S., Robbins, N., Cowen, L.E., 2011. Regulatory Circuitry Governing Fungal Development, Drug Resistance, and Disease. *Microbiol. Mol. Biol. Rev.* 75, 213.
- Shayeghi, M., Doe, C.L., Tavassoli, M., Watts, F.Z., 1997. Characterisation of *Schizosaccharomyces pombe* rad31, a UBA-related gene required for DNA damage tolerance. *Nucleic Acids Res.* 25, 1162.
- Sherlock, G., AM, B., A, M., JC, S., M, F., J, R., 1994. Molecular cloning and analysis of CDC28 and cyclin homologues from the human fungal pathogen *Candida albicans*. *Mol. Gen. Genet.* 245, 716–723.
- Sherwood, R.K., Bennett, R.J., 2008. Microtubule motor protein Kar3 is required for normal mitotic division and morphogenesis in *Candida albicans*. *Eukaryot. Cell* 7, 1460–1474.
- Shiotani, B., Zou, L., 2009. Single-Stranded DNA Orchestrates an ATM-to-ATR Switch at DNA Breaks. *Mol. Cell* 33, 547.
- SI, R., 2003. Ratchets and clocks: the cell cycle, ubiquitylation and protein turnover. *Nat. Rev. Mol. Cell Biol.* 4, 855–864.
- Siegel, J.J., Amon, A., 2012. New insights into the troubles of aneuploidy. *Annu. Rev. Cell Dev. Biol.* 28, 189–214.
- Simões, J., Bezerra, A.R., Moura, G.R., Araújo, H., Gut, I., Bayes, M., Santos, M.A.S., 2016. The Fungus *Candida albicans* Tolerates Ambiguity at Multiple Codons. *Front. Microbiol.* 0, 401.

- Singh, S.M., Steinberg-Neifach, O., Mian, I.S., Lue, N.F., 2002. Analysis of Telomerase in *Candida albicans*: Potential Role in Telomere End Protection. *Eukaryot. Cell* 1, 967.
- Sinha, I., YM, W., R, P., CR, L., WH, Y., Y, W., 2007. Cyclin-dependent kinases control septin phosphorylation in *Candida albicans* hyphal development. *Dev. Cell* 13, 421–432.
- Sinha, R., Häder, D., 2002. UV-induced DNA damage and repair: a review. *Photochem. Photobiol. Sci.* 1, 225–236.
- Skoneczna, A., Kaniak, A., Skoneczny, M., 2015. Genetic instability in budding and fission yeast—sources and mechanisms. *FEMS Microbiol. Rev.* 39, 917–967.
- Smith, A.C., Hickman, M.A., 2020. Host-Induced Genome Instability Rapidly Generates Phenotypic Variation across *Candida albicans* Strains and Ploidy States. *mSphere* 5.
- Soll, D.R., 2004. Mating-type locus homozygosis, phenotypic switching and mating: a unique sequence of dependencies in *Candida albicans*. *BioEssays* 26, 10–20.
- Stead, K., Aguilar, C., Hartman, T., Drexel, M., Meluh, P., Guacci, V.A., 2003. Pds5p regulates the maintenance of sister chromatid cohesion and is sumoylated to promote the dissolution of cohesion. *J. Cell Biol.* 163, 729–741.
- Steiner, N.C., Hahnenberger, K.M., Clarke, L., 1993. Centromeres of the fission yeast *Schizosaccharomyces pombe* are highly variable genetic loci. *Mol. Cell. Biol.* 13, 4578.
- Sterner, D.E., Grant, P.A., Roberts, S.M., Duggan, L.J., Belotserkovskaya, R., Pacella, L.A., Winston, F., Workman, J.L., Berger, S.L., 1999. Functional Organization of the Yeast SAGA Complex: Distinct Components Involved in Structural Integrity, Nucleosome Acetylation, and TATA-Binding Protein Interaction. *Mol. Cell. Biol.* 19, 86.
- Sucher, A.J., Chahine, E.B., Balcer, H.E., 2009. Echinocandins: the newest class of antifungals. *Ann. Pharmacother.* 43, 1647–1657.
- Sudbery, P.E., 2011. Growth of *Candida albicans* hyphae. *Nat. Rev. Microbiol.* 2011 910 9, 737–748.
- Suhandynata, R.T., Quan, Y., Yang, Y., Yuan, W.-T., Albuquerque, C.P., Zhou, H., 2019. Recruitment of the Ulp2 protease to the inner kinetochore prevents its hyper-sumoylation to ensure accurate chromosome segregation. *PLOS Genet.* 15, e1008477.
- Sumara, I., Vorlaufer, E., Stukenberg, P.T., Kelm, O., Redemann, N., Nigg, E.A., Peters, J.M., 2002. The Dissociation of Cohesin from Chromosomes in Prophase Is Regulated by Polo-like Kinase. *Mol. Cell* 9, 515–525.

- Sun, L.L., Li, W.J., Wang, H.T., Chen, J., Deng, P., Wang, Y., Sang, J.L., 2011. Protein phosphatase Pph3 and its regulatory subunit Psy2 regulate Rad53 dephosphorylation and cell morphogenesis during recovery from DNA damage in *Candida albicans*. *Eukaryot. Cell* 10, 1565–1573.
- Sun, S., Hoy, M.J., Heitman, J., 2020. Fungal pathogens. *Curr. Biol.* 30, R1163–R1169.
- Svensson, J.P., Pesudo, L.Q., Fry, R.C., Adeleye, Y.A., Carmichael, P., Samson, L.D., 2011. Genomic phenotyping of the essential and non-essential yeast genome detects novel pathways for alkylation resistance. *BMC Syst. Biol.* 5, 157.
- Sydorsky, Y., T, S., SM, J., S, W., FJ, V., T, M., YT, C., AC, G., B, R., 2010. A novel mechanism for SUMO system control: regulated Ulp1 nucleolar sequestration. *Mol. Cell. Biol.* 30, 4452–4462.
- Symington, L.S., Gautier, J., 2011. Double-strand break end resection and repair pathway choice. *Annu. Rev. Genet.* 45, 247–271.
- T, von der H., 2007. Optimized protein extraction for quantitative proteomics of yeasts. *PLoS One* 2.
- TA, D., Y, L.G., V, C., M, C., P, V., D, C., JP, B., N, G.-G., N, P., 2018. [Yeasts from the CTG clade (*Candida* clade): Biology, impact in human health, and biotechnological applications]. *J. Mycol. Med.* 28, 257–268.
- Tabarés-Seisdedos, R., Rubenstein, J.L.R., 2009. Chromosome 8p as a potential hub for developmental neuropsychiatric disorders: implications for schizophrenia, autism and cancer. *Mol. Psychiatry* 2009 146 14, 563–589.
- Tanaka, K., Nishide, J., Okazaki, K., Kato, H., Niwa, O., Nakagawa, T., Matsuda, H., Kawamukai, M., Murakami, Y., 1999a. Characterization of a Fission Yeast SUMO-1 Homologue, Pmt3p, Required for Multiple Nuclear Events, Including the Control of Telomere Length and Chromosome Segregation. *Mol. Cell. Biol.* 19, 8660.
- Tanaka, K., Nishide, J., Okazaki, K., Kato, H., Niwa, O., Nakagawa, T., Matsuda, H., Kawamukai, M., Murakami, Y., 1999b. Characterization of a Fission Yeast SUMO-1 Homologue, Pmt3p, Required for Multiple Nuclear Events, Including the Control of Telomere Length and Chromosome Segregation. *Mol. Cell. Biol.* 19, 8660.
- Tao, L., Du, H., Guan, G., Dai, Y., Nobile, C.J., Liang, W., Cao, C., Zhang, Q., Zhong, J., Huang, G., 2014. Discovery of a “White-Gray-Opaque” Tristable Phenotypic Switching System in *Candida albicans*: Roles of Non-genetic Diversity in Host Adaptation. *PLOS Biol.* 12, e1001830.
- Taylor, D.L., Ho, J.C.Y., Oliver, A., Watts, F.Z., 2002. Cell-cycle-dependent localisation of Ulp1, a *Schizosaccharomyces pombe* Pmt3 (SUMO)-specific protease. *J. Cell Sci.* 115, 1113–1122.

- Taylor, D.L., Hollingsworth, T.N., McFarland, J.W., Lennon, N.J., Nusbaum, C., Ruess, R.W., 2014. A first comprehensive census of fungi in soil reveals both hyperdiversity and fine-scale niche partitioning. *Ecol. Monogr.* 84, 3–20.
- Thakur, J., Sanyal, K., 2011. The Essentiality of the Fungus-Specific Dam1 Complex Is Correlated with a One-Kinetochore-One-Microtubule Interaction Present throughout the Cell Cycle, Independent of the Nature of a Centromere. *Eukaryot. Cell* 10, 1295.
- Thakur, J., Sanyal, K., 2012. A Coordinated Interdependent Protein Circuitry Stabilizes the Kinetochore Ensemble to Protect CENP-A in the Human Pathogenic Yeast *Candida albicans*. *PLoS Genet.* 8, 1002661.
- Thompson, D.S., Carlisle, P.L., Kadosh, D., 2011a. Coevolution of morphology and virulence in *Candida* species. *Eukaryot. Cell* 10, 1173–1182.
- Thompson, D.S., Carlisle, P.L., Kadosh, D., 2011b. Coevolution of morphology and virulence in *Candida* species. *Eukaryot. Cell* 10, 1173–1182.
- Tishkoff, D.X., Filosi, N., Gaida, G.M., Kolodner, R.D., 1997. A Novel Mutation Avoidance Mechanism Dependent on *S. cerevisiae* RAD27 Is Distinct from DNA Mismatch Repair. *Cell* 88, 253–263.
- Tkach, J.M., Yimit, A., Lee, A.Y., Riffle, M., Costanzo, M., Jaschob, D., Hendry, J.A., Ou, J., Moffat, J., Boone, C., Davis, T.N., Nislow, C., Brown, G.W., 2012. Dissecting DNA damage response pathways by analysing protein localization and abundance changes during DNA replication stress. *Nat. Cell Biol.* 14, 966–976.
- Toczyski, D.P., Galgoczy, D.J., Hartwell, L.H., 1997. CDC5 and CKII Control Adaptation to the Yeast DNA Damage Checkpoint. *Cell* 90, 1097–1106.
- Todd, R.T., Wikoff, T.D., Forche, A., Selmecki, A., 2019. Genome plasticity in *Candida albicans* is driven by long repeat sequences. *Elife* 8.
- Tsai, H., JA, B., I, L., A, K., LS, B., MA, H., MA, T., LN, R., J, B., 2014. Origin replication complex binding, nucleosome depletion patterns, and a primary sequence motif can predict origins of replication in a genome with epigenetic centromeres. *MBio* 5.
- Turner, S.A., Butler, G., 2014. The *Candida* Pathogenic Species Complex. *Cold Spring Harb. Perspect. Med.* 4.
- Tyc, K.M., Herwald, S.E., Hogan, J.A., Pierce, J. V., Klipp, E., Kumamoto, C.A., 2016. The game theory of *Candida albicans* colonization dynamics reveals host status-responsive gene expression. *BMC Syst. Biol.* 10.
- Tyc, K.M., Kühn, C., Wilson, D., Klipp, E., 2014. Assessing the advantage of morphological changes in *Candida albicans*: a game theoretical study. *Front. Microbiol.* 5.

- Tytell, J.D., Sorger, P.K., 2006a. Analysis of kinesin motor function at budding yeast kinetochores. *J. Cell Biol.* 172, 861–874.
- Tytell, J.D., Sorger, P.K., 2006b. Analysis of kinesin motor function at budding yeast kinetochores. *J. Cell Biol.* 172, 861–874.
- Tzeng, Y.L., Datta, A., Strole, C., Kumar Kolli, V.S., Birck, M.R., Taylor, W.P., Carlson, R.W., Woodard, R.W., Stephens, D.S., 2002. KpsF Is the Arabinose-5-phosphate Isomerase Required for 3-Deoxy-d-mannooctulosonic Acid Biosynthesis and for Both Lipooligosaccharide Assembly and Capsular Polysaccharide Expression in *Neisseria meningitidis* *. *J. Biol. Chem.* 277, 24103–24113.
- Uhlmann, F., 2001. Secured cutting: controlling separase at the metaphase to anaphase transition. *EMBO Rep.* 2, 487.
- Uhlmann, F., F, L., K, N., 1999. Sister-chromatid separation at anaphase onset is promoted by cleavage of the cohesin subunit Scc1. *Nature* 400, 37–42.
- Uwamahoro, N., Qu, Y., Jelacic, B., Lo, T.L., Beaurepaire, C., Bantun, F., Quenault, T., Boag, P.R., Ramm, G., Callaghan, J., Beilharz, T.H., Nantel, A., Peleg, A.Y., Traven, A., 2012. The Functions of Mediator in *Candida albicans* Support a Role in Shaping Species-Specific Gene Expression. *PLoS Genet.* 8.
- Van het Hoog, M., Rast, T.J., Martchenko, M., Grindle, S., Dignard, D., Hogues, H., Cuomo, C., Berriman, M., Scherer, S., Magee, B.B., Whiteway, M., Chibana, H., Nantel, A., Magee, P.T., 2007a. Assembly of the *Candida albicans* genome into sixteen supercontigs aligned on the eight chromosomes. *Genome Biol.* 8.
- Van het Hoog, M., Rast, T.J., Martchenko, M., Grindle, S., Dignard, D., Hogues, H., Cuomo, C., Berriman, M., Scherer, S., Magee, B.B., Whiteway, M., Chibana, H., Nantel, A., Magee, P.T., 2007b. Assembly of the *Candida albicans* genome into sixteen supercontigs aligned on the eight chromosomes. *Genome Biol.* 8, R52.
- Vanoosthuyse, V., Valsdottir, R., Javerzat, J.-P., Hardwick, K.G., 2004. Kinetochores Targeting of Fission Yeast Mad and Bub Proteins Is Essential for Spindle Checkpoint Function but Not for All Chromosome Segregation Roles of Bub1p. *Mol. Cell. Biol.* 24, 9786.
- Vernay, A., Schaub, S., Guillas, I., Bassilana, M., Arkowitz, R.A., 2012. A steep phosphoinositide bis-phosphate gradient forms during fungalfilamentous growth. *J. Cell Biol.* 198, 711.
- Veses, V., Gow, N.A.R., 2009. Pseudohypha budding patterns of *Candida albicans*. *Med. Mycol.* 47, 268–275.
- Wan, J., Subramonian, D., Zhang, X.-D., 2012. SUMOylation in Control of Accurate Chromosome Segregation during Mitosis. *Curr. Protein Pept. Sci.* 13, 467.

- Wang, H., Gao, J., Li, W., Wong, A.H.H., Hu, K., Chen, K., Wang, Y., Sang, J., 2012. Pph3 Dephosphorylation of Rad53 Is Required for Cell Recovery from MMS-Induced DNA Damage in *Candida albicans*. *PLoS One* 7, 37246.
- Warenda, A.J., Konopka, J.B., 2002. Septin Function in *Candida albicans* Morphogenesis. *Mol. Biol. Cell* 13, 2732.
- Wellehan, J.F.X., Lierz, M., Phalen, D., Raidal, S., Styles, D.K., Crosta, L., Melillo, A., Schnitzer, P., Lennox, A., Lumeij, J.T., 2016. CHAPTER 2 - Infectious disease. In: SPEER, B.L.B.T.-C.T. in A.M. and S. (Ed.), . W.B. Saunders, pp. 22–106.
- Wells, R.D., 1996. Molecular Basis of Genetic Instability of Triplet Repeats (*). *J. Biol. Chem.* 271, 2875–2878.
- Westermann, S., A, A.-S., HW, W., H, N., J, W., DG, D., E, N., G, B., 2005. Formation of a dynamic kinetochore- microtubule interface through assembly of the Dam1 ring complex. *Mol. Cell* 17, 277–290.
- Whitaker, A.M., Schaich, M.A., Smith, M.S., Flynn, T.S., Freudenthal, B.D., 2017. Base excision repair of oxidative DNA damage: from mechanism to disease. *Front. Biosci. (Landmark Ed.* 22, 1493.
- Wightman, R., Bates, S., Amornrattanapan, P., Sudbery, P., 2004. In *Candida albicans*, the Nim1 kinases Gin4 and Hsl1 negatively regulate pseudohypha formation and Gin4 also controls septin organization. *J. Cell Biol.* 164, 581–591.
- Wysocki, Robert, Bobrowicz, P., Ułaszewski, S., 1997. The *Saccharomyces cerevisiae* ACR3 gene encodes a putative membrane protein involved in arsenite transport. *J. Biol. Chem.* 272, 30061–30066.
- Wysocki, R, P, B., S, U., 1997. The *Saccharomyces cerevisiae* ACR3 gene encodes a putative membrane protein involved in arsenite transport. *J. Biol. Chem.* 272, 30061–30066.
- Xiao, W., Chow, B.L., Hanna, M., Doetsch, P.W., 2001. Deletion of the MAG1 DNA glycosylase gene suppresses alkylation-induced killing and mutagenesis in yeast cells lacking AP endonucleases. *Mutat. Res. Repair* 487, 137–147.
- Xie, J., L, Q., Z, M., BT, G., JC, D., K, Ting, JR, K., J, T., K, Tan, MD, L., T, K., MF, M., DJ, K., C, B., BJ, A., A, S., K, H.W., N, R., LE, C., 2017. The *Candida albicans* transcription factor Cas5 couples stress responses, drug resistance and cell cycle regulation. *Nat. Commun.* 8.
- Xu, N., Dong, Y., Cheng, X., Yu, Q., Qian, K., Mao, J., Jia, C., Ding, X., Zhang, Bing, Chen, Y., Zhang, Biao, Xing, L., Li, M., 2014. Cellular iron homeostasis mediated by the Mrs4–Ccc1–Smf3 pathway is essential for mitochondrial function, morphogenesis and virulence in *Candida albicans*. *Biochim. Biophys. Acta - Mol. Cell Res.* 1843, 629–639.

- Yamano, H., 2019. APC/C: current understanding and future perspectives. *F1000Research* 8.
- Yang, F., Jiang, Y., Cao, Y., Berman, J., 2021. The fitness costs and benefits of trisomy of each *Candida albicans* chromosome. *bioRxiv* 2021.01.21.427689.
- Yang, M., Brand, A., Srikantha, T., Daniels, K.J., Soll, D.R., Gow, N.A.R., 2011. Fig1 Facilitates Calcium Influx and Localizes to Membranes Destined To Undergo Fusion during Mating in *Candida albicans*. *Eukaryot. Cell* 10, 435.
- Yang, S.H., Galanis, A., Witty, J., Sharrocks, A.D., 2006. An extended consensus motif enhances the specificity of substrate modification by SUMO. *EMBO J.* 25, 5083.
- Yona, A.H., Manor, Y.S., Herbst, R.H., Romano, G.H., Mitchell, A., Kupiec, M., Pilpel, Y., Dahan, O., 2012. Chromosomal duplication is a transient evolutionary solution to stress. *Proc. Natl. Acad. Sci.* 109, 21010–21015.
- You, H., RL, S., C, H., AH, C., S, J.-R., S, S., SS, W., S, B., M, D., PW, D., 1999. *Saccharomyces cerevisiae* Ntg1p and Ntg2p: broad specificity N-glycosylases for the repair of oxidative DNA damage in the nucleus and mitochondria. *Biochemistry* 38, 11298–11306.
- Yu, E.Y., 2012. Telomeres and telomerase in *Candida albicans*. *Mycoses* 55, 48–59.
- Yu, S., Evans, K., Eijk, P. van, Bennett, M., Webster, R.M., Leadbitter, M., Teng, Y., Waters, R., Jackson, S.P., Reed, S.H., 2016. Global genome nucleotide excision repair is organized into domains that promote efficient DNA repair in chromatin. *Genome Res.* 26, 1376.
- Zeman, M.K., Cimprich, K.A., 2014. Causes and consequences of replication stress. *Nat. Cell Biol.* 16, 2–9.
- Zhang, A., Petrov, K.O., Hyun, E.R., Liu, Z., Gerber, S.A., Myers, L.C., 2012. The Tlo proteins are stoichiometric components of *Candida albicans* Mediator anchored via the Med3 subunit. *Eukaryot. Cell* 11, 874–884.
- Zhao, R., KJ, D., SR, L., KM, Y., LL, H., DR, S., 2005. Unique aspects of gene expression during *Candida albicans* mating and possible G(1) dependency. *Eukaryot. Cell* 4, 1175–1190.
- Zhou, Y., Liao, M., Zhu, C., Hu, Y., Tong, T., Peng, X., Li, M., Feng, M., Cheng, L., Ren, B., Zhou, X., 2018. ERG3 and ERG11 genes are critical for the pathogenesis of *Candida albicans* during the oral mucosal infection. *Int. J. Oral Sci.* 2018 102 10, 1–8.
- Zhu, C., Gao, P., Jiang, Y., 2010. [Advances in the study of *Candida albicans* gene mutation on azole drug resistance]. *Yao Xue Xue Bao* 45, 821–826.
- Zordan, R.E., Galgoczy, D.J., Johnson, A.D., 2006. Epigenetic properties of

white–opaque switching in *Candida albicans* are based on a self-sustaining transcriptional feedback loop. *Proc. Natl. Acad. Sci.* 103, 12807–12812.